Variation in Effects of Climate Change on Salmonid Demography: Extent, Scale, and Underlying Mechanisms

Brian K. Gallagher

A Thesis
In the Department of
Biology

Presented in Partial Fulfillment of the Requirements
For the Degree of
Doctor of Philosophy (Biology)

at Concordia University
Montreal, Quebec, Canada

January 2024

CONCORDIA UNIVERSITY

SCHOOL OF GRADUATE STUDIES

This is to certify that the thesis prepared

By: *Brian K. Gallagher*

Entitled: *Variation in Effects of Climate Change on Salmonid Demography: Extent, Scale, and Underlying Mechanisms*

And submitted in partial fulfillment of the requirements for the degree of

Doctor of Philosophy (*Biology*)

complies with the regulations of the University and meets the accepted standards with respect to originality and quality.

Signed by the final examining committee:

_____ Chair
Dr. Emma Despland

_____ External Examiner
Dr. Jennifer Sunday

_____ External to Program
Dr. Nicola Smith

_____ Examiner
Dr. James Grant

_____ Examiner
Dr. Pedro Peres-Neto

_____ Thesis Supervisor
Dr. Dylan Fraser

Approved by _____
Dr. Robert Weladji, Graduate Program Director

March 7, 2024 _____
Dr. Pascale Sicotte
Dean, Faculty of Arts and Sciences

ABSTRACT

Variation in Effects of Climate Change on Salmonid Demography: Extent, Scale, and Underlying Mechanisms

Brian K. Gallagher, Ph.D.

Concordia University, 2024

Predicting species responses to climate change is an increasingly important objective in ecological research and natural resource management. However, heterogeneity in demography, life history, and habitat characteristics across multiple spatial scales can generate substantial diversity in population responses, complicating species-level assessments. Therefore, for widely distributed species consisting of many fragmented populations, understanding the mechanisms that underlie population variation can improve predictions of climate impacts across the species range. Using salmonid fishes as a model system, my thesis investigates variation in population responses to climate change at global, regional, and local scales. First, through a global meta-analysis of 156 studies of 23 species, I demonstrated that population responses to temperature and precipitation exhibit significant spatial, temporal, and biological patterns that broadly align with predictions based on salmonid thermal limits. Importantly, I showed that salmonid populations at low latitudes and elevations tend to be most negatively impacted by rising temperatures. Subsequently, I analyzed mark-recapture and stream temperature data collected during field surveys in Cape Race (Newfoundland, Canada) since 2010 to characterize local-scale variation in demography, climate impacts, and thermal regimes among eleven populations of brook trout (*Salvelinus fontinalis*) separated by <5 km. I showed that variation in recruitment, growth, and demographic relationships combined to generate diverse population dynamics that stabilized brook trout abundance across Cape Race, and that thermal regimes driven by groundwater inputs contributed to population diversity. Finally, using population-specific demographic and life history data, I built eco-genetic models that simulated responses to future climate warming across Cape Race brook trout populations, which emphasized the role of life history evolution and thermal habitat variation in determining population persistence. Together, my thesis shows that large-scale gradients in latitude and elevation structure salmonid responses to climate change, but substantial fine-scale variation is embedded within these trends due to heterogeneity in habitat characteristics, human impacts, and eco-evolutionary dynamics experienced by populations. Similar research frameworks that employ diverse methodologies and integrate data across scales will be crucial for understanding the complex impacts of climate change on salmonids and other freshwater fish populations, and should inform the conservation of a wide range of species.

Acknowledgements

This work was financially supported by Concordia University (Graduate Doctoral Fellowship, International Tuition Award, Graduate Student Conference & Exposition Award, and a Concordia University Research Chair awarded to D.J. Fraser), Groupe de Recherché Interuniversitaire en Limnologie (Doctoral Fellowship), Fulbright Canada (Graduate Student Award), and the Natural Sciences and Engineering Research Council of Canada (Discovery Grant awarded to D.J. Fraser). All work was conducted in accordance with Concordia University Animal Research Ethics Protocols, and permits issued by Fisheries and Oceans Canada (2022 permit number: NL-6873-22) and the Newfoundland and Labrador Natural Areas Program.

First and foremost, I would like to thank my supervisor Dr. Dylan Fraser for his continual support throughout my PhD. Since starting my degree in 2019, Dylan has provided me with countless opportunities to travel (to British Columbia, Newfoundland, and Spain to name a few), meet new people, and foster my intellectual development. Dylan also provided much-needed encouragement when, contrary to all initial plans, I left Montreal during the COVID-19 pandemic, moved in with my partner, and worked remotely during the vast majority of my PhD. While it wasn't always easy, Dylan told me to prioritize my happiness and maintain work-life balance, which ended up being crucial for the completion of my PhD in the long run. It is important to have role models in work and in life, and Dylan has been an outstanding role model for me. I will forever be grateful.

I also want to thank my committee members, Dr. Jim Grant and Dr. Pedro Peres-Neto, for their feedback and guidance during my PhD. Jim's insistence on developing a priori predictions for each chapter, as well as carefully thinking about *why* particular patterns might exist, is something that I will undoubtedly take with me as I move forward in my career. Similarly, Pedro's passion for thoughtful application and prudent interpretation of statistical models has been invaluable. Jim and Pedro also provided many helpful editing suggestions and have been generous with their time throughout my PhD, which I greatly appreciate.

The meta-analysis in Chapter 1 would not have been possible without help from BSc honors student Sarah Geargeoura, who did a fantastic job reviewing and extracting data from hundreds of papers. Similarly, the eco-genetic models in Chapter 4 would not have been possible without code, expertise, and feedback provided by Dr. Erin Dunlop at the Ontario Ministry of Natural Resources. The temperature and demographic data from Cape Race, Newfoundland that supported Chapters 2-4 would not exist without thousands of hours of grueling field work conducted by dozens of people over the years, so I am indebted to each and every one of them. I am grateful to Jacob Coon-Come, Alex Engler, Sarah Geargeoura, Mat Hillyard, Ramela Koumrouyan, and Brett Studden for their help with data collection in Newfoundland during the 2021 and 2022 field seasons. Special thanks to Dave Shepherd, Julie Cappelman, and Lucas Ward for their warm hospitality during my time in Newfoundland.

I have been privileged to overlap with many amazing colleagues in the Fraser lab. During the early stages of my PhD, Matthew Yates and Jean-Michel Matte provided feedback on my research ideas that proved to be invaluable. I have also received helpful feedback at various points from Zach Eisenhauer, Hyung-Bae Jeon, Thais Bernos, Elizabeth Lawrence, Julie Gibelli, Sozos Michaelides, Raphael Bouchard, and Jonathan Lemay, and participated in hours of awesome conversations during long car rides with Shannon Clarke, Justin Budyk, and Julien

Beaulieu. I am also thankful for the friends I made outside the Fraser lab, especially Marc-Antoine Poulin, Lo Feyten, Heather Stewart, Dave Hunt, Stanzi Vaubel, and Claire Reising.

Finishing my PhD would have been impossible without the support of my family. My parents have encouraged me to pursue my passion for biology since my earliest days in college, while also keeping me grounded and looking ahead. My siblings Francis, Dan, and Pat have all provided invaluable support, outlets for venting, and an ever-important sense of humor. Everyone in my family has taken time to remind me that, despite occasional difficulties, I am immensely privileged to do what I do - traveling widely, meeting people from around the world, getting payed to go fishing, and learning things that nobody ever knew before.

Finally, my wonderful fiancée Katie has tirelessly supported me during my PhD and accompanied me on countless vacations, hikes, brewery tours, and impromptu restaurant trips that kept me happy and sane. With all of the uncertainty and upheaval in recent years, Katie and our pets (Maggie and Kitty) have been by far my most important source of stability, comfort, affection, and joy. I love you all.

Contribution of Authors

I contributed to research design, data collection, data analysis, data interpretation, and writing of all thesis chapters. Dr. Dylan Fraser contributed to research design, data interpretation, and editing of all thesis chapters. Sarah Geargeoura contributed to data collection and data analysis for Chapter 1. Dr. Erin Dunlop contributed to research design, data analysis, data interpretation, and editing for Chapter 4. Chapters 1, 2, and 3 have been published in peer-reviewed journals, while Chapter 4 is currently in preparation (see below).

Chapter 1 has been published as:

Gallagher, B. K., Geargeoura, S., and Fraser, D. J. (2022). Effects of climate on salmonid productivity: A global meta-analysis across freshwater ecosystems. *Global Change Biology*, 28(24), 7250-7269. DOI: 10.1111/gcb.16446

Chapter 2 has been published as:

Gallagher, B. K., and D.J. Fraser, D. J. (2024). Microgeographic variation in demography and thermal regimes stabilize regional abundance of a widespread freshwater fish. *Ecological Applications*, e2936 (Online). DOI: 10.1002/eap.2936

Chapter 3 has been published as:

Gallagher, B. K., and Fraser, D. J. (2024). Stream groundwater inputs generate fine-scale variation in brook trout phenology and growth across a warming landscape. *Freshwater Biology*, 69, 127-142. DOI: 10.1111/fwb.14198

Chapter 4 is in preparation to be submitted to *Evolutionary Applications* as:

Gallagher, B. K., Dunlop, E. S., and Fraser, D. J. (in prep). Fine-scale thermal habitat variation and life history evolution shape the demography of brook trout populations under future climate change.

All authors reviewed final drafts of manuscripts or thesis chapters and approved of the contents.

Table of Contents

List of Figures

variance-covariance matrix (a, c). Loadings describing the relationship between individual populations and the common trend (see Table 1 for population codes) are also shown (b, d), with dashed horizontal lines denoting strong positive or negative loadings (after Zuur et al. 2003).

Figure 2.3: Variation in three key demographic relationships among Cape Race brook trout populations. Raw data and regression lines are shown for each population (top panels; see Table 1 for population codes), as well as estimates of fixed effects (thick black line with grey 95% confidence band) and population random effects (thin black lines) from generalized linear mixed models (bottom panels; see Table 2). The *recruit-adult relationship* (a, d) plots standardized adult abundance (age-2+ census population size) against standardized recruitment (age-1 census population size) during the previous year. The *stock-recruitment relationship* (b, e) plots the log-transformed ratio of recruits per spawner against the standardized adult abundance when recruits were born. The *density-dependent growth relationship* (c, f) plots standardized juvenile growth (age-1 individual growth rate) against standardized recruitment within each year-class.

Figure 2.4: Effects of selected stream temperature metrics on Cape Race brook trout recruitment (left panels) and juvenile growth (right panels). Raw data and regression lines are shown for each population (top panels; see Table 1 for population codes), as well as estimates of fixed effects (thick black line with grey 95% confidence band) and population random effects (thin black lines) from generalized linear mixed models (bottom panels; see Table 2). The *temperature-recruitment relationship* plots standardized recruitment against mean stream temperature during emergence in May (a, c), while the *temperature-growth relationship* plots non-standardized juvenile growth against degree days accumulated from November 1-August 31 within each year-class (b, d). Note that the GLMM for the *temperature-recruitment relationship* (c) exhibited no variation in population random effects.

Figure 2.5: Portfolio effects across Cape Race brook trout populations. Stacked time-series of abundance (census population size of all individuals age-1 and older) are shown for the seven best-monitored populations (a), with a gap in 2020 due to the the COVID-19 pandemic preventing travel to the study area. Temporal coefficients of variation in abundance (b) are shown for individual populations (dark grey bars), the average across individual populations (black dashed line), and for the total abundance summed across all populations (red bar). A lower coefficient of variation suggests greater stability in abundance throughout the study period.

Figure 2.6: Thermal regimes experienced by Cape Race brook trout populations since 2005. Stream temperatures were reconstructed from air temperature based on data from 2012-2021, then averaged during incubation (a; November-March) and the growing season (b; April-November), fitted by population-specific regression lines with 95% confidence intervals. Note that two groundwater-dominated streams, LC (sky blue) and STBC (yellow green), experienced the warmest incubation temperatures and coldest growing season temperatures.

Figure 3.1: Raw data showing relationship between daily average stream temperature and air temperature in ten Cape Race streams. Different colors are used to highlight stream temperature observations below (black points) and above 16°C (red points), with red points corresponding to periods of possible thermal stress. Note the absence of stream temperatures above 16°C in LC and STBC.

Figure 3.2: Non-linear relationships predicting daily average stream temperature from average air temperature for ten Cape Race streams. Parameter estimates (see Equation 1), sample sizes, and R^2 values for each stream are shown in Table 3.1. Streams are colored based on their maximum temperatures, with darker blue colors used for groundwater-dominated streams (STBC and LC) and dark orange or red colors used for rainfall-dominated streams (LO, UO and HM; see Results).

Figure 3.3: Performance of non-linear regression models predicting daily average stream temperature from air temperature. Kernel densities are shown for mean daily air temperatures from 2012-2021 used to estimate stream temperature via non-linear regression (a), and all daily air temperature observations used to reconstruct stream temperature in ten Cape Race streams from 1980-2021 (b). Root-mean-square error (RMSE) values were calculated for daily stream temperatures predicted directly by regression models (see Table 3.1), as well as average stream temperatures calculated over weekly and monthly time periods from 2012-2021 (c). Lower RMSE values suggest that predicted stream temperatures are closer to observed values. Streams are colored based on their maximum temperatures (see Figure 3.2).

Figure 3.4: Trends (a) and anomalies (b) extracted from reconstructed temperature time-series for ten Cape Race streams. Trends and anomalies were estimated independently during each month and year from 1980-2021 (i.e. trends were estimated with anomalies removed and vice-versa), such that the original time-series can be reproduced by summing the corresponding trend and anomaly values. Monthly estimates each year (transparent points) were fitted with a loess smoother (solid lines) to clarify broader patterns, and anomaly values in (b) were aggregated by month. Streams are colored based on their maximum temperatures (see Figure 3.2).

Figure 3.5: Temporal trends in degree-days accumulated from incubation until emergence (a; November 1st-May 1st) and from incubation until the end of summer (b; November 1st-August 31st) for ten Cape Race streams. Horizontal lines in (a) are shown at 500 and 750 degree-days to denote putative thresholds for the timing of hatch and emergence, respectively. Streams are colored based on their maximum temperatures (see Figure 3.2). Note that groundwater-dominated LC and STBC (royal blue and dark blue lines) accumulated the most degree-days before emergence (a), but accumulated the fewest by the end of the summer in recent years (b).

Figure 3.6: Temperature-dependent growth of young-of-the-year (YOY) brook trout in ten Cape Race streams from 2010-2021. Individual fork length is plotted against degree-days accumulated from the start of the incubation period on November 1st the previous year until the date individuals were captured (transparent points), then fitted with stream-specific regressions (solid lines). The putative degree-day threshold for emergence (750 degree-days; dashed vertical line) is shown for reference. Streams are colored based on their maximum temperatures (see Figure 3.2), and regression equations are reported in Table S2.

Figure 4.1: Empirical life history patterns in eight Cape Race brook trout populations. Mean age (a) and longevity (b) of spawning adults from Bernos and Fraser (2016) are plotted against mean length of spawning adults from Zastavniouk et al. (2017). Similarly, mean age of spawning adults (c) and reproductive effort estimated from von Bertalanffy growth coefficients (d) are plotted against the adult:juvenile growth ratio. Growth ratios were calculated based on predicted size at age-1 (for juveniles) and change in predicted size from age-2 to age-4 (for adults) from von Bertalanffy growth curves, similar to previous methods used by Hutchings (1993). Linear regression equations and R^2 values are shown separately in each panel for reference.

Figure 4.2: Initial growth curves and probabilistic maturation reaction norms (PMRNs) in eight Cape Race brook trout populations, based on empirical data from 2010-2022. Individual length observations are plotted against age estimated using finite mixture models (transparent points). Lester growth curves (solid lines) assuming average population-specific biomass and growing season temperature are shown separately for maturation at age-2 or age-3. Population-specific PMRN intercepts were estimated using logistic regression (dotted lines) and PMRN slopes were assumed to be zero, with a constant width of 20mm (transparent bands). Populations are colored according to their stream thermal regime, with cooler groundwater-dominated streams in blue and warmer rainfall-dominated streams in red (see Chapter 3).

Figure 4.3: Climate change scenarios experienced by eight Cape Race brook trout populations. Air temperature increased by 0°C (solid lines), 3°C (dotted lines), or 6°C (dashed lines) during the last 100 years of each simulation, which then affected stream temperatures experienced by each population during the growing season and summer. Slopes and intercepts for converting air temperature to population-specific stream temperature are shown in Table 4.1. Populations are colored according to their stream thermal regime, with cooler groundwater-dominated streams in blue and warmer rainfall-dominated streams in red (see Chapter 3).

Figure 4.4: Effects of climate change on evolving traits of Cape Race brook trout populations. Results are displayed as violin plots (polygons) that summarize changes in mean genotype values during the last 100 years from twenty independent simulations (points), organized by three traits (rows; top: PMRN intercept, middle: PMRN slope, bottom: maximum growth rate) and three climate scenarios (columns; magnitude of air temperature warming over the same 100 years). Populations are colored according to their stream thermal regime, with cooler groundwater-dominated streams in blue and warmer rainfall-dominated streams in red (see Chapter 3). No data are shown for 'No Evolution' scenarios, where all three traits were fixed through time.

Figure 4.5: Effects of climate change on abundance of Cape Race brook trout populations. Results are displayed as violin plots (polygons) that summarize the percent change in total abundance during the last 100 years from twenty independent simulations (points), organized by two evolutionary scenarios (rows; whether evolution occurred or not) and three climate scenarios (columns; magnitude of air temperature warming over the same 100 years). Declines of 100%, in which population extirpation occurs, are shown for reference (dashed lines). Populations are colored according to their stream thermal regime, with cooler groundwater-dominated streams in blue and warmer rainfall-dominated streams in red (see Chapter 3).

Figure 4.6: Effects of climate change on biomass of Cape Race brook trout populations. Results are displayed as violin plots (polygons) that summarize the percent change in total biomass during the last 100 years from twenty independent simulations (points), organized by two evolutionary scenarios (rows; whether evolution occurred or not) and three climate scenarios (columns; magnitude of air temperature warming over the same 100 years). Declines of 100%, in which population extirpation occurs, are shown for reference (dashed lines). Populations are colored according to their stream thermal regime, with cooler groundwater-dominated streams in blue and warmer rainfall-dominated streams in red (see Chapter 3).

Figure 4.7: Effects of climate change on growth curves of Cape Race brook trout populations. Results are displayed as average size-at-age across twenty independent simulations. Growth

curves are shown for simulation years 100 (high transparency), 200 (intermediate transparency), and 299 (no transparency), and for climate change scenarios corresponding to 0°C (solid lines), 3°C (dotted lines), or 6°C (dashed lines) of warming over the last 100 simulation years. Populations are colored according to their stream thermal regime, with cooler groundwater-dominated streams in blue and warmer rainfall-dominated streams in red (see Chapter 3).

Figure A1.1: Study screening summary, showing each step from the original Web of Science search to the final database after critical appraisal and filtering (see Section A1.3). Flow chart made through the ROSES online tool provided by Haddaway (2020).

Figure A1.2: Map of georeferenced observations from each dataset. Shape files were taken from from the Maps package in R (Deckmyn et al. 2021). Map lines delineate study areas and do not necessarily depict accepted national boundaries.

Figure A1.3: Plots of residuals against predicted values from the best-fit models for the Abundance-Precipitation (a), Abundance-Temperature (b), Growth-Precipitation (c), and Growth-Temperature (d) data sets. Details on model structure in each case can be found in Table 1.3.

Figure A1.4: Funnel plots showing residual values (x-axis) and standard errors (y-axis) of each observation from the best-fit models for the Abundance-Precipitation (a), Abundance-Temperature (b), Growth-Precipitation (c), and Growth-Temperature (d) data sets. Note the residual asymmetry in panel a, where publication bias is evident in observations with low standard error that are skewed towards negative residual values. Corresponding Egger test results are in Table A1.2.

Figure A1.5: Plots of residuals against publication year from the best-fit models for the Abundance-Precipitation (a), Abundance-Temperature (b), Growth-Precipitation (c), and Growth-Temperature (d) data sets. Temporal patterns are visualized with a loess smoother (blue) and its confidence interval (grey shading) in each case. Statistical tests of linear trends with publication year are in Table A1.2.

Figure A1.6: Species contrasts and 95% confidence intervals for Abundance-Precipitation (a), Abundance-Temperature (b), and Growth-Temperature (c) datasets subsetted to contain the five species with the greatest sample size in each case. Contrasts were obtained by adding species as an additional covariate to each best-fit model structure (see Methods; Table 3). Note that all confidence intervals contain zero, and that the first species listed was used for reference in each set of contrasts.

Figure A2.1: Map of the study area, with labels denoting codes for the eleven brook trout populations (red circles) studied in Cape Race, Newfoundland. The full names for each population are provided in Table 2.1.

Figure A2.2: Size distributions for eleven Cape Race brook trout populations. Distributions are displayed as smoothed kernel densities for age-1 (pink) and age-2+ individuals (blue) within each population (rows) and year (columns). Empty panels had no data available (see Section A2.1).

Figure A2.3: Recruitment time-series for eleven Cape Race brook trout populations. Recruitment was estimated as the total census population size multiplied by the proportion of

age-1 individuals derived from length distributions or age-specific counts (see Section A2.1 and Figure A2.2). 95% confidence intervals (error bars) were estimated based on recapture proportions observed across all ages.

Figure A2.4: Juvenile growth rate time-series for eleven Cape Race brook trout populations. Growth rates were estimated as the median length of age-1 individuals divided by their estimated age at the time of sampling (see Section A2.1).

Figure A3.1: Examples of groundwater- and rainfall-dominated streams harboring brook trout in Cape Race, Newfoundland, Canada (photo credits: Dylan Fraser). Panel A (facing upstream) and B (facing downstream, same position): a groundwater seep entering the upper section of Lower Coquita (LC). The seep pours out of the ground 3 m above the confluence with the stream and directly influences the flow, acidity and vegetation downstream. For example, note the tannin-colored water in the bottom right corner of panel B upstream of the groundwater seep that is devoid of aquatic vegetation – here the stream pH is ~5.0-5.3, whereas below the groundwater seep the pH is ~6.3-6.6 and aquatic vegetation is abundant. Panel C: the presence of Miner's Lettuce (*Montia fontana*) (the bright green aquatic plant) below a large groundwater seep that enters a small pond within Bob's Cove River (BC). Panel D: a groundwater-dominated stream characterized by very low current velocity and choked aquatic vegetation (Still There by Chance; STBC). Panels E and F: example of fluctuating streamflow in a rainfall-dominated stream (Upper O'Beck; UO) in the same location in July 2021 (E) and October 2022 (F).

Figure A3.2: Autocorrelation functions based on residual values from air-stream temperature relationships in ten streams in Cape Race, Newfoundland, Canada. Correlations in residuals across various daily time lags (vertical bars) and significance thresholds (blue dashed lines) are shown in each case.

Figure A3.3: Effects of daily precipitation on residual values from air-stream temperature relationships in ten streams in Cape Race, Newfoundland, Canada (panels). A linear trend is shown for each stream (red line), along with its estimated intercept and slope (text in top right corner). Note that all streams exhibit negative slopes.

Figure A3.4: Temporal trends in reconstructed mean stream temperature during the growing season (April-November) in ten streams in Cape Race, Newfoundland, Canada. Estimated intercepts and slopes are shown in the top-left of each panel (see also Table 2). Note the lower average temperatures and reduced slopes predicted in the two groundwater-dominated streams (LC and STBC).

Figure A3.5: Annual variation in reconstructed degree-day accumulation since November 1st in ten streams in Cape Race, Newfoundland, Canada from 1980-2020. Horizontal lines are shown at 500 and 750 degree-days to denote putative thresholds for the timing of hatch and emergence, respectively. The most recent years are plotted in yellow, illustrating phenological shifts (see Table 3.3). Note the earlier phenology and reduced inter-annual variation predicted in the two groundwater-dominated streams (LC and STBC).

Figure A3.6: Violin plots showing within-stream spatial variation in water temperature recorded during transect surveys in ten streams in Cape Race, Newfoundland, Canada. Transects were performed during four summers between mid-June and early-August (see Wood et al. 2014 for details), but not all streams were sampled each year and were not always sampled in the same

order or during the same time of day within years. Note that spatial variation in temperature exceeded 5°C in the majority of cases.

List of Tables

intercept and slope estimates are displayed with standard errors in parentheses. The percentage of variance (pseudo-R^2) explained by the fixed effect and population random effects is shown for each model. The selected stream temperature metric for the *temperature-recruitment* relationship was emergence temperature during May. For the *temperature-growth* relationship, it was cumulative degree-days from November-August (see Appendix 1: Table S2).

Table 2.3: Correlations between model estimates and proposed drivers of brook trout population variation across Cape Race. Correlations were not corrected for multiple comparisons, and significant relationships ($p<0.05$) are marked in bold italic text. Pearson correlations are shown for the groundwater index (GWI), mean recruitment (R), mean juvenile growth rate (G), and mean reproductive success (S), while Mantel correlations are shown for pairwise phylogenetic distance (PD). Correlations could not be calculated for the *temperature-recruitment* relationship because the GLMM exhibited no variation in population random effects (see Results).

Table 3.1: Parameter estimates, sample sizes, R^2 and root-mean-square error (RMSE, in °C) values for non-linear relationships between daily average air temperature and stream temperature for ten Cape Race streams from 2012-2021. Sample sizes for BC and HM are marked with asterisks (*) due to missing data after July 2019 in these streams. For reference, μ is the minimum stream temperature, α is the maximum stream temperature, γ is the slope at the inflection point, and β is the temperature where the inflection point occurs (see Equation 3.1). Thermal regimes are categorized as groundwater-dominated, rainfall-dominated, or intermediate (see Results).

Table 3.2: Temporal trends in reconstructed stream temperature in winter (December-February), spring (March-May), summer (June-August), autumn (September-November), and growing season (April-November) months for ten Cape Race streams from 1980-2021. Trends are expressed as slopes (in $°C \cdot year^{-1}$) from regressing mean temperature on year within each stream, and the corresponding air temperature regression slope is shown for reference (bottom). Thermal regimes are categorized as groundwater-dominated, rainfall-dominated, or intermediate (see Results).

Table 3.3: Summary statistics for dates of degree-day (DD) accumulation since November 1st for putative hatch (500 DD; left side) and emergence (750 DD; right side) thresholds in ten Cape Race streams from 1980-2021. Mean, minimum, and maximum annual dates of degree-day accumulation are shown, with temporal trends displayed as slopes (in days·year-1) from regressing annual date of accumulation on year within each stream. The 40-year change (in days) multiplies the annual slope by 40 to approximate the advancement of developmental timing (in days) over the last four decades in each stream. Thermal regimes are categorized as groundwater-dominated, rainfall-dominated, or intermediate (see Results).

Table 4.1: Population-specific parameters for individual-based eco-genetic models of eight Cape Race brook trout populations. Parameters in bold italic text are evolving traits, shown as initial mean values for genotypes drawn from a normal distribution.

Table 4.2: Shared parameters for individual-based eco-genetic models of eight Cape Race brook trout populations. Values separated by commas represent values used in three different climate change scenarios (for ΔT) and two evolution scenarios for each population (for CV).

Table 4.3: Average change in Cape Race brook trout evolving traits, demography, and phenotypes over the last 100 years of twenty independent simulations, across six scenarios.

Table A1.1: Model results for omnibus test of covariates (Wald-type test statistic with p-values based on a Chi-squared distribution), and fixed effect coefficients for best-fit models from each data set (Abundance-Precipitation (A-P), Abundance-Temperature (A-T), Growth-Precipitation (G-P), Growth-Temperature (G-T)). Covariate abbreviations used for coefficients are from Table 1.1.

Table A1.2: Summary of post-hoc tests of model assumptions, collinearity (variance inflation factors calculated across all levels of each covariate and within levels of temporal covariates), publication bias, taxonomic effects, and robustness of model results to methodological factors (see Table 1) or the inclusion of outlier studies. Results are shown separately for Abundance-Precipitation (A-P), Abundance-Temperature (A-T), Growth-Precipitation (G-P), Growth-Temperature (G-T) datasets. Asterisks (*) denote significant results, while non-significant statistical tests are marked with NS. Detailed contrasts for robustness tests are shown in Table A1.3.

Table A1.3: Detailed results of robustness tests where four methodological variables were added to the best-fit model for each data set (see Methods; variable descriptions and abbreviations in Table 1). Contrast coefficients and their p-values are shown, as well as a description of the variable levels used in each contrast. Results are shown separately for Abundance-Precipitation (A-P), Abundance-Temperature (A-T), Growth-Precipitation (G-P), Growth-Temperature (G-T) datasets. Significant contrasts and p-values are highlighted in bold italic text with an asterisk (*).

Table A2.1: Model selection results from dynamic factor analysis of recruitment (top) and juvenile growth (bottom) time-series in Cape Race brook trout. All models were run with an identity variance-covariance matrix, and only the top 15 models are shown for recruitment (55 models overall). Note that in both cases, AICc values were lowest in the model with no covariates, which significantly outperformed all models with one covariate (T=air temperature, P=precipitation), which in turn outperformed models with two covariates. The number of parameters estimated (k) increased substantially every time a covariate was added to the model.

Table A2.2: Model selection results from generalized linear mixed models (GLMMs) relating recruitment and juvenile growth to various measures of stream temperature. Average stream temperature (T) and degree-days since November 1st (DD) were estimated based on empirical air-stream temperature relationships from 2012-2021 (see Chapter 3 for details).

Table A3.1: Catchment survey data for ten streams in Cape Race, Newfoundland, Canada. Drainage area is expressed in km^2, gradient is reported as the percent change in elevation divided by stream length, depth is shown in cm, velocity is in m·s^{-1}, and relative pond area was calculated as the total perimeter of all ponds divided by stream length. Sinuosity and the width:depth ratio are unitless. Full details on survey methodology are available in Wood et al. (2014).

Table A3.2: Relationships between young-of-the-year brook trout length and degree-days accumulated from November 1st the previous year until the date of capture (see Figure 6). Intercepts, slopes, sample sizes (N), and R^2 values (treating degree-days as a fixed effect) are shown for linear regression models run separately for each stream with no random effects. The

same outputs are also shown for a generalized linear mixed model that included stream as a random effect on intercepts and slopes (bottom), where R^2 Fixed and R^2 Random correspond to the variance explained by the fixed and random effects, respectively. Intercept and slope estimates with a p-value <0.05 are marked with an asterisk (*), while those with a p-value <0.001 are marked with two asterisks (**).

Table A3.3: Correlations between stream characteristics from habitat surveys (predictors) and parameter estimates for non-linear relationships between daily average air temperature and stream temperature in ten streams in Cape Race, Newfoundland, Canada. Significant correlations without multiple comparison adjustments ($p < 0.05$) are shown in bold italic text. For reference, μ is the minimum stream temperature, α is the maximum stream temperature, γ is the slope at the inflection point, and β is the temperature where the inflection point occurs (see Equation 3.1). Note that all significant correlations became non-significant when applying Bonferroni multiple comparison adjustments ($p > 0.0016$).

I. General Introduction

Declines in species abundance contribute to extinction and biodiversity loss throughout the world, thereby altering the structure and function of ecosystems (Pimm and Raven 2000, Dirzo et al. 2014). Climate change is an important driver of biodiversity loss and, crucially, is likely to accelerate extinction rates in the future (Urban 2015). As a result, efforts to describe and predict the effects of climate change have increased dramatically in recent decades, most commonly using climate envelope models based on contemporary species distributions (reviewed by Pearson and Dawson 2003). However, species distribution models are often applied with coarse spatial resolution and may ignore or oversimplify mechanisms that are known to impact responses to climate change in many species, especially environmental heterogeneity and adaptive potential (Skelly et al. 2007, Urban et al. 2016). Moreover, while biodiversity risk assessments are often conducted at the species level, variation in phenotypes, demographics and habitat sensitivities can generate substantial diversity in responses to climate change among populations of the same species, even at very small spatial scales (Richardson et al. 2014, Nadeau et al. 2017). Indeed, many species of fish, amphibians, reptiles, mammals, and plants exhibit large ranges with many genetically and ecologically distinct populations that occupy diverse, fragmented habitats (Schindler et al. 2010, Waterhouse et al. 2017, Pearson et al. 2018, Ony et al. 2020, Rowland et al. 2022), which likely produces enormous variation in population responses to climate change. Moreover, intraspecific population variation can have substantial impacts on community and ecosystem dynamics, often equaling or exceeding the effect of interspecific variation (Des Roches et al. 2018). More detailed research and mechanistic models that describe the ecological and evolutionary effects of climate change across diverse populations will be crucial for improving predictions of climate-induced biodiversity loss (Urban et al. 2023).

Population variation at multiple spatial scales is crucial for the conservation and management of many species under climate change, as it allows the risk of local extinction to be spread among populations experiencing different environmental conditions that affect growth, survival, and evolutionary potential (Schindler and Hilborn 2015, Nadeau and Urban 2023). This is exemplified by salmonids, a family of coldwater fishes consisting of dozens of species that occupy lakes, rivers, and streams around the world (Crawford and Muir 2008, Muhlfeld et al. 2019), supporting commercial, recreational, and subsistence fisheries that are culturally and economically important to many human communities (ASF 2011, PSC 2017). The persistence of many salmonid populations and, by extension, the ecosystem services they provide, is threatened by climate change, especially intense warming and drought (Arismendi et al. 2013, Kovach et al. 2016). However, observed effects of contemporary climate change on population demography are highly variable. For example, increased temperatures have been linked to increased abundance and growth of many salmonid populations in subpolar climates across northern Europe (Jensen et al. 2000, Donadi et al. 2023), while warming is often associated with population declines in Mediterranean climates within southern Europe (Almodovar et al. 2012). Similarly, warming often reduces the abundance of salmonids in low-lying regions of North America and Asia (Nakano et al. 1996, Budy et al. 2008), while nearby populations at high altitudes commonly maintain stable abundance or even increase as the climate warms (Nakano et al. 1996, Coleman and Fausch 2007). Subtle differences in connectivity, reproductive timing, and somatic growth rates can also affect survival and modify responses to climate change among neighboring salmonid populations (Tsuboi et al. 2022, Baldock et al. 2023). Modeling studies that incorporate future climate projections routinely predict sharp declines in abundance or

complete extirpation (Bassar et al. 2016, Ayllon et al. 2019), but these studies typically focus on a single population and have only assessed a very small subset of salmonid population diversity, which may limit the generalizability of current knowledge (O'Sullivan 2021). Collectively, a better understanding of the prevalence, scale, and drivers of population diversity in salmonids can help managers and conservation organizations prioritize which populations should be targeted for protection (Schindler et al. 2010) or active interventions (e.g. White et al. 2023, Beechie et al. 2023) under current and future climate conditions.

In this thesis, I ask "*What are the mechanisms that drive variation in contemporary and future demographic responses to climate change among salmonid fish populations?*" I explore how processes that operate at large and small spatial scales combine to shape population-specific responses to inter-annual variation in temperature and precipitation. Over large scales, I argue that population responses are structured by gradients in latitude and elevation, which strongly influence macroclimatic patterns such as maximum temperature exposure, growing season length, and winter severity (Jensen et al. 2000, Isaak et al. 2015). However, aquatic habitats can exhibit substantial differences in thermal regimes at small scales due to variation in groundwater inputs, watershed geomorphology, and land use, such that habitats at the same latitude and elevation often vary in their susceptibility to climate change (Lisi et al. 2015, Ishiyama et al. 2023). Habitat variation at small scales also contributes to local adaptation in salmonid populations (Fraser et al. 2011), leading to distinct genotypes, phenotypes and demographics that influence population dynamics and responses to human impacts (Schindler et al. 2010). Therefore, I argue that measuring and accounting for local biotic and abiotic heterogeneity is also crucial for understanding how salmonid populations respond to climate change. Overall, the goal of my thesis is to use multiple methods that integrate data across spatial scales in order to support more accurate and generalizable predictions about the future of salmonids in a rapidly changing world, and ultimately inform conservation and management.

In Chapter 1, I conducted a global-scale meta-analysis to examine how observed effects of climate (temperature and precipitation) on salmonid demography (abundance and growth) from 156 studies of 23 species were related to spatial, temporal, and biological variation among populations. For spatial variation, I predicted that increased temperature and reduced precipitation would be associated with declines in salmonid growth and abundance at low latitudes and elevations, but opposite patterns would be observed at high latitudes and elevations where demography is often constrained by suboptimal temperatures. Similarly for temporal variation, I predicted that warming and drought would reduce salmonid abundance and growth during the warmest times of year (e.g. summer months), but increase it during the coldest periods. Finally, for biological variation, I predicted that native populations would respond more negatively to warming than non-native populations due to asymmetric competition, while salmonids occupying lakes would respond more favorably to warming than those in streams because lake stratification increases coldwater habitat availability. Predictions were informed by salmonid thermal limits, but were also influenced by prevailing narratives in the salmonid biology literature, which had never been quantitatively tested across many studies (see Kovach et al. 2016). I interpreted results as *very* broad patterns that were useful but insufficient for population-specific predictions, and highlighted the importance of continued monitoring to understand heterogeneity in salmonid responses to climate change across space and time.

In Chapters 2-4, I focused on local-scale variation in responses to climate change among wild populations of brook trout (*Salvelinus fontinalis*) in Cape Race (Newfoundland, Canada). Cape

Race brook trout are an excellent model system because multiple populations have been studied extensively since the 1980s and are separated by <5 km, thereby experiencing similar climate conditions (Hutchings 1993). Populations are also genetically and phenotypically distinct despite sharing a common ancestor, and are virtually untouched by human activities with the exception of climate change (Wood et al. 2015, Zastavniouk et al. 2017). Specifically in Chapter 2, I analyzed mark-recapture data from eleven brook trout populations in Cape Race from 2010-2022 in order to quantify asynchrony in abundance, somatic growth rates, and demographic relationships among populations. I predicted that Cape Race brook trout would exhibit substantial demographic asynchrony tied to differences in habitat characteristics, life history, and genetics among populations known from previous studies, which would ultimately stabilize species abundance across the study area and buffer against climate change. I interpreted results in light of the pristine nature of Cape Race, which may not be typical for most salmonid populations and can thus offer unique insights into natural (rather than anthropogenic) processes.

In Chapter 3, I collected and analyzed stream temperature data from 2012-2021 to describe thermal regimes experienced by ten Cape Race brook trout populations, then explored how temperature variation influenced phenology, growth and exposure to warming among populations. Based on over a decade of on-the-ground research and consultations with local naturalists, I predicted that neighboring streams would exhibit substantial differences in water temperature due to variation in groundwater inputs, which in turn would strongly influence rates of warming and phenological shifts experienced by each population. Seasonal variation in temperature plays a key role in determining rates of development, growth, and survival of brook trout and other salmonids (Beacham and Murray 1990, Curry et al. 1995), so fine-scale differences in groundwater inputs can potentially diversify population responses to current and future climate change. I interpreted results with respect to variation in watershed geomorphology and the unusual subpolar oceanic microclimate of Cape Race, which may reduce brook trout vulnerability to warming within the study area.

Finally, in Chapter 4, I combined my findings from Chapters 2 and 3 with previous results from common garden experiments and transplant studies in Cape Race brook trout in order to build eco-genetic models (Dunlop et al. 2009) that simulated the effects of climate warming from 2001-2100 on demography and life history evolution in eight populations. I predicted that population abundance will decline and individuals will evolve faster somatic growth rates as rates of atmospheric warming increase, while the effects of warming on population biomass will be more complex, depending on the relative magnitude of climate-induced changes in abundance (which will reduce biomass) and growth (which will increase biomass). Additionally, I predict that evolution will reduce the demographic impacts of climate change, while populations will differ in their responses based upon initial life history patterns and stream thermal regimes, with the latter having the strongest influence on model outcomes (Snyder et al. 2015). I interpreted results based upon past mechanistic modeling work that seeks to understand the role of habitat variation and evolution in fish population responses to climate change (e.g. Reed et al. 2011, Bassar et al. 2016, Ayllón et al. 2019), and speculate how results in Cape Race can inform future research on this topic.

II. Chapter 1: *Effects of climate on salmonid productivity: a global meta-analysis across freshwater ecosystems*

Abstract:

Salmonids are of immense socio-economic importance in much of the world, but are threatened by climate change. This has generated a substantial literature documenting effects of climate variation on salmonid productivity in freshwater ecosystems, but there has been no global quantitative synthesis across studies. I conducted a systematic review and meta-analysis to gain insight into key factors shaping the effects of climate on salmonid productivity, ultimately collecting 1,321 correlations from 156 studies, representing 23 species across 24 countries. Fisher's Z was used as the standardized effect size, and a series of weighted mixed-effects models were compared to identify covariates that best explained variation in effects. Patterns in climate effects were complex, and were driven by spatial (latitude, elevation), temporal (time-period, age-class), and biological (range, habitat type, anadromy) variation within and among study populations. These trends were often consistent with predictions based on salmonid thermal tolerances. Namely, warming and decreased precipitation tended to reduce productivity when high temperatures challenged upper thermal limits, while opposite patterns were common when cold temperatures limited productivity. Overall, variable climate impacts on salmonids suggest that future declines in some locations may be counterbalanced by gains in others. In particular, I suggest that future warming should (1) increase salmonid productivity at high latitudes and elevations (especially >60° and >1,500m), (2) reduce productivity in populations experiencing hotter and dryer growing season conditions, (3) favor non-native over native salmonids, and (4) impact lentic populations less negatively than lotic ones. These patterns should help conservation and management organizations identify populations most vulnerable to climate change, which can then be prioritized for protective measures. My framework enables broad inferences about future productivity that can inform decision making under climate change for salmonids and other taxa, but more widespread, standardized, and hypothesis-driven research is needed to expand current knowledge.

1.1 Introduction:

Climate change is strongly impacting biodiversity throughout the world (Parmesan and Yohe 2003, Woodward et al. 2015). These effects are likely to intensify in the future (Urban 2015), but estimates of effect size can vary considerably depending on the design, location, and focal organism of different studies (Koricheva et al. 2013, Haddaway 2015). Understanding how and why climate change affects biodiversity in natural systems is critically important for improving predictions of biodiversity loss (Urban et al. 2016, Mouquet et al. 2015), as well as for developing adaptive conservation and management strategies (Reside et al. 2018). Although the ecological consequences of climate change can be affected by evolutionary history, spatial scale, and other factors (Nadeau et al. 2017a, 2017b), data synthesis approaches offer a way to disentangle these confounding influences to gain a more integrated understanding across multiple studies. Indeed, data synthesis plays a prominent role in explaining patterns and changes in biodiversity more broadly, and while conclusions can still be disputed (e.g. Dornelas et al. 2014, Vellend et al. 2013, but see Gonzalez et al. 2016), this process can help identify key knowledge gaps that motivate further study.

A growing body of research has focused on synthesizing effects of climate change on fishes (Kovach et al. 2016, Myers et al. 2017, Comte and Olden 2017, Krabenhoft et al. 2020, Comte et

al. 2021), which are culturally and economically important to communities around the world. Salmonids in particular support valuable commercial, recreational, and subsistence fisheries in many regions (ASF 2011, PSC 2017) and are thought to be sensitive to climate change, driving fears of future declines in productivity (defined herein as the rate of population biomass production, which I assume to increase with higher abundance, individual growth, or both). However, there is considerable uncertainty in how different species and populations will respond to future warming, while the factors shaping vulnerability to climate change are thought to be complex and difficult to disentangle (Kovach et al. 2019, Irvine and Fukuwaka 2011). As a result, previous syntheses have not explicitly quantified spatial, temporal, and biological variation in salmonid responses to climate across many empirical studies. My research attempts to fill this knowledge gap by synthesizing effects of climate variables (temperature and precipitation) on a wide range of salmonid populations, providing timely insight into the broad patterns influencing current and future productivity.

Spatial variation likely plays a dominant role in structuring salmonid responses to climate. Salmonids occupy an enormous native and non-native range across the globe (Crawford and Muir 2008), and often exhibit strong gradients in productivity based on latitude and elevation. Previous research suggests that populations at low latitudes (Ayllón et al. 2019, Carlson and Satterthwaite 2011) are expected to respond to climate change differently than those at high latitudes (Pitman et al. 2020, Campana et al. 2020), with similar contrast expected between low-altitude and high-altitude populations (Kanno et al. 2015, Isaak et al. 2016). Specifically, declines in salmonid productivity are expected in areas where temperatures regularly exceed upper thermal limits, and should decline further if low precipitation reduces the volume and thermal buffering capacity of water (Kovach et al. 2016). Therefore, in the warmest areas at low latitudes and elevations, higher temperature is expected to reduce salmonid productivity and increased precipitation should enhance productivity, whereas opposite patterns are expected at high latitudes and elevations (Figure 1.1a,b). Despite the importance of spatial variation in moderating responses to climate, no quantitative research to date has tested these predicted effects at a global scale across salmonid species.

Responses to climate in salmonids also likely depend on the time-period under consideration, as most salmonids occupy temperate regions where temperature and precipitation vary seasonally and may disproportionately affect some life-stages more than others (Jonsson and Jonsson 2009, Nislow and Armstrong 2012, Bassar et al. 2016). Moreover, since salmonid productivity can also be limited by cold temperatures, warming can be beneficial for most of the year but harmful during summer months (Armstrong et al. 2021). Despite a large volume of research on these topics, the vulnerability of specific life-stages to increasing temperatures is still debated (Dahlke et al. 2020; but see Pottier et al. 2022), and the severity of the threat posed by warming temperatures to species persistence remains unresolved (Muñoz et al. 2015; but see Mantua et al. 2015). Similarly, while some research shows that climate impacts can vary based on the size- or age-class being affected (Letcher et al. 2002, 2015), these can differ among systems within studies (e.g. Xu et al. 2010a). Nonetheless, increased temperatures and reduced precipitation should be associated with declines in productivity during the warmest time-periods, with opposite effects expected during the coldest periods, especially for temperature (Figure 1.1c,d). More complex influences of temporal variation should also be considered, as negative impacts of flooding could be observed during vulnerable life-stages such as egg incubation, and timing of key events across the life cycle can vary considerably within and among species (Kovach et al.

2016, 2019). Data synthesis can test these predictions, thereby informing debates and uncertainties about the factors shaping salmonid vulnerability to climate change.

Finally, biological differences among populations have the potential to modify the effects of climate on salmonid productivity (Figure 1.1e,f), but these too await quantification across many studies. For example, effects may differ based on whether salmonids occupy lotic (streams and rivers) or lentic environments (lakes and ponds) due to the prevalence of stratification in lakes, which is expected to increase the availablility of coldwater habitat (Blair et al. 2013) and reduce sensitivity to warming in lentic populations. Additionally, some research has suggested that non-native salmonids may respond more favorably to warming than their native counterparts by exhibiting higher thermal tolerance or outcompeting them for suitable habitats (Al-Chokhachy et al. 2016, Bell et al. 2021), leading me to expect more severe climate-induced declines in productivity within native species. Also, because my work focuses on salmonids in freshwater environments, migration behaviors may play a role, as anadromous populations could respond less strongly to climate variation than freshwater residents due to their shorter periods of residence and exposure to ocean conditions (Mueter et al. 2002). Specifically, warming and drought are expected to reduce productivity more severely in freshwater resident populations than anadromous ones. Finally, observed climate impacts could be influenced by methodological differences, as studies can vary widely in sampling design, the exact salmonid or climate data measured, and how data were transformed and analyzed. Taken together with the spatial and temporal variation discussed previously, it is clear that broad patterns should be detectable in salmonid responses to temperature and precipitation. A simplified overview of a priori predictions for the influence of spatial (latitude, elevation), temporal (age-class, time-period), and biological (range portion, habitat type, anadromy) factors is shown in Figure 1. Rigorously testing these predicted patterns will help clarify key drivers underlying variation in climate impacts, thereby addressing an important knowledge gap in salmonid biology (Kovach et al. 2016, 2019).

I conducted a global systematic literature search and quantitative meta-analysis to illuminate key patterns in the effects of climate variables on salmonid productivity. This research is timely because it can leverage a vast body of past research to inform the future of salmonids in a changing world – a topic that remains rife with uncertainty and disagreement (Muñoz et al. 2015, Mantua et al. 2015, Kovach et al. 2016, Dahlke et al. 2020, Pottier et al. 2022). My objectives were to (1) conduct a systematic review to build a database of standardized effect sizes describing the influence of climate variation on salmonid productivity, (2) identify a parsimonious set of covariates that best explain variation in effect sizes and test predicted spatial, temporal, and biological patterns, and (3) assess publication bias and potential taxonomic, methodological, and geographic influences that may limit current knowledge. This is the first study to carry out these objectives at a global scale for salmonids, providing the most in-depth analysis to date of climate impacts on these iconic coldwater taxa. My structured and hypothesis-driven approach allowed me to identify broad patterns in salmonid-climate relationships, which can then support inferences about future productivity. Such patterns can inform conservation and management decisions by helping agencies identify populations that are likely to be most vulnerable to climate change. More broadly, I believe this approach can be adapted to a host of other taxa to predict and test key drivers of variation in responses to climate change.

1.2 - Methods:

1.2.1 - Literature search and screening criteria:

Throughout this study, I used PRISMA-EcoEvo criteria to guide decision making and reporting (O'Dea et al. 2021). I sought to identify studies reporting correlations between climate variables (temperature or precipitation) and the individual growth or relative abundance (growth or abundance hereafter) of wild salmonid populations in freshwater environments. To increase consistency and maximize focus on natural contexts, I targeted observational studies of populations that did not receive hatchery supplementation during the study period. Correlations were preferred because they are the simplest measure of standardized relationships between continuous variables, and can easily be used to calculate effect size and its sampling variance (see below). While this decision may have reduced data availability, it is paramount to standardize effect sizes for rigorous quantitative analysis (Koricheva et al. 2013). Measures of relative abundance (e.g. density, population size, biomass, survival) and individual growth (e.g. length-at-age, somatic growth rate) were interpreted as surrogates for productivity, but past research has shown that rates of salmonid biomass production are often more sensitive to abundance than growth (Lobón-Cerviá 2009). Similarly, all surrogates of temperature and precipitation were treated equally, although a previous review argued that direct measures of aquatic habitat conditions (e.g. water temperature, streamflow) are preferable to indirect proxies (e.g. air temperature, rainfall; see Kovach et al. 2016). It would have been ideal to quantify differences between the many proxies used to describe climate and salmonid productivity, but this was impractical because relationships between these proxies and the processes of interest varied, and were often unknown or unreported.

A comprehensive literature search was conducted during the first week of July 2020 through the Web of Science advanced search portal, including all available collections since 1900. Search terms were adapted from Kovach et al. (2016), but expanded to include more salmonid taxa, yielding 2,989 studies. The specific search string was:

TS=(trout OR char(r) OR salmon* OR whitefish* OR grayling*) AND TS=(streamflow OR stream temperature OR lake temperature) AND TS=(abundance OR survival OR growth)*

where TS denotes a set of search topics, AND/OR are Boolean operators, and asterisks enable truncated word searches (e.g. salmon* identifies salmon, salmonid, salmoninae, etc.). Web of Science was the only literature search method used and may not be exhaustive, but I chose to avoid other methods (e.g. alternative search engines, compiling studies from past reviews) in order to maximize consistency and save time.

Titles and abstracts were screened for relevance based on whether relationships between salmonid data and climate variables were mentioned, or if it seemed plausible that relevant raw data could be reported. Title and abstract screening was first conducted by co-author Sarah Geargeoura (BSc honors student, Concordia University) and followed up in full by me for verification. All studies deemed relevant by one or both authors were collated, yielding 700 studies for subsequent screening. Google Scholar was used to retrieve full-texts, which were available for 603 relevant studies. Each study was subsequently scanned to determine whether the study design was suitable (review papers and modeling studies without empirical data were excluded), and whether correlations (with sample sizes) or raw data were reported. Overall, 182 studies satisfied these criteria and were subjected to data extraction. If not directly reported by

authors, correlations and sample sizes were calculated in a spreadsheet from raw data extracted manually from tables, or from figures with the *Digitize* package in R (Poisot 2011). Non-linear relationships were ignored unless they were shown in figures, in which case the data were extracted and used to calculate linear correlation coefficients. This practice was uncommon (ten observations from six studies), and did not strongly impact effects (correlation between linear and non-linear R^2 values=0.94). In total, this process yielded 1,735 observations. I was satisfied with this outcome, and therefore decided not to allocate more time towards increasing the number of observations or studies (e.g. contacting authors for missing data).

1.2.2 - Database description:

In addition to correlations and sample sizes, a wide range of other data were collected in the initial database, including relevant spatial, temporal, biological, and methodological covariates. Study coordinates and elevation data directly reported by authors were preferred, but georeferencing was conducted in Google Maps and elevations were inferred using the *Elevatr* R package (Hollister et al. 2021) when necessary. A detailed account of the methods used and data recorded in this process can be found in Appendix 1 (see section A1.1), while details about covariates, their usage, and categorical levels are in Table 1.1. Once the initial database was completed, it was subjected to critical appraisal to ensure the validity and comparability of observations (Haddaway 2015), while filtering out duplicates and observations with insufficient sample size ($n<5$; section A1.2). After six critical appraisal and filtering steps, the final database contained 1,321 correlations from 156 studies, featuring 23 species within six genera, and spanning 24 countries across five continents. Overall, my database (see Gallagher et al. 2022) had considerably greater sample size, taxonomic breadth, and geographic contrast than a previous systematic review by Kovach et al. (2016). A summary of the study filtering process is provided in Figure A1.1 (after Haddaway 2020), while the final database and a full bibliography of the included studies can be found in Gallagher et al. (2022). Note that repeated measures within studies were often present (range: 1-102 correlations per study), and this non-independence was accounted for during data analysis.

1.2.3 - Statistical analysis:

The filtered database was imported into R, and analyzed using the *Metafor* package (Viechtbauer 2010). The *escalc()* function was used to calculate Fisher's Z based on the formula:

$$Z = \frac{1}{2}\ln\left(\frac{(1+r)}{(1-r)}\right) \qquad (Eq.\,1.1)$$

where *ln* is the natural logarithm and *r* is the correlation coefficient. This transformation alleviates problems with correlations becoming skewed as they approach ±1, while retaining the magnitude and direction of effects. The asymptotic variance (V_Z) for each Fisher's Z estimate was calculated by:

$$V_Z = \frac{1}{(n-3)} \qquad (Eq.\,1.2)$$

where *n* is the sample size. In all subsequent analyses, Fisher's Z was used as the standardized effect size, while the inverse of the variance was used to weight observations (Koricheva et al. 2013).

The database was then divided into four datasets based on the type of response and predictor variables used within each correlation: Abundance-Precipitation (n=362), Abundance-Temperature (n=610), Growth-Precipitation (n=66), and Growth-Temperature (n=283). Abundance and growth were both assumed to be positively related to population productivity. Each dataset was analyzed separately using the *rma.mv()* function, which allows for linear mixed-effects models to be built with a nested random effect structure (Viechtbauer 2010). Across all models in this analysis, response variables from each correlation (which were assigned unique within-study codes) were nested within study to create a consistent random effect structure. When appropriate, variances were partititioned among studies, within studies, and due to sampling variance, which were used to calculate indices of heterogeneity and test their statistical significance (Nakagawa et al. 2017, Senior et al. 2016). Variance components also influenced weights for each effect size by downweighing repeated measures within and among studies according to the variance observed at each level, thereby alleviating pseudoreplication. An explicit demonstration of this random effect structure and its handling of repeated measures can be obtained through R code that I have made publicly available (see Gallagher et al. 2022).

1.2.4 - Model selection:

Due to the large number of potential covariates in my data, I sought to test competing models in a stepwise forward selection framework that reflected the structure of my data and was guided by mechanistic hypotheses (see Figure 1.1). Model selection was conducted separately for each dataset, but I ensured the same framework was applied consistently to all datasets. All covariates were incorporated as fixed effects, with models fit using maximum likelihood and compared based on AICc values. The model with the lowest AICc was selected in each stage, although the most parsimonious model was preferred in cases where AICc values differed by less than two (Johnson and Omland 2004). Note that taxonomic variation was not explicitly considered during model selection due to unbalanced sample sizes and concerns that estimating species-specific coefficients would yield over-parameterized models, so this was addressed in subsequent analyses (section 1.2.6).

The first stage of model selection sought to identify the best set of spatial covariates (latitude, elevation, and their interaction; Table 1.1) because these effects are of considerable biological interest, and were expected to be relatively strong and consistent across datasets. In all analyses, latitude was expressed as an absolute value for simplicity, but 98% of observations were from the northern hemisphere (Figure A1.2). There was limited spatial contrast in the Growth-Precipitation dataset due to low sample size, so the interaction between latitude and elevation was not explored.

The selected model from the first stage was then used as the base model for the second stage, where temporal covariates based on age-class (four levels), season (five levels), life-stage (seven levels), or life-stage*age (ten levels; see Table 1.1 and section A1.1 for details) were added individually and compared. Note that most levels of life-stage*age were identical to life-stage, but estimates from the growing season were broken up by age-class (Table 1.1). These factors were of interest because they could suggest differential vulnerabilities to climate change based on size, age, or specific events in the life cycle. However, the relative importance of each temporal covariate may vary across datasets, especially since model selection penalized more complex covariates. There were few observations during the growing season in the Growth-Precipitation dataset (n=35) such that age differences were unlikely to be informative, so I chose

to omit life-stage*age from model selection. For all other temporal covariates and datasets, there was sufficient contrast (n>10 within two or more levels) to proceed with model selection, but I noted all cases where sample sizes did not meet this threshold for specific levels (see Results).

Finally, the selected model from the second stage moved forward to the third stage, wherein four binary covariates (two levels) denoting biological (range portion, habitat type, anadromy) and methodological differences (study design; see Table 1.1 and section A1.1) were added in all possible combinations. These factors were expected to have less consistent effects across datasets, but could nonetheless help explain variation. Covariates were excluded from model selection if they lacked contrast within a given dataset (n<10 for one of two levels), which ruled out habitat type in Abundance-Precipitation and Growth-Precipitation, and range portion in the Growth-Precipitation and Growth-Temperature datasets. The selected model from the third stage was considered the best-fit model overall for each dataset.

1.2.5 - Best-fit models:

After identifying best-fit models, I summarized model performance using ΔAICc scores, likelihood ratio tests, and pseudo-R^2 values (based on proportional reduction in variance components) relative to alternative models with no covariates. Mean effect sizes and their 95% confidence intervals were estimated from each best-fit model, while variance components were used to run omnibus tests for residual heterogeneity (Viechtbauer 2010) and calculate total heterogeneity within and among studies (Nakagawa et al. 2017). Finally, estimated coefficients for all covariates (or contrasts for categorical levels) were reported and used to make summary plots, while an omnibus test across all covariates was performed for each best-fit model (Viechtbauer 2010).

1.2.6 - Publication bias and model robustness:

Homogeneity of variance was evaluated by inspecting residual plots from all best-fit models. Collinearity was checked in each best-fit model using variance inflation factors (VIF) calculated across all levels of each covariate, while within-level VIF values were also reported for temporal covariates that had more than two levels. All best-fit models were assessed for publication bias by creating funnel plots in *Metafor*. Currently, Egger regression cannot be implemented in models with nested random effects, so instead I added the standard error as an additional covariate in each best-fit model to test for the effect of precision on residuals (Viechtbauer 2010). This test (Egger test hereafter) is analogous to an Egger regression, such that a significant effect of the standard error indicates publication bias. If bias was detected, I identified individual studies that contributed to the pattern, removed them from the dataset, and re-tested for publication bias in the reduced data. Similarly, temporal publication bias was explored by relating residuals from each best-fit model to publication year (Gurevitch et al. 2018).

Possible taxonomic biases were examined by subsetting the Abundance-Precipitation, Abundance-Temperature, and Growth-Temperature datasets to only include the five species with the largest sample size (Growth-Precipitation was excluded due to low sample size), then re-running the best-fit model with and without species as an additional covariate. The decision to select five species was subjective, but I sought to estimate multiple species effects while retaining sufficient sample sizes within species. Species contrast terms were reported and analyzed for significance in each dataset, while 95% confidence intervals for all other coefficients were compared. Support for species-specific intercepts and slopes was assessed

using ΔAICc scores relative to the original best-fit model. Additionally, the effects of four methodological factors (response type, predictor type, data transformation, data extraction method; Table 1) were evaluated by adding them individually to all best-fit models and testing their significance. Finally, influential studies were identified in each dataset using Cook's distance, and their impact was assessed by comparing 95% confidence intervals of all coefficients from models fitted to data with and without these studies.

1.3 - Results:

1.3.1 - Model selection:

Table 1.2 describes all models run and their ΔAICc scores within each stage of model selection, suggesting that each dataset had a different set of covariates that best explained variation. Abundance-Precipitation effect sizes differed according to season and study design, while Abundance-Temperature effects were influenced by latitude, elevation, age-class, study design, and range portion (Tables 2 and 3). Growth-Precipitation effect sizes varied according to life-stage and anadromy, while Growth-Temperature effects had the most complex model that included latitude, elevation, life-stage*age, and habitat type as covariates (Tables 1.2 and 1.3). Across all datasets, best-fit models substantially outperformed models with no covariates (ΔAICc>15; likelihood ratio test $p<0.001$), but the proportional reduction in variance components suggested that relatively little variation was explained (pseudo-R^2=5-41%; Table 3). Mean effect sizes based on predicted values from the best-fit models were positive and significant for the Growth-Precipitation and Growth-Temperature datasets, while 95% confidence intervals contained zero in the Abundance-Precipitation and Abundance-Temperature datasets (Table 3). Residual heterogeneity within and among studies was significant (Wald-type test; $p<0.006$) and accounted for a large percentage of the total variance (40-74%; Table 3) observed in all best-fit models.

1.3.2 - Best-fit models:

In all datasets, omnibus tests showed that covariates had significant explanatory power (Wald-type test $p<0.002$; Table A1.1). Coefficients from the best Abundance-Precipitation model confirmed a significant positive effect of fall precipitation on abundance highlighted in a previous review (Kovach et al. 2016), but this was only evident in temporal studies, which were associated with significantly more positive (or less negative) effect sizes than spatial studies ($p<0.05$; Table A1.1; Figure 1.2). In contrast, a significant negative effect of spring precipitation on abundance was apparent ($p<0.01$; Table A1.1), but only for spatial studies (Figure 1.2).

The best Abundance-Temperature model showed that latitude and elevation had a significant positive influence on effect sizes ($p<0.01$; Table A1.1), such that effects of temperature on abundance were predicted to be negative at low latitudes and elevations, but positive at higher values (latitude>60°; elevation>1,500m; Figure 1.3a-b). Temperature effects did not vary significantly by age-class ($p>0.05$; Table A1.1) but were significantly more positive in temporal study designs ($p<0.05$) and non-native ranges ($p<0.01$; Figure 1.3c).

Within the best Growth-Precipitation model, precipitation had significant positive effects during the growing season ($p<0.001$) and negative effects during incubation ($p<0.01$; Table A1.1). However, the latter was based on a very low sample size (n=2; Figure 1.4), and this model should be interpreted with caution due to the low number of observations in the dataset (n=66

total). Effect sizes varied for precipitation during other life-stages, but precipitation effects were significantly more negative in anadromous populations relative to those observed in freshwater residents ($p<0.05$; Figure 1.4).

Finally, estimates from the best Growth-Temperature model suggested that temperature effects became more positive with increasing latitude and elevation (Figure 1.5a-b). This was only significant for elevation ($p<0.05$; Table A1.1), while temperature effects were also significantly more negative in lotic than lentic habitats ($p<0.05$; Figure 1.5c). Similarly, effect sizes varied across levels of life-stage*age, with significant differences observed during incubation (positive effect; $p<0.05$), overwintering, and the growing season (negative effects; $p<0.05$; Figure 1.5c). Negative effects during the growing season were weaker in age-0 compared to age-1 or age-2+ salmonids (Figure 1.5c), but these differences were not significant ($p>0.05$). Estimates for incubation (n=8) and overwintering (n=12) were likely impacted by low sample sizes.

1.3.3 - Publication bias and model robustness:

Visual inspections of residuals suggested that assumptions of residual homogeneity were satisfied for all best-fit models (Figure A1.3; Table A1.2). Variance inflation factors suggested that collinearity among covariates in each best-fit model was limited (VIF<5; Table A1.2). However, there was evidence of collinearity within the 'multiple' (VIF=6.12) and 'winter' (VIF=6.43) levels of the season covariate in the best-fit Abundance-Precipitation model, but not within other seasons or any of the other datasets (Table A1.2). Funnel plots and Egger tests revealed evidence of publication bias in the Abundance-Precipitation dataset only ($p<0.05$; Table A1.2). This bias appeared to be mostly caused by observations with high precision having residual values that were skewed negative (Figure A1.4). Further investigation identified eleven studies that contributed disproportionately to this bias, which were skewed towards two study areas and correlations based on precipitation data averaged over nine months or more (i.e. season='multiple'). Removing these eleven studies caused publication bias to become non-significant (Egger test $p=0.064$) and reduced collinearity (VIF=2.70 and 1.87 for 'winter' and 'multiple', respectively), while estimated coefficients had overlapping confidence intervals (details in section A1.3). Significant negative relationships between residuals and publication year were detected in the Abundance-Precipitation and Growth-Temperature datasets ($p<0.05$; Table A1.2). However, these patterns were largely driven by positive residuals from very few studies published before 1981, suggesting these trends could be an artifact of the skewed distribution of publication years.

Analysis of the three datasets subsetted by species indicated that results from best-fit models were robust to taxonomic differences. Specifically, whenever species contrasts were added, they were not significantly different than zero, with wide and overlapping confidence intervals (Figure A1.6). Confidence intervals for all coefficients broadly overlapped in models with and without species contrasts, while models with species contrasts were always outperformed by best-fit models without them (ΔAICc>3.5). Interactions between species and intercepts or slopes were also explored for effects of latitude and elevation in the Abundance-Temperature and Growth-Temperature datasets, but these models performed poorly compared to the original best-fit models (ΔAICc range: 8.0-21.5).

Robustness tests suggested that methodological choices often had significant impacts on effect sizes. The best-fit model for the Abundance-Precipitation dataset was robust to all four methodological factors tested ($p>0.05$), but the other datasets showed significant effects of one

or more variables ($p<0.05$; Table A1.2). Adding data transformation and extraction method (Table 1.1) to the best-fit Abundance-Temperature model suggested that correlations based on transformed abundance data (99% of which were log-transformations) and data extracted from figures or tables were associated with more positive effect sizes ($p<0.05$; Table A1.3). Similarly, adding response type to both Growth-Precipitation and Growth-Temperature models suggested that correlations based on weight were significantly different ($p<0.01$) than those based on length or growth rate (Table A1.3). Predictor type also affected the best-fit Growth-Temperature model, such that correlations based on minimum temperature were associated with significantly more negative effect sizes than for average temperature, with no significant differences for other predictor types (Table A1.3). Finally, Cook's distance identified influential studies in each dataset (n=3-6), but removing these studies and re-running each best-fit model yielded similar coefficients with substantial overlap in 95% confidence intervals (Table A1.2).

1.4 - Discussion

I assembled and analyzed the most extensive global database of climate effects on salmonid productivity to date, uncovering substantial variation. This variation exhibited broad spatial, temporal, and biological patterns that often, but not always, aligned with predictions based on salmonid thermal limits (see Figure 1.1). Specifically, spatial variation in latitude and elevation shaped temperature effects on productivity but, interestingly, did not influence precipitation effects. Generally, increased temperature tended to reduce productivity at low latitudes and elevations where warm and stressful thermal regimes predominate, but increase productivity at high latitudes and elevations where cold temperatures limit salmonid growth and abundance. Similarly, temporal variation structured responses to climate during the warmest time-periods, when higher temperature and lower precipitation were both associated with reduced productivity. In addition, there was some evidence that increased flooding during egg incubation or the spring could further diminish productivity, but these patterns were inconsistent and sometimes impacted by low sample size. Finally, biological differences were also important, as abundance of non-native populations and salmonid growth in lentic habitats responded more positively (or less negatively) to higher temperatures, relative to native populations and lotic habitats.

Collectively, these patterns imply that future warming should be expected to (1) enhance productivity at polar latitudes (>60°) and high altitudes (>1,500m), (2) threaten salmonids in areas where precipitation is declining during the warmest months (3) affect native populations more negatively than non-natives, and (4) increase the importance of lentic habitats as climate refugia. These findings can help conservation and management bodies identify and protect salmonid populations that are especially sensitive to climate change, as well as guide future research. However, I also identified key limitations in current knowledge of salmonid responses to climate, as the majority of variation remains unexplained, while geographic bias, methodological inconsistencies, and unbalanced sample sizes likely restricted scope of inference.

1.4.1 - Spatial patterns:

The effects of temperature on salmonid abundance and, to a lesser extent, growth were related to latitude, as warming negatively impacted productivity at low latitudes but had positive effects in polar regions, which is in line with previous research. For example, studies of European brown trout (*Salmo trutta*) suggested that higher temperatures and longer growing seasons should increase productivity in high-latitude populations that are currently constrained by cold temperatures (Jensen et al. 2000, Parra et al. 2009), while Mediterranean populations face

extirpation due to thermal stress as climate change continues (Almodóvar et al. 2012, Ayllón et al. 2019). My results suggest that this pattern may be similar across other salmonids, although most species are not well-represented in my database across their range. Generally, this latitudinal trend supports predictions that salmonids should become more productive within their native range in the Arctic under climate change (especially >60°N), while declines in productivity will be more frequent in low-latitude regions (Reist et al. 2006, Jonsson and Jonsson 2009, Campana et al. 2020). However, the Arctic currently has the highest rates of warming on earth and this trend is expected to continue, so many high-latitude areas could be a boon for salmonids over the next few decades but may become less suitable later this century. Moreover, constraints within polar ecosystems could limit increases in salmonid productivity, as primary and secondary production must rise substantially to sustain higher salmonid biomass in the future (Reist et al. 2006), and high-latitude populations can still be negatively impacted by prolonged heat waves and droughts (von Biela et al. 2022).

Similar to latitude, there was a strong trend in temperature effects due to elevation, such that warmer temperatures were linked to declines in growth and abundance at low elevations, but with increases at high elevations. This pattern supports the notion that high-altitude streams provide a 'coldwater climate shield' for salmonids and will serve as important climate refugia in a warming world (Nakano et al. 1996, Almodóvar et al. 2012, Isaak et al. 2015, Kanno et al. 2015). Mountain streams typically exhibit slower climate velocities that help buffer against warming (Isaak et al. 2016), while previous research on cutthroat trout (*Oncorhynchus clarkii*) in the Rocky Mountains showed that productivity at high elevations is limited by cold summer temperatures (Harig and Fausch 2002, Young et al. 2005, Coleman and Fausch 2007). Thus, there is considerable scope for warming to increase productivity in high-altitude populations (especially >1,500m), and I expect the distribution of productivity to shift towards higher elevations in the future. However, this will be offset by reduced productivity and more frequent extirpation in low-lying areas (Nakano et al. 1996, Almodóvar et al. 2012). Moreover, there is likely to be considerable variation in the rate of elevation shifts at the local level, especially as warming interacts with changes in snowpack and non-native species (Wenger et al. 2011).

The broad spatial patterns in salmonid-temperature relationships I uncovered were in line with my predictions (Figure 1.1a), and suggest that populations occupying low-elevation habitats near low-latitude range margins are most likely to decline with warming. These vulnerable populations can be targets for conservation interventions or restoration by agencies, especially if they harbor unique diversity that might aid persistence (Carlson and Satterthwaite 2011). Similarly, if vulnerable populations support fisheries, managers may need to consider reducing future harvests to remain sustainable under climate change. Changes in precipitation could possibly offset some of these impacts, but model selection did not indicate strong spatial variation in precipitation effects. This is likely because temperature varies more predictably with latitude and altitude than precipitation, which is more influenced by rainshadows, prevailing winds, and proximity to large water bodies (Fick and Hijmans 2017).

1.4.2 - Temporal patterns:

Effects of climate on growth and abundance varied considerably based on the time-period studied, revealing critical periods when climate variation tends to have particularly strong impacts on salmonids. Most notably, warmer temperatures and decreased precipitation during the warmest times of year were both associated with reduced productivity, while increased

precipitation during other time-periods (e.g. spring, egg incubation) was also linked to declines in productivity. These patterns largely matched expectations (especially during the growing season; Figure 1.1c,d) and corroborated previous qualitative reviews that emphasized temporal variation in climate impacts, as well as its utility for improving inferences (Nislow and Armstrong 2012, Kovach et al. 2016). Indeed, multiple studies of brook trout (*Salvelinus fontinalis*) in eastern North America found that temperature and precipitation have the largest impacts during specific seasons or life-stages (Kanno et al. 2015, Bassar et al. 2016, Sweka and Wagner 2022). In contrast, model selection in both temperature datasets supported the inclusion of age (age-class in Abundance-Temperature, life-stage*age in Growth-Temperature), but differences between age-classes varied in direction and were not statistically significant. Thus, the magnitude and direction of future climate change during critical time-periods in the life cycle will be a key determinant of salmonid persistence, while differences among age-classes should be less influential. Continued research on these critical periods should help build upon current knowledge of how temporal climate variation shapes habitat quality (Armstrong et al. 2021), and how this can produce different responses within and among species (Kanno et al. 2015, Bassar et al. 2016, Kanno et al. 2017).

The temporal patterns I found in salmonid responses to climate suggest that declines in productivity should be most frequent in areas where growing season conditions are becoming hotter and dryer, as proposed in previous studies (Arismendi et al. 2013). This type of climate change is especially prominent in western North America (Carlson and Satterthwaite 2011) and Mediterranean Europe (Ayllón et al. 2019), which will create future management and conservation challenges in these regions. However, future responses will likely be complex, as temporal patterns were not always consistent among datasets (e.g. summer precipitation did not show expected positive effects in the Abundance-Precipitation dataset), and their significance sometimes depended on other biological and methodological factors. Additionally, some strong effects were based on low sample sizes (e.g. reproduction and incubation in Figure 1.4, incubation and overwintering in Figure 1.5), and should thus be viewed as preliminary. The paucity of data during migration, reproduction, incubation, and emergence means I cannot resolve uncertainties about the vulnerability of these life-stages to climate change (e.g. Jonsson and Jonsson 2009, Dahlke et al. 2020, Pottier et al. 2022). Finally, I believe inferring the impacts of temporal covariates on salmonid productivity is especially hampered by the use of ambiguous time-periods. Specifically, climate data were frequently averaged over 9-12 month periods (e.g. season=’multiple’), which contributed to publication bias and collinearity issues in the Abundance-Precipitation dataset (see section A1.3 for details). More broadly, this practice obscures inferences about temporal variation in climate effects (section A1.4) and should thus be avoided, as also suggested by Kovach et al. (2016). Instead, assessments of climate impacts should consistently focus on well-defined periods linked to the life cycle of the focal population.

1.4.3 - Biological patterns:

Biological factors such as range portion, habitat type, and anadromy also strongly modified salmonid responses to climate variation. The most striking patterns were the significant differences in temperature effects between native and non-native species, and between lotic and lentic habitats, which both have implications for management and conservation. Specifically, the abundance of non-native salmonids responded more positively to warming on average, relative to native populations. This supports the perception that climate change may allow non-native salmonids to further outcompete or replace their native counterparts in some areas (Budy et al.

2008, Al-Chokhachy et al. 2016), a key warning sign given that many management agencies seek to limit or remove non-natives from critical habitats when feasible (Kanno et al. 2016, Kovach et al. 2017). However, such decisions should still be tailored to species- and population-specific data whenever possible, as Bell et al. (2021) showed that competition with non-native salmonids can significantly threaten some native species, but not others. Additionally, the Growth-Temperature model suggested that warming temperatures during the growing season reduced productivity in lotic habitats, but these effects were negligible in lentic habitats. This pattern could be due to lentic environments, especially large lakes, becoming stratified with warming and providing deepwater thermal refugia that can benefit salmonid growth (Blair et al. 2013). While the role of lentic habitats as potential climate refugia for salmonids has not been extensively studied, protecting or restoring large stratified lakes may be a worthwhile management and conservation option, especially in areas where lakes are known to be more resistant to warming than other habitats (Reist et al. 2006). Migration behaviors also influenced effects in the Growth-Precipitation dataset, such that increased precipitation during the growing season improved growth in non-anadromous salmonids more than anadromous populations. Causes of this pattern are uncertain given the low sample size in this dataset, but could perhaps be due to shorter freshwater residency in anadromous salmonids, which reduces exposure to the warmest time-periods when increased precipitation should be most beneficial. It is also notable that methodological differences in study design, data collection, and transformation influenced patterns in effect size (Figures 1.2 and 1.3c; Table A1.1 and A1.3), which underscores the need to improve standardization across studies.

1.4.4 - Limitations and future work:

Although my quantitative synthesis now provides the most comprehensive global analysis of salmonid responses to climate change, current knowledge is incomplete and significant uncertainty remains. First, my database does not represent the whole salmonid range, with 85% of observations coming from Canada, the United States, British Isles, and Nordic countries, similar to geographic biases highlighted in critiques of past biodiversity syntheses (e.g. Gonzalez et al. 2016). This bias clearly underrepresents non-English speakers and limits scope of inference, such that applications of my findings beyond these regions must be done with care. In future studies, English language bias could be partially remedied by using scientific genus names instead of common names as Web of Science search terms (e.g. “Salmo, Oncorhynchus, and Salvelinus” instead of “salmon, trout, and charr”). This was an oversight in my meta-analysis, even though it likely had a small effect on the studies that were ultimately included. Moreover, although covariates were significant overall, the variance explained was low for effects on abundance (pseudo-R^2=5-10%) and modest for effects on growth (30-41%). This is an important limitation since abundance often has the strongest impact on productivity (Lobón-Cerviá 2009), and much of the unexplained variation (40-75%) was attributed to heterogeneity within and among studies. Such variation is typical in ecological meta-analyses (Senior et al. 2016), and suggests that the broad patterns in productivity I uncovered have limited predictive power at the local level, and that population-specific monitoring data remain critical for conservation and management planning. The variation I observed also likely reflects the remarkable population diversity of salmonids, which managers should seek to maintain in order to promote stability and resilience in a changing world (Schindler et al. 2010).

Our analysis was also impacted by the need to use correlations to derive standardized effect sizes, as these simplified relationships cannot account for factors such as density-dependence

(Matte et al. 2020a), food availability (Railsback 2022), and species interactions (Wenger et al. 2011). Furthermore, I analyzed growth and abundance separately even though these are often coupled (Lobón-Cerviá 2022, Zabel and Achord 2004), and can exhibit complex and variable relationships to actual rates of biomass production (Lobón-Cerviá 2009). Similarly, interactive (Arismendi et al. 2013) or non-linear (Rosenfeld 2017, Lobón-Cerviá and Mortensen 2005) climate effects are not adequately captured with correlations, while the linearity of salmonid-climate relationships are likely influenced by choices in study design and data transformation. Further research that standardizes productivity and climate data while accounting for key ecological processes (e.g. density-dependence; Matte et al. 2020a) would provide more precise and informative effects of climate on salmonids.

Despite some issues with publication bias, collinearity, and unbalanced sample sizes, best-fit models appeared to satisfy assumptions, and were robust to influential studies and taxonomic differences. Although species did not differ significantly in my analyses, divergence in evolutionary histories, habitat preferences, and thermal tolerances within and among species will invariably shape future responses to climate change (McKenzie et al. 2021, Jonsson and Jonsson 2009). My data are probably ill-suited to taxonomic comparisons due to skewed species composition (47% of observations were brown trout or brook trout), so more targeted studies of variation in climate responses within and among species should be a priority for future research. Overall, the patterns my meta-analysis uncovered are not definitive, and more research is needed to mitigate its geographic, taxonomic, and methodological limitations. To this end, I have shared my database (see Gallagher et al. 2022) and encourage others to use it, add more studies, or explore other covariates (e.g. WorldClim data; Fick and Hijmans 2017). Finally, while I recognize that ecological data are complex and often best analyzed with sophisticated models (e.g. Letcher et al. 2015), I urge researchers around the world to report simple correlations (with sample sizes) between salmonid and climate data believed to be most relevant for their own study systems. Together, broader data sharing and more targeted, hypothesis-driven inquiry should further improve predictions of the future of salmonids under climate change.

1.5 - Conclusion:

Patterns revealed by my meta-analysis suggest that native salmonids occupying lotic habitats at low latitudes and elevations are likely to be most vulnerable to future warming, especially in areas where drought will become more frequent during the hottest time-periods. Conversely, increased temperatures will likely enhance productivity at high latitudes and elevations. In combination, these trends can serve as a point of comparison for future studies, and may play an important role in salmonid range shifts over the coming decades (Comte and Olden 2017). More generally, my framework to predict and test patterns in effects of climate variation on growth and abundance enabled us to translate simple correlations from past research into broad inferences about future productivity, underscoring the value of data synthesis to informing conservation and management decisions (Haddaway 2015). While imperfect, my structured quantitative approach - centered around simple questions of where, when, and what kind of effects are measured - should be useful for explaining patterns in responses to climate in other organisms. Overall, future impacts of climate change will be complex but are unlikely to be entirely negative, and local responses will exhibit substantial variation around the broad patterns highlighted in this study. Such varied responses to climate change in salmonids imply that, while some populations will inevitably decline, this will be offset by expansion and increased productivity in others (Mantua et al. 2015). For biodiversity at large, this balance between gains and losses in species

productivity through time is critically important for the future of life in an increasingly human-dominated world (Dornelas et al. 2014, 2019). My synthesis suggests that this uncertain balance also applies to salmonids, with far-reaching implications for these coldwater fishes, and the ecosystems and people that depend on them.

Tables & Figures:

Table 1.1: List of all potential covariates, plus their abbreviations (abbrev.), usage during quantitative meta-analysis (model selection stage 1-3, or post-selection tests; see Methods), and number of levels (categorical variables only). Note that variables used in stages 1, 2, and 3 of model selection correspond to spatial, temporal, and biological or methodological covariates, respectively, and were tested in a stepwise forward selection framework. Details for data collection protocols can be found in the Supplementary Material (section A1.1), while the full database, metadata, and R code are freely accessible online (see Gallagher et al. 2022).

Covariate	Abbrev.	Usage	N Levels	Description or levels
Latitude	L	Stage 1	Cont.	*Absolute value of latitude* (° from equator)
Elevation	E	Stage 1	Cont.	*Elevation* (meters above sea level)
Age-class	AC	Stage 2	4	*Age-0*, *age-1*, *age-2+*, *or multiple*
Season	SE	Stage 2	5	*Fall, spring, summer, winter, or multiple*
Life-stage	LS	Stage 2	7	*Incubation, emergence, growing season, overwintering, migration, reproduction, or multiple*
Life-stage*Age	LSA	Stage 2	10	Same as Life-stage, but growing season is broken up by age into *growing season_0, growing season_1, growing season_2+*, and *growing season_multiple* levels
Study design	S	Stage 3	2	*Spatial or temporal*
Anadromy	A	Stage 3	2	*Anadromous or resident*
Range portion	N	Stage 3	2	*Native or non-native*
Habitat type	H	Stage 3	2	*Lotic or lentic*
Publication year	YR	Publication bias	Cont.	*Year* when study was published
Response type	RT	Robustness tests	7	*Abundance, population growth, stock-recruitment, survival* (abundance only), *length, weight, or growth rate* (growth only)
Predictor type	PT	Robustness tests	6	*Average, maximum, minimum, percentile, PCA* (temperature or precipitation), or *degree-day* (temperature only)
Data transformation	DT	Robustness tests	2	*Yes* or *no*
Extraction method	DM	Robustness tests	2	*Direct reporting* or *manual extraction*

Table 1.2: Full list of unique model numbers and corresponding equations within three stages of stepwise model selection. ΔAICc scores are shown for each model in the Abundance-Precipitation (labeled A-P; 16 models tested overall), Abundance-Temperature (A-T; 24 models), Growth-Precipitation (G-P; 10 models), and Growth-Temperature (G-T; 16 models) datasets. Abbreviations used in model equations are taken from Table 1, with Z denoting the standardized effect size and r denoting the nested random effect structure (see Methods). Some models were ignored (denoted by '-') due to limited contrast in covariates within some datasets (see Methods). The selected models in stages 1 and 2 are denoted by an asterisk (*). All models within 2 ΔAICc units of the selected model are highlighted in bold italic text, and the model with the fewest fixed effects was selected in these cases. The best model overall for each dataset is denoted by three asterisks (***).

Stage	Number	Model Equation	A-P (n=362)	A-T (n=610)	G-P (n=66)	G-T (n=283)
1	1	Z = r	***0.00****	9.97	***0.00****	3.26
1	2	Z = L + r	2.03	8.24	2.10	3.66
1	3	Z = E + r	***0.59***	8.70	***1.51***	2.16
1	4	Z = L + E + r	2.33	***1.02****	3.72	***0.00****
1	5	Z = L * E + r	***1.52***	***0.00***	-	2.08
2	-	Stage 1 (selected)	11.44	2.33	20.03	13.91
2	6	Stage 1 + LS	10.77	10.93	***0.00****	2.70
2	7	Stage 1 + AC	7.77	***0.00****	23.41	9.57
2	8	Stage 1 + SE	***0.00****	7.87	13.13	16.26
2	9	Stage 1 + LSA	14.45	16.59	-	***0.00****
3	-	Stage 2 (selected)	4.19	10.96	2.05	2.44
3	10	Stage 2 + S	***0.00*****	7.57	2.33	3.48
3	11	Stage 2 + A	4.82	10.25	***0.26*****	4.67
3	12	Stage 2 + N	6.01	2.82	-	-
3	13	Stage 2 + H	-	13.02	-	***0.16*****
3	14	Stage 2 + S + A	***0.06***	7.17	***0.00***	5.72
3	15	Stage 2 + S + N	***1.61***	***0.00*****	-	-
3	16	Stage 2 + S + H	-	9.43	-	***0.00***
3	17	Stage 2 + A + N	6.02	3.04	-	-
3	18	Stage 2 + A + H	-	11.87	-	2.40
3	19	Stage 2 + N + H	-	4.67	-	-
3	20	Stage 2 + S + A + N	***0.62***	***0.45***	-	-
3	21	Stage 2 + S + A + H	-	8.13	-	2.24
3	22	Stage 2 + S + N + H	-	***1.35***	-	-
3	23	Stage 2 + A + N + H	-	4.12	-	-
3	24	Stage 2 + S + A + N + H	-	***0.68***	-	-

Table 1.3: Summary of best-fit models for the Abundance-Precipitation (labeled A-P), Abundance-Temperature (A-T), Growth-Precipitation (G-P), and Growth-Temperature (G-T) datasets according to stepwise model selection. Abbreviations used in model equations are taken from Table 1.1. Each ΔAICc (with p-values for likelihood ratio tests) and pseudo-R^2 value was calculated relative to models with no covariates (Number=1 in Table 1.2; see Methods). Heterogeneity tests are based on a Wald-type test statistic, while the total heterogeneity (summed within and among studies) was calculated based on variance components. Significant p-values are marked with an asterisk (*).

Dataset	Best-Fit Model Equation	ΔAICc	Pseudo-R^2	Mean Effect	Wald Test	Total % Heterogeneity
A-P	Z = SE + S + r	15.63 (p<0.001)*	0.05	0.06 (p>0.05)	589 (p<0.001)*	59.3
A-T	Z = L + E + AC + S + N + r	22.24 (p<0.001)*	0.10	-0.07 (p>0.05)	1563 (p<0.001)*	70.1
G-P	Z = LS + A + r	21.82 (p<0.001)*	0.41	0.23 (p<0.05)*	91 (p=0.005)*	40.2
G-T	Z = L + E + LSA + H + r	19.44 (p<0.001)*	0.30	0.26 (p<0.05)*	874 (p<0.001)*	73.8

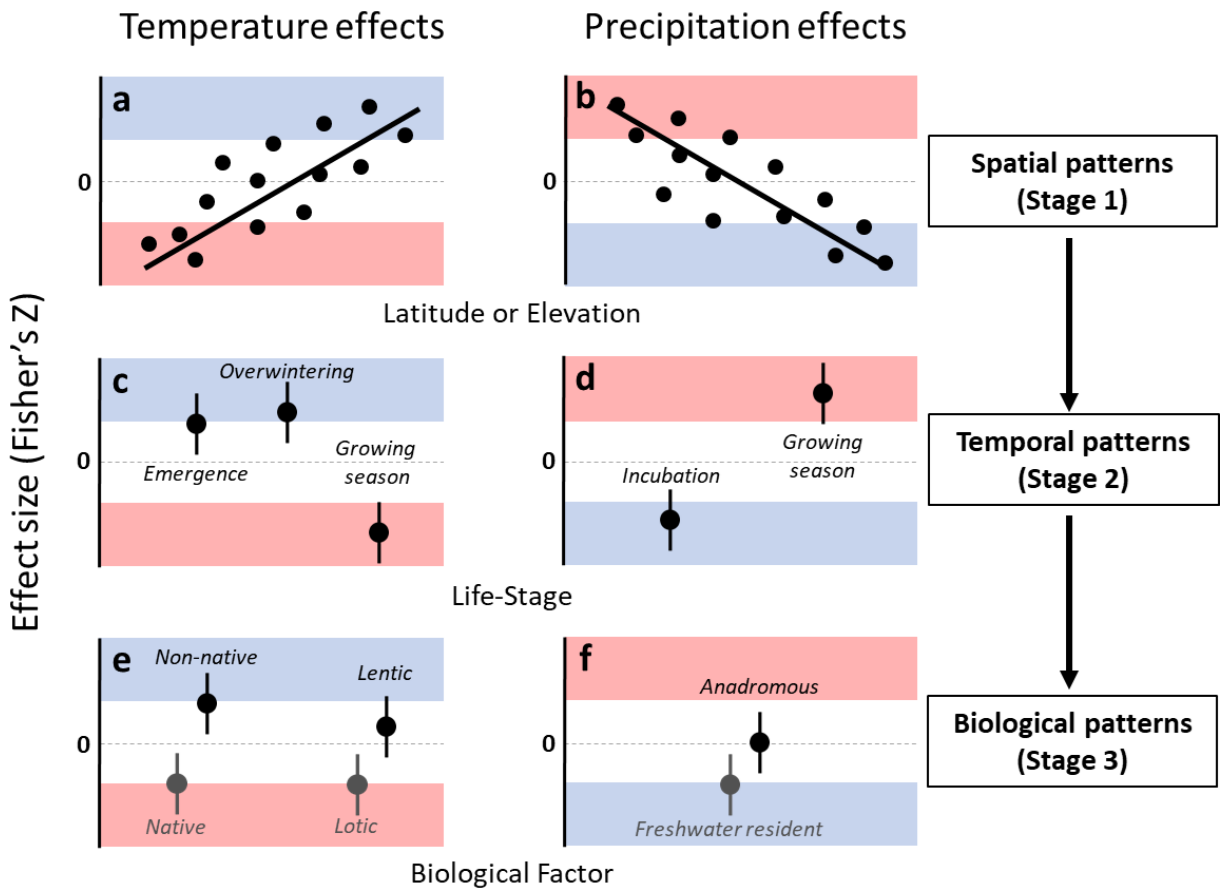

Figure 1.1: Summary of predicted patterns in effects of temperature (panels a, c, and e) and precipitation (panels b, d, and f) on salmonid productivity. Predictions are structured according to spatial (a and b), temporal (c and d), and biological (e and f) patterns that were of most interest, and stages 1-3 (boxes and arrows) correspond to the order variables were inputted into models during the stepwise model selection process (see Methods). All panels have a shaded background to highlight expected climate effects when temperatures exceed upper thermal limits (red shading), or when low temperatures limit productivity (blue shading; see Introduction). Note that predicted effects on productivity were expected to be largely similar for measures of abundance and growth.

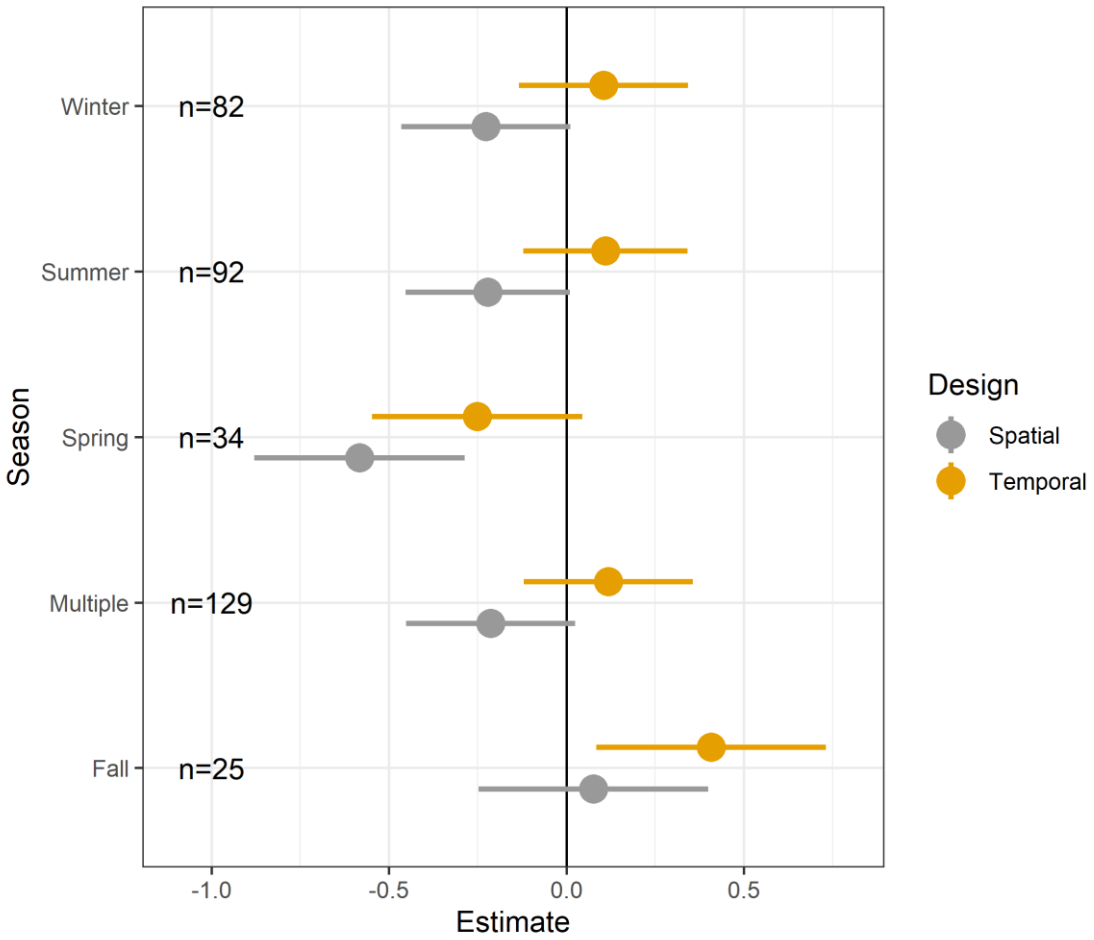

Figure 1.2: Best-fit model for the Abundance-Precipitation dataset, showing categorical coefficients and 95% confidence intervals plotted by season for spatial (silver) or temporal (gold) study designs (see Table A1.1). Total sample sizes for each level of season are shown for reference.

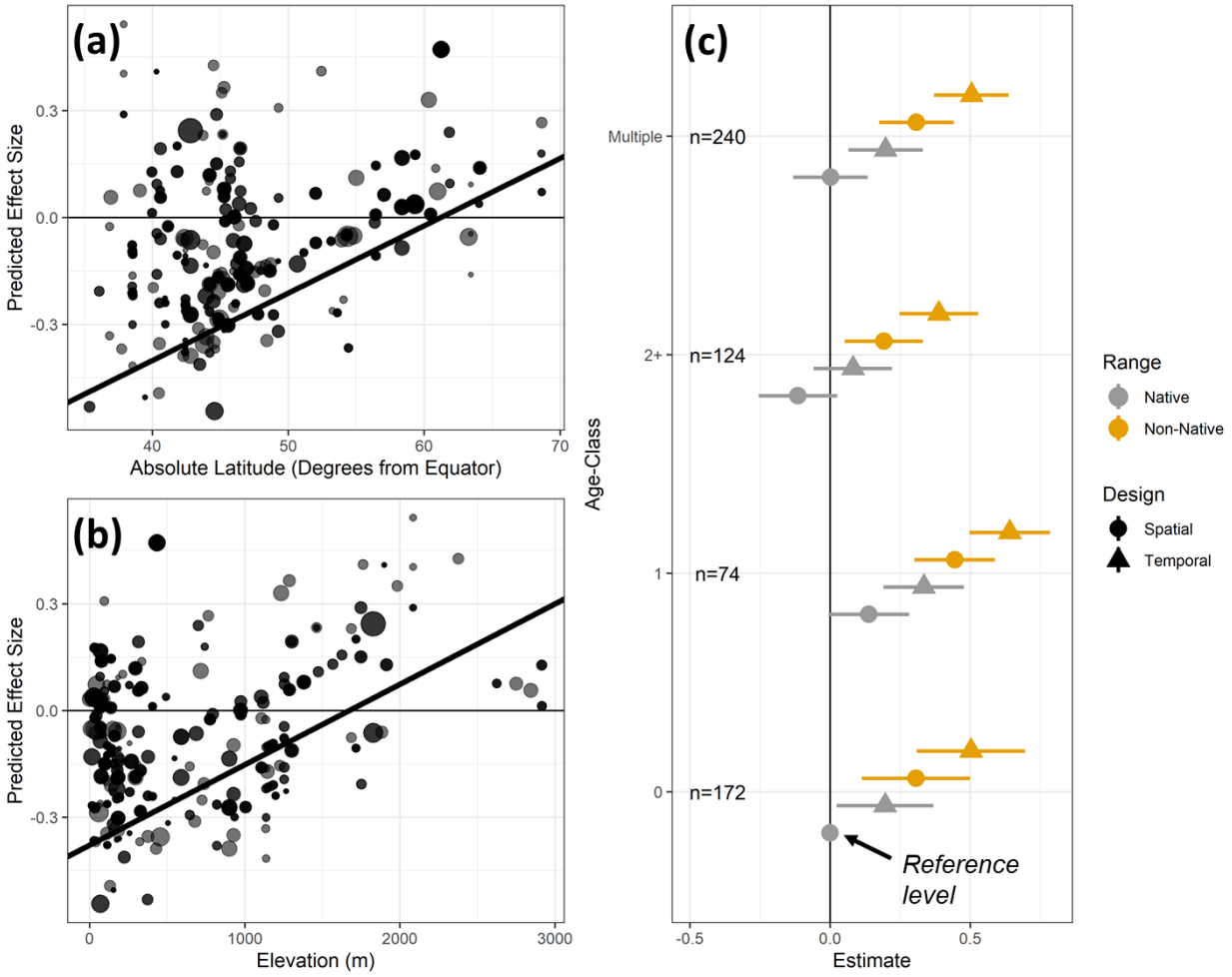

Figure 1.3: Best-fit model for the Abundance-Temperature dataset. Predicted values are plotted by latitude (a) and elevation (b), with fitted slope and intercepts corresponding to a reference level (c; arrow). Intercepts in a and b were adjusted to reflect the mean elevation and latitude, respectively, while points were sized according to the inverse of their sampling variance (see Methods). Categorical coefficients and 95% confidence intervals (c) are plotted by age-class for native (silver) or non-native (gold) range portions, and spatial (circles) or temporal (triangles) study designs. Coefficients in c were estimated as contrasts relative to a reference level (bottom; see text) while controlling for latitude and elevation (see Table A1.1). Total sample sizes for each level of age-class are shown in panel c for reference.

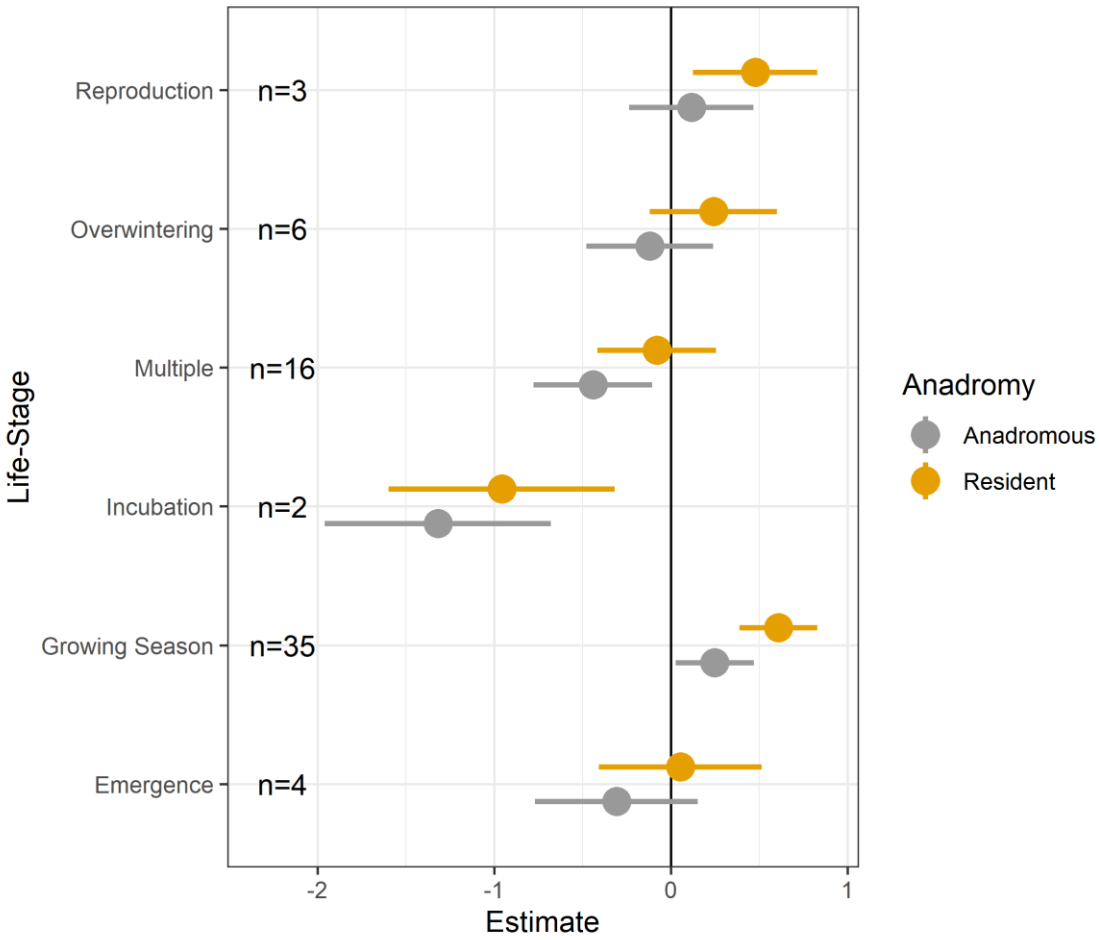

Figure 1.4: Best-fit model for the Growth-Precipitation dataset, showing categorical coefficients and 95% confidence intervals plotted by life-stage for anadromous (silver) or freshwater resident (gold) populations (see Table A1.1). Total sample sizes for each level of life-stage are shown for reference.

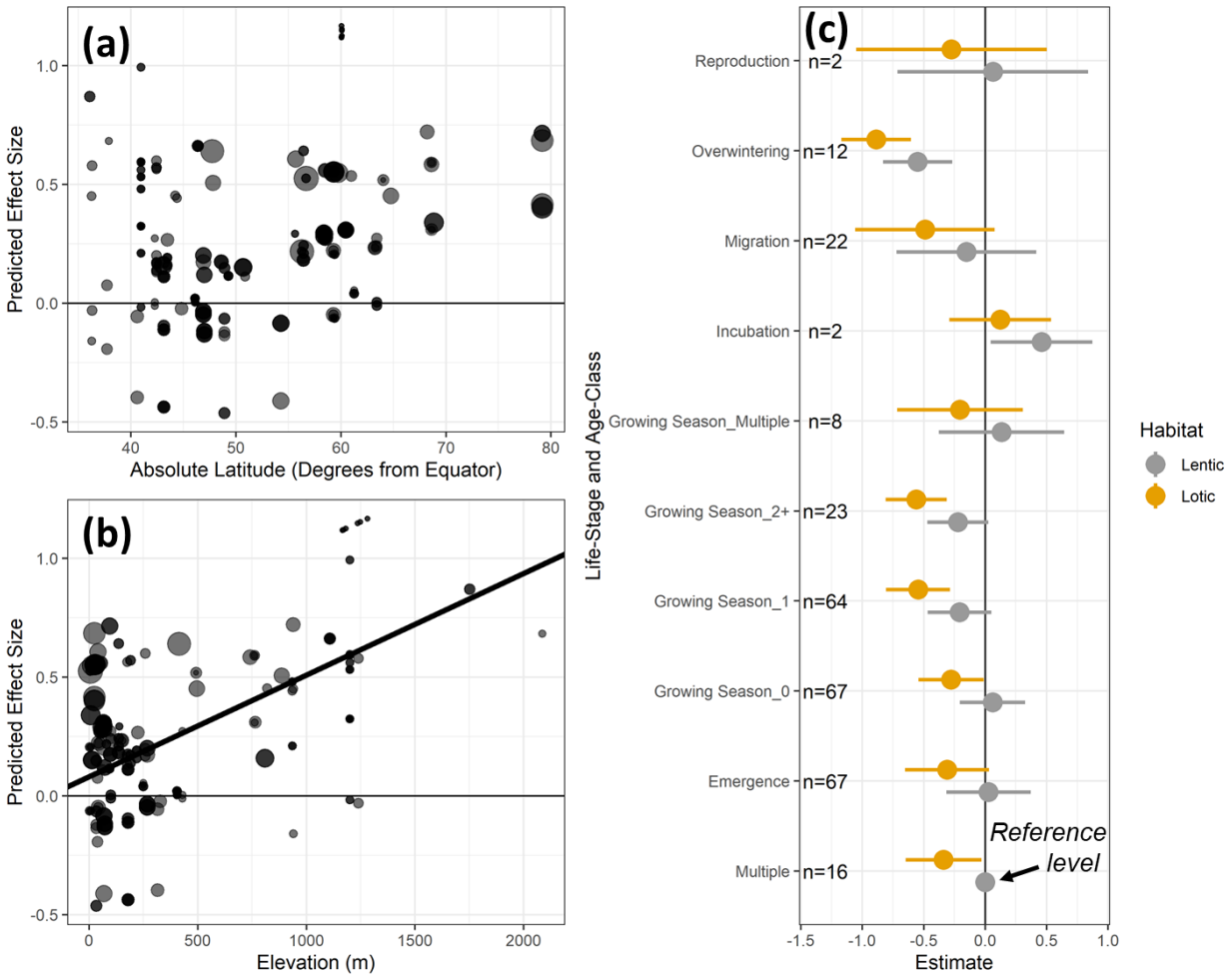

Figure 1.5: Best-fit model for the Growth-Temperature dataset. Predicted values are plotted by latitude (a) and elevation (b), with fitted slope and intercept corresponding to a reference level (c; arrow). The relationship with latitude in panel a was not signficant, so the fitted line is not shown. Points in panels a and b are sized according to the inverse of their sampling variance (see Methods). Categorical coefficients and 95% confidence intervals (c) are plotted by life-stage*age for lentic (silver) or lotic (gold) habitat types (see Table A1.1). Coefficients in c were estimated as contrasts relative to a reference level (bottom; see text) while controlling for latitude and elevation. Total sample sizes for each level of life-stage*age are shown in panel c for reference.

III. Chapter 2: *Microgeographic variation in demography and thermal regimes stabilize regional abundance of a widespread freshwater fish*

Abstract:

Predicting the persistence of species under climate change is an increasingly important objective in ecological research and management. However, biotic and abiotic heterogeneity can drive asynchrony in population responses at small spatial scales, complicating species-level assessments. For widely distributed species consisting of many fragmented populations, such as brook trout (*Salvelinus fontinalis*), understanding drivers of asynchrony in population dynamics can improve predictions of range-wide climate impacts. I analyzed demographic time-series from mark-recapture surveys of eleven natural brook trout populations in eastern Canada over 13 years to examine the extent, drivers, and consequences of fine-scale population variation. The focal populations were genetically differentiated, occupied a small area (~25 km^2) with few human impacts, and experienced similar climate conditions. Recruitment was highly asynchronous, weakly related to climate variables and showed population-specific relationships with other demographic processes, generating diverse population dynamics. In contrast, individual growth was mostly synchronized among populations and driven by a shared positive relationship with stream temperature. Outputs from population-specific models were unrelated to four of five hypothesized drivers (recruitment, growth, reproductive success, phylogenetic distance), but variation in groundwater inputs strongly influenced stream temperature regimes and stock-recruitment relationships. Finally, population asynchrony generated a portfolio effect that stabilized regional species abundance. My results demonstrate that population demographic and habitat diversity at microgeographic scales can play a significant role in moderating species responses to climate change. Moreover, I suggest that the absence of human activities within study streams preserved natural habitat variation and contributed to asynchrony in brook trout abundance, while the small study area eased monitoring and increased the likelihood of detecting asynchrony. Therefore, anthropogenic habitat degradation, landscape context, and spatial scale must be considered when developing management strategies to monitor and maintain populations that are diverse, stable, and resilient to climate change.

2.1 Introduction:

Population dynamics are often expected to be synchronized at small scales due to the prevalence of spatial autocorrelation in dispersal, environmental conditions, and trophic interactions such as predation (Liebhold et al. 2004). Within species, demographic synchrony among populations has been observed in numerous taxa at scales ranging from centimeters to thousands of kilometers (Liebhold et al. 2004), with shared responses to environmental variation among populations often cited as a key driver (i.e., 'Moran effects' after Moran 1953). In addition, dispersal often facilitates gene flow that increases the similarity of geographically proximate populations, as described in isolation-by-distance models that are ubiquitous in population genetics (Wright 1943). The ecological and genetic similarity driven by gene flow can further synchronize population dynamics, especially in mobile, large-bodied species occupying habitats with limited barriers to dispersal (Jenkins et al. 2010, Carvajal-Quintero 2022).

Despite its prevalence and utility as a conceptual baseline, synchrony can break down due to biotic and abiotic heterogeneity, even at small spatial scales. For example, fine-scale population dynamics in pond-breeding amphibians are expected to be synchronized due to connectivity and environmental similarity, but a recent study of wood frogs within a small area (32 km^2) found

that asynchrony dominated due to local variation in pond size and density-dependence (Rowland et al. 2022). Furthermore, habitat heterogeneity can drive local adaptation that reduces synchrony, even within continuous habitats expected to be open to dispersal and gene flow. For example, many fish species within postglacial lakes exhibit strong morphological, behavioral, and genetic divergence linked to the use of benthic and limnetic habitats (Skúlason et al. 1989, Schluter and McPhail 1992, Doenz et al. 2018). This microgeographic variation within species (after Richardson et al. 2014) is increasingly recognized as a key factor in ecological and evolutionary processes, with effects extending to community and ecosystem dynamics (Bolnick et al. 2011, Des Roches et al. 2018). However, the relative importance of asynchrony driven by microgeographic variation and synchrony driven by spatial autocorrelation is poorly understood in most systems, and more studies are needed that sample many populations (Liebhold et al. 2004).

Asynchrony may be most widespread in species occupying highly fragmented habitats, which often limit dispersal and increase population divergence at microgeographic scales. This pattern has also been observed across numerous taxa and contexts, such as plants within forest fragments (Ony et al. 2020), reptiles on rocky outcrops (Pearson et al. 2018), amphibians in isolated desert springs (Wang 2009), and mammals living on mountainsides (Waterhouse et al. 2017). At evolutionary time-scales, historical differences in habitat fragmentation can determine how colonization, genetic drift, and local adaptation influence diversification among species and populations (Yoder et al. 2010), which can in turn impact contemporary demography (Johansson et al. 2007, Kuhn et al. 2022). Variation arising through these mechanisms can drive asynchrony in population abundance through time, resulting in portfolio effects that stabilize aggregate abundance at larger scales (Bolnick et al. 2011, Schindler et al. 2015). In species that are sensitive to warming, portfolio effects driven by asynchrony can thus increase the likelihood of persistence under climate change (Rowland et al. 2022), while synchronized responses often result in widespread declines (Manderson 2008, Carlson and Satterthwaite 2011). Comparative studies across many naturally fragmented populations can help better characterize the prevalence, causes, and consequences of asynchrony at fine scales.

Salmonid fishes are useful systems to study population asynchrony due to their fine-scale genetic differentiation, as well as remarkable variation in locally adapted phenotypes, life histories, and demographics (Hutchings 1993, Fraser et al. 2011). Moreover, salmonid habitats can be naturally fragmented and differ markedly in hydrology and geomorphology at small scales, driving highly variable local sensitivities to regional air temperature and precipitation patterns (Lisi et al. 2015, Snyder et al. 2015, Isaak et al. 2016). This interplay between population variation and habitat heterogeneity should increase the likelihood of demographic asynchrony in salmonids at microgeographic scales. Indeed, asynchrony in reproductive timing, spawning habitat conditions, and population productivity stabilize abundance of sockeye salmon across southwestern Alaska, perhaps the most iconic example of portfolio effects in a vertebrate (Hilborn et al. 2003, Schindler et al. 2010). Over broader scales, the resilience conferred by asynchrony could help attenuate range shifts in salmonids and other widespread species exhibiting fine-scale population structure (Richardson et al. 2014, Amburgey et al. 2018). In many species, improved knowledge of the causes and consequences of population asynchrony at microgeographic scales may also inform management and conservation under climate change, as there is often considerable local variation in species responses to warming (Urban et al. 2016, Gallagher et al. 2022).

In this study, I assess how microgeographic variation contributes to demographic asynchrony in eleven populations of brook trout (*Salvelinus fontinalis*) in Cape Race (Newfoundland, Canada). Brook trout are a freshwater salmonid fish with a large native range in eastern North America (spanning 35-59°N latitude; NatureServe 2022) and often consist of small, isolated stream populations (Kazyak et al. 2022). I specifically investigated variation in juvenile abundance, growth rates, and demographic responses to climate at a microgeographic scale (~25 km^2), which I expected to display significant asynchrony that stabilizes abundance across the study area (after Schindler et al. 2015). Crucially, because Cape Race brook trout have been studied for decades (Hutchings 1993, Purchase and Hutchings 2008, Matte et al. 2020b), population differences identified in past research were used to explore potential drivers of microgeographic variation. Predictions were constructed around five well-studied population and habitat features: groundwater input, juvenile abundance, juvenile growth, reproductive success, and phylogenetic distance (Table 2.1). First, groundwater is crucial in moderating freshwater thermal regimes (Snyder et al. 2015) and brook trout are known to be sensitive to temperature and precipitation (Kanno et al. 2015, Bassar et al. 2016, Smith and Ridgway 2019), so I predicted variation in groundwater inputs to drive demographic asynchrony. Second, because juvenile abundance (i.e., recruitment) spans three orders of magnitude and is strongly correlated with drainage size in Cape Race (Wood et al. 2014), I predicted greater asynchrony among small populations than large populations due to their susceptibility to demographic stochasticity (Lande 1993) and hydrological variation (Sabo et al. 2010). Next, I predict that populations with reduced juvenile growth rates will exhibit stronger demographic responses to temperature, as life history research suggests small body size increases overwintering mortality (Hutchings 1993). Similarly, adult reproductive success varies considerably (Bernos et al. 2016) and is positively associated with spawning habitat diversity (Belmar-Lucero et al. 2012), so I predicted that populations with low reproductive success (and therefore fewer spawning areas) will be more strongly impacted by temperature and precipitation patterns. Finally, given the well-described genetic structure in Cape Race, I expected closely related populations (i.e., lower phylogenetic distance) to exhibit more similar growth and abundance patterns as a result of sharing similar demographic histories, habitats and selection pressures (Fraser et al. 2014, Wood et al. 2014).

Our results inform the management of fragmented populations by characterizing microgeographic variation in brook trout and exploring its drivers and consequences, which should be relevant for other species. The fact that Cape Race streams are well-studied and pristine may also illuminate mechanisms that explain the relative importance of synchrony and asynchrony in different contexts, thereby identifying management strategies that can promote and maintain diversity among natural populations.

2.2 - Methods:

2.2.1 - Study area:

This study focuses on eleven brook trout populations in Cape Race, a coastal barren landscape in southeastern Newfoundland dominated by blanket bogs, streams, and ponds (population codes: BC, DY, HM, LC, LO, MC, STBC, UC, UO, WC, WN; Figure A2.1). Proximity to the Grand Banks, where the Labrador Current meets the Gulf Stream, results in cool, wet, and foggy weather year-round. The focal streams are short (0.3-8.2 km; Wood et al. 2014), separated by 5 km or less, and harbor brook trout with a common origin dating back to the last deglaciation 10-12 kya (Danzmann et al. 1998). Brook trout are the only vertebrates in most Cape Race streams.

Landlocked Atlantic salmon (*Salmo salar*) are also present in three streams (LO, UO, WN), but they are rare in LO and significantly outnumbered by brook trout in UO (~5-fold difference) and WN (~20-fold difference) while exhibiting much more limited spatial distributions (Bernos et al. 2018). Importantly, Cape Race drainages are uninhabited and mostly protected within Mistaken Point Ecological Reserve, providing a rare opportunity to study effects of climate change on a system with minimal confounding human impacts.

Cape Race brook trout are genetically differentiated despite their close proximity and exposure to similar climate conditions (Fraser et al. 2014). In addition, populations vary in abundance and life history (Hutchings 1993, Fraser et al. 2019), while streams differ in size, habitat variability, and thermal regimes driven by the prevalence of groundwater seeps (Wood et al. 2014, see Chapter 3; Table 2.1). Although most populations are physically isolated, previous habitat and genetic surveys found evidence of connectivity within the O'Beck (LO and UO) and Coquita (LC, MC, UC) drainages (Table 2.1). Specifically, LO and UO are separated by a short (~50m) boulder field that occasionally floods, while MC receives individuals from both UC and LC (Bernos et al. 2016). MC does not contribute individuals to UC due to an impassable waterfall at its upstream end, while acidic conditions at its downstream end likely reduce brook trout survival (Yates et al. 2019) and limit exchange with LC except during times of flooding. Connectivity can influence demographic processes and was therefore considered when interpreting results, but models were also re-run without connected populations to ensure that patterns were robust (see Results).

2.2.2 - Demographic data:

Brook trout have been monitored almost every year from 2010 to 2022 (no data were collected in 2020 due to COVID-19 travel restrictions), and I focused on the best-studied populations (Table 2.1). Mark-recapture data were obtained through backpack electrofishing surveys that sampled the entire length of each stream. First, a marking event was conducted where all captured brook trout were marked with adipose fin clips and released. Several days later, this was followed by one or more recapture events that estimated the proportion of marked individuals in a random sample of the population (Krebs 2014). I aimed to observe population-level recapture rates (i.e., proportion of marked individuals during recapture events) of at least 25%, and achieved this in 73% of my observations (mean=37%, range=4-80%). Individual fork lengths were measured and weight was recorded for a subsample of fish during marking events, but these data were unavailable for some populations and years (see Appendix 2; Section A2.1). The Petersen method was most commonly used to estimate population abundance (i.e., census population size) from a single recapture event (93% of observations), but the Schnabel method was employed when multiple recapture events were conducted (Wood et al. 2014).

Abundance estimates included all fish age-1 or older, and a total of 122 annual observations were available from 11 populations. However, my objectives required data for individual age-classes that experienced similar environmental (e.g., temperature) and ecological conditions (e.g., conspecific density). Age-1 brook trout can be confidently distinguished from older fish based on size cutoffs (Figure A2.2), so length distributions or age-specific count data were used to separate age-1 from age-2+ individuals for each population each year, and then generate estimates of age-specific abundance and growth rates (details in Appendix 2: Section A2.1). Estimated age-1 abundance (recruitment hereafter; n=122 observations), age-2+ abundance (adult abundance hereafter; n=122 observations), and age-1 individual somatic growth rates

(juvenile growth hereafter; n=105 observations) from 11 populations were the focus of statistical analysis (Figures A2.3 and A2.4). Juvenile growth was calculated as the median fork length of age-1 individuals divided by their estimated age in years (units of $mm \cdot year^{-1}$). Abundance could not be confidently estimated in age-0 brook trout because they were small (mean fork length=42 mm) and thus poorly selected by electrofishing (Dolan and Miranda 2003), especially during early summer sampling dates.

2.2.3 - Climate and stream temperature data:

I used the DayMet database to obtain daily climate data for the study area from 1980-2021 (Thornton et al. 2020; available: https://daymet.ornl.gov/single-pixel/). Monthly average air temperature and precipitation from DayMet reasonably matched data from a nearby weather station with less consistent records (R2=0.96 and 0.62 for temperature and precipitation, respectively; ECCC 2021). I used different time-periods to link climate data to brook trout recruitment or growth to reflect distinct hypotheses. Recruitment was related to mean air temperature and precipitation during reproduction (October 8-31), incubation (November-March), emergence (May), first summer (July-August), and first winter (December-February), which are of interest in salmonid research (Gallagher et al. 2022). In contrast, growth was related to mean temperature and precipitation during the first growing season (April-November) and non-growing season (December-March) after emergence, since these are critical periods for brook trout to gain (Xu et al. 2010) or lose body mass (Hutchings et al. 1999). All climate variables were checked for collinearity, which was limited (variance inflation factors <5).

Cape Race streams also exhibit substantial variation in thermal regimes, with daily summer stream temperatures differing by up to 13°C based on the relative influence of groundwater (Table 2.1). To account for this in demographic analyses, I used non-linear regression to relate DayMet air temperature to daily average stream temperature data collected by automated loggers placed on the stream bottom during four periods from 2012-2021 (Mohseni and Stefan 1999; see Chapter 3 for details). Model fits were satisfactory for all populations (monthly R^2 range=0.88-0.98; monthly RMSE range=0.69-1.15°C), and air temperatures were thus used to reconstruct stream temperatures experienced by each population since 2005, a plausible birth year for the oldest individuals sampled in 2010 (Bernos et al. 2016). Reconstructed stream temperatures were used to calculate annual averages during the same time-periods outlined previously for climate variables. In addition, cumulative degree-days were calculated from stream temperatures during November-August every year within each population (spanning incubation, emergence, and first summer), which generated additional metrics for analyses of juvenile growth. One population, MC, was excluded from all stream temperature reconstructrions because data were unavailable from 2018-2021.

In all analyses of recruitment and juvenile growth (see below), climate data or stream temperatures were lagged to correspond to the time when each year-class experienced a particular time-period (e.g., age-1 fish sampled in 2010 were born in October 2008, incubated from November 2008-March 2009, emerged in May 2009, etc.).

2.2.4 - Population asynchrony:

All analyses were run using R version 4.2.1 (R Core Team 2022), and visualized with *ggplot2* (Wickham 2016). First, patterns in recruitment and juvenile growth of Cape Race brook trout were summarized using a simple correlation analysis. Pairwise correlations between all

populations were plotted for both metrics, along with correlations between each population time-series and sampling year to indicate temporal trends. The distribution and average values of all pairwise correlations (n=66) and temporal trends (n=11) were then summarized to assess whether correlations and trends were centered around zero or skewed in a particular direction.

Next, trends and synchrony in recruitment and juvenile growth time-series were characterized using dynamic factor analysis (DFA) within the *MARSS* package (Holmes et al. 2012). DFA is a multivariate technique designed to identify common trends across short, non-stationary time-series (Zuur et al. 2003). Common trends were modeled with a non-linear autoregressive random walk, while loadings were estimated that describe the relationship between population-specific time-series and the common trend (i.e., positive loadings imply that populations track the common trend, while those with negative values track the inverse of the common trend; Holmes et al. 2012). In both recruitment and growth analyses, population time-series and climate variables were standardized to Z-scores (mean=0, SD=1), then modeled with a single common trend and an identity variance-covariance matrix. This approach minimized the number of estimated parameters and ensured that covariance among time-series was reflected in population loadings (Holmes et al. 2012). Alternative models were built with all possible combinations of one or two climate covariates to explain residual variation in recruitment (55 models including air temperature or precipitation during reproduction, incubation, emergence, summer, and winter) or juvenile growth (10 models including air temperature or precipitation during the growing and non-growing seasons). Models were compared using AICc, and the model with the lowest AICc by two or more units was selected as the best-fit (Johnson and Omland 2004). To ensure that temperature and precipitation extremes did not have stronger effects on recruitment or growth (Maitland and Latzka 2022), I repeated my DFA model selection procedure with maximum values instead of means.

2.2.5 - Demographic relationships and temperature responses:

Population variation in demographic relationships and responses to temperature were assessed using generalized linear mixed models (GLMMs) within the *lme4* package (Bates et al. 2015). For simplicity and comparability, all selected GLMMs were fitted with restricted maximum likelihood, coded with a single fixed effect, and used population as a random effect on both intercepts and slopes. A normal distribution with no link function was used in all cases. Models were subjected to variance partitioning using the *Mu-MIn* package (Barton 2009), which estimated the variance explained (pseudo-R^2) by fixed and random effects. These components were interpreted as proxies for the strength of population variation (random component) relative to any shared underlying relationship (fixed component). While random effects were always coded in a consistent manner, I reported instances when GLMMs estimated no variation in intercepts or slopes (i.e., singular fit; see Bolker et al. 2009). Due to my short time-series and interest in population differences, data were visualized by plotting raw data with population-specific regression lines, as well as plotting fixed and random effects from GLMMs. Finally, to assess potential non-linearity in GLMMs, I used AICc to compare fits from linear models to non-linear models with a quadratic term added as an additional fixed effect.

Three demographic relationships were used to describe key linkages between age-specific abundance and growth rates in GLMMs, while data were standardized to Z-scores to alleviate population differences in most cases. The first relationship was between standardized adult abundance and standardized recruitment the previous year (recruit-adult relationship hereafter),

which was expected to be positive if recruitment drives subsequent population dynamics (Kanno et al. 2015). Adult abundance includes multiple age-classes which may weaken this relationship, but mortality rates are high in Cape Race brook trout (54-69% $year^{-1}$ based on Bernos and Fraser 2016; 56-78% year-1 in Hutchings 1993), so recently recruited age-2 adults should dominate most years. The second relationship was between the log-transformed recruits per spawner ratio and standardized adult abundance when recruits were born (stock-recruitment relationship hereafter), a linearized Ricker model expected to have negative slopes if density-dependent compensation reduced recruitment at high adult abundance (Hilborn and Walters 2013). The third relationship was between standardized juvenile growth and standardized recruitment within year-classes (density-dependent growth relationship hereafter), which was expected to be negative if intraspecific competition reduced growth at high densities (Matte et al. 2020a).

Similarly, population-specific stream temperature data (see Chapter 3) were related to recruitment and juvenile growth using GLMMs with population random effects applied to intercepts and slopes. However, to determine which temperature metric best explained each demographic response, I fit multiple models with different fixed effects via maximum likelihood and selected the best model using AICc. For recruitment, standardized values (Z-scores) were related to average stream temperature during reproduction, emergence, incubation, summer, or winter (temperature-recruitment relationship hereafter). For juvenile growth, raw values (non-standardized) were related to average stream temperature during the growing season and accumulated degree days from November-April or November-August (temperature-growth relationship hereafter). Raw growth data were preferred to test whether stream temperature explained absolute differences in somatic growth among populations (Table 2.1). The best-fit GLMMs for recruitment and growth were re-fitted with restricted maximum likelihood and subjected to variance partitioning.

2.2.6 - Drivers and consequences of population variation:

To assess the five hypothesized drivers of demographic variation among Cape Race populations (see Introduction), I conducted a correlation analysis using population-specific estimates from DFA (loadings) and GLMMs (random effect slopes). Two-sided Pearson correlations were used to test relationships between model outputs and groundwater input, recruitment, juvenile growth rate, and reproductive success (Table 2.1). Similarly, the absolute value of all pairwise differences in population-specific DFA and GLMM estimates were compared to pairwise phylogenetic distances estimated from neutral single-nucleotide polymorphisms (H.-B. Jeon, personal communication), with significance assessed using Mantel tests (10,000 permutations, within the vegan package; Oksanen et al. 2022). Drivers were not strongly correlated with one another (linear regression; R^2 range=0.01-0.16), suggesting negligible collinearity. Note that slopes and intercepts from GLMMs can be highly correlated (Bolker et al. 2009), so strong correlations with random effect slopes may also apply to intercepts. It should be emphasized that this analysis was exploratory in nature, and that power was low in all cases.

Finally, coefficients of variation were calculated to test whether population asynchrony resulted in portfolio effects that increased the temporal stability of brook trout abundance across Cape Race. The coefficient of variation was calculated for abundance (all individuals age-1 and older) as the standard deviation divided by the mean in seven populations with twelve years of data (BC, DY, LC, STBC, UC, UO, WC). For comparison, abundance in all seven populations was summed to obtain a total each year, and the coefficient of variation was calculated for the total

abundance over all twelve sampling years. If the coefficient of variation for total abundance was less than the average across populations, this implies that annual fluctuations in population abundance tend to offset one another and stabilize the aggregate pattern (Schindler et al. 2010). Abundance across multiple age-classes was preferred in this analysis because it captures variation in demographic relationships affected by older individuals. However, coefficients of variation were also calculated the same way for recruitment alone to determine its contribution to portfolio effects. Similarly, total abundance within a given year could not be calculated if any population was missing data, which excluded populations with more gaps in time-series. Nonetheless, coefficients of variation were calculated across different subsets of years to include LO or HM and ensure results were robust.

2.3 - Results:

2.3.1 - Population asynchrony:

Pairwise correlations in recruitment were highly variable in strength and direction (Figure 2.1a), with a symmetrical distribution averaging near zero (mean r=-0.002; Figure 2.1b). Similarly, positive and negative temporal trends in recruitment were evident across populations (Figure 2.1a; bottom row), and the average correlation with year was close to zero (mean r=0.08; Figure 2.1c). In contrast, pairwise correlations in juvenile growth were variable but skewed towards positive values (Figure 2.1d), with an average correlation of 0.21 (Figure 2.1e). Temporal trends in juvenile growth were more variable among populations, with a symmetrical distribution and an average correlation near zero (mean r=-0.04; Figure 2.1f).

Climate variables were uninformative in DFA models for recruitment and juvenile growth, as both best-fit models had no covariates and significantly outperformed all others (ΔAICc<12.6; see Table A2.1). For recruitment, the common trend increased over time and population loadings varied substantially in both magnitude and direction (Figure 2a,b). This implies asynchrony in recruitment, with some populations displaying strong increasing trends (LO, MC, UC, UO) while others are declining (DY and HM) or stable (BC, LC, STBC, WN). For juvenile growth, the common trend was non-linear with an initial increase, followed by a decline, then another increase in recent years (Figure 2.2c). Most population-specific loadings were strongly positive (BC, HM, LO, MC, UO, WN) and only two populations exhibited weak negative loadings (DY and WC), suggesting broad synchrony in individual growth rates among populations (Figure 2.2d).

DFA results were largely similar when excluding populations displaying connectivity or long gaps in time-series (details in Appendix 2: Section A2.2). Model selection results also did not change appreciably when using maximum temperature and precipitation as covariates instead of average values (ΔAICc<14.3; Section A2.3).

2.3.2 - Demographic relationships and temperature responses:

All three demographic relationships showed strong population variation in intercepts and slopes according to GLMMs (Figure 2.3, Table 2.2). The recruit-adult relationship displayed a strong positive fixed effect (slope=0.24; SE=0.12), implying that recruitment drives adult abundance the following year to some extent (Figure 2.3a,d). However, some populations exhibited stronger (DY, HM, STBC, UC, WN) or weaker (LC, LO, UO) slopes and variance partitioning suggested

that population variation in slopes (but not intercepts) explained the same amount of variation (6.1%) as the fixed effect (6.1%; Table 2.2).

The stock-recruitment relationship showed a strong negative fixed effect (slope=-0.25; SE=0.07) consistent with density-dependent reductions in recruitment when adult abundance is high, but the shape of this relationship varied among populations (Figure 2.3b,e). Some populations exhibited lower intercepts and steeper negative slopes (DY and HM) while others had higher intercepts and flatter slopes (BC, LC, STBC), and variance partitioning suggested that population random effects explained more variation (31.5%) than the fixed effect (9.2%; Table 2.2).

Similarly, the density-dependent growth relationship showed a negative fixed effect suggesting that juvenile growth is reduced when recruitment is high, but this effect was relatively weak (slope=-0.14; SE=0.12) and populations differed in their intercepts and slopes (Figure 2.3c,f). Some populations displayed negligible (BC, LO, UO) or even positive (MC) relationships, while variance partitioning showed that population variation in intercepts and slopes was modest (4%) but exceeded the fixed effect (1.9%).

In contrast to demographic relationships, GLMMs suggested that population variation was more limited when relating recruitment and growth to selected stream temperature metrics (Figure 2.4, Table 2.2). For the temperature-recruitment relationship, emergence temperature was selected as the best fixed effect (ΔAICc>2.5; Table A2.2), which had a strong negative impact on recruitment (slope=-0.22; SE=0.11). Although raw data suggested that some populations exhibited stronger negative relationships (LC, STBC, WC; Figure 2.4a), there was no evidence of population variation in intercepts and slopes in the GLMM (Figure 2.4c), so the variance explained by random effects (0%) was less than the fixed effect (3.2%; Table 2.2).

The temperature-growth relationship was best characterized by cumulative degree-days from November-August, which substantially outperformed other fixed effects (ΔAICc>10.1; Table A2.2). Degree-days exhibited a strong and consistent positive effect on juvenile growth across populations (slope=0.02; SE=0.004; Figure 2.4b,d). Although there was evidence of population variation in intercepts and (to a lesser degree) slopes, random effects explained less variance (22.7%) than the fixed effect (26%).

Results from all five GLMM models were robust to the inclusion of connected populations (Appendix 2: Section A2.2). Similarly, non-linear quadratic terms were generally weak, and their inclusion was not supported by model selection in any GLMMs (Section A2.4).

2.3.3 - Drivers and consequences of population variation:

Exploratory correlation analyses showed that predicted drivers of population variation were not strongly related to population-specific estimates from DFA and GLMMs in 28 out of 30 cases (93%), but there were two significant associations (Table 2.3). First, mean age-1 growth rates were negatively correlated to slopes and positively correlated to intercepts from the temperature-growth relationship ($p<0.05$), but this result was likely an artifact (see Discussion). Second, the groundwater index was negatively correlated with intercepts and slopes from the stock-recruitment relationship ($p<0.05$), suggesting that populations in groundwater-dominated streams displayed higher density-independent productivity (based on intercepts) and weaker density-dependent compensation (based on slopes).

Finally, when abundance data were aggregated across the seven best-studied populations (Figure 2.5a), the temporal coefficient of variation (CV=15%) was 2.2 times lower than the average value across individual populations (CV=32%; Figure 2.5b), consistent with a portfolio effect (Schindler et al. 2010). Further analysis suggested this was mostly, but not entirely, driven by variation in recruitment patterns, as the aggregate CV for recruitment alone was 1.9 times lower than the population average. Results held when different subsets of years were evaluated to include LO (2.3-fold difference in CV) and HM (2.4-fold difference), indicating that portfolio effects were robust to the inclusion of additional populations.

2.4 - Discussion:

Brook trout populations in Cape Race exhibited significant demographic variation at a remarkably small spatial scale (~25 km^2), with prominent differences between recruitment and juvenile growth patterns. Recruitment was highly asynchronous and its relationships with other demographic processes were population-specific, which likely combined to diversify population dynamics throughout the study period. Effects of local climate variation on recruitment were weak, showing little evidence of Moran effects that theoretically increase synchrony. In contrast, juvenile growth rates were largely synchronized across Cape Race and strongly influenced by a positive effect of stream temperature that was shared among populations, although variation remained evident in relationships between growth, temperature and density-dependence. Overall, demographic variation stabilized the total abundance of brook trout throughout the study region, but drivers of population differences remained mostly elusive despite decades of past research. Regardless of cause, the microgeographic variation highlighted in this study generated asynchrony among naturally fragmented populations and likely has meaningful impacts on responses to contemporary and future environmental change. For brook trout and other widespread species occupying fragmented habitats, such fine-scale diversity could potentially buffer against regional extirpation and climate-induced range shifts in a warming world.

2.4.1 - Synchrony and asynchrony at a microgeographic scale:

As expected, pairwise correlations and dynamic factor analysis both suggested that asynchrony dominated recruitment patterns in Cape Race. Temperature experienced in May, during brook trout emergence, was the most informative climate covariate identified in this study, but its effect on recruitment was negligible (3.2% variance explained; Figure 2.4c). While some connected populations within drainages exhibited similar trends in recruitment (e.g., MC and UC, LO and UO; Figure 2.2b), asynchrony prevailed nonetheless, similar to observations from recent research on salmonids (Donadi et al. 2023) and other organisms (Moore and Schindler 2022, Rowland et al. 2022). However, these results differ from previous studies of brook trout elsewhere in North America (Zorn and Nuhfer 2007, Warren et al. 2009, Kanno et al. 2016, Sweka and Wagner 2021, Maitland and Latzka 2022), and other stream-dwelling salmonids in Europe (Cattanéo et al. 2003, Alonso et al. 2011, Bret et al. 2016), which generally report synchronized population dynamics at larger scales than the current study. This synchrony is often attributed to Moran effects, where one or more environmental variables are spatially autocorrelated and consistently influence recruitment across the study area (Moran 1953). The asynchrony observed in Cape Race brook trout recruitment could thus be considered unusual, although the reason for this disparity is unclear. It is possible that the study area is less susceptible to the synchronizing effects of local climate due to its northerly position in the species range, cool microclimate, and unusual lack of seasonality in precipitation (Beck et al. 2018). Alternatively, it may be that

natural ecological and habitat variation has been preserved in the pristine streams of Cape Race , while this diversity is often homogenized or lost in more human-impacted systems (Stranko et al. 2008, Carlson and Satterthwaite 2011; see Section 2.4.4 below).

Contrary to predictions, juvenile growth rates tended to be spatially correlated and were positively related to degree-days accumulated between November and August, indicating a synchronized response to temperature within and among populations. Although intercepts and slopes varied, and populations in groundwater-dominated streams (LC and STBC) accumulated fewer degree-days (Figure 2.4b,d), variance partitioning suggested that the temperature-growth relationship was mostly shared across Cape Race. This pattern was also supported indirectly by the common trend estimated via dynamic factor analysis (Figure 2.2c), which was positively correlated with mean air temperature during the growing season ($r=0.55$; p-value=0.053). In contrast, studies of more southerly brook trout populations found that warming negatively impacted individual growth rates during the summer and fall (Robinson et al. 2010, Xu et al. 2010). However, a recent meta-analysis suggested that, on average, warming tends to increase salmonid growth, especially in cold environments where suboptimal temperatures limit growth (Gallagher et al. 2022). Therefore, while water temperatures can exceed brook trout thermal optima in some streams during the summer (Smith and Ridgway 2019, see Chapter 3), the fact that warmer growing seasons increase juvenile growth across Cape Race is unsurprising. Whether or not this pattern will persist under continued warming is uncertain, but should motivate further modeling efforts and comparative studies across the range of brook trout and other widespread species. Additionally, while short time-series limited my ability detect the effects of temperature extremes on juvenile growth, the importance of extreme heat may become evident in the future as Cape Race warms and more data are collected (Letcher et al. 2023, Maitland and Latzka 2022).

Demographic relationships in Cape Race brook trout showed some consistent patterns, but also exhibited considerable population variation, underlining the importance of both shared responses (i.e., synchrony) and population-specific nuance (i.e., asynchrony). The recruit-adult relationship showed that higher recruitment tended to increase adult abundance the following year, supporting prior assertions that recruitment is a key driver of salmonid population dynamics (Warren et al. 2009, Kanno et al. 2016). Similarly, stock-recruitment relationships were consistently negative, implying that per-capita recruitment declined at high adult abundance due to density-dependent compensation, as observed in some brook trout populations (Sweka and Wagner 2021) but not others (Grossman et al. 2010, Huntsman and Petty 2014). Additionally, the density-dependent growth relationship was negative, in accordance with general patterns across salmonids highlighted by a recent meta-analysis (Matte et al. 2020a). However, while patterns in fixed effects were in line with past research, variance explained by population random effects equaled or exceeded fixed effects in all three relationships, suggesting that population variation is an important contributor to fine-scale asynchrony in brook trout. Indeed, differences in demographic relationships should cause population-specific recruitment patterns to propagate through older age classes in diverse ways, generating a complex mosaic of population dynamics across the landscape (Rowland et al. 2022). Overall, variation in demographic relationships among fragmented populations may be an underappreciated source of intraspecific diversity in brook trout and other wide-ranging species, and variance partitioning offers one practical way to quantify this contribution in future studies.

2.4.2 - Drivers of population variation:

In most cases, population-specific model outputs were unrelated to population variation in groundwater influence, recruitment, juvenile growth, reproductive success, or phylogenetic distance (Table 2.3). This could suggest that demographic asynchrony in Cape Race is mostly driven by internal population-specific processes (Munch et al. 2022), or influenced by a more complex set of drivers than those analyzed in this study (Hilborn et al. 2003). However, there were two exceptions to this pattern. First, slopes and (especially) intercepts from the temperature-growth relationship were correlated with average juvenile growth rates, but this result was likely an artifact from using raw growth data. Specifically, Cape Race populations have evolved distinct growth and life history traits reflected in common garden experiments (Fraser et al. 2019) and in the wild (Zastavniouk et al. 2017), such that fast-growing populations would be expected to have higher intercept values in GLMMs (Figure 2.4b). Secondly, a significant correlation was detected between stock-recruitment relationships and an index of stream groundwater inputs, with groundwater-dominated streams (e.g., LC and STBC) exhibiting higher productivity and relaxed density-dependent compensation (Figure 2.3b,e). Similar patterns have been suggested in brook trout elsewhere (Latta 1965, Hartman et al. 2007) and could help explain recent findings highlighting variation in productivity and density-dependent regulation among Cape Race populations (Matte et al. 2020b). Indeed, the relative importance of environmental conditions and density-dependence in shaping salmonid stock-recruitment relationships is still debated (Lobón-Cerviá 2005, 2009), but my results suggest that the strength of each driver is population-specific and influenced by local habitat variation.

More broadly, groundwater can generate substantial differences in thermal regimes among neighboring streams (Snyder et al. 2015), and this was evident in Cape Race (see Chapter 3). For example, the disparate incubation temperatures experienced by Cape Race populations (Figure 2.6a) likely influenced hatch and emergence timing, with warmer winter temperatures likely accelerating development in groundwater-dominated streams. Thermal regimes during the growing season also differed (Figure 2.6b), as groundwater-dominated streams consistently exhibited colder temperatures that may limit brook trout growth, but also warmed less rapidly since 2005 (e.g., increase of 0.55°C in HM, but only 0.15°C in STBC; Figure 2.6b) and did not exceed thermal optima during summer months (see Chapter 3). Together, these patterns suggest that natural variation in groundwater inputs should contribute to asynchrony in phenology, growth, and survival in many stream-dwelling organisms, highlighting the need for fisheries and watershed managers to engage with local groundwater withdrawal policies (Lapides et al. 2022).

2.4.3 - Portfolio effects:

Regional brook trout abundance across Cape Race was more than twice as stable as the average among individual populations, suggesting that asynchrony in recruitment and, to a lesser extent, variation in demographic relationships contributed to a portfolio effect. Similar findings have been observed in anadromous salmonids occupying larger watersheds (Schindler et al. 2010, Moore et al. 2014, Connors et al. 2022), but there has been little research documenting this phenomenon in other widespread species, including many stream-dwelling salmonids. Indeed, the naturally fragmented habitats occupied by brook trout could be instrumental in generating microgeographic variation (Wood et al. 2014) and stabilizing dynamics over larger scales, thereby buffering the species against disturbance (Schindler et al. 2015). While brook trout population dynamics are likely more synchronized in southern range margins with warmer

climates, recent studies in these regions nonetheless show evidence of demographic variation and subtle differences within and among streams (Kanno et al. 2016, Andrew et al. 2022), which can covary with watershed geology (Hartman et al. 2007) and elevation (Kanno et al. 2015). Thus, fine-scale portfolio effects could potentially alleviate regional climate-induced extinction risk throughout much of the species range. This is perhaps even more likely when considering fine-scale thermal heterogeneity driven by groundwater (Figure 2.6), which is often ignored in spatial assessments of brook trout habitat loss (Clark et al. 2001, Flebbe et al. 2006; but see Deitchman et al. 2012), yielding overly pessimistic predictions (Snyder et al. 2015). Range-wide research approaches like those for other widespread vertebrates (e.g., wood frogs; Amburgey et al. 2018) would provide valuable insight into the extent, scale, and drivers of portfolio effects in species such as brook trout.

2.4.4 - Management implications:

Our study highlights the challenges of managing widespread species with innumerable populations. A comprehensive understanding of every population is unattainable, but applying blanket conservation measures across diverse populations could inadvertently homogenize population dynamics (Schindler and Hilborn 2015). In a rapidly changing world, there is considerable interest in developing management strategies that promote stability now and retain options in the future (Moore and Schindler 2022), and Cape Race illustrates the importance of human impacts, landscape context, and scale to achieving these goals.

Cape Race is minimally impacted by human activities, which has preserved natural differences in the quality, quantity, and configuration of habitats that arose over thousands of years (Wood et al. 2014, Zastavniouk et al. 2017), contributing to asynchrony in brook trout abundance. Therefore, protecting local habitat variation may be sufficient to maintain stable abundance across the ~25 streams in Cape Race. These streams are also small (stream length: 0.2-8 km), close together, and relatively easy to sample, facilitating monitoring that can inform population-specific management strategies when needed (e.g., populations at risk of extirpation). However, habitat protection may be ineffective in degraded landscapes (Stranko et al. 2008), so restoration and other active interventions may be necessary to generate asynchrony among populations in highly impacted systems. Similarly, population-specific approaches are impractical across the entire range of many species or in systems with hundreds or thousands of populations across vast areas, so it may be more prudent to monitor key subsets of population diversity and their relationships with habitat heterogeneity across large scales (e.g., Schindler et al. 2010, Connors et al. 2022). In Cape Race and elsewhere, continued long-term monitoring of populations will be crucial for tracking demographic variation across different contexts and future conditions, thereby informing adaptive management under climate change (Schindler and Hilborn 2015).

2.4.5 - Limitations:

While this study uncovered ecologically significant variation in brook trout demography at a remarkably small spatial scale, three main caveats limited my analysis. Firstly, monitoring in Cape Race only began in 2010, so the time-series used in this analysis were relatively short, increasing the likelihood of mischaracterized trends (Bahlai et al. 2021) and precluding tests for dynamic properties such as chaos (Munch et al. 2022). Similarly, only eleven Cape Race populations had sufficient data for this study, which limited scope of inference when assessing drivers of population variation. Future studies of brook trout could gain more robust insight into the prevalence, causes, and consequences of asynchrony by analyzing more populations with

longer time-series across a larger portion of their native range, as done in other salmonids (e.g., Donadi et al. 2023). Secondly, results of this study were based on observations of brook trout age-1 and older, but ignored age-0 (young-of-the-year) individuals that were often too small to be comprehensively sampled by electrofishing (Dolan and Miranda 2003). Age-0 fish are likely most sensitive to density-dependent growth and survival in Cape Race (Matte et al. 2020b), but these processes may not be well-represented by demographic relationships in older age-classes (e.g., Figure 2.3c,f). Finally, overemphasizing population variation could potentially disregard factors that remain important to local and regional species persistence. For example, one population in this study (HM) is small, highly inbred (Bernos et al. 2016), and exposed to the highest water temperatures in Cape Race (>20°C; see Chapter 3), which may explain sharp declines in recent recruitment. Similarly, the populations most influenced by connectivity (LO, MC) accounted for most cases when population-specific demographic relationships opposed expectations (Figure 2.3a-c), perhaps suggesting a stronger impact of connectivity than implied in this study.

2.5 - Conclusion:

Microgeographic variation in recruitment, juvenile growth, and responses to climate in Cape Race brook trout show that asynchrony can prevail at small scales and dampen fluctuations in regional species abundance. Although the prevalence and consequences of microgeographic variation may differ across the species range and some populations will inevitably face extirpation (Hudy et al. 2008, Bassar et al. 2016), such heterogeneity will likely increase the resilience of brook trout to future climate change. This resilience should stabilize, or at least complicate, climate-induced range shifts in brook trout, and could also play an important role in future range dynamics of other widespread species with naturally fragmented habitats (Waterhouse et al. 2017, Pearson et al. 2018, Ony et al. 2020, Rowland et al. 2022). My results also highlight the importance of landscape context and ecosystem state when designing monitoring programs and adaptive management strategies, which should be relevant for many species (Moore and Schindler 2022).

While measuring fine-scale demographic variation is difficult and not equally relevant for all species, my study suggests that ignoring it in spatial assessments of extinction risk may sometimes generate predictions that are too pessimistic, potentially warping management priorities and ignoring bright spots that can benefit conservation efforts (Cvitanovic and Hobday 2018). Similar concerns have been raised for stream thermal regimes, which can vary substantially but are often oversimplified when evaluating climate change vulnerability (Snyder et al. 2015). For brook trout and other widespread species with diverse populations, further research on the influence of microgeographic variation in demography and thermal regimes throughout the native range may yet uncover more potential sources of resilience, but uncertainty will always remain. Therefore, continued efforts to monitor and maintain diversity of all kinds may be the most prudent way to retain conservation options and ecological flexibility in a changing world.

Tables & Figures:

Table 2.1: List of Cape Race brook trout population codes, full names, and proposed drivers of population variation. The groundwater index (GWI; stream-air temperature regression slope from 2018-2020, with lower values suggesting more groundwater input), mean recruitment (R; age-1 abundance), mean juvenile growth rate (G; age-1 individual growth rate; $mm \cdot year^{-1}$), mean reproductive success (S; ratio between effective number of breeders and adult census population size from Bernos et al. 2016) and phylogenetic distance (PD; mean pairwise distance across study populations provided by H.-B. Jeon, personal communication) are shown for each population. Connectivity among populations inferred from past habitat surveys and genetic studies is shown for reference, with "None" denoting isolated populations. In Middle Coquita (MC; denoted with an asterisk *), the groundwater index was estimated using stream temperature data from 2013-2016 and reproductive success data were unavailable.

Population Code	Population Name	GWI	R	G	S	PD	Connectivity
BC	Bob's Cove	0.525	2,181	52.3	0.076	0.579	None
DY	Ditchy	0.702	33	49.4	0.086	0.602	None
HM	Hermitage	0.870	15	55.4	0.076	0.508	None
LC	Lower Coquita	0.349	243	45.8	0.092	0.599	MC
LO	Lower O'Beck	0.824	267	45.2	0.094	0.595	UO
MC	Middle Coquita*	0.646	56	54.3		0.566	LC, UC
STBC	Still There By Chance	0.294	479	46.3	0.031	0.533	None
UC	Upper Coquita	0.677	43	52.7	0.308	0.600	MC
UO	Upper O'Beck	0.796	1,159	51.1	0.024	0.581	LO
WC	Whale Cove	0.612	333	52.8	0.040	0.592	None
WN	Watern	0.524	2,724	52.5	0.023	0.700	None

Table 2.2: Results from generalized linear mixed models (GLMM) estimating demographic relationships (recruit-adult, stock-recruitment, density-dependent growth) and effects of selected stream temperature metrics on demography (temperature-recruitment, temperature-growth) across Cape Race brook trout populations. The number of annual observations (N) and the number of populations (P) included in each analysis are shown for reference. The fixed effect intercept and slope estimates are displayed with standard errors in parentheses. The percentage of variance (pseudo-R^2) explained by the fixed effect and population random effects is shown for each model. The selected stream temperature metric for the temperature-recruitment relationship was emergence temperature during May. For the temperature-growth relationship, it was cumulative degree-days from November-August (see Table A2.2).

			Fixed Effect		Variance Partitioning	
GLMM Relationship	**N**	**P**	**Intercept**	**Slope**	**% Fixed**	**% Population**
Recruit-Adult	95	11	-0.08 (0.09)	0.24 (0.12)	6.1	6.1
Stock-Recruitment	84	11	-0.35 (0.14)	-0.25 (0.07)	9.2	31.5
Density-Dependent Growth	104	11	-0.00 (0.09)	-0.14 (0.12)	1.9	4.0
Temperature-Recruitment	112	10	1.43 (0.75)	-0.22 (0.11)	3.2	0
Temperature-Growth	96	10	13.61 (8.33)	0.02 (0.004)	26.0	22.7

Table 2.3: Correlations between model estimates and proposed drivers of brook trout population variation across Cape Race. Correlations were not corrected for multiple comparisons, and significant relationships ($p<0.05$) are marked in bold italic text. Pearson correlations are shown for the groundwater index (GWI), mean recruitment (R), mean juvenile growth rate (G), and mean reproductive success (S), while Mantel correlations are shown for pairwise phylogenetic distance (PD). Correlations could not be calculated for the temperature-recruitment relationship because the GLMM exhibited no variation in population random effects.

		Pearson r				Mantel r
Model	**Estimate**	**GWI**	**R**	**G**	**S**	**PD**
DFA	Recruitment loading	0.11	-0.11	-0.13	0.23	-0.01
DFA	Growth loading	0.30	0.29	0.13	-0.12	-0.06
GLMM	Recruit-adult slope	-0.11	-0.12	0.35	0.01	-0.13
GLMM	Stock-recruitment slope	***-0.69***	0.17	-0.57	0.11	-0.12
GLMM	Density-dependent growth slope	0.50	0.04	0.25	0.30	-0.06
GLMM	Temperature-recruitment slope	-	-	-	-	-
GLMM	Temperature-growth slope	0.16	-0.33	***-0.74***	0.05	0.00

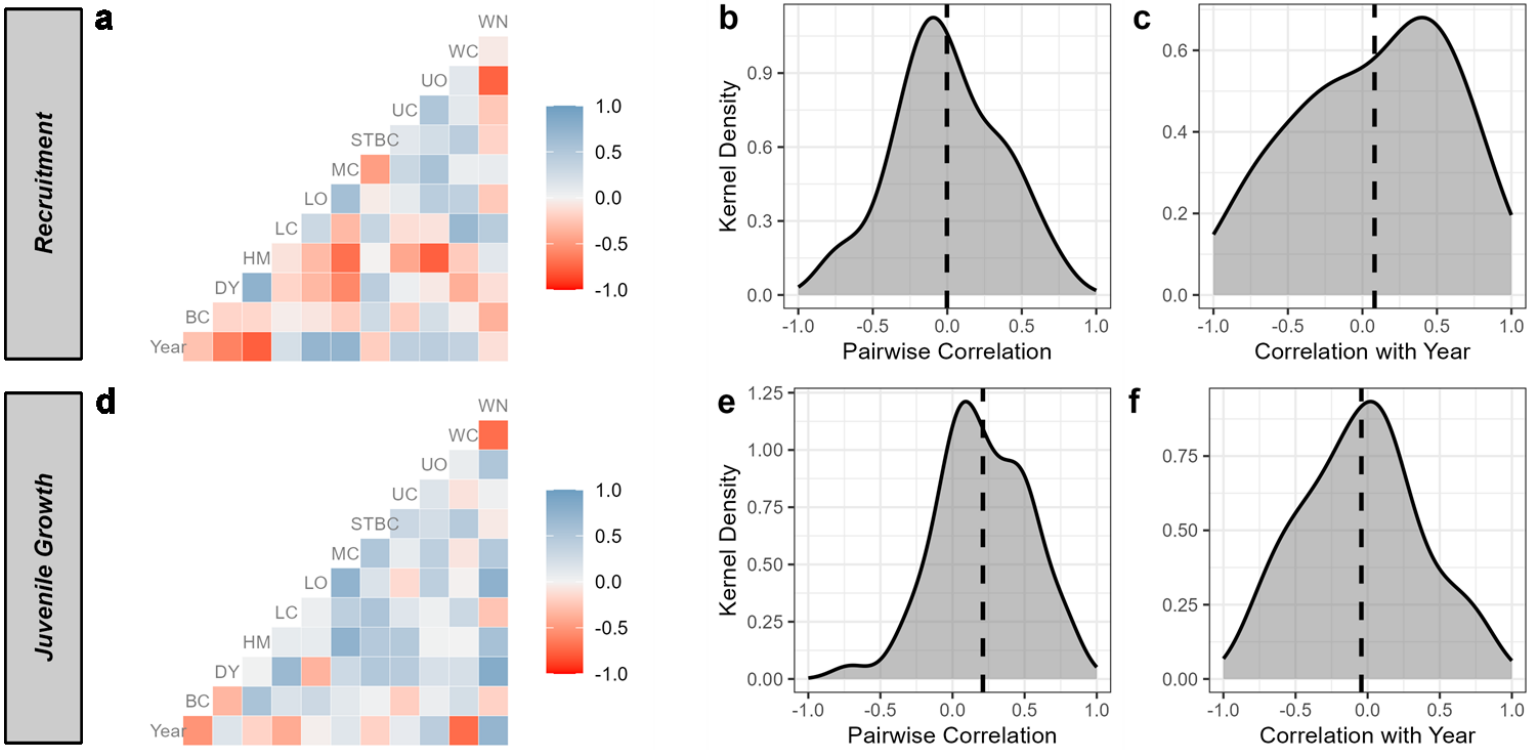

Figure 2.1: Patterns and trends in recruitment (top panels) and juvenile growth (bottom panels) of age-1 Cape Race brook trout. Correlation matrices (a, d) show pairwise correlations between population time-series (top rows) and correlations with sampling year within each population (bottom row). Kernel density plots are shown for all pairwise correlations (b, e) and temporal trends (c, f), with the black dashed lines denoting the average correlation in each case.

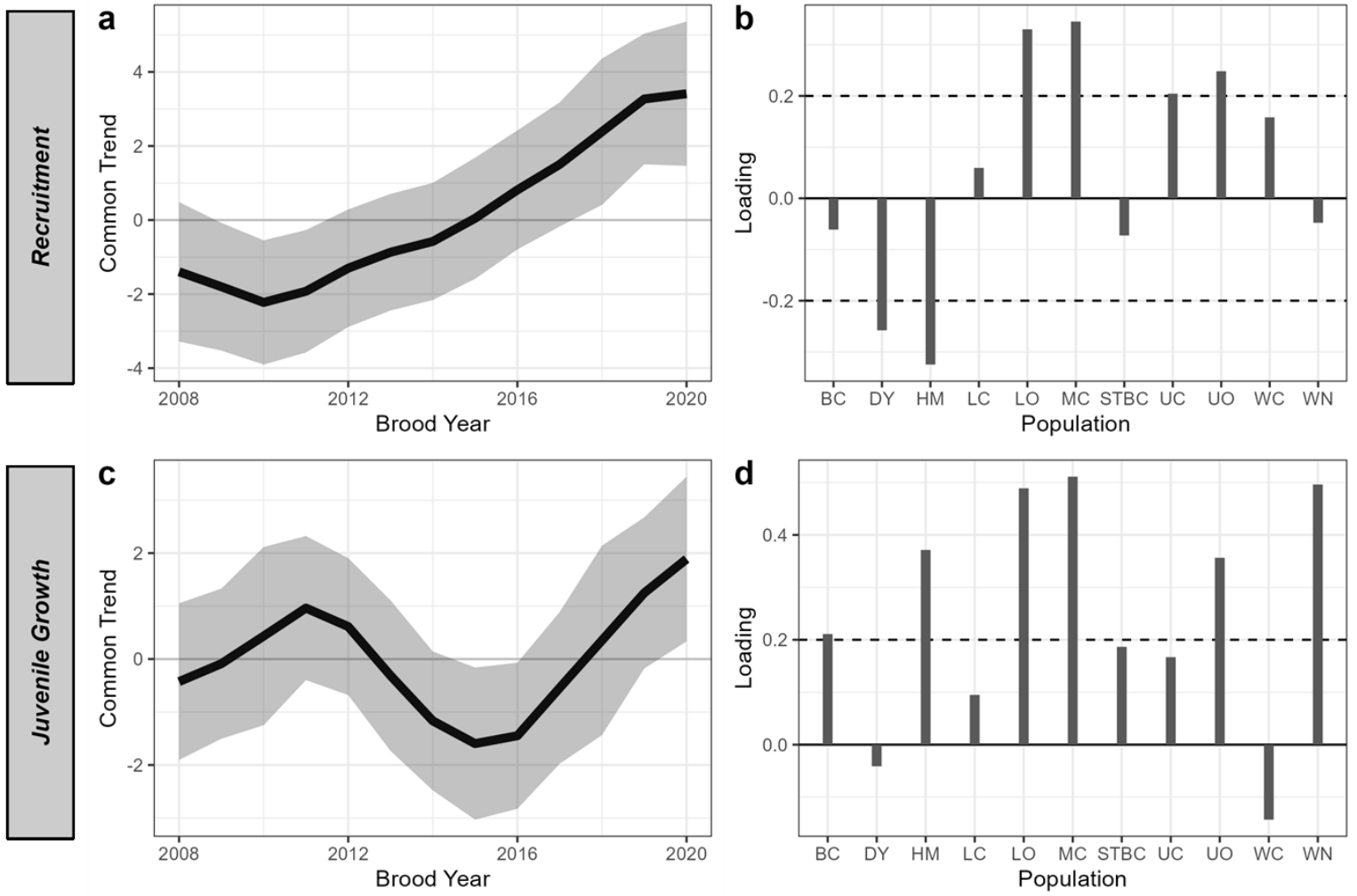

Figure 2.2: Results of dynamic factor analysis of Cape Race brook trout recruitment (top panels) and juvenile growth (bottom panels) time-series. Estimated common trends (thick black line) and 95% confidence intervals (grey bands) are shown for models with no covariates and an identity variance-covariance matrix (a, c). Loadings describing the relationship between individual populations and the common trend (see Table 2.1 for population codes) are also shown (b, d), with dashed horizontal lines denoting strong positive or negative loadings (after Zuur et al. 2003).

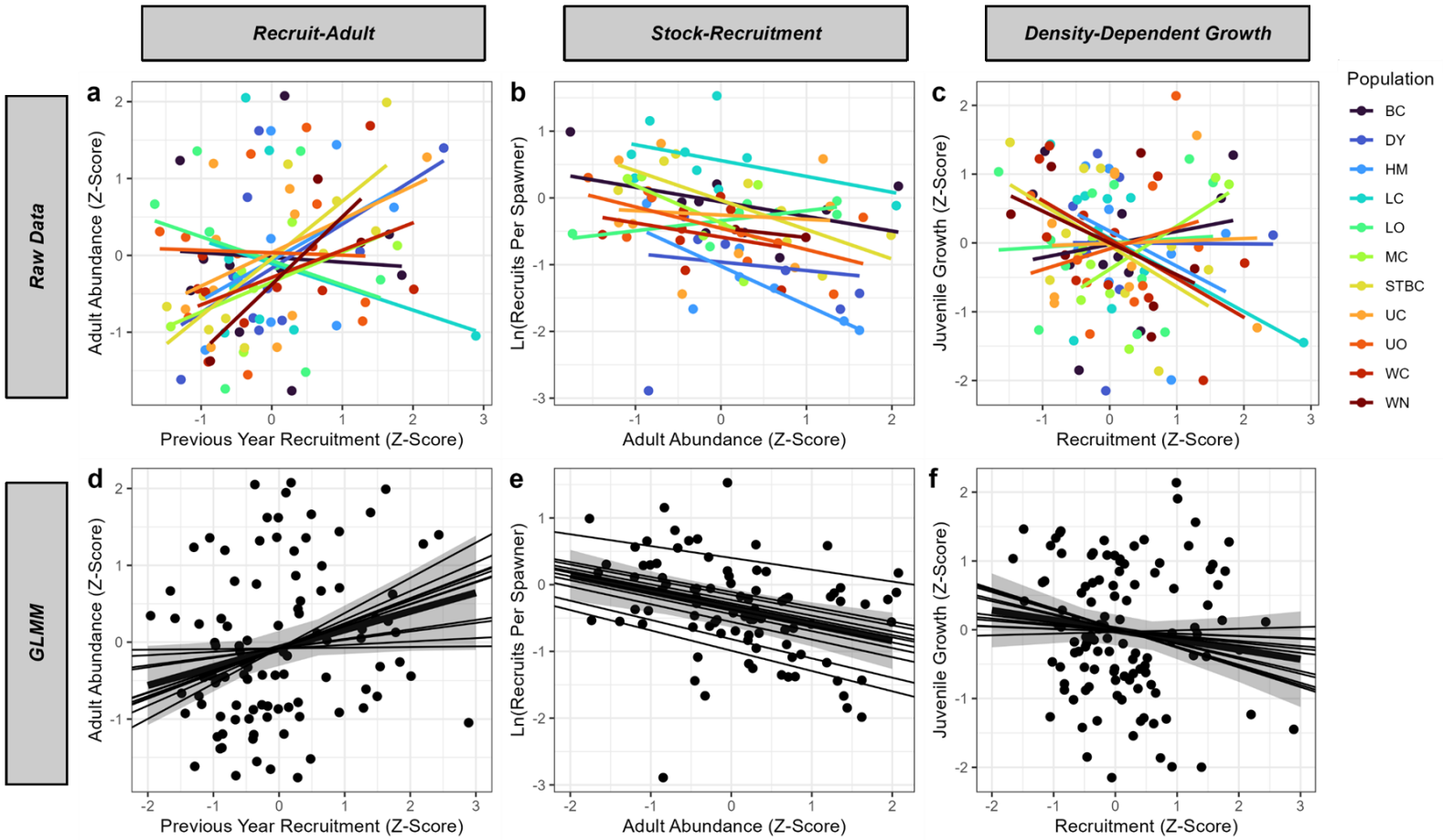

Figure 2.3: Variation in three key demographic relationships among Cape Race brook trout populations. Raw data and regression lines are shown for each population (top panels; see Table 2.1 for population codes), as well as estimates of fixed effects (thick black line with grey 95% confidence band) and population random effects (thin black lines) from generalized linear mixed models (bottom panels; see Table 2.2). The recruit-adult relationship (a, d) plots standardized adult abundance (age-2+ census population size) against standardized recruitment (age-1 census population size) during the previous year. The stock-recruitment relationship (b, e) plots the log-transformed ratio of recruits per spawner against the standardized adult abundance when recruits were born. The density-dependent growth relationship (c, f) plots standardized juvenile growth (age-1 individual growth rate) against standardized recruitment within each year-class.

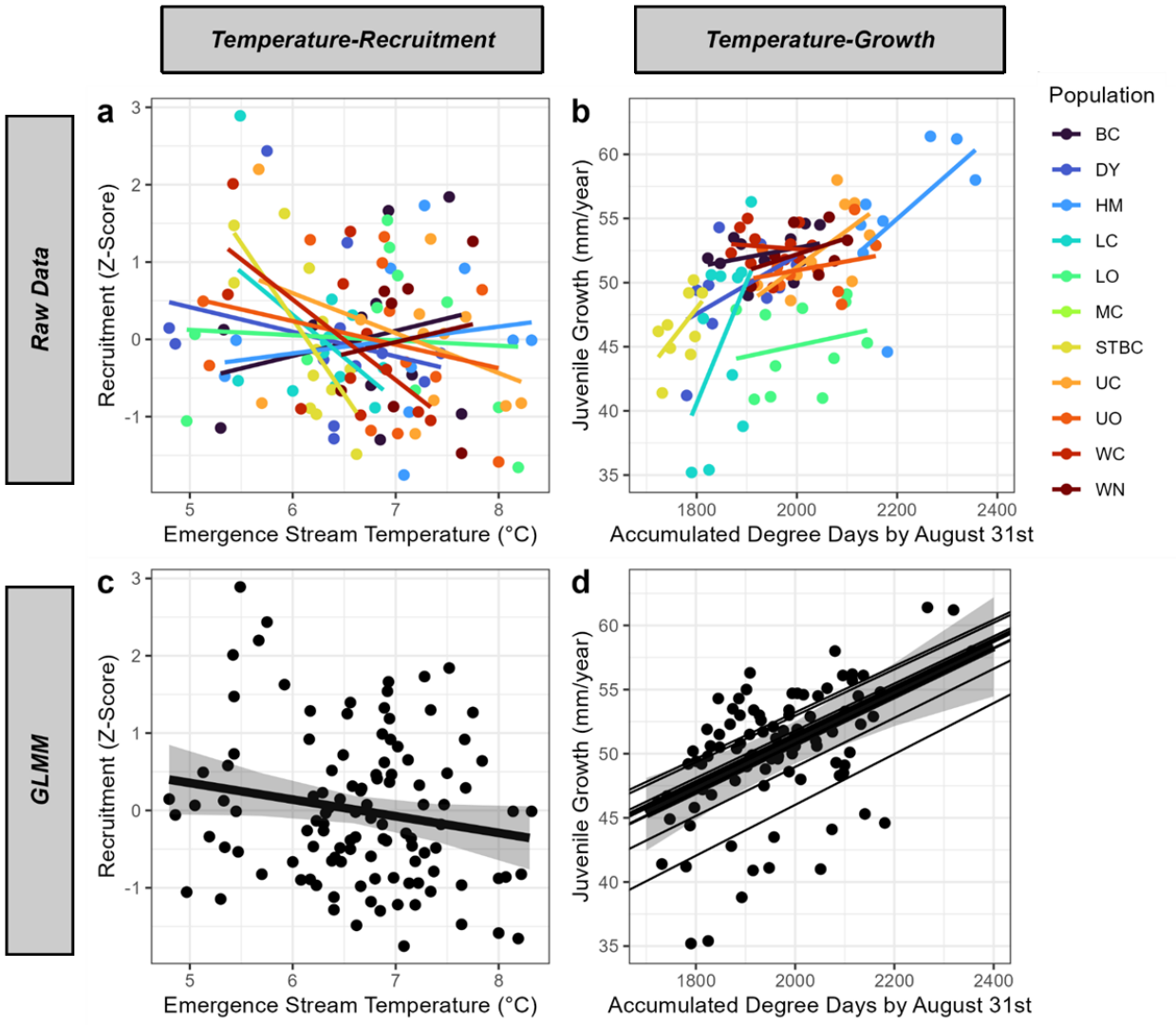

Figure 2.4: Effects of selected stream temperature metrics on Cape Race brook trout recruitment (left panels) and juvenile growth (right panels). Raw data and regression lines are shown for each population (top panels; see Table 2.1 for population codes), as well as estimates of fixed effects (thick black line with grey 95% confidence band) and population random effects (thin black lines) from generalized linear mixed models (bottom panels; see Table 2.2). The temperature-recruitment relationship plots standardized recruitment against mean stream temperature during emergence in May (a, c), while the temperature-growth relationship plots non-standardized juvenile growth against degree days accumulated from November 1-August 31 within each year-class (b, d). Note that the GLMM for the temperature-recruitment relationship (c) exhibited no variation in population random effects.

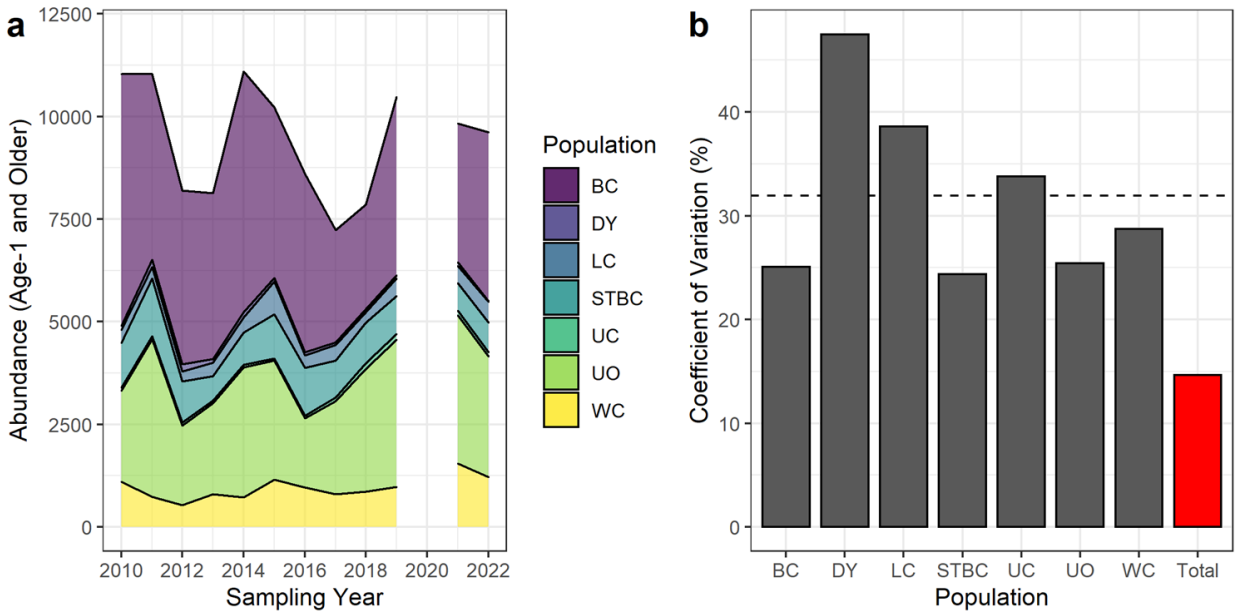

Figure 2.5: Portfolio effects across Cape Race brook trout populations. Stacked time-series of abundance (census population size of all individuals age-1 and older) are shown for the seven best-monitored populations (a), with a gap in 2020 due to the COVID-19 pandemic preventing travel to the study area. Temporal coefficients of variation in abundance (b) are shown for individual populations (dark grey bars), the average across individual populations (black dashed line), and for the total abundance summed across all populations (red bar). A lower coefficient of variation suggests greater stability in abundance throughout the study period.

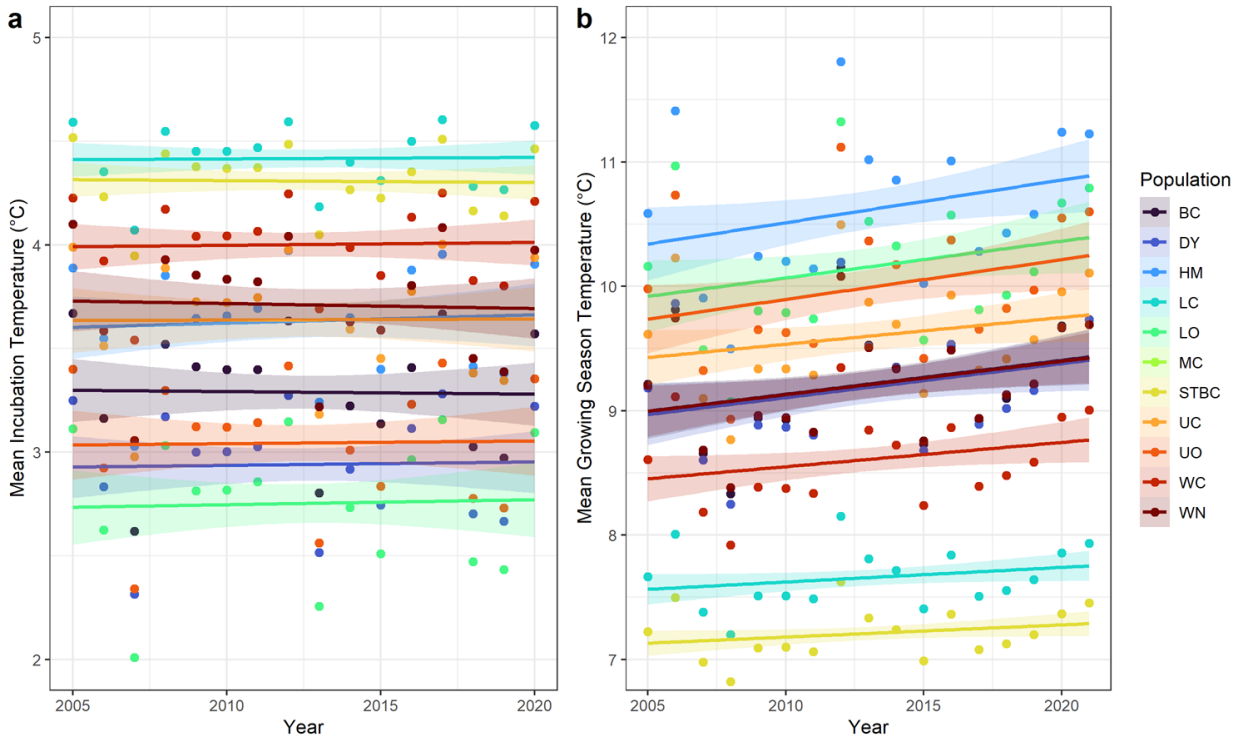

Figure 2.6: Thermal regimes experienced by Cape Race brook trout populations since 2005. Stream temperatures were reconstructed from air temperature based on data from 2012-2021, then averaged during incubation (a; November-March) and the growing season (b; April-November), fitted by population-specific regression lines with 95% confidence intervals. Note that two groundwater-dominated streams, LC (sky blue) and STBC (yellow green), experienced the warmest incubation temperatures and coldest growing season temperatures.

IV. Chapter 3: *Stream groundwater inputs generate fine-scale variation in brook trout phenology and growth across a warming landscape*

Abstract:

Climate change is increasing global atmospheric temperatures, which can reduce abundance and cause range shifts in species that are sensitive to warming. However, fine-scale thermal heterogeneity can drive highly variable local responses to climate change, especially in freshwater environments that differ in groundwater inputs and geomorphology. I used temperature data collected during 2012-2021 from ten small, pristine streams in eastern Canada to characterize thermal variation at a small spatial scale (~25 km2). I then used relationships between daily air and stream temperatures to reconstruct stream temperature since 1980 and assessed how thermal variation influenced the phenology and growth of brook trout (*Salvelinus fontinalis*). Air-stream temperature relationships varied considerably among streams despite their close proximity, with predicted summer temperatures differing up to 9.5°C between warmer rainfall-dominated streams and cooler groundwater-dominated streams. Rainfall-dominated streams warmed more than twice as fast as groundwater-dominated streams across all seasons since 1980, with nearly 4-fold differences in rates of warming evident during summer months. Fine-scale thermal heterogeneity also shaped brook trout phenology, as juveniles in rainfall-dominated streams were estimated to hatch and emerge much later (~70 and 40 days, respectively) and experience faster phenological shifts than in groundwater-dominated streams. Relationships between juvenile brook trout size and accumulated degree-days were positive, but slopes differed over 2-fold and did not vary systematically based on stream hydrology, suggesting more idiosyncratic impacts of warming on early growth. Collectively, my study illustrates how species responses to climate change in freshwater environments can be consistent in direction but vary substantially in magnitude due to the influence of groundwater. Future climate change will likely increase thermal stress experienced by brook trout populations in warmer rainfall-dominated streams, while potentially benefiting those in groundwater-dominated streams where current temperatures are often suboptimal. Observed differences in the rates and ecological impacts of warming among streams suggest that fine-scale thermal variation must be considered when forecasting effects of future climate change on stream fish population dynamics.

3.1 Introduction:

Atmospheric temperatures are increasing globally due to climate change, threatening biodiversity in terrestrial and aquatic habitats (Woodward et al. 2010, Urban et al. 2016). Rapidly warming temperatures can challenge the upper thermal limits of organisms (Sunday et al. 2019) and alter the timing of life history events to track local climate conditions (i.e. phenological shifts; Parmesan and Yohe 2003, Cohen et al. 2018). Although thermal tolerance and phenology are often constrained by shared evolutionary histories and adaptation to past environments, these traits nonetheless vary within and among species (Willis et al. 2008, Bennett et al. 2021, Pottier et al. 2022). Such biological patterns interact with spatial temperature variation, which can be substantial even at fine scales, to produce population-level responses (Suggitt et al. 2011, Scheffers et al. 2014, Lenoir et al. 2017). Thus, the prevalence, causes and consequences of fine-scale temperature differences must be considered when assessing species vulnerability to climate change, and population dynamics must be studied at spatial scales that accurately reflect thermal heterogeneity (Nadeau et al. 2017b).

Responses to warming are particularly complex in freshwater environments, which can exhibit vastly different thermal sensitivity, defined as the expected change in water temperature for every 1° increase in air temperature (Boyer et al. 2021). For example, boreal streams in southwestern Alaska varying in elevation, slope, and contribution of snowmelt to streamflow displayed >5-fold differences in thermal sensitivity during summer months (Lisi et al. 2015). The resulting variation in water temperature shapes salmon phenology and trophic interactions (Lisi et al. 2013, Schindler et al. 2013) and potentially helps stabilize regional abundance in the face of warming (Schindler et al. 2010). Similarly, diverse stream thermal regimes have been noted elsewhere, with groundwater playing a key role in modifying sensitivity to air temperature (Carlson et al. 2019, Daigle et al. 2019, Johnson et al. 2020). Generally, streams dominated by groundwater inputs should have lower thermal sensitivities with more stable temperatures throughout the year (i.e. higher minimums and lower maximums) relative to streams mostly receiving rainfall (Mohseni et al. 1998, Hare et al. 2021). Consequently, fine-scale variation in groundwater contributions can impact the thermal habitats of fishes and strongly influence responses to future climate change, especially in small streams (Meisner et al. 1988, Snyder et al. 2015).

Groundwater plays a key role in generating breeding and rearing habitat for stream fishes. For example, brook trout (*Salvelinus fontinalis*) prefer spawning near groundwater seeps (Curry and Noakes 1995, Ridgway and Blanchfield 1998) where higher discharge, temperature, and dissolved oxygen provide better conditions for developing eggs than surrounding sites (Curry et al. 1995). The warmer winter temperatures at groundwater-dominated sites can significantly advance brook trout phenology (Crisp 1981), while their cooler temperatures during the summer can provide suitable habitat for juveniles after emergence (Borwick et al. 2006). Similar patterns have been documented in other coldwater fish species (Beacham and Murray 1990), and recent research suggests that groundwater-dominated streams harbor distinct and more temporally stable ecological communities (Ishiyama et al. 2023, Hitt et al. 2023). Thus, brook trout can serve as a model for understanding the diverse impacts of groundwater on coldwater fish populations. However, the extent to which groundwater influences ecological processes at small spatial scales remains poorly understood, as previous studies assessed brook trout thermal habitat across relatively large areas (maximum distance between streams: ~25 km in Kanno et al. 2014, ~65 km in Snyder et al. 2015, ~500 km in Carlson et al. 2019). Improved understanding of the spatial scale of temperature variation and its consequences can also inform brook trout conservation and management, as population status and habitat loss are often assessed at coarse scales that aggregate many streams within larger catchments (Hudy et al. 2008, Fesenmyer et al. 2017). If stream thermal sensitivity differs at much smaller scales due to groundwater, this approach may overestimate current and future habitat loss (Snyder et al. 2015).

In this chapter, I assessed fine-scale variation in thermal regimes among ten small streams in Cape Race (Newfoundland, Canada) separated by 5 km or less and explored the ecological impacts of stream temperature on brook trout populations. Cape Race is an excellent focal system because brook trout have been extensively studied for decades (Hutchings 1993, Fraser et al. 2019), and streams exhibit considerable variation in summer water temperatures (Belmar-Lucero et al. 2012, Wood et al. 2014). Although detailed hydrological data are unavailable, field surveys and consultations with local naturalists (J. Cappelman, personal communication) suggest that streams differ in the prevalence of groundwater seeps, which are distinguishable by cool temperatures, less acidic pH, and high densities of miner's lettuce (*Montia fontana*; Purchase and

Hutchings 2008, Belmar-Lucero et al. 2012; see Figure A3.1). The extent to which groundwater dynamics generate variation in stream thermal regimes is important for brook trout populations, as habitat suitability may decline at temperatures above 16°C (Kovach et al. 2019, Smith and Ridgway 2019) and the species is sensitive to warming in Cape Race (Wells et al. 2016) and elsewhere (Bassar et al. 2016, Kanno et al. 2016). Additionally, brook trout populations in different streams are frequently distinguishable based on genetic markers (Kazyak et al. 2021) and can exhibit substantial phenotypic differences at small spatial scales (Hutchings 1993, Belmar-Lucero et al. 2012). If thermal habitats differ at similarly fine scales, brook trout populations likely experience enormous variation in environmental and ecological conditions across their range, which has the potential to stabilize species abundance and increase resilience to climate change (Schindler et al. 2010).

In general, I predict that Cape Race streams will exhibit different thermal regimes based on the relative contributions of groundwater and rainfall to each stream. Specifically, my objectives were to (1) characterize relationships between water temperature and air temperature in each stream, (2) reconstruct and compare long-term trends in stream temperature since 1980, (3) explore the consequences of stream thermal regimes for brook trout phenology and growth, and (4) use independent catchment survey data to explore potential causes of thermal habitat variation. The phenological responses of most salmonids to climate change is poorly understood (Kovach et al. 2016), and groundwater likely generates thermal heterogeneity at smaller scales than current knowledge suggests (Snyder et al. 2015). My study addresses these knowledge gaps by linking fine-scale stream temperature variation to the ecology of brook trout populations across Cape Race. This approach should produce more accurate inferences about the effects of contemporary and future climate change on brook trout, which may be applicable to other freshwater fish species.

3.2 - Methods:

3.2.1 - Study area:

Cape Race is a coastal barren with little riparian vegetation and flat, low-elevation topography covered by blanket bogs (stream elevation = 20-51 m). These characteristics, coupled with the small study area (~5 km x 5 km), suggest that air temperature and other factors that may influence water temperature (Mohseni and Stefan 1999, Lenoir et al. 2017) are likely very similar across streams. Furthermore, the underlying geology is mostly homogeneous and dominated by Precambrian sedimentary rock (Liu and Matthews 2017). The focal catchments are uninhabited with no dams, and thus represent natural hydrologic conditions with minimal human disturbance. Cape Race exhibits a subpolar oceanic microclimate that is rare in eastern North America (Cfc Köppen classification; Rubel et al. 2017), characterized by mild winters, cool summers, and high precipitation all year. Brook trout populations in Cape Race are genetically distinct at a scale of tens to hundreds of meters (Fraser et al. 2014, Wood et al. 2014, Yates et al. 2019), and differ markedly in abundance, body size, behavior, life history and morphology (Hutchings 1993, Wood et al. 2014, Wood et al. 2015, Zastavniouk et al. 2017).

3.2.2 - Air-stream temperature relationships:

Water temperature data in ten Cape Race streams (abbreviated names: BC, DY, HM, LC, LO, STBC, UC, UO, WC, WN; Table A3.1) were recorded every 1.5-2 hours by data loggers placed on the streambed. Data were intermittently collected during three periods from 2012-2016 using

HOBO pendent loggers (July-September 2012, July 2013-June 2015, June-August 2016; see Wells et al. 2016, 2019) and continuously collected from June 2018-December 2021 using HOBO U20L loggers (Onset Computer Corporation, Bourne, Massachusetts, USA). Importantly, data were available during each season across multiple years, covering temperature extremes during summer (nine years: 2012-2016, 2018-2021) and winter months (six years: 2013-2014, 2018-2021). However, U20L loggers were not found in BC or HM during the summer of 2021, so data were only available until July 2019 in these two streams. I averaged stream temperatures within each stream to obtain daily time-series, which were subsequently filtered to remove periods when loggers were out of the water to download data. This process resulted in 959 (BC) to 1,885 (UO) daily temperature observations in each stream from 2012-2021 (Table 3.1). Most study streams have distinct and unconnected drainages, with the exception of those in the Coquita (LC and UC, separated by a waterfall and a ~150 m section of dried streambed) and O'Beck drainages (LO and UO, separated by a ~50 m boulder field that is dry under baseflow conditions but sporadically floods). Despite differences in geomorphology that may affect thermal regimes (e.g. relative pond area; Table A3.1), all streams are short (0.2-8.1 km) and shallow (mean depth range: 11-42cm; Wood et al. 2014) so local air temperature is likely the strongest driver of stream temperature.

To quantify air-stream temperature relationships, air temperature data from the same period were gathered from the DayMet database, which provides continuous gridded climate data throughout North America since 1980 (Thornton et al. 2020). Specifically, the single-pixel extraction tool (available: https://daymet.ornl.gov/single-pixel/) was used to obtain daily average air temperature data at 2-meter height for the middle of the study area (46.6464° N, 53.2064° W) from 2012-2021. Average air temperatures from DayMet closely matched those from a weather station at Cape Race Lighthouse, which had limited temporal coverage (R^2=0.93; ECCC 2021). Air temperatures (T_{air}) were aligned with daily average stream temperatures (T_{stream}), and stream-specific relationships were fitted using non-linear Type-I least squares. The model estimated T_{stream} as a function of T_{air} and four parameters based on the equation:

$$T_{stream} = \mu + \frac{\alpha - \mu}{1 + e^{\gamma(\beta - T_{air})}} \qquad (Eq. 3.1)$$

where μ is the minimum stream temperature, α is the maximum stream temperature, γ is the inflection point (steepest slope) of the relationship, and β is the temperature at which this inflection point occurs (Mohseni et al. 1998, Morrill et al. 2005). Errors were assumed to be independent and normally distributed, but the consequences of this assumption were evaluated in subsequent analyses (see below). However, this approach does not account for non-stationarity in relationships and is not recommended for estimating stream temperatures under future climate conditions (Arismendi et al. 2014; see Discussion).

To evaluate model performance, residuals were plotted against predicted values and root-mean-square error (RMSE) was calculated for daily stream temperature and for weekly and monthly averages. Ideally, residuals should be unbiased and evenly distributed across all predicted stream temperatures, while RMSE values should be below 1°C (Daigle et al. 2019). Stream temperatures often exhibit strong temporal autocorrelation (Johnson et al. 2020), so residual autocorrelation functions were plotted within each stream and all air-stream temperature relationships were re-estimated with an autoregressive error structure using the *nlme* package in R (Pinheiro et al. 2022). Finally, precipitation can affect stream temperature positively (Ishiyama

et al. 2023) or negatively (Carlson et al. 2019), so residuals from air-stream temperature relationships from March-November were regressed on daily precipitation data from the DayMet database to explore its effects within each stream. This period was selected because precipitation often influences stream temperature most strongly during the warmest months (Carlson et al. 2019), while wintertime effects may be unreliable in Cape Race because high winds often limit accumulation of snow.

3.2.3 - Reconstruction of historical stream temperatures:

Air-stream temperature relationships served as reasonable proxies for thermal regimes experienced by brook trout populations in Cape Race, despite some limitations (see Results). Therefore, these relationships were considered suitable for reconstructing historical stream temperatures to support further analysis. For each stream, I plugged parameter estimates from air-stream temperature relationships (Table 3.1) into Equation 1 to estimate stream temperatures from DayMet air temperature records every day from 1980-2021. This process generated a continuous time-series of stream temperatures spanning over four decades in ten Cape Race streams. Because this extrapolated well beyond the time-periods used to fit non-linear regression models, I compared the distribution of air temperatures during the regression period (2012-2021) to all observations during the reconstruction period (1980-2021). Reconstructed stream temperatures were summarized each year by averaging daily values in each stream during the winter (December-February), spring (March-May), summer (June-August), autumn (September-November), and the longer growing season (April-November).

To assess how differences in stream thermal regimes impact brook trout development and phenology, I calculated cumulative degree-days in each stream every day from November 1st until August 31st the following year. Although my approach for estimating degree-days did not account for population variation in reproductive timing (see Discussion), the period from November-August captured thermal conditions during incubation, emergence, and the first summer that most strongly influence rates of growth and development (Wood and Fraser 2015). A base temperature of 0°C was used in all streams (i.e. a daily average temperature of 5°C would add 5 degree-days to the cumulative total). Inaccurate base temperatures can be problematic (Chezik et al. 2014), but a recent review suggested that base temperatures of 0°C are likely adequate for salmonids like brook trout (Honsey et al. 2022).

3.2.4 - Characterizing rates of warming and phenology:

I used summaries of reconstructed stream temperatures (see section 3.2.3) to assess seasonal rates of warming across Cape Race, and compared them to rates for air temperature during the same period (after Carlson et al. 2019). I estimated warming rates as slopes from the regression of mean annual temperature on year from 1980-2021 (in units of $°C \cdot year^{-1}$). Additionally, I calculated monthly averages from daily temperature reconstructions from 1980-2021, then extracted trends and anomalies during each month and year using time-series analysis conducted within the *forecast* package in R (Hyndman et al. 2022). I adopted this method to complement regression-based approaches because trends and anomalies are independent (i.e. trends are estimated with anomalies removed and vice-versa) and explicitly account for autocorrelation and seasonality in time-series (Daigle et al. 2019), which can potentially bias regression slopes.

Annual summaries of cumulative degree-days were used to explore variation in the timing of brook trout development and phenological shifts among streams, with particular focus on

hatching and emergence. Common garden experiments suggest that Cape Race brook trout populations reared at 5°C hatch after accumulating 490-520 degree-days and respond similarly when developmental temperatures are altered (Wood and Fraser 2015). Studies of other brook trout populations suggest that emergence occurs 150-250 degree-days after hatching (Grande and Anderson 1990, Argent and Flebbe 1999). Thus, I used putative thresholds of 500 degree-days for hatching and 750 degree-days for emergence in each stream. I identified the date each year when these developmental thresholds were reached, calculated the mean and range of dates within each stream, and regressed these dates (converted to ordinal days) on year to obtain slopes from 1980-2021 (in units of days·year^{-1}). This approach assumes identical degree-day thresholds and start dates for incubation (November 1st) across all streams and years, and thus may not fully represent conditions experienced in the wild (see Discussion).

3.2.5 - Effects of thermal regimes on fish growth:

To test the influence of thermal regimes on brook trout growth after emergence, observed fork lengths of young-of-the-year (YOY) were regressed against cumulative degree-days experienced from November 1st in the preceding year until individuals were sampled. YOY were captured via backpack electrofishing during annual mark-recapture surveys from 2010-2021 (Wood et al. 2014; N = 5,531 across all streams and years). Stream-specific regression equations were used to assess growth differences among populations. Similarly, I incorporated all data into a generalized linear mixed model (GLMM) with stream as a random effect on intercepts and slopes, then conducted variance partitioning to quantify the relative importance of growth variation among populations. The efficacy of the putative emergence threshold was also evaluated by back-calculating lengths at 750 degree-days from stream-specific regression equations and comparing these to emergence lengths reported in laboratory studies of Cape Race brook trout (Wood and Fraser 2015, Fraser et al. 2019). Finally, this analysis was repeated using YOY growth rates (length divided by estimated age in years; see Chapter 2) in order to ensure that inter-annual differences in the timing of YOY surveys did not significantly influence results.

3.2.6 - Spatial variation and influence of catchment characteristics:

Detailed catchment surveys were conducted in at least eight streams over four summers (late-June to early-August) between 2010 and 2015, which quantified drainage characteristics via satellite imagery and measured a suite of variables across transects within each stream. Stream transects were conducted one day each year at 5-49 points spaced 25-100 meters apart depending on stream length, with larger streams having more and more widely-spaced transects (see Wood et al. 2014). Surface water temperatures measured during each transect were used to characterize spatial variation in summer stream temperature, which was important because time-series from temperature loggers were only collected from a single location. Transects in small streams were completed in 1-3 hours, but the largest streams (BC, UO, WC, WN) took 4-8.5 hours to sample and spatial variation was thus influenced by time of sampling to some extent (see Discussion). Finally, a correlation analysis was used to relate parameter estimates from air-stream temperature relationships (Equation 3.1) to eight variables measured during catchment surveys (drainage area, sinuosity, gradient, flow velocity, depth, width:depth ratio, pH, and relative pond area; Table A3.1). This yielded a total of 32 correlations that were used to infer potential drivers of thermal regimes, but this analysis should be considered exploratory in nature and was thus implemented with and without multiple comparison adjustments.

3.3 - Results:

3.3.1 - Air-stream temperature relationships:

Streams exhibited considerable temperature differences from 2012-2021, especially in the frequency of temperatures above 16°C (Figure 3.1). During the summer, observed temperatures differed between the warmest and coldest streams by as much as 13°C within the same day. Parameter estimates similarly varied among streams, suggesting diverse air-stream temperature relationships (Table 3.1, Figure 3.2). Streams such as STBC and LC were characterized by relatively high minimum temperatures (μ = 2.5-3.5°C) and low maximum temperatures (α = 9-10°C; Figure 3.2), which point to significant groundwater influence. In contrast, streams such as HM and LO exhibited low minimum temperatures (μ = 0-1.5°C) and high maximum temperatures (α = 17-19°C; Figure 3.2), suggesting they primarily receive surface water (see Discussion). To ease interpretation, I grouped streams into three categories based on estimated thermal sensitivities during the growing season: groundwater-dominated (STBC and LC; thermal sensitivity <0.45 after Hitt et al. 2023), rainfall-dominated (HM, LO, UO; thermal sensitivity >0.70), and intermediate (DY, BC, WN, UC, WC; thermal sensitivity = 0.45-0.70). These categories are not absolute and may not be applicable elsewhere, but reasonably describe the continuum of air-stream temperature relationships I observed.

Air temperatures used in regressions from 2012-2021 (Figure 3.3a) were representative of the historic range in Cape Race from 1980-2021 (Figure 3.3b), but skewed towards warmer air temperatures collected during summer months. Model fits were satisfactory, with R^2 values of 0.79-0.92 (Table 3.1), and predicted stream temperatures following 1:1 relationships with observations. Residuals largely satisfied assumptions of homoscedasticity, although variance was reduced as predicted temperatures approached 0°C in some streams (DY, LO, UO). Daily RMSE values based on predicted stream temperatures were relatively high (1.05-1.97°C; Table 3.1), but improved when data were averaged across weekly (0.83-1.52°C) and monthly (0.69-1.15°C) intervals (Figure 3.3c). Autocorrelation was pervasive in the residuals from all streams (Figure A3.2), but re-fitting relationships with autoregressive errors yielded very similar parameter estimates and daily RMSE values (1.05-1.98°C). Daily precipitation had a negative effect on residuals in every stream (Figure A3.3), and showed similar patterns for 3-day and 5-day running average precipitation.

3.3.2 - Variation in rates of warming and phenology:

Positive slopes for all streams and seasons indicated pervasive warming in Cape Race since 1980 (Table 3.2), but slopes varied substantially in magnitude. During winter, air temperatures increased by 0.0314°C·year^{-1}, while the slowest (LC; 0.0058°C·year^{-1}) and fastest (LO; 0.0125°C·year^{-1}) rates of stream temperature warming differed 2.1-fold (Table 3.2). Warming was less dramatic for spring air temperature (0.0115°C·year^{-1}) but still differed 2.3-fold between streams with the slowest (STBC; 0.0031°C·year^{-1}) and fastest (LO; 0.0071°C·year^{-1}) rates. Summer exhibited the highest rate of warming for air temperature (0.0482°C·year^{-1}), with 3.9-fold differences between streams with the fastest (HM; 0.0356°C·year^{-1}) and slowest (STBC; 0.0091°C·year^{-1}) increases. Rates of warming were similarly high during the autumn, as air temperature increased by 0.0451°C·year^{-1}, while streams with the slowest (STBC) and fastest (HM) rates of warming differed 2.8-fold, increasing 0.0140°C and 0.0399°C·year^{-1}, respectively (Table 3.2). During the growing season (April-November), air temperatures increased by 0.0379°C·year^{-1}, while stream temperature rose fastest in HM (0.0304°C·year^{-1}) and slowest in

STBC (0.0096°C·year^{-1}), representing a 3.2-fold difference (Table 3.2, Figure A3.4). When compared against rates of atmospheric warming across all periods except winter, rainfall-dominated streams exhibited thermal sensitivities of 0.62-0.88, while groundwater-dominated streams had much lower sensitivities ranging from 0.19-0.31 (Table 3.2). These patterns were corroborated by time-series analysis of reconstructed stream temperatures where groundwater-dominated streams exhibited slower rates of warming (especially since 2000; Figure 3.4a) and dampened seasonality (Figure 3.4b) compared to rainfall-dominated streams.

Annual degree-day accumulation in each stream indicated that thermal regimes varied significantly during brook trout development, while hatching and emergence appeared to occur earlier in recent years due to warming (Figure A3.5). These patterns were confirmed in estimates of hatch and emergence timing, where mean hatch dates spanned ~2.5 months, from as early as February 25th (LC) to as late as May 9th (LO). Similarly, mean emergence dates spanned ~1.5 months, ranging from April 25th in LC to June 11th in LO (Table 3.3). Phenology shifted towards earlier dates in every stream since 1980, but the rate of these shifts differed among streams by 2.2-fold for hatching and 1.6-fold for emergence (Table 3.3). Groundwater-dominated streams (LC and STBC) had the smallest shifts, with slopes of -0.29 and -0.22 days·year^{-1} for hatching and emergence, respectively. In contrast, rainfall-dominated streams such as HM and UO had larger phenological shifts, with slopes of -0.60 days·year^{-1} for hatching and -0.33 days·year^{-1} for emergence. These rates imply that Cape Race brook trout currently hatch 11-25 days earlier and emerge 9-15 days earlier than four decades ago (Table 3.3). Degree-day accumulation also exhibited notable discrepancies before emergence and at the end of summer, as groundwater-dominated streams accumulated the most degree-days from November-April (Figure 3.5a), but the fewest from November-August (Figure 3.5b).

3.3.3 - Effects of thermal regimes on fish growth:

Accumulated degree-days had a significant positive effect on YOY brook trout length in every stream ($p < 0.001$), although regression slopes differed 2.5-fold among populations (Figure 3.6; Table A3.2). Contrary to expectations, slopes did not differ systematically based on thermal regime, with groundwater-dominated streams displaying both the steepest (STBC; slope = 0.041mm·degree-day^{-1}) and shallowest slopes (LC; slope = 0.017mm·degree-day^{-1}; Table A3.2). The GLMM integrating data across all streams yielded similar results, with pseudo-R^2 values suggesting that the variance explained by population-specific intercepts and slopes (35%) exceeded the fixed effect (27%; Table A3.2). The putative 750 degree-day threshold for emergence appeared to be reasonable, as estimated lengths at this threshold (mean = 26mm, range = 17-33mm based on regression equations; Table A3.2) were more variable but otherwise similar to emergence lengths of Cape Race brook trout observed in common garden experiments (mean = 23mm, range = 20-25mm; Wood and Fraser 2015, Fraser et al. 2019). Results were very similar when YOY growth rates were used as the response variable instead of lengths, with roughly four-fold differences in slopes between LC (0.008mm·day^{-1}·degree-day^{-1}) and STBC (0.037mm·day^{-1}·degree-day^{-1}).

3.3.4 - Spatial variation and influence of catchment characteristics:

Surface water temperatures measured during summertime transect surveys indicated significant spatial variation within each stream, often exceeding 5°C (Figure A3.6). While the date and time of stream sampling varied within years and likely influenced spatial patterns (see Discussion), groundwater-dominated streams were usually coldest (Figure A3.6). Correlating additional

habitat survey data to parameter estimates from air-stream temperature relationships uncovered seven significant associations ($p < 0.05$; Table A3.3). The minimum stream temperature parameter (μ) was positively correlated with stream gradient ($r = 0.85$) and negatively associated with average velocity ($r = -0.64$). Maximum stream temperature (α) was negatively correlated with stream gradient ($r = -0.87$), while the inflection point slope (γ) was negatively related to drainage area ($r = -0.84$). Finally, temperature at the inflection point (β) was negatively associated with stream gradient ($r = -0.69$), and positively correlated with width:depth ratio ($r = 0.67$) and relative pond area ($r = 0.64$). However, no correlations remained significant after using the Bonferroni method to adjust for multiple comparisons ($p > 0.0016$).

3.4 - Discussion:

I uncovered substantial differences in water temperature among streams separated by less than 5 km, which alter rates of warming experienced by fish populations and generate variation in phenology and growth. Thermal regimes were well-characterized by air-stream temperature relationships from 2012-2021, which diverged by over 9.5°C in estimated maximum stream temperatures. Based on reconstructed temperatures since 1980, warming and phenological advancement were ubiquitous across Cape Race, albeit with significant variation in magnitude. Warming rates varied more than 2-fold among streams across all seasons and differed nearly 4-fold during the summer, while advancement in the timing of brook trout hatching and emergence differed 2.2-fold and 1.6-fold, respectively. Because climate conditions, underlying geology, and landscape attributes were similar across the small study area, temperature variation among streams appeared to be influenced by differences in groundwater inputs, with groundwater-dominated streams always displaying the slowest rates of change. Such fine-scale heterogeneity in thermal regimes has significant implications for stream fish habitat suitability, growth, and phenology under continued warming, and may play a key role in diversifying species responses to future climate change. However, my results are likely shaped by the remote high-latitude setting and unusual local climate of Cape Race, so caution is warranted when applying these findings elsewhere.

3.4.1 - Thermal regimes under climate change:

Air-stream temperature relationships highlighted significant variation in thermal regimes across Cape Race, especially in the prevalence of high stream temperatures that may negatively impact brook trout during summer months (Figures 3.1 and 3.2). Optimal growth for brook trout occurs at 12-16°C (Kovach et al. 2019, Smith and Ridgway 2019) and may decline when chronically exposed to higher temperatures. For Cape Race populations, field experiments conducted over ~2 months showed reduced growth and survival above 15°C (Yates et al. 2019) while short-term laboratory experiments suggested that behavioral stress responses are initiated at 17-18°C (Wells et al. 2016). Based on these thresholds, brook trout occupying rainfall-dominated streams (HM, LO and UO) are clearly exposed to much more thermal stress than those in groundwater-dominated streams (LC and STBC), which seldom experience temperatures above 16°C. Rates of warming observed in groundwater-dominated streams were also much slower than rainfall-dominated streams (Table 3.2; Figure 3.4), suggesting that future temperature differences among streams may widen if this pattern persists. However, stream temperature records in Cape Race contained multiple gaps that likely prevented this study from capturing the full range of conditions, as recent hydrology studies recommend using at least five years of continuous stream temperature data to characterize thermal sensitivity (Daigle et al. 2019, Boyer et al. 2021).

Additionally, I did not account for temporal autocorrelation or non-stationarity in air-stream temperature relationships, which will change in the future if climate change impacts the recharge, routing, and depth of groundwater (Arismendi et al. 2014, Hare et al. 2021). Despite these limitations, the large differences in observed stream temperature (Figure 3.1) and satisfactory model performance over longer periods (monthly RMSE = 0.69-1.15°C; Figure 3.3) support the use of air-stream temperature relationships to broadly describe thermal regimes experienced by brook trout.

I focused on predicting average daily stream temperature, but its variance must also be considered, especially at high temperatures. For example, the maximum stream temperature parameter (α) in HM was ~19°C, but the warmest observed stream temperatures were as low as 15°C and as high as 23°C (Figure 3.1). Similarly, stream temperature data were recorded at one location in each stream, but summer temperatures routinely differed by 5°C or more along the entire stream length (Figure A3.6), and the smallest drainages (e.g. DY, LC, UC) tend to exhibit greater spatial temperature variation (Wood et al. 2014). Hourly fluctuations in stream temperature can also be substantial (Kanno et al. 2014), and this was evident in the most detailed Cape Race temperature logger data available from 2018-2021. Specifically, median differences between the highest and lowest stream temperatures observed each day ranged from 1.6-2.9°C, but within-day differences exceeded 9°C on rare occasions in every stream. This pattern also impacted temperatures recorded during transect surveys that took 4-8 hours in large streams (see Methods), so the data in Figure A3.6 likely overestimate spatial variation. Nonetheless, the combination of residual error, spatial variation, and subdaily fluctuations highlight that thermal regimes in Cape Race streams are much more complex than my analysis suggests. Indeed, such spatiotemporal variability may create cooler refuges that buffer brook trout populations against the adverse effects of high summer temperatures, even within the warmest streams (Wang et al. 2020, Morgan and O'Sullivan 2022).

The variation and complexity of stream temperatures across Cape Race demonstrates that brook trout thermal habitat differs substantially at finer scales than previously documented (Kanno et al. 2014, Snyder et al. 2015, Carlson et al. 2019). Variable rates of warming estimated among streams imply that these differences may increase in the future, impacting brook trout habitat quality during the summer. More broadly, my results suggest that characterizing the distribution of thermal refuges among streams should continue to be a research priority in areas occupied by coldwater fishes (Kovach et al. 2019, Isaak and Young 2022). This also applies to spatial variation within streams, as groundwater seeps occur midway along the length of some Cape Race streams with intermediate thermal regimes (e.g. BC, WC), and are perhaps better characterized as rainfall-dominated upstream with groundwater-dominated thermal refuges downstream.

3.4.2 - Phenology and growth under climate change:

By combining reconstructed stream temperatures with previous research on brook trout development in Cape Race and elsewhere, I estimated substantial fine-scale variation in phenology that aligned with thermal regimes in accordance with past research (Crisp 1981, Beacham and Murray 1990). Remarkably, eggs were estimated to hatch up to 74 days earlier (February 25th vs. May 9th) and emergence was estimated to occur 47 days earlier (April 25th vs. June 11th; Table 3.3) in groundwater-dominated streams such as LC and STBC than in rainfall-dominated streams (Figure A3.5). This disparity is surprising given that developmental rates of

Cape Race populations are similar in common garden conditions (Wood and Fraser 2015), but can be explained by differences in incubation temperature. Specifically, groundwater-dominated streams were predicted to be ~3°C warmer than most nearby streams during the incubation period, thereby accumulating more degree-days and accelerating development (Figure 3.5a). In addition, while the timing of hatch and emergence shifted earlier in every stream, groundwater-dominated streams exhibited slower phenological shifts, perhaps reflecting their more stable temperatures overall (Figure 3.4). Similar variation in hatch and emergence times in Chinook salmon can mediate spatial patterns in growth (Kaylor et al. 2021, 2022), but the consequences of the disparate phenologies observed among Cape Race brook trout populations are currently less clear (see below). Moreover, reproductive timing was not accounted for when reconstructing degree-day accumulations, as spawning ground surveys (see Fraser et al. 2019) indicate that brook trout reproduce at least one to two weeks later in groundwater-dominated streams. Similarly, more stable incubation temperatures in groundwater-dominated streams may increase degree-day thresholds needed to hatch and emerge (Grande and Anderson 1990), while some Cape Race populations actively prefer spawning near groundwater seeps within streams (Purchase and Hutchings 2008). Combined, these processes should generate less extreme phenological variation across wild populations than my estimates suggest, although differences in developmental temperature likely remain substantial.

Young-of-the-year brook trout increased in size as they accumulated more degree-days in every stream (Figure 3.6, Table A3.3), but no consistent patterns distinguished groundwater-dominated from rainfall-dominated streams. Nonetheless, slopes of these relationships differed 2.5-fold in groundwater-dominated STBC and LC (Table A3.3), highlighting that effects of temperature on individual growth can vary considerably among streams with similar thermal regimes. Differences in slopes may reflect genetically-based growth rates observed in common garden experiments (Fraser et al. 2019) and spatial variation within streams, while differences in intercepts could be due to population divergence in egg size, which positively influences emergence length (Hutchings 1991). Age-1 brook trout growth rates in Cape Race similarly increased with accumulated degree-days, corroborating this pattern (see Chapter 2). Overall, warming currently appears to increase individual growth rates in Cape Race brook trout, but it is unclear whether this pattern will persist in the future, especially in rainfall-dominated streams with high and rapidly increasing temperatures (e.g. HM, LO, UO). Indeed, continued warming may reduce growth in rainfall-dominated streams while benefiting populations in groundwater-dominated streams, where temperatures are currently suboptimal throughout much of the growing season.

The diverse effects of stream temperature on brook trout phenology and growth imply that Cape Race populations are not responding to climate change the same way. For example, differences in phenology should spread the risk of exposure to episodic events such as floods, droughts, or heatwaves, thereby reducing the likelihood of synchronous declines in survival and growth across populations (Kovach et al. 2016, Kaylor et al. 2021). Additionally, effects of temperature on growth differed considerably among streams with similar thermal regimes, adding another layer of variation that may help stabilize productivity through portfolio effects (Lisi et al. 2013, Kaylor et al. 2022). Improved understanding of fine-scale population and habitat diversity across the species range could provide insights into the resilience of brook trout and the ecosystem services they provide (e.g. supporting fisheries and acting as apex predators in small streams). Identifying and conserving key facets of this diversity will be critical for maintaining healthy

brook trout populations (Fesenmyer et al. 2017), and are likely relevant for the management of other species.

3.4.3 - Factors influencing stream thermal regimes:

Groundwater is likely the dominant influence on stream thermal regimes in Cape Race, although this can only be inferred indirectly in the present study. Streams such as LC and STBC exhibited warmer winter temperatures and much cooler summer temperatures than other streams (Figures 3.2 and 3.4), consistent with signals of groundwater influence (Snyder et al. 2015, Carlson et al. 2019, Hare et al. 2021). In addition to its effect on temperature, groundwater may also dampen fluctuations in streamflow (Mann et al. 1989), and neutralize acidic conditions that reduce brook trout survival (Yates et al. 2019) but are otherwise prevalent in the bog-covered landscape of Cape Race (Figure A3.1). Among eight drainage characteristics explored as predictors of thermal regimes, stream gradient had the strongest influence. High-gradient streams were associated with lower maximum and higher minimum temperatures (Table A3.3), suggesting larger groundwater contributions. Additionally, the inflection point of air-stream temperature relationships exhibited steeper slopes in smaller drainages, while inflection points occurred at higher air temperatures in relatively wide streams (Table A3.3). These patterns demonstrate the importance of catchment characteristics to fish thermal habitat (Lisi et al. 2015, Daigle et al. 2019), but all correlations became non-significant after multiple comparison adjustments and may not be relevant beyond Cape Race.

Stream geomorphology, particularly the presence of ponds within drainages, may also help explain variation in thermal sensitivity among streams. For example, HM was very warm during the summer but exhibited higher winter temperatures (μ = 1.55°C) than other rainfall-dominated streams. This is likely because HM is a deep and slow-moving pond over most of its length (Table A3.1), making it more likely to freeze and thus insulate water from heat loss during the winter (Mohseni and Stefan 1999). A similar dynamic may also influence winter thermal regimes and spatial variation within streams such as BC, UO, and WC, which all contain multiple interconnected ponds (Table A3.1). Although more data are needed to determine the influence of ponds on thermal regimes in Cape Race, air-stream temperature inflection points tended to occur at higher temperatures in drainages with high relative pond area (Table A3.3). Finally, stream temperatures in Cape Race are invariably shaped by the region's unusually cool and wet microclimate, which has few analogues throughout the native range of brook trout and may explain why the highest predicted stream temperatures in Cape Race (~17-19°C) were lower than similar studies conducted in Canada (~23-24°C in Quebec; Daigle et al. 2019) and the United States (~22-23°C in Virginia and Michigan; Snyder et al. 2015, Carlson et al. 2019). Therefore, while fine-scale variation in groundwater contributions may influence stream thermal regimes throughout much of the species range, its consequences will depend on current and future climate conditions, with temperatures expected to exceed thermal optima more often in warmer regions at low latitudes and elevations (Gallagher et al. 2022).

3.5 - Conclusion:

I found considerable temperature variation among small, pristine streams separated by less than 5 km, which likely alters brook trout growth and phenology at a remarkably small spatial scale. Such fine-scale variation has largely been overlooked in past assessments of brook trout conservation status and climate vulnerability (Flebbe et al. 2006, Hudy et al. 2008, Fesenmyer et al. 2017), so future research should develop tools that enable managers to incorporate stream-

specific thermal regimes into decision making. More widespread data collection would facilitate this process, as paired air-stream temperature monitoring (Ishiyama et al. 2023), thermal infrared cameras (Morgan and O'Sullivan 2022, Iwasaki et al. 2023), and high-resolution models (e.g. DeWeber and Wagner 2014) offer promising ways to identify and preserve thermal refuges for many species.

While more refined studies of local groundwater dynamics in Cape Race and elsewhere would be valuable, the fine-scale thermal heterogeneity observed in this study has important conservation implications nonetheless. Firstly, fine-scale differences in stream temperature can play an essential yet underappreciated role in generating response diversity within species, which can provide a buffer against climate change and other human impacts (Schindler et al. 2010, Lisi et al. 2013). Secondly, projected effects of future warming that do not account for stream-specific thermal sensitivities may overestimate the risk of local extirpation in coldwater fishes, as previously noted (Snyder et al. 2015). Finally, matching the spatial scale of population dynamics to the temperatures experienced by those populations (Nadeau et al. 2017b) may be especially difficult in freshwater environments due to their natural fragmentation and variable responses to warming (Daigle et al. 2019, Hare et al. 2021). Overall, my study highlights how for brook trout and other widespread stream fishes, continued efforts to characterize diversity in thermal regimes, phenology and growth at the smallest scale possible should improve forecasts of climate change responses (Urban et al. 2016), and may provide more insights into mechanisms that will shape future persistence.

Tables & Figures:

Table 3.1: Parameter estimates, sample sizes, R^2 and root-mean-square error (RMSE, in °C) values for non-linear relationships between daily average air temperature and stream temperature for ten Cape Race streams from 2012-2021. Sample sizes for BC and HM are marked with asterisks (*) due to missing data after July 2019 in these streams. For reference, μ is the minimum stream temperature, α is the maximum stream temperature, γ is the slope at the inflection point, and β is the temperature where the inflection point occurs (see Equation 3.1). Thermal regimes are categorized as groundwater-dominated, rainfall-dominated, or intermediate (see Results).

Stream	Thermal Regime	μ	α	γ	β	Sample Size	R^2	RMSE
BC	Intermediate	0	16.63	0.21	8.07	959*	0.88	1.87
DY	Intermediate	0.50	16.17	0.26	8.22	1,732	0.90	1.81
HM	Rainfall	1.55	19.25	0.28	9.16	1,119*	0.91	1.92
LC	Groundwater	3.11	10.66	0.28	7.23	1,714	0.79	1.39
LO	Rainfall	0	17.67	0.28	7.82	1,808	0.91	1.94
STBC	Groundwater	2.68	9.73	0.25	6.16	1,652	0.83	1.05
UC	Intermediate	1.01	15.09	0.27	7.01	1,647	0.86	1.97
UO	Rainfall	0.17	18.27	0.24	8.45	1,885	0.92	1.79
WC	Intermediate	2.26	13.58	0.27	8.09	1,878	0.89	1.37
WN	Intermediate	0	17.04	0.18	8.30	1,635	0.90	1.52

Table 3.2: Temporal trends in reconstructed stream temperature in winter (December-February), spring (March-May), summer (June-August), autumn (September-November), and growing season (April-November) months for ten Cape Race streams from 1980-2021. Trends are expressed as slopes (in $°C \cdot year^{-1}$) from regressing mean temperature on year within each stream, and the corresponding air temperature regression slope is shown for reference (bottom). Thermal regimes are categorized as groundwater-dominated, rainfall-dominated, or intermediate (see Results).

Stream	Thermal Regime	Winter	Spring	Summer	Autumn	Growing Season
BC	Intermediate	0.0119	0.0060	0.0271	0.0311	0.0237
DY	Intermediate	0.0106	0.0060	0.0274	0.0336	0.0248
HM	Rainfall	0.0099	0.0062	0.0356	0.0399	0.0304
LC	Groundwater	0.0058	0.0032	0.0113	0.0165	0.0115
LO	Rainfall	0.0125	0.0071	0.0292	0.0391	0.0279
STBC	Groundwater	0.0063	0.0031	0.0091	0.0140	0.0096
UC	Intermediate	0.0113	0.0060	0.0205	0.0300	0.0209
UO	Rainfall	0.0120	0.0067	0.0322	0.0376	0.0283
WC	Intermediate	0.0077	0.0044	0.0195	0.0246	0.0180
WN	Intermediate	0.0119	0.0057	0.0267	0.0288	0.0226
Air	-	0.0314	0.0115	0.0482	0.0451	0.0379

Table 3.3: Summary statistics for dates of degree-day (DD) accumulation since November 1st for putative hatch (500 DD; left side) and emergence (750 DD; right side) thresholds in ten Cape Race streams from 1980-2021. Mean, minimum, and maximum annual dates of degree-day accumulation are shown, with temporal trends displayed as slopes (in days·year^{-1}) from regressing annual date of accumulation on year within each stream. The 40-year change (in days) multiplies the annual slope by 40 to approximate the advancement of developmental timing (in days) over the last four decades in each stream. Thermal regimes are categorized as groundwater-dominated, rainfall-dominated, or intermediate (see Results).

		Hatch Timing (500 DD)					**Emergence Timing (750 DD)**				
Stream	**Thermal Regime**	**Mean**	**Min**	**Max**	**Slope**	**40-Year Change**	**Mean**	**Min**	**Max**	**Slope**	**40-Year Change**
BC	Intermediate	17-Apr	23-Mar	13-May	-0.53	-21	30-May	11-May	19-Jun	-0.34	-13
DY	Intermediate	1-May	10-Apr	25-May	-0.49	-20	9-Jun	21-May	27-Jun	-0.29	-12
HM	Rainfall	31-Mar	2-Mar	27-Apr	-0.62	-25	22-May	5-May	9-Jun	-0.33	-13
LC	Groundwater	25-Feb	14-Feb	13-Mar	-0.29	-11	25-Apr	15-Apr	7-May	-0.23	-9
LO	Rainfall	9-May	16-Apr	3-Jun	-0.48	-19	11-Jun	22-May	1-Jul	-0.31	-12
STBC	Groundwater	1-Mar	16-Feb	17-Mar	-0.29	-11	28-Apr	18-Apr	11-May	-0.22	-9
UC	Intermediate	1-Apr	6-Mar	30-Apr	-0.59	-24	21-May	4-May	9-Jun	-0.34	-13
UO	Rainfall	28-Apr	4-Apr	23-May	-0.55	-22	5-Jun	16-May	25-Jun	-0.33	-13
WC	Intermediate	12-Mar	23-Feb	3-Apr	-0.45	-18	10-May	27-Apr	26-May	-0.29	-11
WN	Intermediate	30-Mar	2-Mar	28-Apr	-0.56	-23	19-May	2-May	7-Jun	-0.34	-14

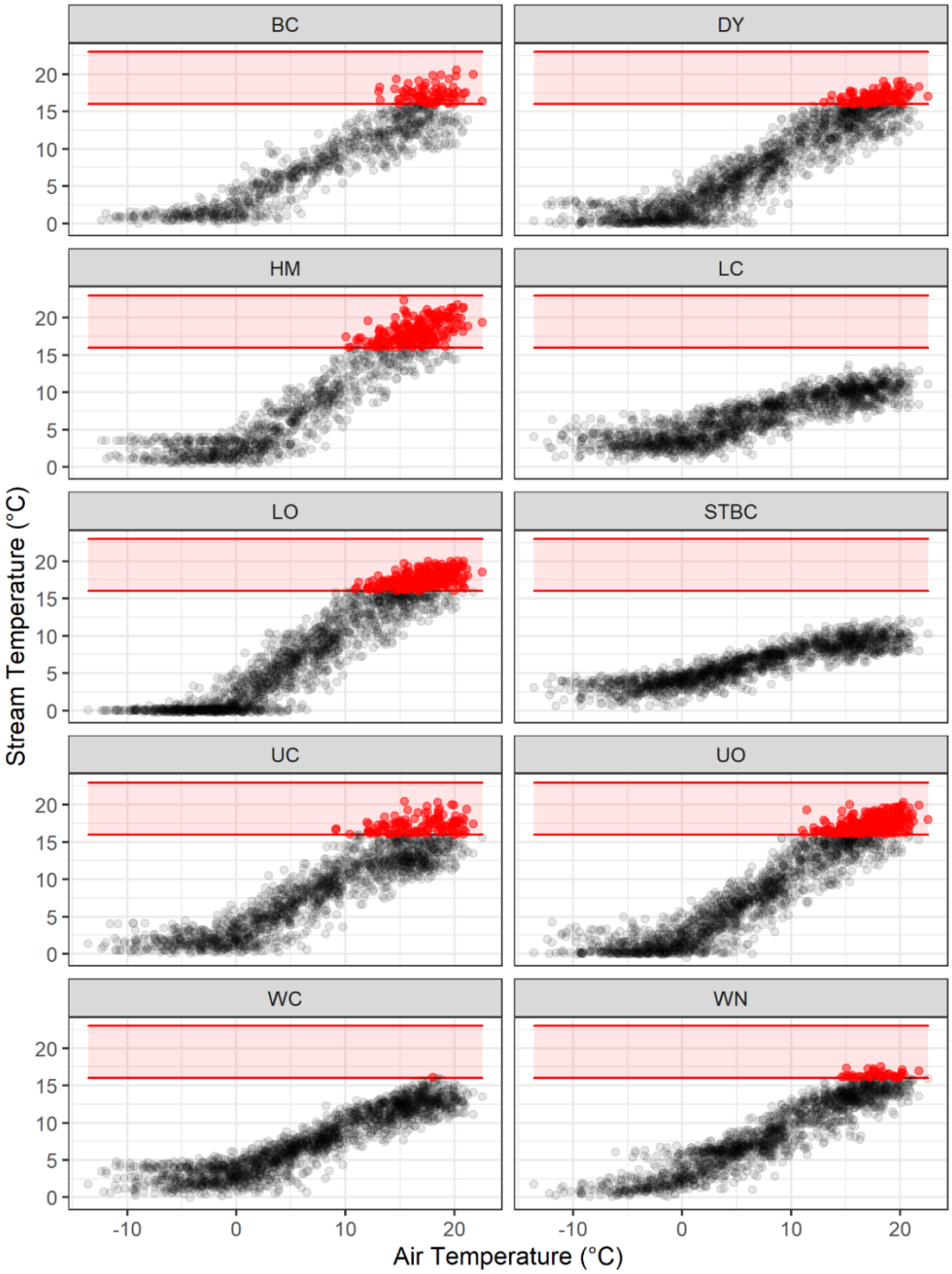

Figure 3.1: Raw data showing relationship between daily average stream temperature and air temperature in ten Cape Race streams. Different colors are used to highlight stream temperature observations below (black points) and above 16°C (red points), with red points corresponding to periods of possible thermal stress. Note the absence of stream temperatures above 16°C in LC and STBC.

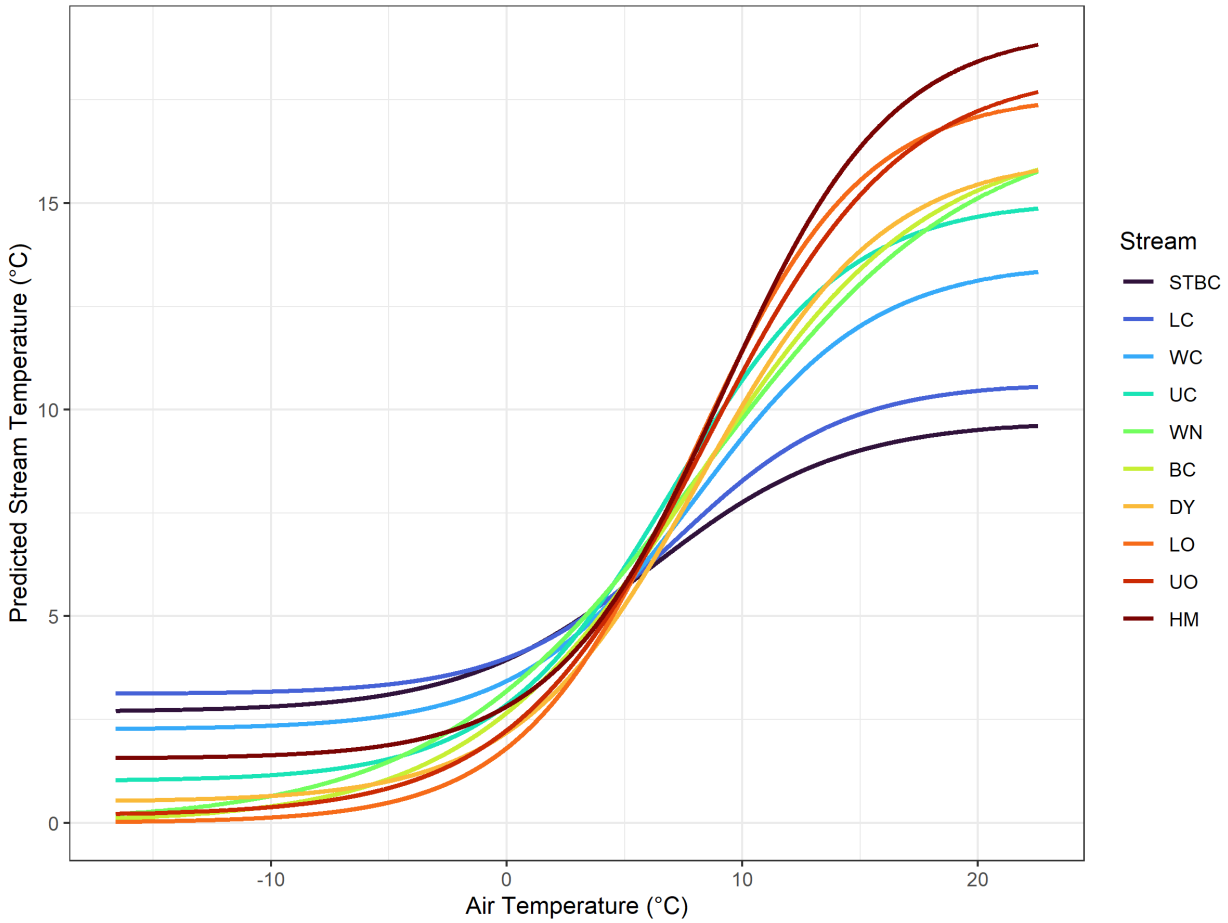

Figure 3.2: Non-linear relationships predicting daily average stream temperature from average air temperature for ten Cape Race streams. Parameter estimates (see Equation 3.1), sample sizes, and R^2 values for each stream are shown in Table 3.1. Streams are colored based on their maximum temperatures, with darker blue colors used for groundwater-dominated streams (STBC and LC) and dark orange or red colors used for rainfall-dominated streams (LO, UO and HM; see Results).

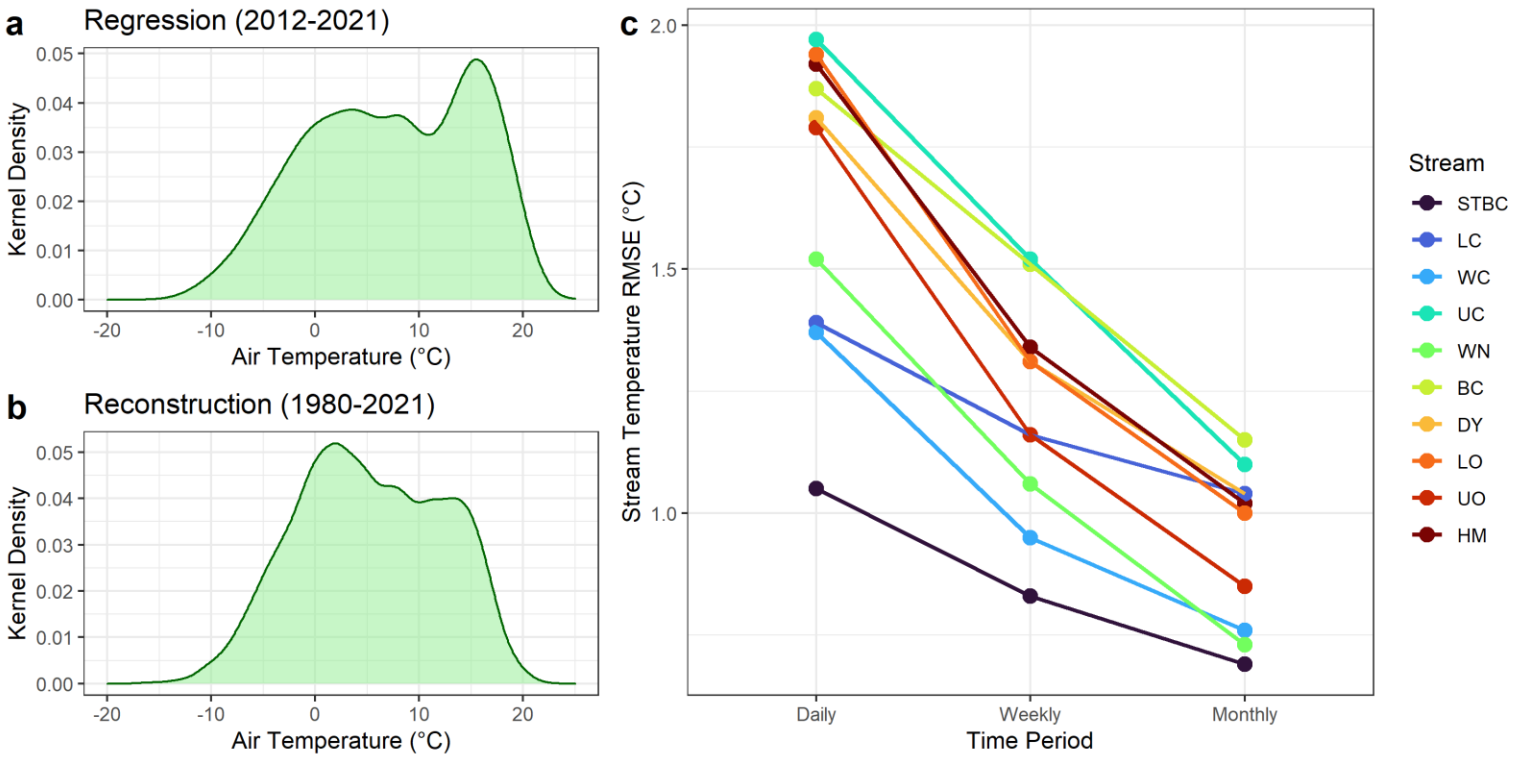

Figure 3.3: Performance of non-linear regression models predicting daily average stream temperature from air temperature. Kernel densities are shown for mean daily air temperatures from 2012-2021 used to estimate stream temperature via non-linear regression (a), and all daily air temperature observations used to reconstruct stream temperature in ten Cape Race streams from 1980-2021 (b). Root-mean-square error (RMSE) values were calculated for daily stream temperatures predicted directly by regression models (see Table 3.1), as well as average stream temperatures calculated over weekly and monthly time periods from 2012-2021 (c). Lower RMSE values suggest that predicted stream temperatures are closer to observed values. Streams are colored based on their maximum temperatures (see Figure 3.2).

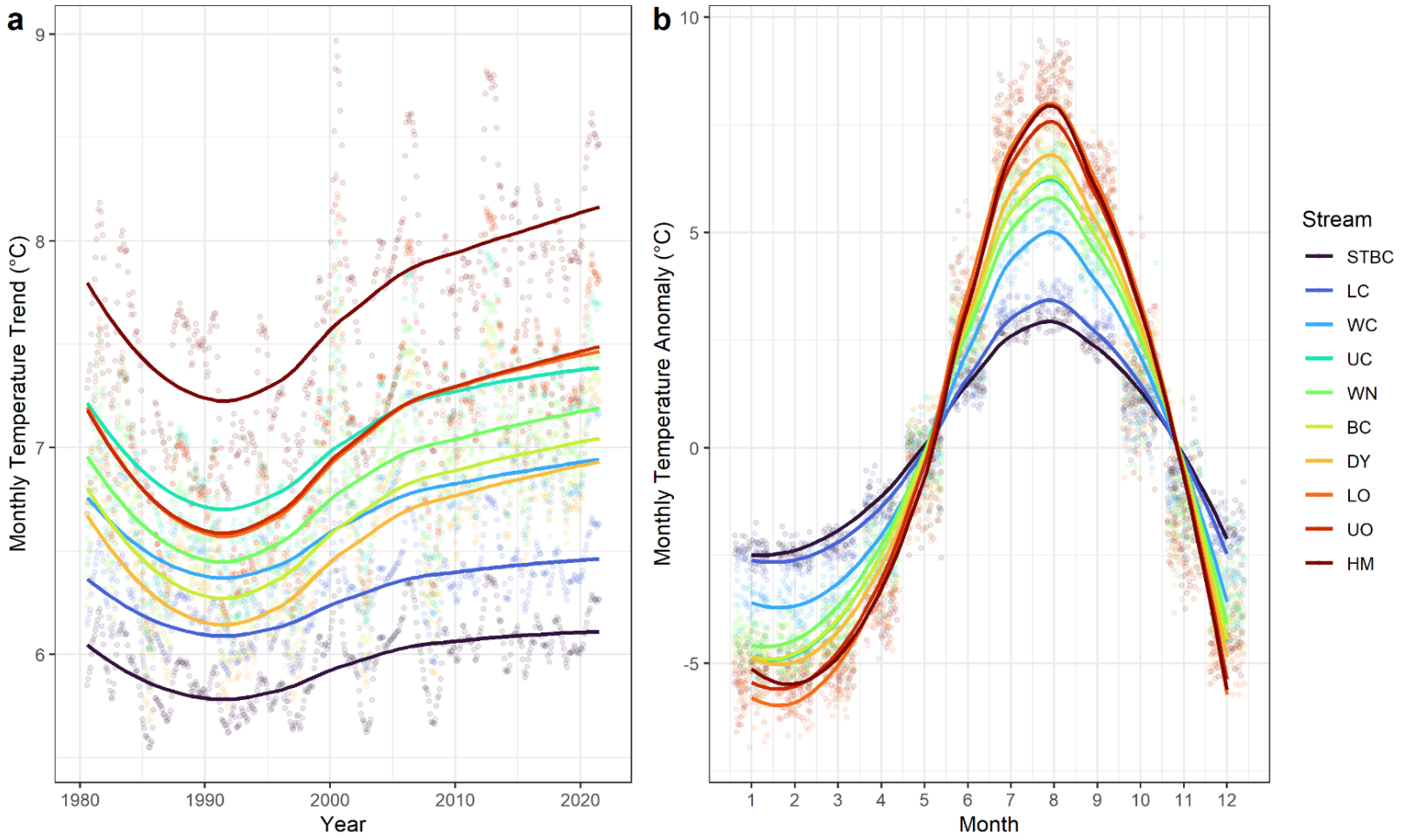

Figure 3.4: Trends (a) and anomalies (b) extracted from reconstructed temperature time-series for ten Cape Race streams. Trends and anomalies were estimated independently during each month and year from 1980-2021 (i.e. trends were estimated with anomalies removed and vice-versa), such that the original time-series can be reproduced by summing the corresponding trend and anomaly values. Monthly estimates each year (transparent points) were fitted with a loess smoother (solid lines) to clarify broader patterns, and anomaly values in (b) were aggregated by month. Streams are colored based on their maximum temperatures (see Figure 3.2).

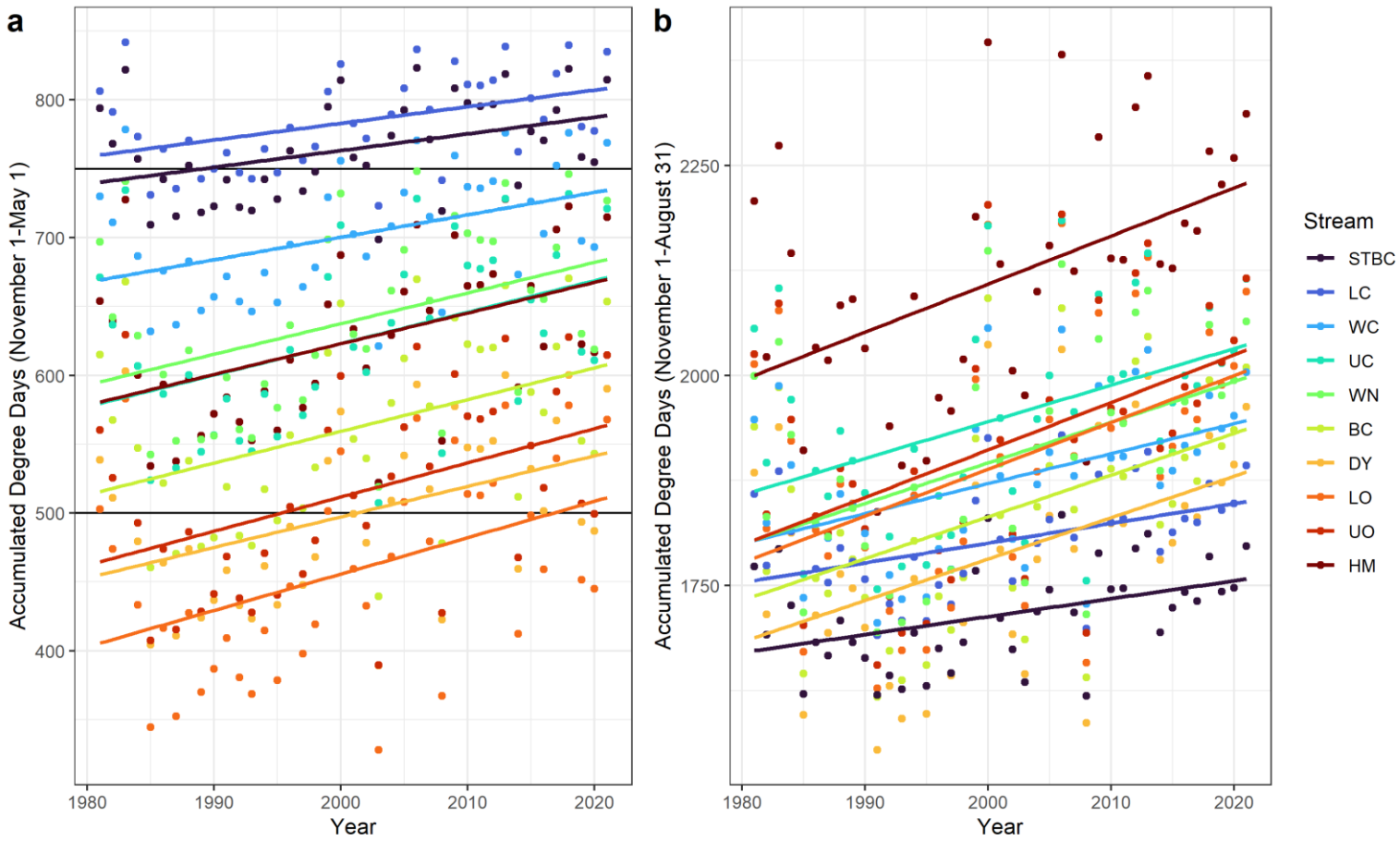

Figure 3.5: Temporal trends in degree-days accumulated from incubation until emergence (a; November 1st-May 1st) and from incubation until the end of summer (b; November 1st-August 31st) for ten Cape Race streams. Horizontal lines in (a) are shown at 500 and 750 degree-days to denote putative thresholds for the timing of hatch and emergence, respectively. Streams are colored based on their maximum temperatures (see Figure 3.2). Note that groundwater-dominated LC and STBC (royal blue and dark blue lines) accumulated the most degree-days before emergence (a), but accumulated the fewest by the end of the summer in recent years (b).

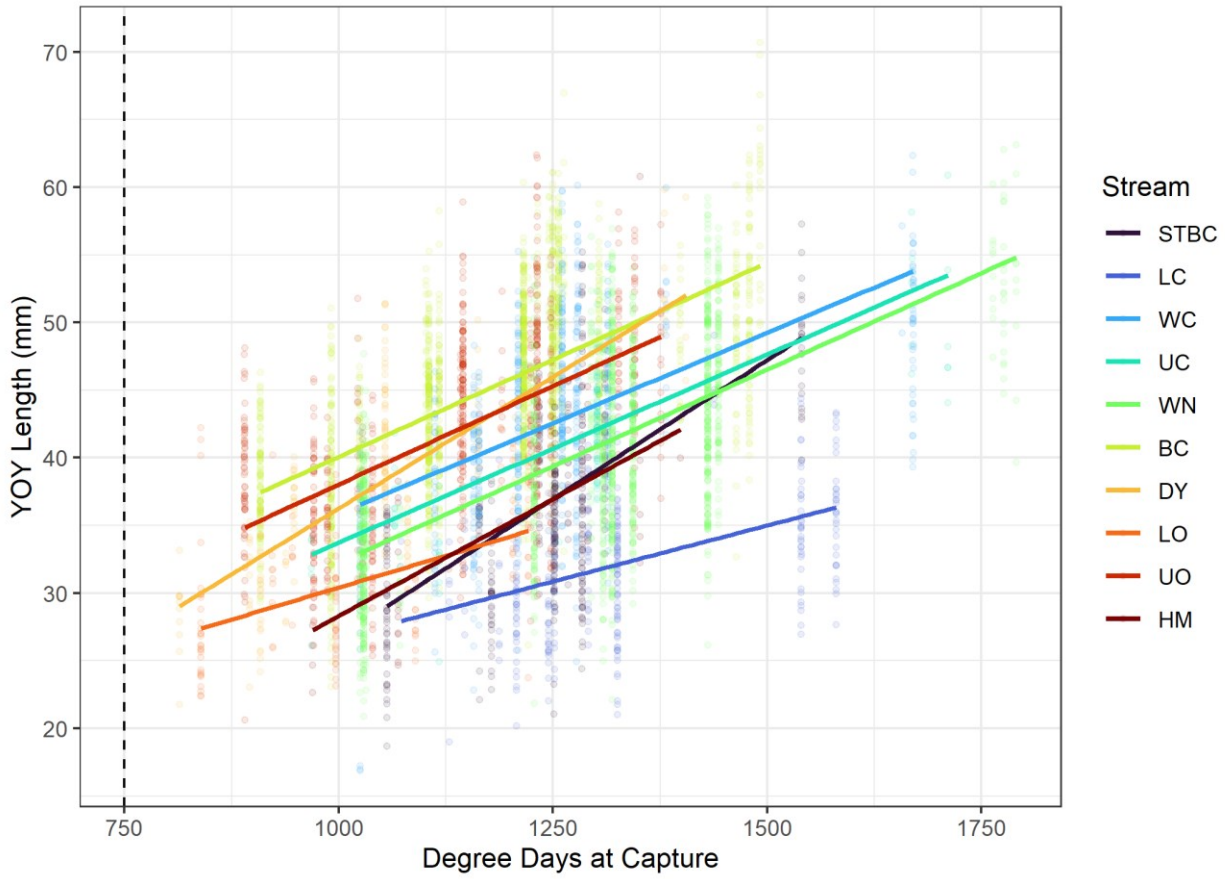

Figure 3.6: Temperature-dependent growth of young-of-the-year (YOY) brook trout in ten Cape Race streams from 2010-2021. Individual fork length is plotted against degree-days accumulated from the start of the incubation period on November 1st the previous year until the date individuals were captured (transparent points), then fitted with stream-specific regressions (solid lines). The putative degree-day threshold for emergence (750 degree-days; dashed vertical line) is shown for reference. Streams are colored based on their maximum temperatures (see Figure 3.2), and regression equations are reported in Table A3.2.

V. Chapter 4: *Fine-scale thermal habitat variation and life history evolution shape the demography of brook trout populations under future climate change*

Abstract:

Many species are at risk of extinction due to climate change, but climate vulnerability can vary considerably among populations of the same species due to multiple mechanisms that are often poorly understood. This is especially likely in species with fine-scale population structure that occupy diverse habitats and exhibit high capacities for phenotypic change via plasticity or evolution. Thus, for many species, there is a need to understand how habitat characteristics, phenotypic plasticity, and evolution contribute to population persistence under climate change. In this chapter, I built individual-based eco-genetic models to simulate the effects of climate change on eight populations of wild brook trout (*Salvelinus fontinalis*) separated by <3 kilometers in Cape Race, Newfoundland, Canada. Models were parameterized with empirical data from mark-recapture surveys, life history studies, common garden experiments, and stream temperature measurements. Three evolving traits governed individual growth and maturation, while stream temperature and density-dependence also influenced growth via phenotypic plasticity. Within each population, six scenarios were explored that represented three rates of atmospheric warming over the next century (0°, 3°, or 6°C), both with and without evolution allowed to occur (genetic CV set to 0.12 or 0, respectively). I found that warming generally caused populations to evolve faster growth, larger size-at-maturation, and earlier age-at-maturation, but less phenotypic change occurred in populations inhabiting colder groundwater-dominated streams. Population biomass tended to decline as rates of warming increased, but the magnitude of decline varied considerably among populations, with extirpation occurring exclusively in warmer rainfall-dominated streams in scenarios when evolution could not occur. Plasticity was sufficient to rescue some populations from extirpation under climate change, but evolution consistently dampened demographic declines and was necessary to rescue populations inhabiting the warmest streams. The critical role of population-specific thermal regimes and life history evolution is broadly applicable for stream-dwelling species, and underscores the importance of accounting for habitat suitability and local adaptation when modeling species responses to climate change.

4.1 Introduction:

Life history evolution is crucial for understanding how variation in individual growth, survival and maturation influence fitness across populations and species, which directly impacts persistence in different environments (Stearns 1992). Life histories can evolve rapidly over ecological time scales (30 generations or less; Hairston and Walton 1986, Reznick et al. 1990, Stockwell and Weeks 1999), which alter eco-evolutionary dynamics that link genetically-based phenotypes to population dynamics (Hendry 2017). Human activities can play a role in eliciting rapid changes in life history traits, with fisheries known to exhibit particularly strong impacts (Fugere and Hendry 2018). Indeed, there is evidence that intense size-selective harvest of Atlantic cod increased mortality of fast-growing individuals, which ultimately selected for slower growth and earlier maturation, thereby reducing population productivity and recovery potential (Olsen et al. 2004, 2005). However, the impacts of climate change on life history evolution have not been extensively studied, despite the potential of consistent warming to impose directional selection on body size, development, and fecundity (Grainger and Levine 2022). Moreover, how evolutionary responses to climate change differ among populations due to

pre-existing variation in life history traits and thermal habitat characteristics is not well understood (Nadeau et al. 2017b).

The extent to which detailed population-specific information is needed for accurate biological risk assessment under climate change is highly relevant for conservation and management decisions. For example, if multiple populations respond similarly to warming temperatures over a large area, then population-specific data may not be needed to accurately characterize the current status and future risk of each population. Moreover, population-specific data is often unavailable while gathering it is costly and labor intensive, so there could be many circumstances where this approach is not the best use of conservation resources (Iacona et al. 2018). Similar concerns apply when considering the mechanisms that impact life history and population dynamics - genotypes, phenotypes, plasticity mediated by environmental conditions, and feedbacks between them can all shape demography (Hendry 2017) but may not be equally relevant in all situations (Bailey et al. 2009). The utility of population-specific information and mechanistic detail in predicting ecological and evolutionary responses to climate change can be assessed through the development of simulation models based on empirical data, which provide a tractable way to compare outcomes across a wide range of scenarios while disentangling mechanistic impacts (Ezard et al. 2009, Norberg et al. 2012).

The development of biologically realistic models of future climate change responses will likely play an increasingly important role in the conservation and management of biodiversity (Urban et al. 2016). Such models allow researchers to compare the risk of extinction across species or populations (Cotto et al. 2016) and quantify the influence of specific processes on model outcomes. Modern software and computing capabilities have facilitated recent development of biological models with unprecedented detail, such as end-to-end (Rose et al. 2015), individual-based (Ayllón et al. 2019) and eco-genetic models (Dunlop et al. 2009). Despite these advances, the data needed to parameterize complex models are unavailable in most taxa (Hoffman and Sgro 2011), which highlights the need to identify well-studied species that are suitable for model development. In addition, there has been little research comparing model outcomes across geographically proximate populations within species, even though population divergence can be considerable at small spatial scales (Richardson et al. 2014) and population comparisons can provide insight into local adaptation while minimizing confounding phylogenetic and biogeographic influences (Hutchings 1993).

Among vertebrates, salmonid fishes are excellent candidates for application of mechanistic models because the evolutionary history, heritability, and plasticity of life history and other phenotypes have been extensively studied (Stearns and Hendry 2004, Carlson and Seamons 2008). Additionally, salmonids commonly exhibit large genetic and phenotypic differences at small spatial scales, which makes them especially useful for comparative analyses among populations (Hutchings 1993, Hilborn et al. 2003). For salmonid species such as brook trout (*Salvelinus fontinalis*), mechanistic models have previously been developed to study the evolution of alternative life history tactics (Thériault et al. 2008) and impacts of compensatory density-dependence on demographic responses to climate change within populations (Bassar et al. 2016), but a model integrating both approaches across many populations has not been attempted. More generally, the role of evolution and phenotypic plasticity in responses to climate change is a critical knowledge gap in salmonid biology (Kovach et al. 2019), and a recent review suggested that only eight published studies have explicitly modeled the effects of climate change on eco-evolutionary dynamics in wild fish populations (O'Sullivan 2021). Therefore, a better

understanding of the combined effects of life history evolution and plasticity on future population dynamics would benefit salmonid conservation and management efforts.

In this chapter, I developed individual-based eco-genetic models that projected the impacts of climate warming on multiple populations of brook trout over the 21st century (~30-50 generations). Importantly, these models can track how two distinct mechanisms contribute to temporal shifts in life history phenotypes - genetic change due to evolution and non-genetic change due to phenotypic plasticity, which accounts for the influence of environmental conditions. Thus, the phenotypes expressed by each individual at a given time are determined by genetic trait values inherited from the previous generation, plus any modifying effects of the environment (e.g. temperature). My objectives were to (1) build individual-based eco-genetic models that simulated demography and life history evolution in eight populations of brook trout, (2) compare population responses across three different climate change scenarios, and (3) assess the influence of life history evolution on climate change responses in each population. In general, I predict that increasing levels of climate warming will increase growth and length-at-maturity at the individual level, while reducing abundance at the population level. I also predict that population-specific responses to climate change will vary, and will be most strongly influenced by observed differences in thermal habitat among populations (see Chapter 3). Changes in biomass will be more complex, and will differ based on the magnitude of population-specific increases in growth (which positively affects biomass) and declines in abundance (which negatively affects biomass). This framework will provide crucial insights into how much population-specific data and mechanistic detail affect predictions about population dynamics under climate change.

4.2 Methods:

4.2.1 - Study system and model parameterization:

Models were built to represent eight genetically distinct brook trout populations in Cape Race, Newfoundland, Canada (population abbreviations: BC, DY, HM, LC, STBC, UC, UO, and WC). These populations exhibit a gradient of life history strategies, despite sharing a common evolutionary origin (Danzmann et al. 1998) and experiencing similar climate conditions due to their geographic proximity (separated by <3 km). This gradient is best captured by two contrasting populations: UC exhibited low growth, low survival (i.e. shorter lifespan), early maturation, and high reproductive effort, while WC displayed high growth, high survival, delayed maturation, and low reproductive effort (Figure 4.1). Other populations showed consistent patterns between these extremes, as larger adult body size was positively associated with average age and maximum age of spawning adults (Figure 4.1a,b), while the ratio between adult and juvenile growth was negatively correlated with reproductive effort (Figure 4.1d). Life history patterns were remarkably similar to seminal research on Cape Race brook trout by Hutchings (1993, 1994, 1996), who studied three populations that were not included in this chapter. Hutchings (1993) argued that population variation in growth and survival emerged from differences in the availability of food and overwintering habitat within each stream, and my results suggest this may be a general phenomenon across Cape Race. However, my research also suggests that thermal habitat plays a critical role, as populations in colder groundwater-dominated streams such as LC and STBC exhibit lower growth, higher juvenile survival, and should warm significantly less in the future than warmer rainfall-dominated streams such as DY, HM and UO (Yates et al. 2019, see Chapters 2 and 3).

The evolving life history traits of interest in this study were maximum growth rate and probabilistic maturation reaction norms (PMRNs hereafter) describing the size and age at which individuals mature (Heino et al. 2002). PMRNs were expressed as a linear function with slope and intercept terms, with the PMRN intercept corresponding to the median length-at-maturation when the slope is equal to zero (Heino et al. 2002). Model parameterization was informed by recent research in Cape Race brook trout, which has shown genetically-based population differences in maximum growth rates in common garden experiments (Fraser et al. 2019), while growth rates of wild individuals decline with conspecific density (Matte et al. 2020b) and increase with stream temperature during the growing season (see Chapters 2 and 3). Additionally, empirical length and weight data were available for thousands of individuals from mark-recapture surveys conducted in each population between 2010 and 2022 (Wood et al. 2014; see Chapter 2), while the size and age of spawning individuals has been described in targeted field studies (Bernos and Fraser 2016, Zastavniouk et al. 2017). Detailed age data are unavailable for Cape Race populations in recent years, but age-0 and age-1 individuals can be confidently distinguished based on length frequency distributions (see Appendix 2). To estimate age in older individuals, I used finite mixture models in the *mixtools* package in R (Benaglia et al. 2009) to separate the length distribution into three discrete normal distributions representing age-2, age-3, and age-4+. This process was repeated for every sampling year with length data available from 2010-2022, and used to assign individuals to age-classes each year (after Hoxmeier and Dieterman 2011).

Growth curves were constructed to relate individual size to estimated age using the von Bertalanffy model, as well as an alternative model by Lester et al. (2004) that estimated growth separately before and after maturation. PMRN slopes were assumed to be zero, while PMRN intercepts representing the length at which the probability of maturation is 50% were estimated via logistic regression. Population-specific growth and maturation patterns are summarized in Figure 4.2, which support previous observations that populations with relatively low adult growth rates (e.g. LC, STBC, UC) tend to mature at smaller sizes and earlier ages, and likely invest more energy into reproduction. Further details about model structure and parameterization are described in the sections below. Population-specific parameters are listed in Table 4.1, while Table 4.2 shows relevant parameters that were shared across all populations.

4.2.2 - Climate change:

All models were constructed to run over 300 years with an annual time step. The first 200 years exhibited stable temperature to allow populations to reach equilibrium (Dunlop et al. 2009), then temperature was subsequently increased at a constant rate during the last 100 years, representing climate change from 2001 to 2100. Annual mean temperature acted as the key environmental forcing on brook trout populations, and affected individual growth and mortality (see Sections 4.2.4 and 4.2.5). Air temperature at a given time (T_t) was determined by:

$$T_t = \begin{cases} T_0 \; if \; t \leq 200 \\ T_0 + (\Delta T \cdot (t - 200)) \; if \; t > 200 \end{cases} \qquad (Eq. 4.1)$$

where T_0 is the initial air temperature, ΔT is the rate of air temperature warming (in °C·year^{-1}).

Air temperature was assumed to be identical for all populations, but stream temperatures experienced by each population varied based on stream thermal sensitivity, moderated by local

groundwater inputs (see Chapter 3). The mean growing season stream temperature from April-November (GT_t) was calculated from air temperature based on the equation:

$$GT_t = GT_{int} + \left(GT_{slope} \cdot T_t\right) \qquad (Eq. 4.2)$$

where GT_{int} and GT_{slope} represent the intercept and slope from regression equations converting annual air temperature to growing season stream temperature experienced by each population. Similarly, mean summer stream temperature from June-August (ST_t) was calculated from air temperature using a linear conversion:

$$ST_t = ST_{int} + \left(ST_{slope} \cdot T_t\right) \qquad (Eq. 4.3)$$

where ST_{int} and ST_{slope} represent the population-specific intercept and slope from conversion equations. Both stream temperature metrics were simulated without stochasticity, and air temperature was increased by 0°, 3°, or 6°C over the last 100 years of each simulation (see Section 4.2.6). Variation in stream temperature conversion equations (Table 4.1) resulted in each population experiencing different thermal regimes (Figure 4.3), with populations inhabiting rainfall-dominated streams (DY, HM, UO) exhibiting higher mean values and faster rates of warming than those in groundwater-dominated streams (LC, STBC).

4.2.3 - Reproduction and inheritance:

For populations to persist and evolve through time, new individuals need to be added each year through reproduction, and acquire evolving traits through inheritance. To initiate this process, the number of offspring at time *t* was calculated as the sum of fecundity across all mature females. Fecundity (f_t) of individual females increased with length (L_t) according to the function:

$$f_t = c \cdot L_t^d \qquad (Eq. 4.4)$$

where *c* is a constant and *d* is an exponential term. This allowed larger fish to produce more offspring (Gobin et al. 2016), which is supported by empirical studies of Cape Race brook trout populations (Hutchings 1993, Fraser et al. 2019). The number of recruits that enter the model at time *t* (R_t) was determined by a population-specific Ricker stock-recruitment function:

$$R_t = \alpha \cdot S_{t-1} \cdot e^{(-\beta \cdot S_{t-1})} \cdot \epsilon_R \qquad (Eq. 4.5)$$

where S_{t-1} is the total number of mature adults of both sexes during the previous time step (when reproduction occurred), α is the density-independent term describing the maximum number of recruits per spawner and β is the density-dependent compensation term that determines the shape of the curve when adult abundance is high (Hilborn and Walters 1992; Table 4.1). The multiplicative error term ε_R was drawn from a lognormal distribution with a mean of one and a shared coefficient of variation, in order to add stochasticity to the number of recruits produced each year. Stock-recruitment parameters were tuned to roughly reproduce the average total abundance of each population observed in mark-recapture surveys from 2010-2022, which varies over three orders of magnitude among Cape Race populations (DY, HM, and UC have relatively low abundance; see N_{mean} in Table 4.1). Notably, recruitment was much lower than the number of offspring, but adults that produced more offspring (i.e. larger females) were assumed to produce more recruits, which has been observed in Cape Race (Morrissey and Ferguson 2009).

The parentage of all recruited individuals was tracked and used to determine evolving trait genotypes. Individual genotypes followed a quantitative genetic model of inheritance, with

random mating of males and females. Sexes were treated equally for all phenotypes, and all simulations were initialized with a 50:50 sex ratio. Individual offspring inherited three evolving traits that characterized growth (maximum growth rate) and maturation (PMRN intercept and slope), with segregation-recombination variances that equaled half of parental values (Dunlop et al. 2009). Offspring genotypes were not identical, but drawn from a normal distribution centered on mid-parent values with a variance determined by a shared genetic coefficient of variation (Gobin et al. 2021). Models of inheritance were informed by common garden experiments conducted in Cape Race brook trout populations (Table 4.2), which established the genetic basis for growth (Fraser et al. 2019) and estimated heritability and quantitative genetic variation for a suite of early life history traits (Wood et al. 2015). Specifically, I assumed a heritability (h^2) of 0.39 and a genetic coefficient of variation (CV_G) of 0.12 (but see Section 4.2.6). This heritability was within the observed range for growth and life-history traits from a past review of salmonids (Carlson and Seamons 2008), as well as estimates from wild juveniles in one Cape Race brook trout population (Morrissey and Ferguson 2011).

4.2.4 - Growth and maturation:

Individuals grew larger and matured with age based upon evolving trait genotypes and plasticity (i.e. density-dependence and stream temperature) within each population. Increasing temperatures driven by climate change (Figure 4.3) therefore acted as a selective pressure that could alter the phenotypic and genetic composition of populations. Individual growth was age-structured and modeled using the biphasic growth model of Lester et al. (2004), which accounts for the allocation of energy towards gonads after maturity. Maturation status of each individual was determined before growth occurred at each time step. For immature individuals, length at a given time step (L_t) increased linearly according to the equation:

$$L_t = h_t \cdot A_t \qquad (Eq. 4.6)$$

where h_t is the annual growth rate and A_t denotes age in years at time step t.

For mature individuals, length increased according to an asymptotic function:

$$L_t = \left(\frac{3}{3+g}\right) \cdot L_{t-1} + \left(3 \cdot \frac{h_t}{3+g}\right) \qquad (Eq. 4.7)$$

where g is the population-specific reproductive effort, which was calculated from the von Bertalanffy growth coefficient estimated from mature individuals (Lester et al. 2004).

In both cases, expressed growth rates (h_t) were a function of the maximum growth rate genotype (h_{max}) that each individual inherited from its parents, and scaled according to population biomass (B_t) and average stream temperature during the growing season (GT_t) experienced during that time step (modified from Gobin et al. 2021; Figure 4.2). This was modeled by the equation:

$$h_t = \left(\frac{h_{max}}{m + n \cdot B_t}\right) + 1.67 \cdot \left(GT_t - GT_{ref}\right) \qquad (Eq. 4.8)$$

where n represents the loss of food due to competition among individuals, m represents the loss of food due to other causes (after Walters and Post 1993), GT_{ref} is the reference growing season stream temperature representing the average across all populations from 2010-2022, and 1.67 is the effect of relative growing season stream temperature on growth (i.e. if GT_t exceeds GT_{ref} by

1°C, h_t increases by 1.67 mm·year^{-1} on average). Growing season temperature was assumed to positively and linearly influence growth rates based on data from mark-recapture surveys (see Chapters 2 and 3). Thus, expressed growth was density- and temperature-dependent, and these effects acted as non-evolving sources of phenotypic plasticity (Table 4.2).

Population biomass at a given time was obtained by summing the weights (W_t) of all individuals age-1 and older. Weights were determined by population-specific length-weight relationships:

$$W_t = a \cdot L_t^b \qquad (Eq. 4.9)$$

where a is a constant and b is an exponential term (Table 4.1).

Individual maturity status (M_t) was treated as a binary variable (i.e. 0 for immature, 1 for mature) and determined by population-specific PMRNs (Figure 4.2). During each time step, the probability of maturing (p_{mat}) at a given age (A_t) and length (L_t) was estimated from a function:

$$p_{mat} = f(A_t, L_t \mid I, S, w) \qquad (Eq. 4.10)$$

where I is the PMRN intercept genotype and S is the PMRN slope genotype that each individual inherited from its parents, and w is the PMRN width that described the range of sizes at which individuals can mature at each age. A random number drawn above or below the estimated probability determined individual maturity status (Gobin et al. 2016). Initial population means for PMRN slopes were assumed to be zero with a width of 20mm (Figure 4.2), while PMRN intercepts were estimated via logistic regression as the length at 50% maturation based on lengths of wild adults (Zastavniouk et al. 2017) and a similar number of putatively immature age-0 and age-1 individuals collected during mark-recapture surveys. Although detailed data on the lengths of immature fish at older age-classes were unavailable, assumed PMRNs reflect the fact that Cape Race brook trout are short-lived and mature at a relatively narrow range of ages (two to four years; Hutchings 1993).

4.2.5 - Mortality:

Mortality of individuals after recruitment occurred at the end of each time step. The annual probability of natural mortality (p_{mort}) was calculated by the equation:

$$p_{mort} = \left(1 - e^{-Z} + (M_t \cdot C)\right) + \left(0.0284 \cdot \left(ST_t - ST_{ref}\right)\right) \qquad (Eq. 4.11)$$

where Z is the population-specific instantaneous mortality rate, M_t is individual maturity status (immature=0, mature=1), C is the population-specific cost of reproduction, ST_t is the population-specific summer stream temperature, and ST_{ref} is the fixed reference summer stream temperature representing the average across all populations from 2010-2022. Similar to maturity status, a random number drawn above or below the estimated probability determined individual survival.

Instantaneous mortality rates were based on longevity data collected by Bernos and Fraser (2016) and estimated using a model from Hoenig (1983). Increasing summer stream temperature was assumed to increase mortality based on recent transplant experiments of Cape Race brook trout, which found that exposure to high summer temperatures (>15°C over ~3 months) increased mortality (Yates et al. 2019). This response was similar across populations, and was further supported by laboratory experiments that showed limited population variation in thermal tolerance (Wells et al. 2016). Similarly, the effect of maturity status reflects consistent increases

in overwintering mortality observed after spawning (Hutchings 1994, Morrissey and Ferguson 2009), as the cost of reproduction (C) was assumed to be related to reproductive effort (g). Specifically, populations with high reproductive effort (LC, STBC, UC) exhibited a 30% increase in mortality after maturity (see Morrissey and Ferguson 2009), while those with intermediate effort (BC, HM, UO) displayed a 20% increase, and those with low effort (DY, WC) had only a 10% increase (Table 4.1).

4.2.6 - Model scenarios and comparative analysis:

Climate models suggest an average of 2-3°C of atmospheric warming is most plausible by the end of the century, and recent studies suggest that higher emission scenarios (e.g. RCP8.5) are probably unrealistic (Burgess et al. 2023). Nonetheless, northern regions such as Newfoundland are warming faster than the global average (increase of 0.35°C·decade^{-1} from 1980-2021; see Chapter 3), so I tested three climate scenarios with annual air temperature increases of 0°C, 3°C, and 6°C by the end of the century. This was done by adjusting the value of the ΔT parameter to equal 0, 0.03, or 0.06 respectively (Table 4.2). Additionally, each climate scenario was run with evolving trait genotypes allowed to change over time according to their heritability and genetic variance, or held constant at their initial values by setting genetic variance to zero (Table 4.2), yielding a total of six scenarios tested for all eight populations. To compare effects of climate change across scenarios, I calculated observed changes over the last 100 years of twenty independent simulations for three evolving trait genotypes (maximum growth rate, PMRN intercept and slope), two measures of population demography (total abundance and biomass), and three phenotypic traits (expressed growth rate, female length and age at maturation). Growth curves were also constructed to visualize how length-at-age for individuals age 1 to 5 changed over time (simulation years 100, 200, and 299) across all six scenarios.

4.3 Results:

4.3.1 - Evolving trait genotypes:

As expected, none of the three evolving trait genotypes changed over time in simulations where genetic variation was set to zero, regardless of the climate scenario (Table 4.3). However, significant changes in genotypes often occurred in simulations when traits were allowed to evolve, but the magnitude varied by trait, population, and climate scenario (Table 4.3, Figure 4.4).

PMRN intercepts (I; see Equation 4.10) exhibited varying degrees of evolutionary change over the last 100 simulation years under 0°C of warming, ranging from a reduction of 2.8 mm in HM to an increase of 16.4 mm in STBC. Specifically, PMRN intercepts tended to increase most in populations inhabiting cold groundwater-dominated streams (LC, STBC) and decline in populations with low abundance occupying warm rainfall-dominated streams (DY, HM), but changed relatively little in other populations (BC, UC, UO, WC; Table 4.3). Similar patterns were observed in other climate change scenarios, but average outcomes became more clearly linked to stream thermal regimes with 3° and 6°C of warming (Figure 4.4; see top row). This was exemplified by PMRN intercepts in UO, which were relatively stable without warming but declined over time as warming intensified, ultimately becoming more similar to other rainfall-dominated streams (Table 4.3). Notably, there appeared to be more variation across simulations in populations exhibiting low abundance (DY, HM, UC), which became more prominent as the amount of warming increased (Figure 4.4).

PMRN slopes (*S*; see Equation 4.10) were initially assumed to be flat (slope = 0 mm·year^{-1}) and did not change considerably on average over the last 100 simulation years. Across all populations and climate change scenarios, the largest observed evolutionary changes in PMRN slopes were an increase of 0.059 mm·year^{-1} (DY under 6°C of warming) and a decrease of 0.089 mm·year^{-1} (HM under 6°C of warming; Table 4.3). Considering that Cape Race brook trout rarely live beyond age-5 (Figure 4.1b), simulated changes in slopes translate to a difference in median length-at-maturity of only 0.3-0.5 mm over the lifetime of most individuals, which is probably not biologically significant. Moreover, outcomes varied across simulations in every population, with a range of change spanning zero (Figure 4.4; see middle row).

Maximum growth rates (h_{max}; see Equation 4.8) consistently increased over time across all simulations, but the magnitude of evolutionary change differed across thermal regimes (Figure 4.4; see bottom row). Under 0°C of warming, growth rates increased by 31.2 to 51.8 mm·year^{-1}, but changes in growth were lower for populations within cold groundwater-dominated streams (LC, STBC; Table 4.3). Similar patterns were observed as rates of warming increased, with populations generally evolving faster maximum growth rates under 3°C (36.2 to 56 mm·year^{-1}) and 6°C of warming (38.4 to 54.5 mm·year^{-1}) while maintaining comparable population differences (Table 4.3). Similar to PMRN intercepts, greater variation across simulations was evident in populations with low abundance (DY, HM, UC; Figure 4.4).

4.3.2 - Population demography:

Simulated population demography showed that brook trout abundance and biomass remained stable or increased modestly when warming did not occur (0°C scenario), while increasing temperatures by 3° or 6°C tended to reduce population abundance and biomass (Table 4.3). However, there was considerable population variation in demographic outcomes that was largely driven by stream thermal regimes within each scenario (Figures 4.5 and 4.6). Changes in abundance and biomass were calculated over the last 100 simulation years, but were expressed as percent differences in order to account for disparities among populations in average biomass (range = 1.4 to 62.5 kg) and spawner abundance (range = 44 to 2,015 individuals; Table 4.1).

Climate change tended to reduce abundance in simulations with no evolution, but the magnitude of population decline differed based on stream thermal regime (Figure 4.5; see top row). Population abundance changed little on average under 0°C of warming, ranging from a 5% decline to a 7% increase in abundance (Table 4.3). In contrast, abundance declined in every population exposed to 3°C of warming, with severe declines of 53 to 98% in populations occupying warm rainfall-dominated streams (DY, HM, UO) while more modest declines of 16 to 22% were observed in populations inhabiting cold rainfall-dominated streams (LC, STBC; Table 4.3). Abundance declined even more precipitously under 6°C of warming, ranging from complete extirpation (100% decline) of HM within the warmest stream to a 22% decline of STBC in the coldest stream (Table 4.3).

Overall, life history evolution appeared to dampen climate-induced declines in abundance, but populations experiencing the warmest thermal regimes were still more negatively affected than those inhabiting cooler streams in every scenario (Figure 4.5; see bottom row). In models where populations were allowed to evolve over time, relatively small changes in abundance occurred when temperatures warmed by 0°C, spanning a 2% decline to a 17% increase on average (Table 4.3). When temperatures warmed by 3°C, abundance declined by 24 to 38% in warm rainfall-

dominated streams (DY, HM, UO) but only declined by 8 to 19% within cold groundwater-dominated streams (LC, STBC; Table 4.3). Similarly under 6°C of warming, a 74% decline in abundance occurred for the population inhabiting the warmest stream (HM), while a decline of only 25% was observed in the coldest stream (STBC; Table 4.3).

In general, changes in simulated biomass exhibited similar patterns to population abundance (Figure 4.6), but were more complex due to the evolution of increased maximum growth and divergent PMRN intercepts (see Section 4.3.1), which indirectly affected individual maturation schedules, length, and weight. For biomass in model scenarios with no evolution (Figure 4.6; see top row), most populations were relatively stable with 0°C of warming, with changes varying from a 4% decline to a 9% increase (Table 4.3). Conversely, biomass was reduced in every population under 3°C (8 to 99% declines) and 6°C of warming (17 to 100% declines), with the most severe reductions occurring in the three warmest rainfall-dominated streams (DY, HM, UO; Table 4.3). In model scenarios when evolution was allowed to occur (Figure 4.6; see bottom row), biomass increased in every population under 0°C of warming (13 to 26% rise; Table 4.3). With 3°C of warming, biomass rose slightly by 2 to 9% in populations occupying cold groundwater-dominated streams (LC, STBC), but declined by 32% within the warmest stream (HM) and was reduced slightly in other populations (0.2 to 9% declines; Table 4.3). Biomass fell in every population under 6°C of warming, but declines were strongly ordered by stream thermal regime, ranging from 3% in STBC to 40% in HM (Table 4.3).

4.3.3 - Phenotypes:

Climate-induced changes in three phenotypic traits related to growth (expressed growth rate) and maturation (length- and age-at-maturation for females) were assessed, which integrated changes in evolving trait genotypes and plasticity due to changes in stream temperature and density-dependent growth (see Equation 4.8). Differences in the average phenotype of all surviving individuals were calculated over the last 100 simulation years as a proxy for shifts in phenotypic composition within each population across all six scenarios. Similar to evolving trait genotypes and population demography, simulated results mostly varied according to stream thermal regime within each scenario (Table 4.3). However, when evolution was not allowed to occur, phenotypic change could not be calculated in two populations with low abundance, DY (6°C scenario) and HM (3° and 6°C scenarios) because steep declines in abundance meant that no individuals remained during the last year of most simulations (Figure 4.5).

Expressed growth rate phenotypes (h_t; see Equation 4.8) generally increased over time in every population and scenario. In scenarios when evolution was not allowed to occur, changes were small and variable on average under 0°C of warming (range: decrease of 2.8 mm·year^{-1} to increase of 1.5 mm·year^{-1}), but individuals consistently grew faster under 3° (3.6 to 22 mm·year^{-1} increase), and 6°C (5.6 to 43.1 mm·year^{-1} increase) of warming (Table 4.3). Larger gains in growth were evident in populations inhabiting warm rainfall-dominated streams, such as UO. Increases in simulated growth were disproportionately higher in scenarios when evolution was allowed to occur, as expressed growth progressively rose under 0° (range: 0.2 to 6.8 mm·year^{-1} increase), 3° (5.2 to 30.8 mm·year^{-1} increase), and 6°C (10.9 to 86.5 mm·year^{-1} increase) of warming, with the smallest increases occurring in populations within colder streams (LC, STBC) and larger increases in populations occupying warmer streams (DY, HM, UO; Table 4.3).

Female length-at-maturation phenotypes most commonly increased within simulations, but exhibited idiosyncratic changes across populations and scenarios. In scenarios without evolution, changes were small under 0°C of warming (range: 2.8 mm decrease to 3.3 mm increase), but became more skewed towards larger length-at-maturation with 3° (5.9 mm decrease to 35.4 mm increase), and 6°C of warming (9.4 mm decrease in UC, increase of 0.1 to 28.4 mm elsewhere; Table 4.3). Results were not strongly ordered by stream thermal regime, but females tended to mature at modestly larger sizes in populations within cold groundwater-dominated streams (LC, STBC; Table 4.3). In scenarios with evolution, length-at-maturation declined slightly on average in DY and UC under 0°C of warming (0.8 to 1 mm decrease) but rose in other populations (2.6 to 15.4 mm increase), with the largest increases in groundwater-dominated LC and STBC (Table 4.3). Similar patterns occurred as rates of warming increased, as females matured at smaller sizes in two relatively warm streams (DY, UO), but otherwise exhibited larger length-at-maturation under 3°C (increase of 4.5 to 19.8 mm) and 6°C (increase of 6.4 to 19.8 mm) of warming, while larger increases tended to occur in populations within relatively cold streams such as LC, STBC, and WC (Table 4.3).

Female age-at-maturation phenotypes most commonly declined across simulations, indicating a general shift towards earlier reproduction under climate change. With 0°C of atmospheric warming, shifts in average age-at-maturation were small and variable in scenarios without evolution (range: 0.04 year decrease to 0.11 year increase) and with evolution allowed to occur (0.15 year decrease to 0.29 year increase; Table 4.3). With 3°C of atmospheric warming, female age-at-maturation was consistently reduced in scenarios when evolution was not allowed to occur (0.09 to 0.48 year decrease) and when evolution did occur (0.01 to 0.54 year decrease; Table 4.3). Similar patterns occurred under 6°C of atmospheric warming, as females always matured at younger ages in scenarios both without (0.28 to 0.75 year decrease) and with evolution (0.17 to 0.81 year decrease; Table 4.3). When rates of warming were higher (3° and 6°C), the largest reductions in age-at-maturation tended to occur in populations occupying warmer streams (DY, HM, UO), while shifts were less pronounced within cooler streams (LC, STBC, WC; Table 4.3).

4.3.4 - Growth curves:

For nearly all populations, increasing the rate of climate warming led to progressively larger simulated length-at-age (Figure 4.7). Additionally, when evolution was not allowed to occur (Figure 4.7; see top panels), length-at-age remained largely static as simulations progressed through time, but tended to increase over time when evolution did occur (Figure 4.7; see bottom panels). The only exception to this pattern was HM, which was stable or showed shifts towards smaller size-at-age under climate change and over time within simulations, possibly due to a combination of demographic stochasticity (see Section 4.3.2) and its exposure to the warmest stream temperatures in Cape Race (Figure 4.3), which reduced samples sizes via high mortality. With the exception of HM, the degree to which growth curves changed in each population appeared to be largely driven by stream thermal regime and population-specific reproductive effort (Table 4.1). Specifically, two populations in warm rainfall-dominated streams (DY, UO) exhibited the biggest increases in length-at-age as the rate of warming increased, with average simulated lengths at age-5 exceeding 350 mm under 6°C of warming and when evolution occurred (Figure 4.7). This is substantially larger than any individual observed in current Cape Race monitoring programs (maximum length ~ 230 mm; Figure 4.2). In contrast, two populations occupying the coldest groundwater-dominated streams exhibited the smallest

climate-induced increases in modeled length-at-age (LC, STBC), with age-5 lengths never exceeding 200 mm.

4.4 Discussion:

By simulating the effects of climate warming on life history evolution, demography, and phenotypes of Cape Race brook trout populations, I uncovered substantial variation in multiple responses. Through a combination of evolution and phenotypic plasticity, increasing rates of warming from 0° to 3° to 6°C over 100 years generally caused individuals to develop faster growth rates, larger sizes-at-maturation, and earlier ages-at-maturation over time, which should increase body size and reproductive output in every population. These gains were offset by higher mortality as rates of warming increased, which reduced abundance and caused severe declines in some populations under 3° and 6°C of warming. However, declines in abundance were dampened when evolution was allowed to occur, which generally increased the magnitude of phenotypic change within simulations. How these processes combined to shape changes in population biomass was strongly influenced by stream thermal regime, as populations inhabiting colder groundwater-dominated streams (LC, STBC) exhibited less phenotypic change and smaller increases in mortality than those in warmer rainfall-dominated streams (DY, HM, UO). As a result, population biomass in groundwater-dominated streams declined only slightly (under 6°C) or sometimes even increased (under 3°C), while biomass within rainfall-dominated streams was consistently reduced and some populations were extirpated completely under 6°C of warming. Therefore, my models suggest that brook trout as a species will exhibit diverse responses to future climate change, even among geographically proximate populations. The vital role of fine-scale thermal habitat variation, phenotypic plasticity, and life history evolution is broadly relevant for predicting biodiversity loss, and highlights the importance of conserving natural habitat variation and adaptive potential in many species.

4.4.1 - Importance of thermal habitat

The variation observed in model outcomes across Cape Race shows that demographic responses to climate change in brook trout are likely to be population-specific, even at very small spatial scales. Although populations were separated by <3 kilometers, thermal habitat differed significantly and appeared to be the most influential driver of future population demography. This is best illustrated by simulated changes in biomass, which integrated shifts in abundance, growth phenotypes, and stream temperature within each population. In the scenario with evolution under 6°C of atmospheric warming, biomass was predicted to decline by 32% over 100 years in the population inhabiting the warmest rainfall-dominated stream in Cape Race (HM), but only declined by 3% in the population occupying the coldest groundwater-dominated stream (STBC; Table 4.3). Between these extremes, changes in population biomass were ordered by thermal regime (Figure 4.6), with the average percent change in population biomass showing a strong correlation with population-specific ST_{slope} values ($r = -0.93$; Tables 4.1 and 4.3). This suggests that, for species with diverse populations like brook trout, caution is warranted when interpreting coarse-scale models of climate vulnerability that average over many discrete populations (e.g. Clark et al. 2001, Flebbe et al. 2006; see Chapter 2). Similarly, model predictions from one population may not necessarily support accurate inferences about other populations, or indeed the species as a whole, especially without information about the thermal

sensitivity of occupied streams (Snyder et al. 2015). Comparable population-specific responses to climate change are likely common in other species, especially those with large ranges, fragmented habitats, and significant population differentiation (Amburgey et al. 2018, Rowland et al. 2022).

My results differed from a previous study that projected the effects of climate change on four more southerly brook trout populations, which suggested that warming was likely to drive every population to extirpation (Bassar et al. 2016). However, thermal regimes experienced by populations in Bassar et al. (2016) were very similar, while average summer stream temperatures and rates of warming in Cape Race differed considerably (Figure 4.3; see Chapter 3). This could suggest that fine-scale population variation in demographic responses to climate change is not universal, but depends on geographic and landscape contexts that influence local thermal regimes. For example, compared to other well-studied trout streams in the United States and Canada (e.g. Bassar et al. 2016, Carlson et al. 2019, Daigle et al. 2019, Lu et al. 2023), streams in Cape Race are more physically isolated and exhibit relatively cool stream temperatures, likely because they are situated at a higher latitude with a cool microclimate (see Chapter 3). Additionally, drainages in Cape Race are uninhabited by humans and thus unimpacted by land use change or groundwater withdrawal, which can homogenize stream temperature (Stranko et al. 2008, Lapides et al. 2022). Overall, diversity in thermal regimes should contribute to the stability and resilience of brook trout populations under future climate change, both in Cape Race (see Chapter 2) and elsewhere (Valentine et al. 2024). Nonetheless, simulated abundance and biomass declined in every Cape Race population under 6°C of warming, highlighting the importance of mitigating climate change as much as possible (IPCC 2023). To understand key drivers of variation in climate-induced biodiversity loss, more mechanistic modeling studies are needed to improve predictions of demographic responses to climate change across a wide range of species, populations, and environmental contexts (O'Sullivan 2021, Urban et al. 2023).

Thermal habitat also influenced the magnitude of climate-induced genetic and phenotypic shifts in Cape Race brook trout, as populations within cooler groundwater-dominated streams (LC, STBC) exhibited relatively little change in maximum growth genotypes, expressed growth rates, and female maturation patterns within simulations (Table 4.3). Indeed, warming stream temperature acted as a driver of plasticity and selection (see Section 4.4.2 below), while initial temperatures and rates of warming were both considerably lower in colder streams. Modeled growth curves also shifted towards larger size-at-age in every population, but generally changed more in warmer streams (DY, UO) than in colder streams (Figure 4.7). However, changes in growth curves could not be explained by thermal regimes alone, as growth increased considerably more in WC than in UC, even though WC experienced cooler temperatures (Figure 4.7). This could be due to much lower reproductive effort in WC (g = 0.47 in WC, g = 0.92 in UC). High reproductive effort in UC, which has the shortest lifespan out of any study population (Figure 4.1b), constrains the amount of energy allocated towards growth after maturation occurs (Lester et al. 2004), making changes in growth less pronounced. This may also partially explain why growth curves were relatively static in groundwater-dominated LC and STBC, which exhibited high reproductive effort (g = 0.77 and 0.92, respectively; Table 4.1). Demographic stochasticity may have also played a role, as the least abundant populations (DY, HM, UC) showed more variable phenotypic and demographic shifts across simulations (Figures 4.4 and 4.6), likely due to random fluctuations in survival having larger per-capita effects in small populations (Lande et al. 1993).

4.4.2 - Effects of life history evolution on persistence

Life history evolution in Cape Race brook trout considerably dampened declines in simulated population abundance and biomass due to climate change, supporting the notion that adaptive potential will be a key determinant of future persistence (Reed et al. 2011, Urban et al. 2023). Under 6°C of warming, the population occupying the warmest stream (HM) was always extirpated when evolution did not occur (i.e. genetic variance was set to zero), but abundance declined by 74% and biomass was only reduced by 32% when populations evolved through time. Similar demographic buffering was evident in other populations, especially for biomass (Figure 4.6), likely because evolution enabled larger and more rapid changes in life history phenotypes under climate change. Indeed, expressed growth rates increased progressively as rates of warming rose from 0° to 3° to 6°C, and this pattern was even stronger when evolution was allowed to occur (Table 4.3). In the scenario with evolution under 6°C of warming, expressed growth roughly doubled in four populations (BC, DY, HM, UO) on average over the course of 300 simulation years, or 100-150 generations. Mechanistically, increased growing season temperatures and warming-induced declines in population biomass both resulted in faster growth rates through phenotypic plasticity (Equation 4.8), and this often resulted in considerably larger individual body size under climate change, even when evolution did not occur (Figure 4.7). When evolution took place, increases in growth were intensified because fecundity increased exponentially with body size and individual contributions to the next generation were proportional to fecundity (see Section 4.2.3), which should select for adults with higher maximum growth genotypes. Faster expressed growth rates also likely contributed to females maturing earlier and at larger sizes in most populations under climate change (Table 4.3), which should increase adult length, weight, fecundity, and frequency of reproduction over time. Together, these phenotypic changes increased individual-level biomass production and offset losses caused by climate-induced reductions in survival, thus explaining the beneficial effect of life history evolution on population biomass within simulations (Figure 4.6). My results support prior assertions that population-specific life histories in Cape Race are adaptive and influence fitness (Hutchings 1993, 1994, Fraser et al. 2019), but plasticity in individual growth also plays an important role (Hutchings 1996).

There is considerable interest in evolutionary rescue (Carlson et al. 2014) and plastic rescue (Snell-Rood et al. 2018) under climate change, which describe the ability of phenotypic change via evolution or plasticity to prevent extirpation. For example, two previous modeling studies in salmonids showed that warmer temperature and changes in precipitation under climate change will likely lead to extirpation, overwhelming the rescue effects of plasticity (Bassar et al. 2016) and evolution (Ayllón et al. 2019). However, my research shows that plastic rescue and evolutionary rescue should both contribute to persistence in Cape Race brook trout under climate change. For populations in streams with cold (LC, STBC, WC) or intermediate thermal regimes (BC, UC), plasticity alone was sufficient to prevent extirpation under 6°C of warming, although declines in abundance were dampened when evolution occurred (Figure 4.5). In contrast, plastic rescue was insufficient for populations inhabiting the warmest streams (DY, HM, UO) under 6°C of warming, but these populations persisted when plasticity and evolutionary rescue occurred together (Figure 4.5). Thus, the combined effects of phenotypic change through plasticity and life history evolution enabled all eight simulated Cape Race populations to persist in a warming world, but the relative importance of evolutionary rescue varied by thermal regime. This further underscores the need for more modeling studies across a greater range of environments in

salmonids (O'Sullivan 2021), and suggests that habitat heterogeneity could influence the strength of plastic rescue and evolutionary rescue in other species (Nadeau et al. 2017b).

4.4.3 - Limitations

My research, like any modeling study, includes assumptions and simplifications that limit the generalizability results, which could be improved upon in future work. First, my current models captured a simplified range of future atmospheric warming scenarios over the next century, but using empirical climate projections based on shared socioeconomic pathways (SSPs) would be more realistic (Burgess et al. 2023, IPCC 2023). I also did not account for climate-induced changes in precipitation, which can intensify or offset the effects of warming on salmonids (see Chapter 1). Although I did not observe strong precipitation effects in Cape Race (see Chapter 2), multiple studies in the United States found that increased rainfall during brook trout incubation and emergence is associated with lower juvenile abundance (Warren et al. 2009, Sweka and Wagner 2022, Maitland and Latzka 2022, Valentine et al. 2024). In Newfoundland, recent ensemble projections suggest air temperature will increase by 4-6°C and precipitation will increase 0-10% by the end of this century (Leduc et al. 2019, Sobie et al. 2023). Thus, depending on the exact climate model and emission scenario considered, my simulations that assumed 6°C of atmospheric warming this century may be unrealistic. Downscaled projections from multiple climate models across various SSPs are available from the Canadian government (Sobie et al. 2023) and other global databases (e.g. Karger et al. 2023), which should be leveraged to create more representative climate scenarios for Cape Race populations in the future.

Second, current models may not accurately represent life history evolution in Cape Race brook trout populations. For example, I assumed heritability and genetic variance values based on a common garden experiment conducted on juveniles from multiple Cape Race populations (Wood et al. 2015). These values were within the observed range from other studies of salmonids, but were relatively high (Carlson and Seamons 2008, Gobin et al. 2021), and could have thus overestimated the rate of evolution. The assumed heritability may also not apply to all life-stages in wild populations (Morrissey and Ferguson 2011), while natural selection can potentially reduce the genetic variance of fitness-linked traits over time (Stearns and Hendry 2004). Correlations and tradeoffs between life history traits were also not accounted for, even though they can significantly affect evolution (Stearns 1992). Most notably, the substantial increase in maximum growth genotypes could suggest that growth-mortality tradeoffs were not sufficiently strong, even though they were indirectly included through the effects of temperature. Similarly, salmonid life history traits are highly polygenic (Tsai et al. 2015, Ali et al. 2020; but see Pearse et al. 2014) and may thus be influenced by correlations among genetic loci that influence multiple traits. More research is needed on genetic and phenotypic correlations among life history traits in Cape Race brook trout, as well as the genomic basis of traits and the maintenance of individual genetic variation.

Finally, the exact contribution of climate change, stream thermal regimes, evolution, and plasticity to model outcomes has not been quantified in the current study. For example, while stream thermal regimes clearly structured population-specific responses to climate warming in Cape Race, the abundance and reproductive effort of each population also influenced patterns of phenotypic change (see Section 4.4.1). Additionally, I did not assess model outcomes without density-dependent growth (after Gobin et al. 2021), which likely exacerbated climate-induced increases in growth because population biomass often declined at the same time (Figure 4.6). In

the future, a more generalized model parameterization coupled with a targeted sensitivity analysis (Dunlop et al. 2009, Bernos et al. 2023) is needed to quantify the importance of stream thermal regimes, especially compared to the impacts of more realistic climate scenarios (e.g. projections from multiple SSPs; IPCC 2023), density-dependence, and other population attributes that affected model outcomes (e.g. initial population abundance and life history traits).

4.5 Conclusion:

To my knowledge, this is one of very few assessments of climate change impacts that accounts for variation in habitat characteristics, life history traits, demography, and evolutionary potential across many wild populations (Urban et al. 2016). My research is also the first to apply this modeling approach to brook trout, which was enabled by decades of past research in Cape Race (Hutchings 1993, Wood et al. 2014, Fraser et al. 2019). My work illustrates how thermal regimes, plasticity, and evolution will all play a significant role in shaping future population demography within species under climate change. In accordance with initial predictions, abundance declined while individual growth rates and sizes-at-maturation mostly increased as the climate warmed. Together, this caused biomass to decline in every population under 6°C of warming, but the exact decline varied based on thermal habitat. Specifically, simulated biomass was only slightly reduced in groundwater-dominated streams, which experienced colder average stream temperatures and slower rates of warming, while biomass declined more substantially in warmer rainfall-dominated streams. However, phenotypic plasticity and life history evolution dampened declines in abundance and, when combined, allowed every population to withstand up to 6°C of warming across simulations, with evolutionary rescue playing a more critical role in populations occupying the warmest streams.

Collectively, the diversity in responses to climate change observed among Cape Race brook trout populations is remarkable considering they are separated by <3 km, share a common ancestor (Danzmann et al. 1998), and are exposed to the same climate. This fine-scale population variation may be broadly applicable to salmonids (Schindler et al. 2010; see Chapter 2), as well as other species that are genetically and ecologically distinct at small spatial scales while occupying diverse habitats with varying thermal sensitivities (Nadeau et al. 2017b; see Chapter 3). By building more mechanistic models that capture population diversity in thermal habitat, life history traits, plasticity, and evolutionary potential across a range of conditions, biodiversity scientists should gain further insight into the fate of species and the stability of species ranges in a warmer future.

4.6 Tables & Figures:

Table 4.1: Population-specific parameters for individual-based eco-genetic models of eight Cape Race brook trout populations. Parameters in bold italic text are evolving traits, shown as initial mean values for genotypes drawn from a normal distribution.

Parameter	Process	BC	DY	HM	LC	STBC	UC	UO	WC	Description
α	Demography	12	15	11	9	8	15	11	9	Density-independent term for Ricker stock-recruitment function
β	Demography	3.7e-4	1.9e-2	2.6e-2	4.6e-3	3.6e-3	2.3e-2	8.0e-4	2.3e-3	Density-dependent term for Ricker stock-recruitment function
Z	Demography	0.77	0.84	0.70	0.72	0.65	0.91	0.70	0.70	Instantaneous mortality rate for immature individuals
C	Demography	0.15	0.08	0.14	0.22	0.20	0.27	0.14	0.07	Reproductive cost, which additively increases mortality after maturation
B_{mean}	Demography	62.5	2.5	1.9	3.9	9.9	1.4	47.6	22.4	Mean biomass (kg), excluding age-0 individuals
N_{mean}	Demography	2015	62	44	141	462	44	1622	616	Mean number of spawners
I	***Maturation***	***100.6***	***99.8***	***111.7***	***94.2***	***90.8***	***99.6***	***101.4***	***110.6***	***Initial PMRN intercept (mm)***
S	***Maturation***	***0***	***0***	***0***	***0***	***0***	***0***	***0***	***0***	***Initial PMRN slope with age (mm/year)***
$\boldsymbol{h_{max}}$	***Growth***	***114.8***	***109.4***	***114.4***	***109.3***	***121.8***	***121.4***	***108.0***	***119.4***	***Initial maximum growth rate (mm/year)***
g	Growth	0.59	0.47	0.57	0.77	0.92	0.92	0.52	0.47	Reproductive effort derived from von Bertalanffy growth coefficient
a	Growth	1.1e-5	2.7e-5	1.6e-5	2.1e-5	2.7e-5	6.7e-6	2.5e-5	1.5e-5	Constant for length-weight relationship
b	Growth	3.02	2.85	2.95	2.87	2.82	3.13	2.84	2.96	Exponent for length-weight relationship
ST_{int}	Climate change	8.33	8.44	9.39	7.52	7.14	9.35	8.98	8.12	Intercept for converting air temperature to summer stream temperature
ST_{slope}	Climate change	0.65	0.68	0.87	0.29	0.23	0.53	0.78	0.49	Slope for converting air temperature to summer stream temperature
GT_{int}	Climate change	5.34	5.06	5.70	5.66	5.52	5.96	5.34	5.59	Intercept for converting air temperature to growing season stream temperature
GT_{slope}	Climate change	0.67	0.71	0.85	0.35	0.30	0.63	0.80	0.52	Slope for converting air temperature to growing season stream temperature

Table 4.2: Shared parameters for individual-based eco-genetic models of eight Cape Race brook trout populations. Values separated by commas represent values used in three different climate change scenarios (for ΔT) and two evolution scenarios for each population (for CV_G).

Parameter	Process	Value	Description
c	Demography	5.3e-4	Constant for length-fecundity relationship
d	Demography	2.45	Exponent for length-fecundity relationship
ε_R	Demography	0.2	Coefficient of variation in recruitment
w	Maturation	20	PMRN width (5-95% probability of maturation, in mm)
n	Growth	-0.39	Effect of biomass (relative to the population average, B_{mean}) on intraspecific competition for food
m	Growth	1	Effect of biomass on other causes of food loss
GT_{ref}	Climate change	9.72	Reference growing season stream temperature for growth effect
ST_{ref}	Climate change	11.68	Reference summer stream temperature for mortality effect
T_0	Climate change	5.24	Initial mean annual air temperature
ΔT	Climate change	0, 0.03, 0.06	Rate of increase in annual air temperature per year
h^2	Evolution	0.39	Heritability of all evolving traits, based on common garden experiments
CV_G	Evolution	0, 0.12	Coefficient of genetic variation of all evolving traits

Table 4.3: Average change in Cape Race brook trout evolving traits, demography, and phenotypes over the last 100 years of twenty independent simulations, across six scenarios.

			No Evolution			Evolution		
Change in Output	**Type**	**Population**	**0°C**	**3°C**	**6°C**	**0°C**	**3°C**	**6°C**
PMRN Intercept (mm)	Evolving Trait Genotype	BC	N/A	N/A	N/A	0.4	1.4	0.1
		DY	N/A	N/A	N/A	-0.6	-8.4	-6.6
		HM	N/A	N/A	N/A	-2.8	-1.8	-8.2
		LC	N/A	N/A	N/A	7.0	5.8	5.4
		STBC	N/A	N/A	N/A	16.4	12.3	11.8
		UC	N/A	N/A	N/A	2.9	4.1	0.4
		UO	N/A	N/A	N/A	1.0	-3.0	-7.0
		WC	N/A	N/A	N/A	0.7	0.6	0.2
PMRN Slope (mm/year)	Evolving Trait Genotype	BC	N/A	N/A	N/A	0	0.01	0
		DY	N/A	N/A	N/A	0	0.03	0.06
		HM	N/A	N/A	N/A	0.05	-0.06	-0.08
		LC	N/A	N/A	N/A	0.03	0	0.01
		STBC	N/A	N/A	N/A	0.05	0.02	0.04
		UC	N/A	N/A	N/A	0.03	-0.02	-0.02
		UO	N/A	N/A	N/A	0.01	0	-0.02
		WC	N/A	N/A	N/A	0	-0.03	0.01
Max Growth (mm/year)	Evolving Trait Genotype	BC	N/A	N/A	N/A	47.9	49.2	52.1
		DY	N/A	N/A	N/A	46.7	44.1	51.3
		HM	N/A	N/A	N/A	47.8	51.6	50.2
		LC	N/A	N/A	N/A	36.4	38.9	40.5
		STBC	N/A	N/A	N/A	31.2	36.2	38.4
		UC	N/A	N/A	N/A	51.8	56.0	54.5
		UO	N/A	N/A	N/A	43.1	46.9	53.2
		WC	N/A	N/A	N/A	44.8	46.4	48.0
Abundance (% change)	Demography	BC	1	-32	-83	1	-41	-60
		DY	-5	-53	-99	13	-25	-47
		HM	7	-98	-100	16	-38	-74
		LC	0	-22	-33	3	-19	-27
		STBC	4	-16	-22	-2	-8	-25
		UC	5	-47	-76	17	-26	-41
		UO	7	-78	-96	8	-24	-57
		WC	-1	-24	-46	7	-32	-45
Biomass (% change)	Demography	BC	2	-27	-68	13	-9	-30
		DY	-4	-42	-96	27	-6	-25
		HM	-3	-99	-100	26	-32	-32
		LC	3	-11	-23	18	2	-6
		STBC	4	-8	-17	14	9	-3
		UC	9	-23	-58	21	-5	-11
		UO	1	-58	-92	23	-8	-40
		WC	0	-21	-41	20	0	-17

			No Evolution			Evolution		
Change in Output	**Type**	**Population**	**0°C**	**3°C**	**6°C**	**0°C**	**3°C**	**6°C**
Expressed Growth (mm/year)	Phenotype	BC	0	10.4	31.9	3.5	19.7	38.4
		DY	1.2	13.4	-	5.2	22.6	39.2
		HM	-2.8	-	-	6.8	30.8	86.5
		LC	0.6	3.7	6.3	1.3	7.4	12.2
		STBC	-1.2	3.6	5.6	0.2	5.2	10.9
		UC	1.5	14.6	25.8	3.2	10.9	25.9
		UO	-0.7	22.0	43.1	3.8	24.5	51.9
		WC	-0.4	7.3	16.0	1.1	14.5	25.5
Female Length at Maturation (mm)	Phenotype	BC	-0.2	-4.2	28.4	3.3	19.8	9.3
		DY	3.3	9.8	-	-0.8	-9.2	-5.5
		HM	-2.8	-	-	4.0	13.9	6.4
		LC	0.8	5.2	8.0	7.4	11.1	9.3
		STBC	0.9	1.2	0.1	15.4	14.7	17.4
		UC	-1.2	5.8	-9.4	-1.0	4.5	13.5
		UO	-1.2	35.4	22.2	2.6	-14.5	-10.4
		WC	-0.5	-5.9	0.6	3.6	15.6	19.8
Female Age at Maturation (years)	Phenotype	BC	0	-0.48	-0.61	-0.04	-0.21	-0.65
		DY	0.11	-0.28	-	-0.15	-0.50	-0.67
		HM	0	-	-	-0.05	-0.42	-0.75
		LC	0	-0.15	-0.28	0.03	-0.20	-0.44
		STBC	-0.01	-0.15	-0.29	0.29	-0.01	-0.17
		UC	-0.03	-0.23	-0.75	-0.02	-0.38	-0.65
		UO	0.01	-0.09	-0.65	-0.06	-0.54	-0.81
		WC	-0.04	-0.38	-0.56	-0.03	-0.17	-0.35

Note: Non-applicable values (N/A) were used for cells where evolving trait genotypes were fixed through time in 'No Evolution' scenarios, and dashes (-) were used for cells where population declines meant that average phenotypes could not be calculated for some populations and scenarios (see DY and HM).

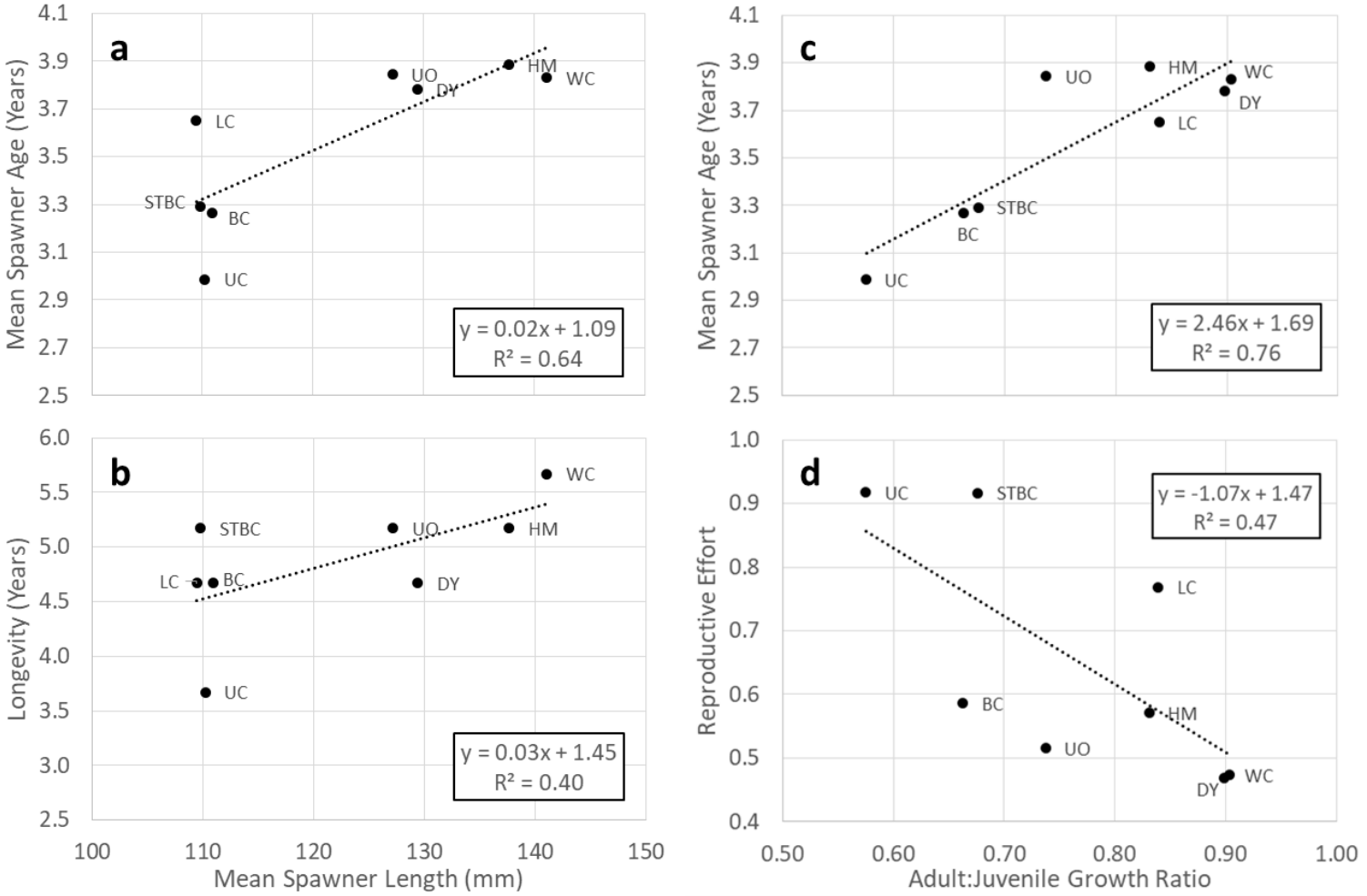

Figure 4.1: Empirical life history patterns in eight Cape Race brook trout populations. Mean age (a) and longevity (b) of spawning adults from Bernos and Fraser (2016) are plotted against mean length of spawning adults from Zastavniouk et al. (2017). Similarly, mean age of spawning adults (c) and reproductive effort estimated from von Bertalanffy growth coefficients (d) are plotted against the adult:juvenile growth ratio. Growth ratios were calculated based on predicted size at age-1 (for juveniles) and change in predicted size from age-2 to age-4 (for adults) from von Bertalanffy growth curves, similar to previous methods used by Hutchings (1993). Linear regression equations and R^2 values are shown separately in each panel for reference.

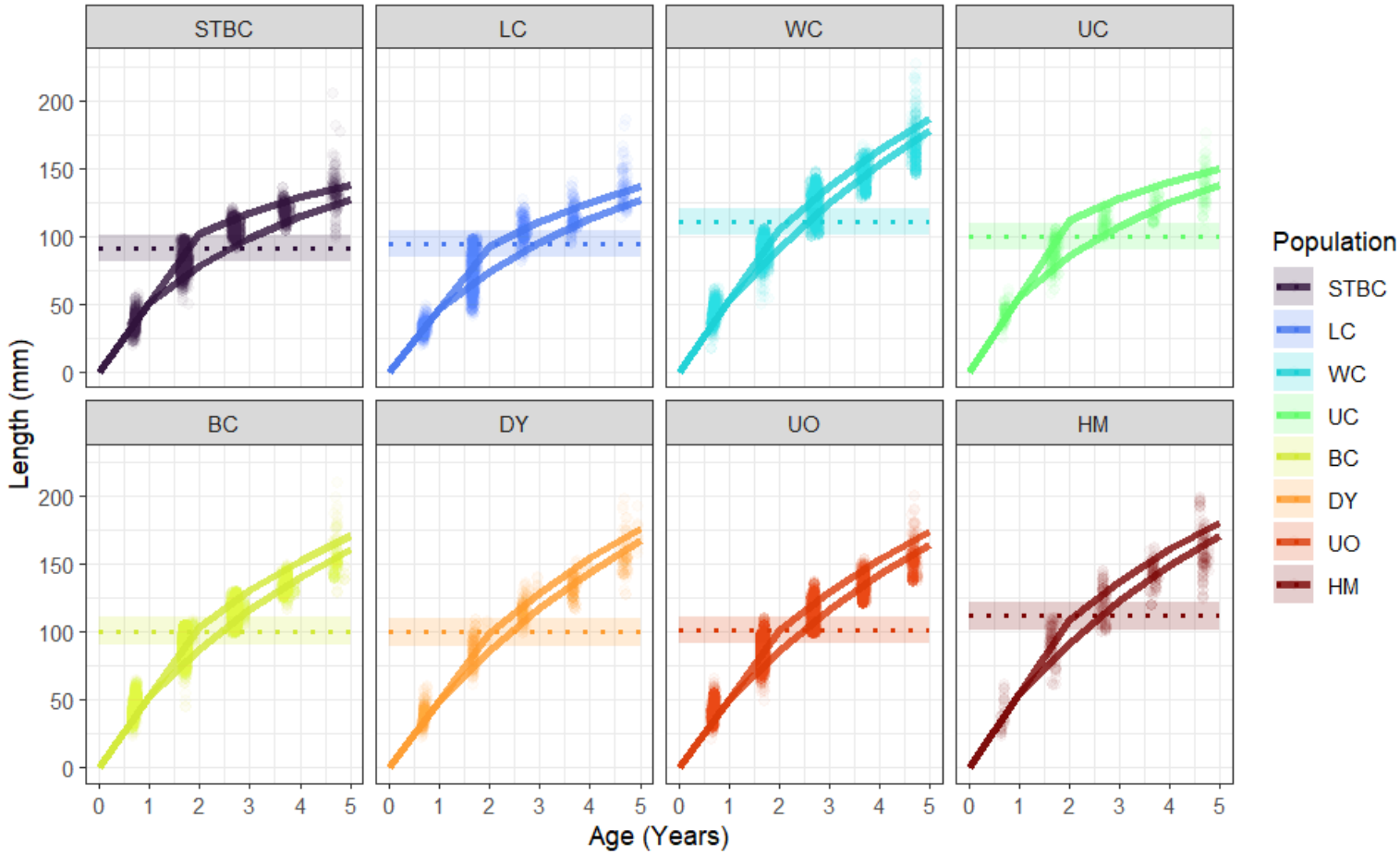

Figure 4.2: Initial growth curves and probabilistic maturation reaction norms (PMRNs) in eight Cape Race brook trout populations, based on empirical data from 2010-2022. Individual length observations are plotted against age estimated using finite mixture models (transparent points). Lester growth curves (solid lines) assuming average population-specific biomass and growing season temperature are shown separately for maturation at age-2 or age-3. Population-specific PMRN intercepts were estimated using logistic regression (dotted lines) and PMRN slopes were assumed to be zero, with a constant width of 20mm (transparent bands). Populations are colored according to their stream thermal regime, with cooler groundwater-dominated streams in blue and warmer rainfall-dominated streams in red (see Chapter 3).

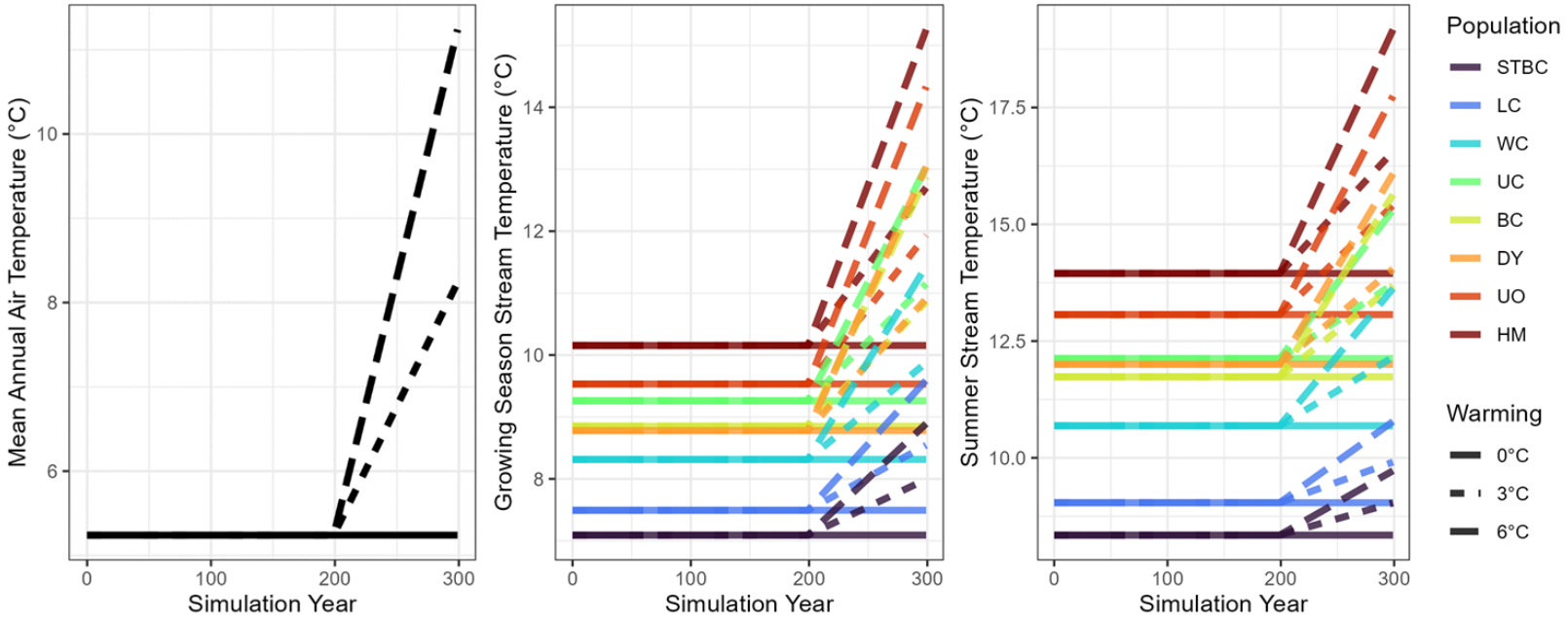

Figure 4.3: Climate change scenarios experienced by eight Cape Race brook trout populations. Air temperature increased by 0°C (solid lines), 3°C (dotted lines), or 6°C (dashed lines) during the last 100 years of each simulation, which then affected stream temperatures experienced by each population during the growing season and summer. Slopes and intercepts for converting air temperature to population-specific stream temperature are shown in Table 4.1. Populations are colored according to their stream thermal regime, with cooler groundwater-dominated streams in blue and warmer rainfall-dominated streams in red (see Chapter 3).

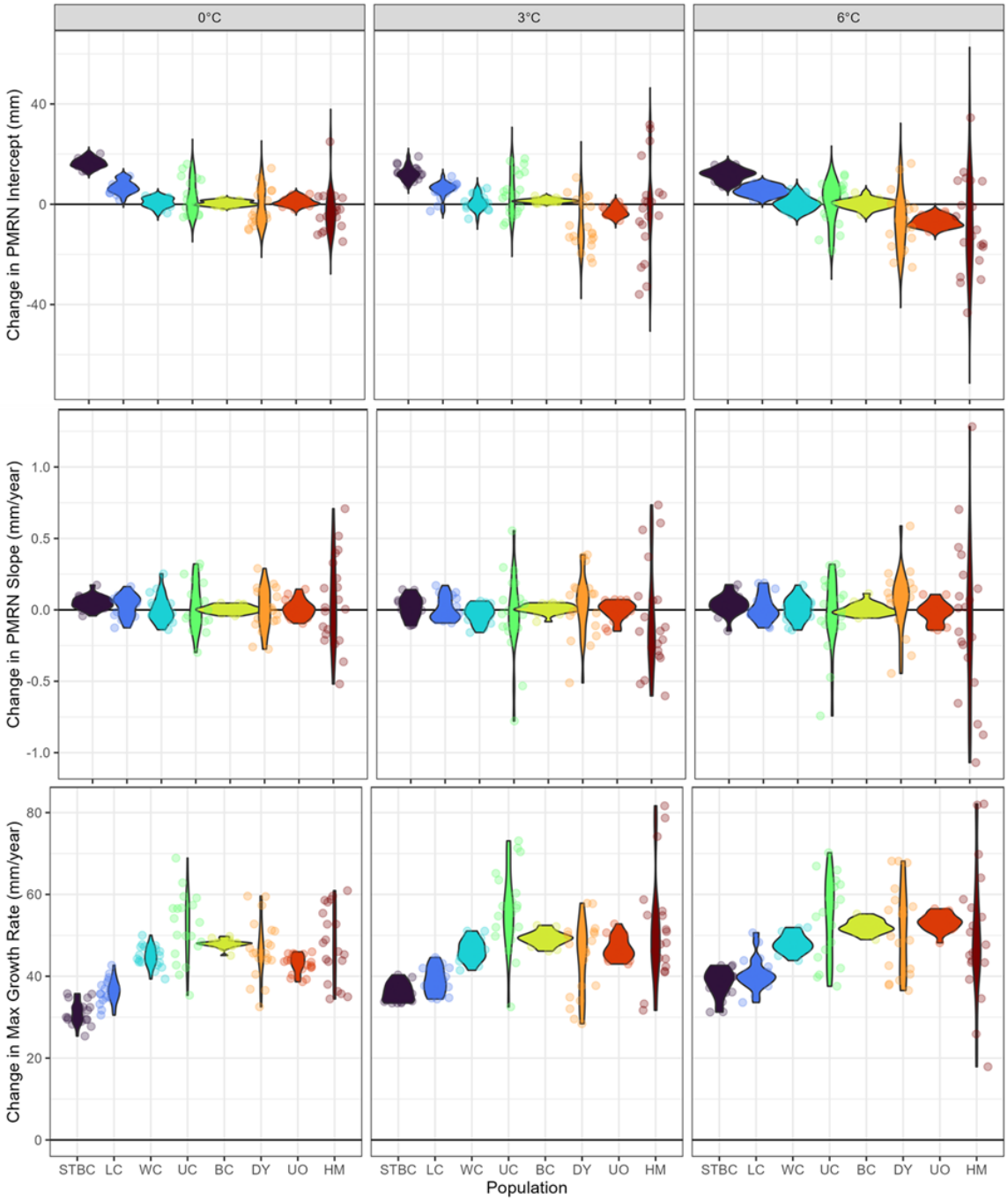

Figure 4.4: Effects of climate change on evolving traits of Cape Race brook trout populations. Results are displayed as violin plots (polygons) that summarize changes in mean genotype values during the last 100 years from twenty independent simulations (points), organized by three traits (rows; top: PMRN intercept, middle: PMRN slope, bottom: maximum growth rate) and three climate scenarios (columns; magnitude of air temperature warming over the same 100 years). Populations are colored according to their stream thermal regime, with cooler groundwater-dominated streams in blue and warmer rainfall-dominated streams in red (see Chapter 3). No data are shown for 'No Evolution' scenarios, where all three traits were fixed through time.

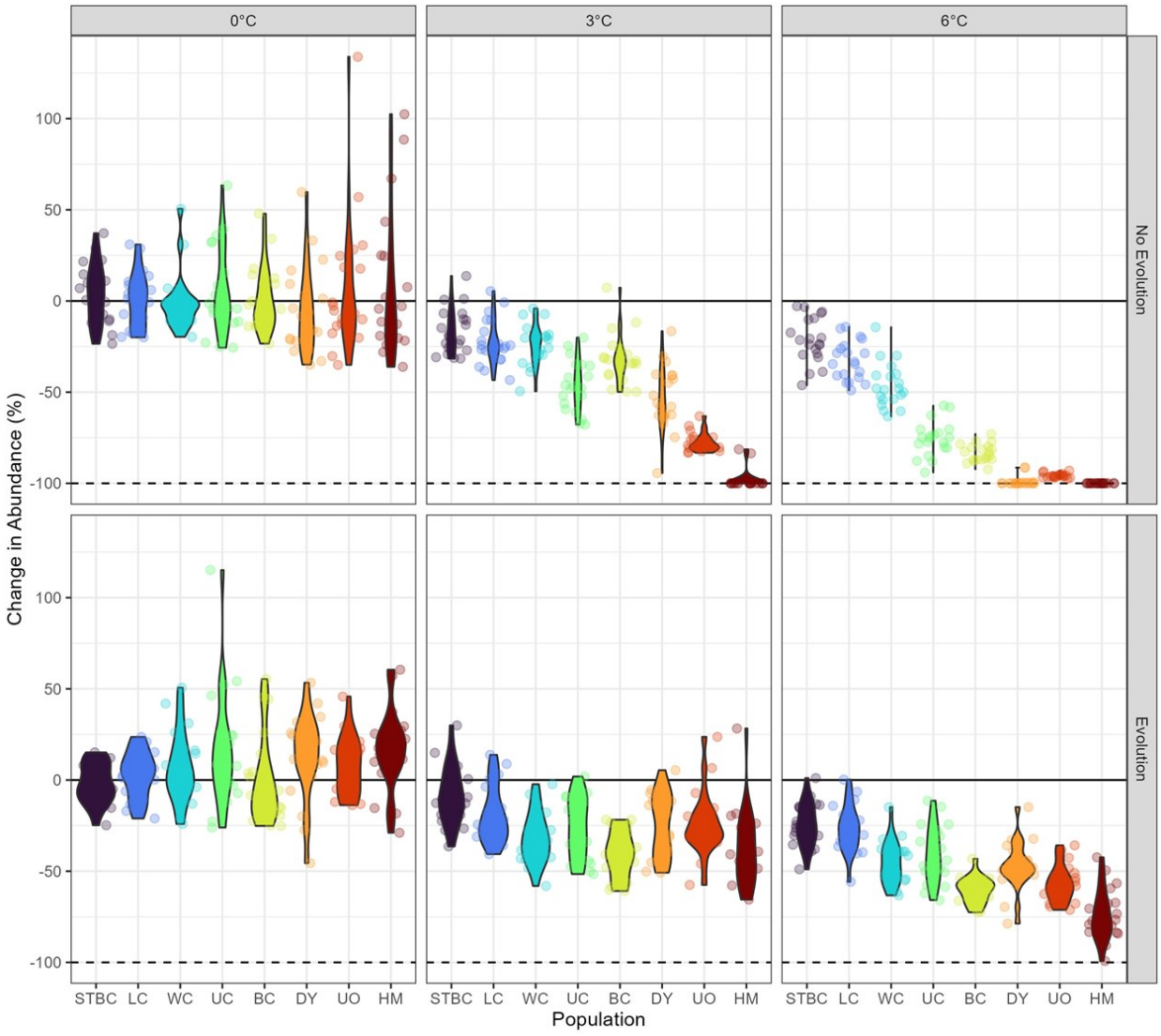

Figure 4.5: Effects of climate change on abundance of Cape Race brook trout populations. Results are displayed as violin plots (polygons) that summarize the percent change in total abundance during the last 100 years from twenty independent simulations (points), organized by two evolutionary scenarios (rows; whether evolution occurred or not) and three climate scenarios (columns; magnitude of air temperature warming over the same 100 years). Declines of 100%, in which population extirpation occurs, are shown for reference (dashed lines). Populations are colored according to their stream thermal regime, with cooler groundwater-dominated streams in blue and warmer rainfall-dominated streams in red (see Chapter 3).

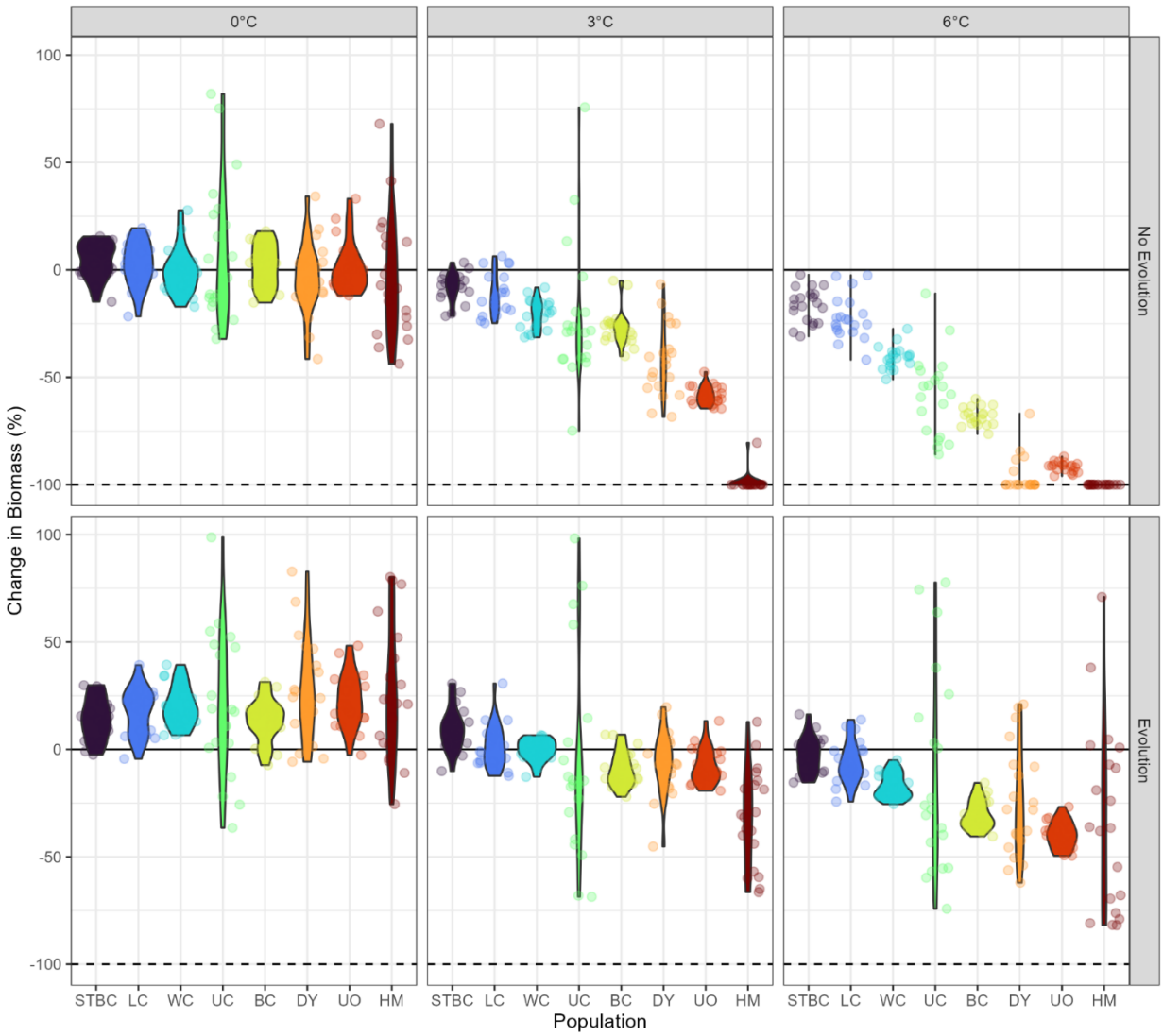

Figure 4.6: Effects of climate change on biomass of Cape Race brook trout populations. Results are displayed as violin plots (polygons) that summarize the percent change in total biomass during the last 100 years from twenty independent simulations (points), organized by two evolutionary scenarios (rows; whether evolution occurred or not) and three climate scenarios (columns; magnitude of air temperature warming over the same 100 years). Declines of 100%, in which population extirpation occurs, are shown for reference (dashed lines). Populations are colored according to their stream thermal regime, with cooler groundwater-dominated streams in blue and warmer rainfall-dominated streams in red (see Chapter 3).

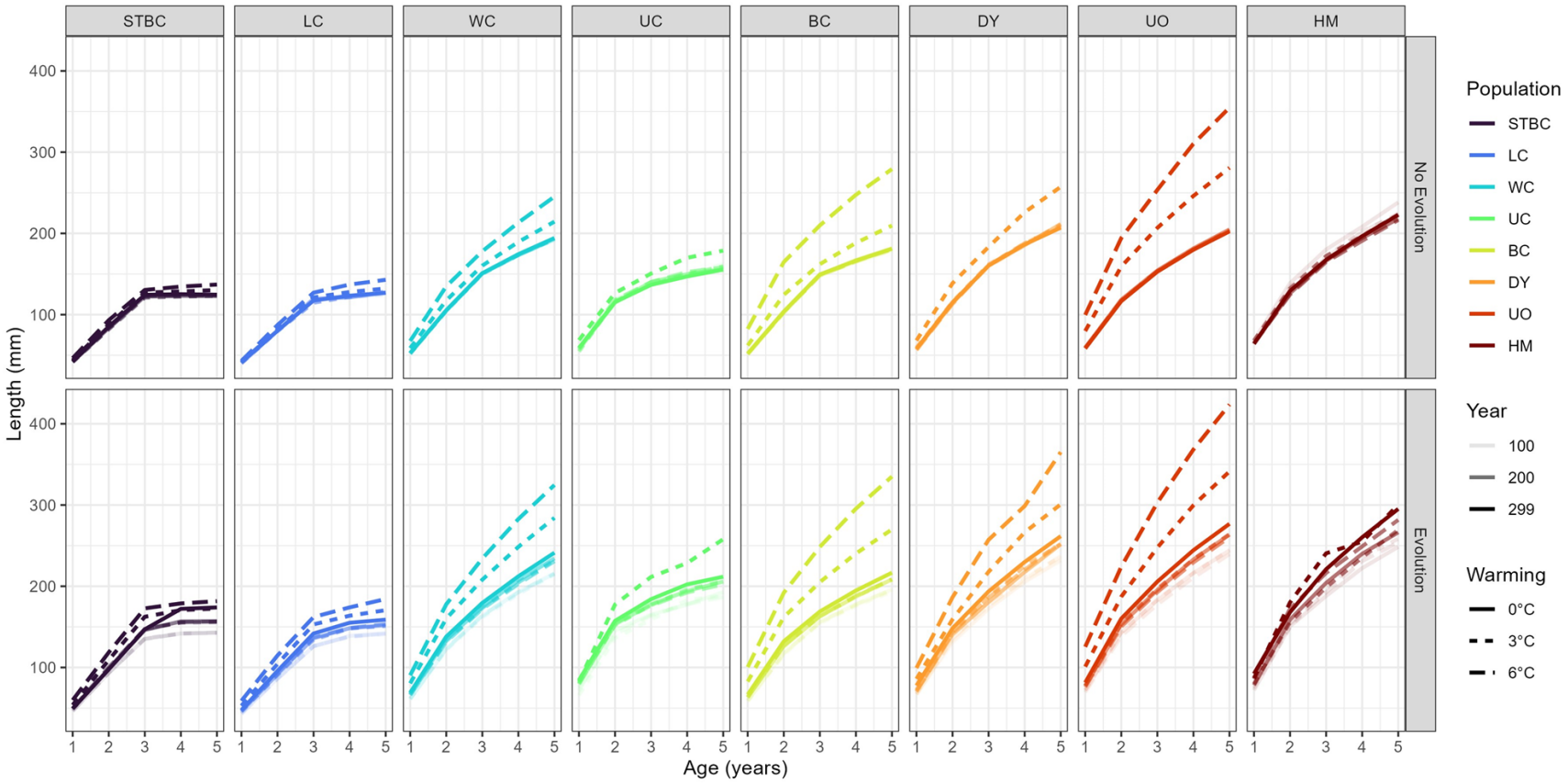

Figure 4.7: Effects of climate change on growth curves of Cape Race brook trout populations. Results are displayed as average size-at-age across twenty independent simulations. Growth curves are shown for simulation years 100 (high transparency), 200 (intermediate transparency), and 299 (no transparency), and for climate change scenarios corresponding to 0°C (solid lines), 3°C (dotted lines), or 6°C (dashed lines) of warming over the last 100 simulation years. Populations are colored according to their stream thermal regime, with cooler groundwater-dominated streams in blue and warmer rainfall-dominated streams in red (see Chapter 3).

VI. General Conclusion

The central question of my thesis was "*What are the mechanisms that drive variation in contemporary and future demographic responses to climate change among salmonid fish populations?*" In particular, I was interested in exploring the extent and spatial scale of population diversity in salmonids, as well as the processes that underpin this diversity. Salmonids are an excellent model for pursuing these questions because populations are often highly subdivided and occupy variable freshwater habitats, which can generate significant demographic differences across multiple scales (Schindler et al. 2010). Moreover, the basic ecology and evolution of salmonids is well-studied (Stearns and Hendry 2004), while most species are targeted by conservation and management efforts because they support valuable subsistence, recreational, and commercial fisheries (ASF 2011, PSC 2017). As climate change continues to increase air temperature and alter precipitation patterns over the coming decades, it is more important than ever to understand how population variation in demography, life history traits, and physical habitats can buffer salmonids against severe declines, and potentially inform the conservation of many less-studied species (Moore and Schindler 2022).

By combining a global meta-analysis across 23 species (Chapter 1) and fine-scale studies of multiple populations of brook trout (*Salvelinus foninalis*) in eastern Canada (Chapters 2, 3, and 4), my research suggests that salmonids exhibit highly variable responses to climate change, spanning multiple scales and arising through multiple mechanisms. Together, these features should stabilize salmonid abundance at large spatial scales through portfolio effects and reduce the likelihood of rapid climate-induced range shifts. Nonetheless, I identified some geographic and hydrological contexts, notably those linked to excessive stream temperatures, which appeared to disproportionately increase the risk of population extirpation under climate change. My findings have significant implications for the conservation and management of salmonids in a changing world, and may provide insights into the effects of climate change on other species with large ranges, fine-scale population differentiation, and diverse thermal habitats.

Extent of variation:

How common is variation in responses to climate change among salmonid populations? My thesis suggests that it is nearly ubiquitous, but the magnitude of variation is not always the same. For example, in Chapter 1, I showed that effects of temperature and precipitation on salmonid demography (i.e. abundance and individual growth rates) varied considerably around the world, and were mostly unexplained by spatial, temporal, or biological covariates. This was especially true for the effects of climate on abundance (variance explained: 5-10%), while covariates were more informative for explaining effects on growth (variance explained: 30-41%). Similarly in Chapter 2, I showed that abundance patterns among neighboring brook trout populations in Cape Race (Newfoundland, Canada) were highly asynchronous and largely unrelated to climate, while growth was synchronized and positively influenced by stream temperature. A consistent positive effect of temperature on brook trout growth was further corroborated in young-of-the-year individuals in Chapter 3. Therefore, salmonid growth appears to exhibit stronger and less variable relationships with climate than abundance. However, this could mostly be because temporal variation in abundance far exceeds variation in growth. For example, in Cape Race brook trout, abundance of age-1 juveniles fluctuated 3- to 9-fold over time, while juvenile growth only varied 1.3- to 1.5-fold (see Chapter 2). Although linking abundance to climate change to is difficult, it should remain a research priority because abundance is most crucial for

determining rates of biomass production (Lobón-Cerviá 2009) and ecosystem services provided by salmonid populations (e.g. harvest; Hilborn et al. 2003, Connors et al. 2022).

Other studies of salmonids have emphasized the role of connectivity, habitat characteristics, and anthropogenic disturbance in determining the extent of population variation in responses to climate change, particularly for abundance. For example, neighboring populations of brook trout (Bassar et al. 2016, Andrew et al. 2022) and other fish species (Alonso et al. 2011, Larsen et al. 2021) within dendritic stream networks often exhibit similar abundance patterns. This is mostly thought to be due to physical connectivity and exchange of individuals, as well as relatively small differences in stream temperature and streamflow among adjacent mainstem streams, which together should drive more similar population dynamics (Larsen et al. 2021; but see Rogers and Schindler 2008). Likewise, salmonid abundance trends are often less variable in areas that have been heavily impacted by human activities, especially damming, introduction of captive-bred individuals, and overharvest, leading to a collapse of regional portfolio effects (Moore et al. 2010, Carlson and Satterthwaite 2011, O'Sullivan et al. 2020). Researchers have also noted that land use practices such as increasing impervious surface area (Stranko et al. 2008), withdrawing groundwater (Lapides et al. 2022), or clearing forests (Hartman et al. 1996) can degrade salmonid habitats, and make some streams entirely unsuitable through changes in thermal regimes and sediment loads. Overall, anthropogenic impacts often homogenize habitats and reduce ecological contrast among salmonid populations, thereby eroding demographic variation. Therefore, the portfolio effect driven by asynchronous abundance that I observed across Cape Race brook trout populations in Chapter 2 might arise from the pristine and isolated nature of the study area, similar to other systems with minimal human impacts (e.g. sockeye salmon in Bristol Bay, Alaska; Schindler et al. 2010). Overall, my thesis supports prior assertions that natural habitat variation should be conserved as much as possible in order to maximize demographic diversity and stability of salmonid populations under future climate change (Schindler and Hilborn 2015).

Spatial scale:

At what spatial scale does most variation occur in salmonid population responses to climate change? My thesis could not answer this question definitively, but I uncovered important sources of variation at continental (entire watersheds across >1,000 kilometers), regional (collections of subwatersheds across 10s to 100s of kilometers), and local scales (individual streams separated by <10 kilometers). At continental and regional scales, my work in Chapter 1 showed that although most variation was unexplained, demographic responses to temperature in salmonid populations were strongly linked to latitude and elevation. Specifically, warmer temperatures were associated with reduced growth and abundance at low latitudes and elevations, while opposite patterns were observed at high latitudes and elevations. However, at the local scale, my research on Cape Race brook trout in Chapter 2 suggested that substantial variation in demography and climate impacts can exist among salmonid populations separated by <5 kilometers. In Chapter 3, I further suggested that local thermal habitat differences played an instrumental role in generating variation in phenology, growth, and survival among Cape Race populations. Thermal habitat was also a key determinant of population-specific responses to future warming uncovered by eco-genetic models in Chapter 4. Importantly, local-scale habitat diversity in Cape Race was not obviously related to large-scale processes, since every stream had very similar latitude, elevation, air temperature, precipitation, vegetation, and underlying geology. Altogether, my research suggests that salmonid population responses to climate change

are related to large-scale gradients in latitude and elevation, but local variation is likely more prevalent and less predictable. Therefore, I caution against over-relying on coarse-scale spatial assessments of conservation status and climate vulnerability (e.g. Clark et al. 2001, Flebbe et al., 2006), and suggest integrating data across scales is most crucial for predicting responses in salmonids and other species (see below).

Similar to stream-dwelling salmonids, many species consist of numerous genetically and ecologically distinct populations distributed over a large area, which thereby sample diverse regional climates and local habitat types. This is perhaps most common in species occupying fragmented landscapes such as many freshwater systems, isolated habitat patches such as springs or wetlands, and rugged terrain such as mountains or outcrops (Johansson et al. 2007, Waterhouse et al. 2017, Pearson et al. 2018; see Chapter 2). To confidently predict responses to future climate change in these species, data describing local population demography, habitat conditions, and climate exposure should ideally be gathered from many representative locations across the species range, then analyzed together. Although local-scale biological and habitat data are expensive and labor-intensive to collect (Iacona et al. 2018), this task can be accomplished through long-term monitoring and targeted range-wide collaboration. For example, wood frogs (*Rana sylvatica*) have been monitored by multiple research groups for decades across hundreds of sites in North America, informing studies that link local-scale population demography to climate change (e.g. Miller and Grant 2015, Rowland et al. 2022). Local data has also been pooled to identify range-wide patterns in population responses to climate, spanning nearly 20 latitudinal degrees (Amburgey et al. 2018). This approach offers promise for other species, including salmonids such as brook trout (see section below: *Implications for future research*).

Underlying mechanisms:

What are the mechanisms that generate variation in salmonid population responses to climate change? Given the importance and idiosyncratic nature of local-scale variation in population demography (see previous section), I emphasize two mechanisms operating at small spatial scales within my study system in Cape Race, which are likely broadly relevant for salmonids. First, my research in Chapter 3 showed that brook trout populations were exposed to vastly different thermal regimes due to variation in stream groundwater inputs, which has been observed in other trout streams in the United States (Snyder et al. 2015, Carlson et al. 2019) and Canada (Daigle et al. 2019). Thermal regimes in Cape Race appeared to be linked to local geomorphology, especially stream gradient and the prevalence of ponds within drainages, while other studies have found that groundwater inputs can differ based on underlying geology (Hitt et al. 2023, Ishiyama et al. 2023). Other processes can also generate fine-scale variation in stream thermal regimes, such as snowmelt contributions, forest cover, and upstream land use (DeWeber and Wagner 2014, Lisi et al. 2015). Combined, these processes likely produce massive range-wide temperature variation for salmonids and other freshwater species, and will play a key role in determining population-specific exposure to atmospheric warming. Nonetheless, future stream temperatures will likely exceed salmonid thermal limits in many areas, so local coldwater refugia will be vital for maintaining viable populations (Isaak and Young 2023, Mejia et al. 2023).

Second, my work in Chapter 4 and past research in Cape Race (Hutchings 1993, Fraser et al. 2019) suggest that neighboring brook trout populations have evolved distinct life histories that are adapted to local habitat conditions, affecting individual schedules of survival, growth, and reproduction. Furthermore, projections from mechanistic models in Chapter 4 suggested that

Cape Race brook trout possess considerable adaptive potential that should allow populations to persist in a warming climate through a combination of life history evolution and phenotypic plasticity. Although contemporary life history patterns and future projections were also influenced by stream thermal regimes in Cape Race, these results highlight the crucial role of fine-scale local adaptation and evolutionary potential in diversifying population responses to climate change. The importance of evolutionary processes to the demography and persistence of salmonids is well-established (Fraser et al. 2011, Reed et al. 2011), but my research is the first to compare adaptive responses to climate change among many salmonid populations separated by <3 kilometers. Similar local-scale evolutionary responses to climate change have been documented in wood frogs (Skelly et al. 2007, Arietta and Skelly 2021), suggesting that potential for rapid adaptation may be common in other wide-ranging vertebrates (but see Radchuk et al. 2019 for an exception in birds).

Implications for future research:

How should researchers study population variation in demographic responses to climate change in the future? I contend that brook trout can serve as a useful model for integrating data across scales to inform conservation and management under climate change in a wide range of species. Brook trout are native to 21 US states and seven Canadian provinces (NatureServe 2022), and have a strong propensity for fine-scale genetic and phenotypic differentiation (Hutchings 1993, Zastavniouk et al. 2017), resulting in thousands of unique populations. Importantly, because brook trout support lucrative recreational fisheries, hold cultural significance, and serve as a coldwater indicator species, they are among the most data-rich freshwater species, with researchers and agencies monitoring population abundance over multiple decades in hundreds of locations (e.g. Zorn and Nuhfer 2007, Kanno et al. 2015, Kratzer et al. 2021). However, much like the species itself, monitoring efforts are highly fragmented and exchange across management jurisdictions is limited, making it difficult to quantify abundance trends throughout the species range. Building collaborative networks to gather these data and analyze them together (similar to Amburgey et al. 2018) would be enormously beneficial for brook trout. Indeed, a recent study synthesized brook trout abundance data from nine agencies in the southeastern United States, which generated novel insights into the spatial scale of population asynchrony, as well as the effects of seasonal temperature and precipitation patterns on demography (Valentine et al. 2024). Expanding the spatial scale of this database to include the rest of the native range in the United States and Canada is a clear next step. Bayesian state-space models can be applied to estimate demographic trends in brook trout populations while accounting for the hierarchical structure of stream networks, with individual stream segments nested within small subwatersheds and larger watersheds (Pregler et al. 2019). Coupled with information on the spatial scale of population differentiation in brook trout (Kazyak et al. 2022), and improved fine-scale stream temperature models (e.g. DeWeber and Wagner 2014, Walker et al. 2020), it may be possible to predict the range-wide biogeography of brook trout responses to future climate change with rare confidence and mechanistic detail. Similar research efforts that integrate multiple datasets across spatial scales have been attempted in populations of Pacific salmon (Mueter et al. 2002) and European brown trout (Parra et al. 2009, Donadi et al. 2023), and could potentially be applied to a wide range of species (Nadeau et al. 2017a, 2017b).

Finally, further research is needed to determine the extent to which existing trait variation and evolutionary potential can buffer species against extirpation in a changing world. This is especially relevant for widespread species with highly subdivided populations, which may be

most likely to display local-scale variation in life history, thermal tolerance, and other traits (Richardson et al. 2014). Salmonid populations often exhibit well-studied genetic and phenotypic differences at small scales (Schindler et al. 2010), and can therefore serve as a useful model for researching trait variation and evolvability more generally (Stearns and Hendry 2004, Carlson and Seamons 2008). However, these processes have not been studied as extensively in brook trout as in many other salmonid species. For example, while life history patterns in lentic brook trout populations have been explored in some parts of Canada and the Great Lakes (Magnan et al. 2005, Ridgway 2008, Adams et al. 2016), very little published information exists for stream-dwelling populations, especially in southern regions that are most vulnerable to warming (see Chapter 1). Similarly, common garden experiments are rarely conducted in brook trout, so heritabilities and genetic variances of life history traits and thermal tolerances are unknown in the vast majority of populations (but see Wells et al. 2016, Fraser et al. 2019). A collaborative approach to studying range-wide life history variation in brook trout could reveal spatial correlates and constraints on adaptive potential, which could then be built into mechanistic models to explore their effects on future demography (see Chapter 4). Overall, brook trout demonstrate that better data, models, and collaborations should help improve predictions of evolutionary responses to climate chance among natural populations, which should also be beneficial for many other species (Urban et al. 2023).

VII. References

Adams, B. K., Cote, D., and Fleming, I. A. (2016). Stochastic life history modeling for managing regional-scale freshwater fisheries: an experimental study of brook trout. *Ecological Applications*, *26*(3), 899-912.

Al-Chokhachy, R., Schmetterling, D., Clancy, C., Saffel, P., Kovach, R., Nyce, L., Liermann, B., Fredenberg, W. and Pierce, R. (2016). Are brown trout replacing or displacing bull trout populations in a changing climate? *Canadian Journal of Fisheries and Aquatic Sciences*, *73(9),* 1395-1404.

Ali, A., Al-Tobasei, R., Lourenco, D., Leeds, T., Kenney, B., and Salem, M. (2020). Genome-wide identification of loci associated with growth in rainbow trout. *BMC genomics*, *21*(1), 1-16.

Almodóvar, A., Nicola, G. G., Ayllón, D., and Elvira, B. (2012). Global warming threatens the persistence of Mediterranean brown trout. *Global Change Biology*, *18*(5), 1549-1560.

Alonso, C., García de Jalón, D., Álvarez, J., and Gortázar, J. (2011). A large-scale approach can help detect general processes driving the dynamics of brown trout populations in extensive areas. *Ecology of Freshwater Fish*, *20*(3), 449-460.

Amburgey, S. M., Miller, D. A., Campbell Grant, E. H., Rittenhouse, T. A., Benard, M. F., Richardson, J. L., Urban, M.C., Hughson, W., Brand, A.B., Davis, C.J. and Hardin, C. R. (2018). Range position and climate sensitivity: The structure of among-population demographic responses to climatic variation. *Global Change Biology*, 24(1), 439-454.

Andrew, R. G., Schwinghamer, C. W., Hartman, K. J., and Briggs, E. E. (2022). Climate change influence on brook trout populations in the Central Appalachians. *Ecology of Freshwater Fish*, *31*(4), 710-725.

Argent, D. G., and Flebbe, P. A. (1999). Fine sediment effects on brook trout eggs in laboratory streams. *Fisheries Research*, *39*(3), 253-262.

Arietta, A. A., and Skelly, D. K. (2021). Rapid microgeographic evolution in response to climate change. *Evolution*, *75*(11), 2930-2943.

Arismendi, I., Safeeq, M., Johnson, S. L., Dunham, J. B., and Haggerty, R. (2013). Increasing synchrony of high temperature and low flow in western North American streams: double trouble for coldwater biota? *Hydrobiologia*, *712*(1), 61-70.

Arismendi, I., Safeeq, M., Dunham, J. B., and Johnson, S. L. (2014). Can air temperature be used to project influences of climate change on stream temperature? *Environmental Research Letters*, *9*(8), 084015.

Armstrong, J. B., Fullerton, A. H., Jordan, C. E., Ebersole, J. L., Bellmore, J. R., Arismendi, I., Penaluna, B. E. and Reeves, G. H. (2021). The importance of warm habitat to the growth regime of cold-water fishes. *Nature Climate Change*, *11*(4), 354-361.

ASF (Atlantic Salmon Federation). 2011. Economic value of wild Atlantic salmon. Final report prepared by Gardner Pinfold Consultants Inc.

Ayllón, D., Railsback, S. F., Harvey, B. C., Quirós, I. G., Nicola, G. G., Elvira, B., and Almodóvar, A. (2019). Mechanistic simulations predict that thermal and hydrological effects of climate change on Mediterranean trout cannot be offset by adaptive behaviour, evolution, and increased food production. *Science of the Total Environment*, 693, 133648.

Bahlai, C. A., White, E. R., Perrone, J. D., Cusser, S., and Whitney, K. S. (2021). The broken window: An algorithm for quantifying and characterizing misleading trajectories in ecological processes. *Ecological Informatics*, *64*, 101336.

Bailey, J. K., Schweitzer, J. A., Ubeda, F., Koricheva, J., LeRoy, C. J., Madritch, M. D., Rehill, B. J., Bangert, R. K., Fischer, D. G., Allan, G. J. and Whitham, T. G. (2009). From genes to ecosystems: a synthesis of the effects of plant genetic factors across levels of organization. *Philosophical Transactions of the Royal Society B: Biological Sciences*, *364*(1523), 1607-1616.

Barton, K. (2009) Mu-MIn: Multi-model inference. R Package Version 0.12.2/r18. http://R-Forge.R-project.org/projects/mumin/.

Bassar, R. D., Letcher, B. H., Nislow, K. H., and Whiteley, A. R. (2016). Changes in seasonal climate outpace compensatory density-dependence in eastern brook trout. *Global Change Biology*, 22(2), 577-593.

Bates, D., Mächler, M., Bolker, B., and Walker, S. (2015). Fitting linear mixed-effects models using lme4. *Journal of Statistical Software*, 67(1), 1-48. doi:10.18637/jss.v067.i01.

Beacham, T. D., and Murray, C. B. (1990). Temperature, egg size, and development of embryos and alevins of five species of Pacific salmon: a comparative analysis. *Transactions of the American Fisheries Society*, *119*(6), 927-945.

Beck, H. E., Zimmermann, N. E., McVicar, T. R., Vergopolan, N., Berg, A., and Wood, E. F. (2018). Present and future Köppen-Geiger climate classification maps at 1-km resolution. *Scientific Data*, *5*(1), 1-12.

Bell, D. A., Kovach, R. P., Muhlfeld, C. C., Al-Chokhachy, R., Cline, T. J., Whited, D. C., Schmetterling, D. A., Lukacs, P. M. and Whiteley, A. R. (2021). Climate change and expanding invasive species drive widespread declines of native trout in the northern Rocky Mountains, USA. *Science Advances*, 7(52), eabj5471.

Belmar-Lucero, S., Wood, J. L., Scott, S., Harbicht, A. B., Hutchings, J. A., and Fraser, D. J. (2012). Concurrent habitat and life history influences on effective/census population size ratios in stream-dwelling trout. *Ecology and Evolution*, 2(3), 562-573.

Benaglia, T., Hunter, D. R., Chauveau, D., and Young, D. S. (2009). Mixtools, a package for analyzing finite mixture models. *Journal of Statistical Software*, *32*, 1-29.

Bennett, J. M., Sunday, J., Calosi, P., Villalobos, F., Martínez, B., Molina-Venegas, R., Araújo, M. B., Algar, A. C., Clusella-Trullas, S., Hawkins, B. A., Keith, S. A. and Olalla-Tárraga, M. Á. (2021). The evolution of critical thermal limits of life on Earth. *Nature Communications*, *12*(1), 1-9.

Bernos, T. A., and Fraser, D. J. (2016). Spatiotemporal relationship between adult census size and genetic population size across a wide population size gradient. *Molecular Ecology*, 25(18), 4472-4487.

Bernos, T. A., Yates, M. C., and Fraser, D. J. (2018). Fine-scale differences in genetic and census population size ratios between two stream fishes. *Conservation Genetics*, *19*(2), 265-274.

Bernos, T. A., Day, C., Hill, J., Morissette, O., Jeffries, K. M., and Mandrak, N. E. (2023). Simulating the effects of long-distance dispersal and landscape heterogeneity on the eco-evolutionary outcomes of range expansion in an invasive riverine fish, Tench (Tinca tinca). *Molecular Ecology*, 32, 3403–3418.

Blair, J. M., Ostrovsky, I., Hicks, B. J., Pitkethley, R. J., and Scholes, P. (2013). Growth of rainbow trout (Oncorhynchus mykiss) in warm-temperate lakes: implications for environmental change. *Canadian Journal of Fisheries and Aquatic Sciences*, *70*(5), 815-823.

Bolker, B. M., Brooks, M. E., Clark, C. J., Geange, S. W., Poulsen, J. R., Stevens, M. H. H., and White, J. S. S. (2009). Generalized linear mixed models: a practical guide for ecology and evolution. *Trends in Ecology and Evolution*, *24*(3), 127-135.

Bolnick, D. I., Amarasekare, P., Araújo, M. S., Bürger, R., Levine, J. M., Novak, M., Rudolf, V. H., Schreiber, S. J., Urban, M. C. and Vasseur, D. A. (2011). Why intraspecific trait variation matters in community ecology. *Trends in Ecology and Evolution*, *26*(4), 183-192.

Borwick, J., Buttle, J., and Ridgway, MS (2006). A topographic index approach for identifying groundwater habitat of young-of-year brook trout (Salvelinus fontinalis) in the land lake ecotone. *Canadian Journal of Fisheries and Aquatic Sciences* , *63* (2), 239-253.

Boyer, C., St-Hilaire, A., and Bergeron, N. E. (2021). Defining river thermal sensitivity as a function of climate. *River Research and Applications*, *37*(10), 1548-1561.

Bret, V., Bergerot, B., Capra, H., Gouraud, V., and Lamouroux, N. (2016). Influence of discharge, hydraulics, water temperature, and dispersal on density synchrony in brown trout populations (Salmo trutta). *Canadian Journal of Fisheries and Aquatic Sciences*, *73*(3), 319-329.

Budy, P., Thiede, G. P., McHugh, P., Hansen, E. S., and Wood, J. (2008). Exploring the relative influence of biotic interactions and environmental conditions on the abundance and distribution of exotic brown trout (Salmo trutta) in a high mountain stream. *Ecology of Freshwater Fish*, *17*(4), 554-566.

Burgess, M. G., Becker, S. L., Langendorf, R. E., Fredston, A., and Brooks, C. M. (2023). Climate change scenarios in fisheries and aquatic conservation research. *ICES Journal of Marine Science*, fsad045.

Campana, S. E., Casselman, J. M., Jones, C. M., Black, G., Barker, O., Evans, M., M., Guzzo, M. M., Kilada, R., Muir, A. M., and Perry, R. (2020). Arctic freshwater fish productivity and colonization increase with climate warming. *Nature Climate Change*, *10*(5), 428-433.

Carline, R. F. (2006). Regulation of an unexploited brown trout population in Spruce Creek, Pennsylvania. *Transactions of the American Fisheries Society*, *135*(4), 943-954.

Carlson, A. K., Taylor, W. W., and Infante, D. M. (2019). Developing precipitation-and groundwater-corrected stream temperature models to improve brook charr management amid climate change. *Hydrobiologia*, *840*, 379-398.

Carlson, S. M., and Satterthwaite, W. H. (2011). Weakened portfolio effect in a collapsed salmon population complex. *Canadian Journal of Fisheries and Aquatic Sciences*, *68*(9), 1579-1589.

Carlson, S. M., and Seamons, T. R. (2008). A review of quantitative genetic components of fitness in salmonids: implications for adaptation to future change. *Evolutionary Applications*, 1(2), 222-238.

Carlson, S. M., Cunningham, C. J., and Westley, P. A. (2014). Evolutionary rescue in a changing world. *Trends in Ecology and Evolution*, 29(9), 521-530.

Carvajal-Quintero, J., Comte, L., Giam, X., Olden, J. D., Brose, U., Erős, T., Filipe, A. F., Fortin, M. J., Irving, K., Jacquet, C. and Larsen, S. (2022). Scale of population synchrony confirms macroecological estimates of minimum viable range size. *Ecology Letters*. Online.

Cattanéo, F., Hugueny, B., and Lamouroux, N. (2003). Synchrony in brown trout, Salmo trutta, population dynamics: A 'Moran effect'on early-life stages. *Oikos*, *100*(1), 43-54.

Chezik, K. A., Lester, N. P., and Venturelli, P. A. (2014). Fish growth and degree-days II: selecting a base temperature for an among-population study. *Canadian Journal of Fisheries and Aquatic Sciences*, 71(9), 1303-1311.

Clark, M. E., Rose, K. A., Levine, D. A., and Hargrove, W. W. (2001). Predicting climate change effects on Appalachian trout: Combining GIS and individual-based modeling. *Ecological Applications*, *11*(1), 161-178.

Clews, E., Durance, I., Vaughan, I. P., and Ormerod, S. J. (2010). Juvenile salmonid populations in a temperate river system track synoptic trends in climate. *Global Change Biology*, *16*(12), 3271-3283.

Cohen, J. M., Lajeunesse, M. J., and Rohr, J. R. (2018). A global synthesis of animal phenological responses to climate change. *Nature Climate Change*, *8*(3), 224-228.

Coleman, M. A., and Fausch, K. D. (2007). Cold summer temperature limits recruitment of age-0 cutthroat trout in high-elevation Colorado streams. *Transactions of the American Fisheries Society*, *136*(5), 1231-1244.

Comte, L., and Olden, J. D. (2017). Climatic vulnerability of the world's freshwater and marine fishes. *Nature Climate Change*, *7*(10), 718-722.

Comte, L., Olden, J. D., Tedesco, P. A., Ruhi, A., and Giam, X. (2021). Climate and land-use changes interact to drive long-term reorganization of riverine fish communities globally. *Proceedings of the National Academy of Sciences*, *118*(27).

Connors, B. M., Siegle, M. R., Harding, J., Rossi, S., Staton, B. A., Jones, M. L., Brown, R., Bechtol, B., Doherty, B., Cox, S., and Sutherland, B. J. (2022). Chinook salmon diversity contributes to fishery stability and trade-offs with mixed-stock harvest. *Ecological Applications*, *32*(8), e2709.

Copeland, T., and Meyer, K. A. (2011). Interspecies synchrony in salmonid densities associated with large-scale bioclimatic conditions in central Idaho. *Transactions of the American Fisheries Society*, *140*(4), 928-942.

Cotto, O., Wessely, J., Georges, D., Klonner, G., Schmid, M., Dullinger, S., Thuiller, W., and Guillaume, F. (2017). A dynamic eco-evolutionary model predicts slow response of alpine plants to climate warming. *Nature Communications*, 8(1), 1-9.

Crawford, S. S., and Muir, A. M. (2008). Global introductions of salmon and trout in the genus Oncorhynchus: 1870–2007. *Reviews in Fish Biology and Fisheries*, *18*(3), 313-344.

Crisp, D. T. (1981). A desk study of the relationship between temperature and hatching time for the eggs of five species of salmonid fishes. *Freshwater Biology*, *11*(4), 361-368.

Curry, R. A., Noakes, D. L., and Morgan, G. E. (1995). Groundwater and the incubation and emergence of brook trout (Salvelinus fontinalis). *Canadian Journal of Fisheries and Aquatic Sciences*, *52*(8), 1741-1749.

Curry, R. A., and Noakes, D. L. (1995). Groundwater and the selection of spawning sites by brook trout (Salvelinus fontinalis). *Canadian Journal of Fisheries and Aquatic Sciences*, *52* (8), 1733-1740.

Cvitanovic, C., and Hobday, A. J. (2018). Building optimism at the environmental science-policy-practice interface through the study of bright spots. *Nature Communications*, *9*(1), 3466.

Dahlke, F. T., Wohlrab, S., Butzin, M., and Pörtner, H. O. (2020). Thermal bottlenecks in the life cycle define climate vulnerability of fish. *Science*, *369*(6499), 65-70.

Daigle, A., Boyer, C., and St-Hilaire, A. (2019). A standardized characterization of river thermal regimes in Québec (Canada). *Journal of Hydrology*, *577*, 123963.

Danzmann, R. G., Morgan II, R. P., Jones, M. W., Bernatchez, L., and Ihssen, P. E. (1998). A major sextet of mitochondrial DNA phylogenetic assemblages extant in eastern North American brook trout (Salvelinus fontinalis): distribution and postglacial dispersal patterns. *Canadian Journal of Zoology*, *76*(7), 1300-1318.

Deckmyn, A., Minka, T. P., Brownrigg, R., Becker, R. A., and Wilks, A. R. (2021) maps: Draw Geographical Maps. R package version 3.4.0, https://CRAN.R-project.org/package=maps.

Deitchman, R., and Loheide, S. P. (2012). Sensitivity of Thermal Habitat of a Trout Stream to Potential Climate Change, Wisconsin, United States 1. *JAWRA Journal of the American Water Resources Association*, *48*(6), 1091-1103.

Des Roches, S., Post, D. M., Turley, N. E., Bailey, J. K., Hendry, A. P., Kinnison, M. T., Schweitzer, J. A., and Palkovacs, E. P. (2018). The ecological importance of intraspecific variation. *Nature Ecology and Evolution*, 2(1), 57-64.

DeWeber, J. T., and Wagner, T. (2014). A regional neural network ensemble for predicting mean daily river water temperature. *Journal of Hydrology*, *517*, 187-200.

Doenz, C. J., Bittner, D., Vonlanthen, P., Wagner, C. E., and Seehausen, O. (2018). Rapid buildup of sympatric species diversity in Alpine whitefish. *Ecology and Evolution*, *8*(18), 9398-9412.

Dolan, C. R., and Miranda, L. E. (2003). Immobilization thresholds of electrofishing relative to fish size. *Transactions of the American Fisheries Society*, *132*(5), 969-976.

Donadi, S., Näslund, J., Sandin, S., Sers, B., Vasemägi, A., and Degerman, E. (2023). Contrasting long-term trends in juvenile abundance of a widespread cold-water salmonid along a latitudinal gradient: effects of climate, stream size and migration strategy. *Ecography*, Online (https://doi.org/10.1111/ecog.06522).

Dornelas, M., Gotelli, N. J., McGill, B., Shimadzu, H., Moyes, F., Sievers, C., and Magurran, A. E. (2014). Assemblage time series reveal biodiversity change but not systematic loss. *Science*, *344*(6181), 296-299.

Dornelas, M., Gotelli, N. J., Shimadzu, H., Moyes, F., Magurran, A. E., and McGill, B. J. (2019). A balance of winners and losers in the Anthropocene. *Ecology Letters*, *22*(5), 847-854.

Dunlop, E. S., Heino, M., and Dieckmann, U. (2009). Eco-genetic modeling of contemporary life-history evolution. *Ecological Applications*, 19(7), 1815-1834.

ECCC (Environment and Climate Change Canada). (2021). Historical climate data for Cape Race (AUT). Accessed October 12, 2021. Available online: https://climate.weather.gc.ca/climate_data/daily_data_e.html?StationID=6590

Ezard, T. H., Côté, S. D., and Pelletier, F. (2009). Eco-evolutionary dynamics: disentangling phenotypic, environmental and population fluctuations. *Philosophical Transactions of the Royal Society B: Biological Sciences*, 364(1523), 1491-1498.

Fesenmyer, K. A., Haak, A. L., Rummel, S. M., Mayfield, M., McFall, S. L., and Williams, J. E. (2017). Eastern brook trout conservation portfolio, range-wide habitat integrity and future security assessment, and focal area risk and opportunity analysis. *Final report to National Fish and Wildlife Foundation*.

Fick, S. E., and Hijmans, R. J. (2017). WorldClim 2: new 1-km spatial resolution climate surfaces for global land areas. *International Journal of Climatology*, *37*(12), 4302-4315.

Flebbe, P. A., Roghair, L. D., and Bruggink, J. L. (2006). Spatial modeling to project southern Appalachian trout distribution in a warmer climate. *Transactions of the American Fisheries Society*, *135*(5), 1371-1382.

Fraser, D. J., Weir, L. K., Bernatchez, L., Hansen, M. M., and Taylor, E. B. (2011). Extent and scale of local adaptation in salmonid fishes: review and meta-analysis. *Heredity*, 106(3), 404-420.

Fraser, D. J., Debes, P. V., Bernatchez, L., and Hutchings, J. A. (2014). Population size, habitat fragmentation, and the nature of adaptive variation in a stream fish. *Proceedings of the Royal Society B: Biological Sciences*, *281*(1790), 20140370.

Fraser, D. J., Walker, L., Yates, M. C., Marin, K., Wood, J. L., Bernos, T. A., and Zastavniouk, C. (2019). Population correlates of rapid captive-induced maladaptation in a wild fish. *Evolutionary Applications*, 12(7), 1305-1317.

Froese, R., and Pauly, D. (2010). FishBase. (website: https://www.fishbase.se/search.php)

Fugère, V., and Hendry, A. P. (2018). Human influences on the strength of phenotypic selection. *Proceedings of the National Academy of Sciences*, *115*(40), 10070-10075.

Gallagher, B. K., Geargeoura, S., and Fraser, D. J. (2022). Effects of climate on salmonid productivity: A global meta-analysis across freshwater ecosystems. *Global Change Biology*, *28*(24), 7250-7269.

Gallagher, B. K., and Fraser, D. J. (2024). Microgeographic variation in demography and thermal regimes stabilize regional abundance of a widespread freshwater fish. *Ecological Applications*, e2936.

Gallagher, B. K., and Fraser, D. J. (2024). Stream groundwater inputs generate fine-scale variation in brook trout phenology and growth across a warming landscape. *Freshwater Biology*, *69*(1), 127-142.

Gallagher, B.K., Geargeoura, S., and Fraser, D.J. (2022), Data and code - Effects of climate on salmonid productivity: a global meta-analysis across freshwater ecosystems, Dryad, Dataset, https://doi.org/10.5061/dryad.t76hdr83z

Gobin, J., Lester, N. P., Fox, M. G., and Dunlop, E. S. (2016). Effects of changes in density-dependent growth and recruitment on sustainable harvest of lake whitefish. *Journal of Great Lakes Research*, *42*(4), 871-882.

Gobin, J., Fox, M. G., and Dunlop, E. S. (2021). Maturation reaction norm evolution under varying conditions of eco-evolutionary change. *Canadian Journal of Fisheries and Aquatic Sciences*, *78*(11), 1639-1649.

Gonzalez, A., Cardinale, B. J., Allington, G. R., Byrnes, J., Arthur Endsley, K., Brown, D. G., Hooper, D. U., Isbell, F., O'Connor, M. I. and Loreau, M. (2016). Estimating local biodiversity change: a critique of papers claiming no net loss of local diversity. *Ecology*, *97*(8), 1949-1960.

Grainger, T. N., and Levine, J. M. (2022). Rapid evolution of life-history traits in response to warming, predation and competition: A meta-analysis. *Ecology letters*, *25*(2), 541-554.

Grande, M., and Andersen, S. (1990). Effect of two temperature regimes from a deep and a surface water release on early development of salmonids. *Regulated Rivers: Research and Management*, *5*(4), 355-360.

Grossman, G. D., Ratajczak, R. E., Wagner, C. M., and Petty, J. T. (2010). Dynamics and regulation of the southern brook trout (Salvelinus fontinalis) population in an Appalachian stream. *Freshwater Biology*, *55*(7), 1494-1508.

Grossman, G. D., Carline, R. F., and Wagner, T. (2017). Population dynamics of brown trout (Salmo trutta) in Spruce Creek Pennsylvania: A quarter-century perspective. *Freshwater Biology*, *62*(7), 1143-1154.

Gurevitch, J., Koricheva, J., Nakagawa, S., and Stewart, G. (2018). Meta-analysis and the science of research synthesis. *Nature*, *555*(7695), 175-182.

Haddaway, N. R. (2015). A call for better reporting of conservation research data for use in meta-analyses. *Conservation Biology*, 29(4), 1242-1245.

Haddaway, N. R. (2020) ROSES_flowchart(): An R package and ShinyApp. doi: 10.5281/zenodo.4294810.

Hairston Jr, N. G., and Walton, W. E. (1986). Rapid evolution of a life history trait. *Proceedings of the National Academy of Sciences*, *83*(13), 4831-4833.

Hare, D. K., Helton, A. M., Johnson, Z. C., Lane, J. W., and Briggs, M. A. (2021). Continental-scale analysis of shallow and deep groundwater contributions to streams. *Nature Communications*, *12*(1), 1-10.

Harig, A. L., and Fausch, K. D. (2002). Minimum habitat requirements for establishing translocated cutthroat trout populations. *Ecological Applications*, *12*(2), 535-551.

Hartman, G. F., Scrivener, J. C., and Miles, M. J. (1996). Impacts of logging in Carnation Creek, a high-energy coastal stream in British Columbia, and their implication for restoring fish habitat. *Canadian Journal of Fisheries and Aquatic Sciences*, *53*(S1), 237-251.

Hartman, K. J., Adams, M. B., Owen, M. D., Shingleton, M., and Keyser, P. D. (2007). Evidence of stock-recruitment relationship in Appalachian brook trout. In *Proceedings of the Annual Conference of the Southeast Association of Fish and Wildlife Agencies* (Vol. 61, pp. 40-45).

Heino, M., Dieckmann, U., and Godø, O. R. (2002). Estimating reaction norms for age and size at maturation with reconstructed immature size distributions: a new technique illustrated by application to Northeast Arctic cod. *ICES Journal of Marine Science*, *59*(3), 562-575.

Hendry, A. P. (2017). Eco-evolutionary dynamics. Princeton University Press.

Hilborn, R., and Walters, C. J. (1992). Stock and recruitment. In: *Quantitative Fisheries Stock Assessment: Choice, Dynamics and Uncertainty*, 241-296.

Hilborn, R., and Walters, C. J. (Eds.). (2013). *Quantitative fisheries stock assessment: choice, dynamics and uncertainty*. Springer Science and Business Media.

Hilborn, R., Quinn, T. P., Schindler, D. E., and Rogers, D. E. (2003). Biocomplexity and fisheries sustainability. *Proceedings of the National Academy of Sciences*, 100(11), 6564-6568.

Hitt, N. P., Rogers, K. M., Kessler, K. G., Briggs, M. A., and Fair, J. H. (2023). Stabilising effects of karstic groundwater on stream fish communities. *Ecology of Freshwater Fish*. (Online)

Hoenig, J. M. (1983). Empirical use of longevity data to estimate mortality rates. *Fishery Bulletin*, *81*, 898-903.

Hoffmann, A. A., and Sgro, C. M. (2011). Climate change and evolutionary adaptation. *Nature*, 470(7335), 479-485.

Hollister J., Shah, T., Robitaille A., Beck, M., and Johnson, M. (2021). elevatr: Access Elevation Data from Various APIs. doi: 10.5281/zenodo.5809645, R package version 0.4.2, https://github.com/jhollist/elevatr/.

Holmes, E. E., Ward, E. J., and Wills, K. (2012). MARSS: multivariate autoregressive state-space models for analyzing time-series data. *R Journal*, *4*(1).

Honsey, A. E., Rypel, A., and Venturelli, P. A. (2022). Guidance for selecting base temperatures when using degree-days in fish growth analyses. *Canadian Journal of Fisheries and Aquatic Sciences*, (Online).

Hoxmeier, R. J. H., and Dieterman, D. J. (2011). *Application of mixture models for estimating age and growth of stream dwelling brook trout*. Study 675. Technical Report F-26-R, Minnesota Department of Natural Resources, Lake City, MN.

Hudy, M., Thieling, T. M., Gillespie, N., and Smith, E. P. (2008). Distribution, status, and land use characteristics of subwatersheds within the native range of brook trout in the eastern United States. *North American Journal of Fisheries Management*, *28*(4), 1069-1085.

Huntsman, B. M., and Petty, J. T. (2014). Density-dependent regulation of brook trout population dynamics along a core-periphery distribution gradient in a central Appalachian watershed. *PLoS One*, *9*(3), e91673.

Hutchings, J. A. (1991). Fitness consequences of variation in egg size and food abundance in brook trout Salvelinus fontinalis. *Evolution*, *45*(5), 1162-1168.

Hutchings, J. A. (1993). Adaptive life histories effected by age-specific survival and growth rate. *Ecology*, 74(3), 673-684.

Hutchings, J. A. (1994). Age-and size-specific costs of reproduction within populations of brook trout, Salvelinus fontinalis. *Oikos*, 12-20.

Hutchings, J. A. (1996). Adaptive phenotypic plasticity in brook trout, Salvelinus fontinalis, life histories. *Ecoscience*, 3(1), 25-32.

Hutchings, J. A., Pickle, A., McGregor-Shaw, C. R., and Poirier, L. (1999). Influence of sex, body size, and reproduction on overwinter lipid depletion in brook trout. *Journal of Fish Biology*, *55*(5), 1020-1028.

Hyndman R, Athanasopoulos G, Bergmeir C, Caceres G, Chhay L, O'Hara-Wild M, Petropoulos F, Razbash S, Wang E, Yasmeen F (2022). *forecast: Forecasting functions for time series and linear models*. R package version 8.19, https://pkg.robjhyndman.com/forecast/.

Iacona, G. D., Sutherland, W. J., Mappin, B., Adams, V. M., Armsworth, P. R., Coleshaw, T., ... and Possingham, H. P. (2018). Standardized reporting of the costs of management interventions for biodiversity conservation. *Conservation Biology*, *32*(5), 979-988.

Intergovernmental Panel on Climate Change (IPCC). (2023). Section 2: Current status and trends. In: *Climate Change 2023: Synthesis Report. Contribution of Working Groups I, II and III to the Sixth Assessment Report of the Intergovernmental Panel on Climate Change* [Core Writing Team, H. Lee and J. Romero (eds.)]. IPCC, Geneva, Switzerland, pp. 35-115.

Irvine, J. R., and Fukuwaka, M. A. (2011). Pacific salmon abundance trends and climate change. *ICES Journal of Marine Science*, *68*(6), 1122-1130.

Isaak, D. J., and Hubert, W. A. (2004). Nonlinear response of trout abundance to summer stream temperatures across a thermally diverse montane landscape. *Transactions of the American Fisheries Society*, *133*(5), 1254-1259.

Isaak, D. J., and Young, M. (2023). Cold-water habitats, climate refugia, and their utility for conserving salmonid fishes. *Canadian Journal of Fisheries and Aquatic Sciences*, *80*(7): 1187-1206.

Isaak, D. J., Young, M. K., Nagel, D. E., Horan, D. L., and Groce, M. C. (2015). The cold-water climate shield: delineating refugia for preserving salmonid fishes through the 21st century. *Global Change Biology*, *21*(7), 2540-2553.

Isaak, D. J., Young, M. K., Luce, C. H., Hostetler, S. W., Wenger, S. J., Peterson, E. E., Ver Hoef, J. M., Groce, M. C., Horan, D. L. and Nagel, D. E. (2016). Slow climate velocities of mountain streams portend their role as refugia for cold-water biodiversity. *Proceedings of the National Academy of Sciences*, 113(16), 4374-4379.

Ishiyama, N., Sueyoshi, M., Molinos, J. G., Iwasaki, K., Negishi, J. N., Koizumi, I., Nagayama, S., Nagasaka, A., Nagasaka, Y., and Nakamura, F. (2023). Underlying geology and climate interactively shape climate change refugia in mountain streams. *Ecological Monographs*, e1566.

Iwasaki, K., Fukushima, K., Nagasaka, Y., Ishiyama, N., Sakai, M., and Nagasaka, A. (2023). Real-time monitoring and postprocessing of thermal infrared video images for sampling and mapping groundwater discharge. *Water Resources Research*, *59*(4), e2022WR033630.

Jenkins, D. G., Carey, M., Czerniewska, J., Fletcher, J., Hether, T., Jones, A., Knight, S., Knox, J., Long, T., Mannino, M., and McGuire, M. (2010). A meta-analysis of isolation by distance: relic or reference standard for landscape genetics? *Ecography*, *33*(2), 315-320.

Jensen, A. J., and Johnsen, B. O. (1999). The functional relationship between peak spring floods and survival and growth of juvenile Atlantic salmon (Salmo salar) and brown trout (Salmo trutta). *Functional Ecology*, *13*(6), 778-785.

Jensen, A. J., Forseth, T., and Johnsen, B. O. (2000). Latitudinal variation in growth of young brown trout Salmo trutta. *Journal of Animal Ecology*, *69*(6), 1010-1020.

Johansson, M., Primmer, C. R., and Merilä, J. (2007). Does habitat fragmentation reduce fitness and adaptability? A case study of the common frog (Rana temporaria). *Molecular Ecology*, *16*(13), 2693-2700.

Johnson, J. B., and Omland, K. S. (2004). Model selection in ecology and evolution. *Trends in Ecology and Evolution*, *19*(2), 101-108.

Johnson, Z. C., Johnson, B. G., Briggs, M. A., Devine, W. D., Snyder, C. D., Hitt, N. P., Hare, D. K. and Minkova, T. V. (2020). Paired air-water annual temperature patterns reveal hydrogeological controls on stream thermal regimes at watershed to continental scales. *Journal of Hydrology*, *587*, 124929.

Jonsson, B., and Jonsson, N. (2009). A review of the likely effects of climate change on anadromous Atlantic salmon Salmo salar and brown trout Salmo trutta, with particular reference to water temperature and flow. *Journal of Fish Biology*, *75*(10), 2381-2447.

Kanno, Y., Vokoun, J. C., and Letcher, B. H. (2014). Paired stream–air temperature measurements reveal fine-scale thermal heterogeneity within headwater brook trout stream networks. *River Research and Applications*, *30*(6), 745-755.

Kanno, Y., Letcher, B. H., Hitt, N. P., Boughton, D. A., Wofford, J. E., and Zipkin, E. F. (2015). Seasonal weather patterns drive population vital rates and persistence in a stream fish. *Global Change Biology*, *21*(5), 1856-1870.

Kanno, Y., Pregler, K. C., Hitt, N. P., Letcher, B. H., Hocking, D. J., and Wofford, J. E. (2016a). Seasonal temperature and precipitation regulate brook trout young-of-the-year abundance and population dynamics. *Freshwater Biology*, *61*(1), 88-99.

Kanno, Y., Kulp, M. A., and Moore, S. E. (2016b). Recovery of native Brook Trout populations following the eradication of nonnative Rainbow Trout in southern Appalachian Mountains streams. *North American Journal of Fisheries Management*, *36*(6), 1325-1335.

Kanno, Y., Kulp, M. A., Moore, S. E., and Grossman, G. D. (2017). Native brook trout and invasive rainbow trout respond differently to seasonal weather variation: Spawning timing matters. *Freshwater Biology*, *62*(5), 868-879.

Karger, D. N., Chauvier, Y., and Zimmermann, N. E. (2023). chelsa-cmip6 1.0: a python package to create high resolution bioclimatic variables based on CHELSA ver. 2.1 and CMIP6 data. *Ecography*, e06535.

Kaylor, M. J., Armstrong, J. B., Lemanski, J. T., Justice, C., and White, S. M. (2022). Riverscape heterogeneity in estimated Chinook Salmon emergence phenology and implications for size and growth. *Ecosphere*, *13*(7), e4160.

Kaylor, M. J., Justice, C., Armstrong, J. B., Staton, B. A., Burns, L. A., Sedell, E., and White, S. M. (2021). Temperature, emergence phenology and consumption drive seasonal shifts in fish growth and production across riverscapes. *Journal of Animal Ecology*, *90*(7), 1727-1741.

Kazyak, D. C., Lubinski, B. A., Kulp, M. A., Pregler, K. C., Whiteley, A. R., Hallerman, E., E., Coombs, J. A., Kanno, Y., Rash, J. M., Morgan, R. P., Habera, J. and King, T. L. (2022). Population genetics of brook trout in the southern Appalachian mountains. *Transactions of the American Fisheries Society*, *151*(2), 127-149.

Kennedy, P., and Meyer, K. A. (2015). Trends in abundance and the influence of bioclimatic factors on Westslope cutthroat trout in Idaho. *Journal of Fish and Wildlife Management*, *6*(2), 305-317.

Koricheva, J., Gurevitch, J., and Mengersen, K. (Eds.). (2013). *Handbook of meta-analysis in ecology and evolution*. Princeton University Press.

Kovach, R. P., Muhlfeld, C. C., Al-Chokhachy, R., Dunham, J. B., Letcher, B. H., and Kershner, J. L. (2016). Impacts of climatic variation on trout: a global synthesis and path forward. *Reviews in Fish Biology and Fisheries*, 26(2), 135-151.

Kovach, R. P., Al-Chokhachy, R., Whited, D. C., Schmetterling, D. A., Dux, A. M., and Muhlfeld, C. C. (2017). Climate, invasive species and land use drive population dynamics of a cold-water specialist. *Journal of Applied Ecology*, *54*(2), 638-647.

Kovach, R. P., Jonsson, B., Jonsson, N., Arismendi, I., Williams, J. E., Kershner, J. L., Al-Chokhachy, R., Letcher, B., and Muhlfeld, C. (2019). Climate change and the future of trout and char. *In: Trout and Char of the World*. American Fisheries Society.

Krabbenhoft, T. J., Myers, B. J., Wong, J. P., Chu, C., Tingley, R. W., Falke, J. A., Kwak, T. J., Paukert, C. P. and Lynch, A. J. (2020). FiCli, the Fish and Climate Change Database, informs climate adaptation and management for freshwater fishes. *Scientific Data*, *7*(1), pp.1-6.

Kratzer, J. F., McHugh, P., Kirn, R., and Eldridge, W. H. (2021). Comparison of brook trout abundance and distribution in Vermont's streams between the 1950s and the 2000s. *Northeastern Naturalist*, *28*(2), 189-201.

Krebs, C. J. (2014). *Ecological methodolgy, 3rd edition*. Addison-Wesley Educational Publishers, Inc.

Kuhn, A., Gehara, M., Andrianarimalala, M. S., Rabibisoa, N., Randriamahatantsoa, B., Overcast, I., Raxworthy, C. J., Ruane, S., and Burbrink, F. T. (2022). Drivers of unique and asynchronous population dynamics in Malagasy herpetofauna. *Journal of Biogeography*, *49*(4), 600-616.

Lande, R. (1993). Risks of population extinction from demographic and environmental stochasticity and random catastrophes. *The American Naturalist*, *142*(6), 911-927.

Lapides, D. A., Maitland, B. M., Zipper, S. C., Latzka, A. W., Pruitt, A., and Greve, R. (2022). Advancing environmental flows approaches to streamflow depletion management. *Journal of Hydrology*, *607*, 127447.

Larsen, S., Comte, L., Filipa Filipe, A., Fortin, M. J., Jacquet, C., Ryser, R., Tedesco, P. A., Brose, U., Erős, T., Giam, X., Irving, K., Ruhi, A., Sharma, S., and Olden, J. D. (2021). The geography of metapopulation synchrony in dendritic river networks. *Ecology Letters*, *24*(4), 791-801.

Latta, W. C. (1965). Relationship of young-of-the-year trout to mature trout and groundwater. *Transactions of the American Fisheries Society, 94(1)*, 32-39.

Leduc, M., Mailhot, A., Frigon, A., Martel, J. L., Ludwig, R., Brietzke, G. B., Giguère, M., Brissette, F., Turcotte, R., Braun, M., and Scinocca, J. (2019). The ClimEx project: A 50-member ensemble of climate change projections at 12-km resolution over Europe and

northeastern North America with the Canadian Regional Climate Model (CRCM5). *Journal of Applied Meteorology and Climatology*, *58*(4), 663-693.

Lenoir, J., Hattab, T., and Pierre, G. (2017). Climatic microrefugia under anthropogenic climate change: implications for species redistribution. *Ecography*, *40*(2), 253-266.

Lester, N. P., Shuter, B. J., and Abrams, P. A. (2004). Interpreting the von Bertalanffy model of somatic growth in fishes: the cost of reproduction. *Proceedings of the Royal Society of London B: Biological Sciences*, *271*(1548), 1625-1631.

Letcher, B. H., Gries, G., and Juanes, F. (2002). Survival of stream-dwelling Atlantic salmon: effects of life history variation, season, and age. *Transactions of the American Fisheries Society*, *131*(5), 838-854.

Letcher, B. H., Schueller, P., Bassar, R. D., Nislow, K. H., Coombs, J. A., Sakrejda, K., Morrissey, M., Sigourney, D. B., Whiteley, A. R., O'Donnell, M .J. and Dubreuil, T .L. (2015). Robust estimates of environmental effects on population vital rates: an integrated capture–recapture model of seasonal brook trout growth, survival and movement in a stream network. *Journal of Animal Ecology*, 84(2), 337-352.

Letcher, B. H., Nislow, K. H., O'Donnell, M. J., Whiteley, A. R., Coombs, J. A., Dubreuil, T. L., and Turek, D. B. (2023). Identifying mechanisms underlying individual body size increases in a changing, highly seasonal environment: The growing trout of West brook. *Journal of Animal Ecology*, *92*(1), 78-96.

Liebhold, A., Koenig, W. D., and Bjørnstad, O. N. (2004). Spatial synchrony in population dynamics. *Annual Review of Ecology, Evolution, and Systematics*, 467-490.

Lisi, P. J., Schindler, D. E., Bentley, K. T., and Pess, G. R. (2013). Association between geomorphic attributes of watersheds, water temperature, and salmon spawn timing in Alaskan streams. *Geomorphology*, *185*, 78-86.

Lisi, P. J., Schindler, D. E., Cline, T. J., Scheuerell, M. D., and Walsh, P. B. (2015). Watershed geomorphology and snowmelt control stream thermal sensitivity to air temperature. *Geophysical Research Letters*, *42*(9), 3380-3388.

Liu, A. G., and Matthews, J. J. (2017). Great Canadian Lagerstätten 6. Mistaken Point Ecological Reserve, Southeast Newfoundland. *Geoscience Canada*, *44*(2), 63-76.

Lobón-Cerviá, J. (2009). Recruitment as a driver of production dynamics in stream-resident brown trout (Salmo trutta). *Freshwater Biology*, *54*(8), 1692-1704.

Lobón-Cerviá, J. (2022). Does recruitment trigger negative density-dependent feedback loops in stream-dwelling salmonids? *Canadian Journal of Fisheries and Aquatic Sciences*, *79*(7), 1145-1153.

Lobón-Cerviá, J., and Mortensen, E. (2005). Population size in stream-living juveniles of lake-migratory brown trout Salmo trutta L.: the importance of stream discharge and temperature. *Ecology of Freshwater Fish*, *14*(4), 394-401.

Lu, X., Kanno, Y., Valentine, G., Rash, J., and Hooten, M. (2023). Multi-scale spatial models reveal the interplay of weather and habitat effects on cold-water fish. *Authorea Preprint*.

Magnan, P., Proulx, R., and Plante, M. (2005). Integrating the effects of fish exploitation and interspecific competition into current life history theories: an example with lacustrine brook trout (Salvelinus fontinalis) populations. *Canadian Journal of Fisheries and Aquatic Sciences*, *62*(4), 747-757.

Maitland, B. M., and Latzka, A. W. (2022). Shifting climate conditions affect recruitment in Midwestern stream trout, but depend on seasonal and spatial context. *Ecosphere*, *13*(12), e4308.

Manderson, J. P. (2008). The spatial scale of phase synchrony in winter flounder (Pseudopleuronectes americanus) production increased among southern New England nurseries in the 1990s. *Canadian Journal of Fisheries and Aquatic Sciences*, *65*(3), 340-351.

Manhard, C. V., Joyce, J. E., Smoker, W. W., and Gharrett, A. J. (2017). Ecological factors influencing lifetime productivity of pink salmon (Oncorhynchus gorbuscha) in an Alaskan stream. *Canadian Journal of Fisheries and Aquatic Sciences*, *74*(9), 1325-1336.

Mann, R. H. K., Blackburn, J. H., and Beaumont, W. R. C. (1989). The ecology of brown trout Salmo trutta in English chalk streams. *Freshwater Biology*, *21*(1), 57-70.

Mantua, N. J., Crozier, L. G., Reed, T. E., Schindler, D. E., and Waples, R. S. (2015). Response of chinook salmon to climate change. *Nature Climate Change*, *5*(7), 613-615.

Matte, J. M., Fraser, D. J., and Grant, J. W. (2020a). Density-dependent growth and survival in salmonids: Quantifying biological mechanisms and methodological biases. *Fish and Fisheries*, 21, 588-600.

Matte, J. M., Fraser, D. J., and Grant, J. W. (2020b). Population variation in density-dependent growth, mortality and their trade-off in a stream fish. *Journal of Animal Ecology*, 89(2), 541-552.

McKenzie, D. J., Zhang, Y., Eliason, E. J., Schulte, P. M., Claireaux, G., Blasco, F. R., Nati, J. J., and Farrell, A. P. (2021). Intraspecific variation in tolerance of warming in fishes. *Journal of Fish Biology*, *98*(6), 1536-1555.

Meisner, J. D., Rosenfeld, J. S., and Regier, H. A. (1988). The role of groundwater in the impact of climate warming on stream salmonines. *Fisheries*, *13*(3), 2-8.

Mejia, F. H., Ouellet, V., Briggs, M. A., Carlson, S. M., Casas-Mulet, R., Chapman, M., ... and Torgersen, C. E. (2023). Closing the gap between science and management of cold-water refuges in rivers and streams. *Global Change Biology*, *29*(19), 5482-5508.

Miller, D. A., and Grant, E. H. C. (2015). Estimating occupancy dynamics for large-scale monitoring networks: amphibian breeding occupancy across protected areas in the northeast United States. *Ecology and Evolution*, *5*(21), 4735-4746.

Mohseni, O., and Stefan, H. G. (1999). Stream temperature/air temperature relationship: a physical interpretation. *Journal of Hydrology*, *218*(3-4), 128-141.

Mohseni, O., Stefan, H. G., and Erickson, T. R. (1998). A nonlinear regression model for weekly stream temperatures. *Water Resources Research*, *34*(10), 2685-2692.

Moore, J. W., and Schindler, D. E. (2022). Getting ahead of climate change for ecological adaptation and resilience. *Science*, *376*(6600), 1421-1426.

Moore, J. W., Yeakel, J. D., Peard, D., Lough, J., and Beere, M. (2014). Life-history diversity and its importance to population stability and persistence of a migratory fish: steelhead in two large North American watersheds. *Journal of Animal Ecology*, *83*(5), 1035-1046.

Moran, P. A. (1953). The statistical analysis of the Canadian lynx cycle. *Australian Journal of Zoology*, *1*(3), 291-298.

Morgan, A. M., and O'Sullivan, A. M. (2023). Cooler, bigger; warmer, smaller: Fine-scale thermal heterogeneity maps age class and species distribution in behaviourally thermoregulating salmonids. *River Research and Applications*, *39*(2), 163-176.

Morrill, J. C., Bales, R. C., and Conklin, M. H. (2005). Estimating stream temperature from air temperature: implications for future water quality. *Journal of Environmental Engineering*, *131*(1), 139-146.

Morrissey, M. B., and Ferguson, M. M. (2009). Marker-assisted determination of the relationship between body size and reproductive success and consequences for evaluation of adaptive life histories. *Molecular Ecology*, *18*(20), 4330-4340.

Morrissey, M. B., and Ferguson, M. M. (2011). A test for the genetic basis of natural selection: An individual-based longitudinal study in a stream-dwelling fish. *Evolution*, *65*(4), 1037-1047.

Mouquet, N., Lagadeuc, Y., Devictor, V., Doyen, L., Duputié, A., Eveillard, D., Faure, D., Garnier, E., Gimenez, O., Huneman, P. and Jabot, F. (2015). Predictive ecology in a changing world. *Journal of Applied Ecology*, *52*(5), 1293-1310.

Mueter, F. J., Peterman, R. M., and Pyper, B. J. (2002). Opposite effects of ocean temperature on survival rates of 120 stocks of Pacific salmon (Oncorhynchus spp.) in northern and southern areas. *Canadian Journal of Fisheries and Aquatic Sciences*, *59*(3), 456-463.

Munch, S. B., Rogers, T. L., Johnson, B. J., Bhat, U., and Tsai, C. H. (2022). Rethinking the prevalence and relevance of chaos in ecology. *Annual Review of Ecology, Evolution, and Systematics*, *53*, 227-249.

Muñoz, N. J., Farrell, A. P., Heath, J. W., and Neff, B. D. (2015). Adaptive potential of a Pacific salmon challenged by climate change. *Nature Climate Change*, *5*(2), 163-166.

Myers, B.J., Lynch, A.J., Bunnell, D.B., Chu, C., Falke, J.A., Kovach, R.P., Krabbenhoft, T.J., Kwak, T.J. and Paukert, C.P. (2017). Global synthesis of the documented and projected effects of climate change on inland fishes. *Reviews in Fish Biology and Fisheries*, *27*(2), 339-361.

Myrvold, K. M., and Kennedy, B. P. (2015b). Interactions between body mass and water temperature cause energetic bottlenecks in juvenile steelhead. *Ecology of Freshwater Fish*, *24*(3), 373-383.

Nadeau, C. P., Urban, M. C., and Bridle, J. R. (2017a). Climates past, present, and yet-to-come shape climate change vulnerabilities. *Trends in Ecology and Evolution*, *32*(10), 786-800.

Nadeau, C. P., Urban, M. C., and Bridle, J. R. (2017b). Coarse climate change projections for species living in a fine-scaled world. *Global Change Biology*, *23*(1), 12-24.

Nakagawa, S., Noble, D. W., Senior, A. M., and Lagisz, M. (2017). Meta-evaluation of meta-analysis: ten appraisal questions for biologists. *BMC Biology*, *15*(1), 1-14.

Nakano, S., Kitano, F., and Maekawa, K. (1996). Potential fragmentation and loss of thermal habitats for charrs in the Japanese archipelago due to climatic warming. *Freshwater Biology*, *36*(3), 711-722.

NatureServe. (2022). NatureServe Network biodiversity location data accessed through NatureServe Explorer [web application]. NatureServe, Arlington, Virginia. (Available online: https://explorer.natureserve.org/).

Neuswanger, J. R., Wipfli, M. S., Evenson, M. J., Hughes, N. F., and Rosenberger, A. E. (2015). Low productivity of Chinook salmon strongly correlates with high summer stream discharge in two Alaskan rivers in the Yukon drainage. *Canadian Journal of Fisheries and Aquatic Sciences*, *72*(8), 1125-1137.

Nislow, K. H., and Armstrong, J. D. (2012). Towards a life-history-based management framework for the effects of flow on juvenile salmonids in streams and rivers. *Fisheries Management and Ecology*, *19*(6), 451-463.

Norberg, J., Urban, M. C., Vellend, M., Klausmeier, C. A., and Loeuille, N. (2012). Eco-evolutionary responses of biodiversity to climate change. *Nature Climate Change*, 2(10), 747.

O'Dea, R. E., Lagisz, M., Jennions, M. D., Koricheva, J., Noble, D. W., Parker, T. H., Gurevitch, J., Page, M. J., Stewart, G., Moher, D. and Nakagawa, S. (2021). Preferred reporting

items for systematic reviews and meta-analyses in ecology and evolutionary biology: a PRISMA extension. *Biological Reviews*, 96(5), 1695-1722.

Oksanen J., Simpson G., Blanchet F., Kindt R., Legendre P., Minchin P., O'Hara R., Solymos P., Stevens M., Szoecs E., Wagner H., Barbour M., Bedward M., Bolker B., Borcard D., Carvalho G., Chirico M., De Caceres M., Durand S., Evangelista H., FitzJohn R., Friendly M., Furneaux B., Hannigan G., Hill M., Lahti L., McGlinn D., Ouellette M., Ribeiro Cunha E., Smith T., Stier A., Ter Braak C., and Weedon J. (2022). vegan: Community Ecology Package. R package version 2.6-4 (link: https://CRAN.R-project.org/package=vegan).

Olsen, E. M., Heino, M., Lilly, G. R., Morgan, M. J., Brattey, J., Ernande, B., and Dieckmann, U. (2004). Maturation trends indicative of rapid evolution preceded the collapse of northern cod. *Nature*, *428*(6986), 932-935.

Olsen, E. M., Lilly, G. R., Heino, M., Morgan, M. J., Brattey, J., and Dieckmann, U. (2005). Assessing changes in age and size at maturation in collapsing populations of Atlantic cod (Gadus morhua). *Canadian Journal of Fisheries and Aquatic Sciences*, *62*(4), 811-823.

Ony, M. A., Nowicki, M., Boggess, S. L., Klingeman, W. E., Zobel, J. M., Trigiano, R. N., and Hadziabdic, D. (2020). Habitat fragmentation influences genetic diversity and differentiation: Fine-scale population structure of Cercis canadensis (eastern redbud). *Ecology and Evolution*, *10*(8), 3655-3670.

O'Sullivan, R. J. (2021). Natural selection, evolution, and demography of salmonine populations experiencing intrusion from non-local stock. PhD Thesis, University College Cork.

O'Sullivan, R. J., Aykanat, T., Johnston, S. E., Rogan, G., Poole, R., Prodöhl, P. A., De Eyto, E., Primmer, C. R., McGinnity, P and Reed, T. E. (2020). Captive-bred Atlantic salmon released into the wild have fewer offspring than wild-bred fish and decrease population productivity. *Proceedings of the Royal Society B*, *287*(1937), 20201671.

Parmesan, C., and Yohe, G. (2003). A globally coherent fingerprint of climate change impacts across natural systems. *Nature*, 421(6918), 37-42.

Parra, I., Almodóvar, A., Nicola, G. G., and Elvira, B. (2009). Latitudinal and altitudinal growth patterns of brown trout Salmo trutta at different spatial scales. *Journal of Fish Biology*, *74*(10), 2355-2373.

Pearse, D. E., Miller, M. R., Abadía-Cardoso, A., and Garza, J. C. (2014). Rapid parallel evolution of standing variation in a single, complex, genomic region is associated with life history in steelhead/rainbow trout. *Proceedings of the Royal Society B: Biological Sciences*, *281*(1783), 20140012.

Pearson, S. K., Bull, C. M., and Gardner, M. G. (2018). Selection outweighs drift at a fine scale: lack of MHC differentiation within a family living lizard across geographically close but disconnected rocky outcrops. *Molecular Ecology*, *27*(9), 2204-2214.

Pinheiro J, Bates D, R Core Team (2022). *nlme: Linear and Nonlinear Mixed Effects Models*. R package version 3.1-161, https://CRAN.R-project.org/package=nlme.

Pitman, K. J., Moore, J. W., Sloat, M. R., Beaudreau, A. H., Bidlack, A. L., Brenner, R. E., Hood, E. W., Pess, G. R., Mantua, N. J., Milner, A. M. and Radić, V. (2020). Glacier retreat and Pacific salmon. *BioScience*, *70*(3), 220-236.

Poisot, T. (2011). The digitize package: extracting numerical data from scatterplots. *The R Journal*, 3.1: 25-26.

Pottier, P., Burke, S., Drobniak, S. M., and Nakagawa, S. (2022a). Methodological inconsistencies define thermal bottlenecks in fish life cycle: a comment on Dahlke et al. 2020. *Evolutionary Ecology*, 1-6.

Pottier, P., Burke, S., Zhang, R. Y., Noble, D. W., Schwanz, L. E., Drobniak, S. M., and Nakagawa, S. (2022b). Developmental plasticity in thermal tolerance: Ontogenetic variation, persistence, and future directions. *Ecology Letters*, *25*(10), 2245-2268.

Pregler, K. C., Hanks, R. D., Childress, E. S., Hitt, N. P., Hocking, D. J., Letcher, B. H., ... and Kanno, Y. (2019). State-space analysis of power to detect regional brook trout population trends over time. *Canadian Journal of Fisheries and Aquatic Sciences*, *76*(11), 2145-2155.

PSC (Pacific Salmon Commission). 2017. Economic impact of Pacific salmon fisheries. Final report prepared by GSGislason and Associates Ltd. and the University of Alaska Anchorage Institute of Social and Economic Research.

Purchase, C. F., and Hutchings, J. A. (2008). A temporally stable spatial pattern in the spawner density of a freshwater fish: evidence for an ideal despotic distribution. *Canadian Journal of Fisheries and Aquatic Sciences*, *65*(3), 382-388.

R Core Team (2022). R: A language and environment for statistical computing. R Foundation for Statistical Computing, Vienna, Austria. https://www.R-project.org/.

Radchuk, V., Reed, T., Teplitsky, C., van de Pol, M., Charmantier, A., Hassall, C., ... and Kramer-Schadt, S. (2019). Adaptive responses of animals to climate change are most likely insufficient. *Nature Communications*, *10*(1), 3109.

Railsback, S. F. (2022). What We Don't Know About the Effects of Temperature on Salmonid Growth. *Transactions of the American Fisheries Society*, *151*(1), 3-12.

Reed, T. E., Schindler, D. E., Hague, M. J., Patterson, D. A., Meir, E., Waples, R. S., and Hinch, S. G. (2011). Time to evolve? Potential evolutionary responses of Fraser River sockeye salmon to climate change and effects on persistence. *PLoS One*, *6*(6), e20380.

Reist, J. D., Wrona, F. J., Prowse, T. D., Power, M., Dempson, J. B., King, J. R., and Beamish, R. J. (2006). An overview of effects of climate change on selected Arctic freshwater and anadromous fishes. *AMBIO: A Journal of the Human Environment*, *35*(7), 381-387.

Reside, A. E., Butt, N., and Adams, V. M. (2018). Adapting systematic conservation planning for climate change. *Biodiversity and Conservation*, *27*(1), 1-29.

Reznick, D. A., Bryga, H., and Endler, J. A. (1990). Experimentally induced life-history evolution in a natural population. *Nature*, *346*(6282), 357-359.

Richardson, J. L., Urban, M. C., Bolnick, D. I., and Skelly, D. K. (2014). Microgeographic adaptation and the spatial scale of evolution. *Trends in Ecology and Evolution*, 29(3), 165-176.

Ridgway, M. S. (2008). A roadmap for coasters: landscapes, life histories, and the conservation of brook trout. *Transactions of the American Fisheries Society*, *137*(4), 1179-1191.

Ridgway, M. S., and Blanchfield, P. J. (1998). Brook trout spawning areas in lakes. *Ecology of Freshwater Fish*, *7*(3), 140-145.

Robinson, J. M., Josephson, D. C., Weidel, B. C., and Kraft, C. E. (2010). Influence of variable interannual summer water temperatures on brook trout growth, consumption, reproduction, and mortality in an unstratified Adirondack lake. *Transactions of the American Fisheries Society*, *139*(3), 685-699.

Rogers, L. A., and Schindler, D. E. (2008). Asynchrony in population dynamics of sockeye salmon in southwest Alaska. *Oikos*, *117*(10), 1578-1586.

Rose, K. A., Fiechter, J., Curchitser, E. N., Hedstrom, K., Bernal, M., Creekmore, S., Haynie, A., Ito, S.I., Lluch-Cota, S., Megrey, B.A and Edwards, C. A. (2015). Demonstration of a fully-coupled end-to-end model for small pelagic fish using sardine and anchovy in the California Current. *Progress in Oceanography*, 138, 348-380.

Rosenfeld, J. S. (2017). Developing flow–ecology relationships: Implications of nonlinear biological responses for water management. *Freshwater Biology*, *62*(8), 1305-1324.

Rowland, F. E., Schyling, E. S., Freidenburg, L. K., Urban, M. C., Richardson, J. L., Arietta, A. A., Rodrigues, S. B., Rubinstein, A. D., Benard, M. F.and Skelly, D. K. (2022). Asynchrony, density dependence, and persistence in an amphibian. *Ecology*, *103*(7), e3696.

Rubel, F., Brugger, K., Haslinger, K., and Auer, I. (2017). The climate of the European Alps: Shift of very high resolution Köppen-Geiger climate zones 1800–2100. *Meteorologische Zeitschrift*, *26*(2), 115-125.

Sabo, J. L., Finlay, J. C., Kennedy, T., and Post, D. M. (2010). The role of discharge variation in scaling of drainage area and food chain length in rivers. *Science*, *330*(6006), 965-967.

Scheffers, B. R., Edwards, D. P., Diesmos, A., Williams, S. E., and Evans, T. A. (2014). Microhabitats reduce animal's exposure to climate extremes. *Global Change Biology*, *20*(2), 495-503.

Schindler, D. E., and Hilborn, R. (2015). Prediction, precaution, and policy under global change. *Science*, *347*(6225), 953-954.

Schindler, D. E., Armstrong, J. B., Bentley, K. T., Jankowski, K., Lisi, P. J., and Payne, L. X. (2013). Riding the crimson tide: mobile terrestrial consumers track phenological variation in spawning of an anadromous fish. *Biology Letters*, *9*(3), 20130048.

Schindler, D. E., Hilborn, R., Chasco, B., Boatright, C. P., Quinn, T. P., Rogers, L. A., and Webster, M. S. (2010). Population diversity and the portfolio effect in an exploited species. *Nature*, 465(7298), 609-612.

Schluter, D., and McPhail, J. D. (1992). Ecological character displacement and speciation in sticklebacks. *The American Naturalist*, *140*(1), 85-108.

Senior, A. M., Grueber, C. E., Kamiya, T., Lagisz, M., O'Dwyer, K., Santos, E. S., and Nakagawa, S. (2016). Heterogeneity in ecological and evolutionary meta-analyses: its magnitude and implications. *Ecology*, *97*(12), 3293-3299.

Skelly, D. K., Joseph, L. N., Possingham, H. P., Freidenburg, L. K., Farrugia, T. J., Kinnison, M. T., and Hendry, A. P. (2007). Evolutionary responses to climate change. *Conservation Biology*, 1353-1355.

Skúlason, S., Noakes, D. L., and Snorrason, S. S. (1989). Ontogeny of trophic morphology in four sympatric morphs of arctic charr Salvelinus alpinus in Thingvallavatn, Iceland. *Biological Journal of the Linnean Society*, *38*(3), 281-301.

Smith, D. A., and Ridgway, M. S. (2019). Temperature selection in brook charr: lab experiments, field studies, and matching the Fry curve. *Hydrobiologia*, *840*(1), 143-156.

Snell-Rood, E. C., Kobiela, M. E., Sikkink, K. L., and Shephard, A. M. (2018). Mechanisms of plastic rescue in novel environments. *Annual Review of Ecology, Evolution, and Systematics*, *49*, 331-354.

Snyder, C. D., Hitt, N. P., and Young, J. A. (2015). Accounting for groundwater in stream fish thermal habitat responses to climate change. *Ecological Applications*, *25*(5), 1397-1419.

Sobie, S. R., Zwiers, F. W., and Curry, C. L. (2021). Climate model projections for Canada: a comparison of CMIP5 and CMIP6. *Atmosphere-Ocean*, *59*(4-5), 269-284.

Stearns, S. C. (1992). The evolution of life histories. Oxford University Press.

Stearns, S. C., and Hendry, A. P. (2004). The salmonid contribution to key issues in evolution. *In: Evolution illuminated: Salmon and their relatives*. Oxford University Press, New York, NY.

Stockwell, C. A., and Weeks, S. C. (1999). Translocations and rapid evolutionary responses in recently established populations of western mosquitofish (Gambusia affinis). In *Animal Conservation forum* (Vol. 2, No. 2, pp. 103-110). Cambridge University Press.

Stranko, S. A., Hilderbrand, R. H., Morgan, R. P., Staley, M. W., Becker, A. J., Roseberry-Lincoln, A., Perry, E. S. and Jacobson, P. T. (2008). Brook trout declines with land cover and temperature changes in Maryland. *North American Journal of Fisheries Management*, *28*(4), 1223-1232.

Suggitt, A. J., Gillingham, P. K., Hill, J. K., Huntley, B., Kunin, W. E., Roy, D. B., and Thomas, C. D. (2011). Habitat microclimates drive fine-scale variation in extreme temperatures. *Oikos*, *120*(1), 1-8.

Sunday, J., Bennett, J. M., Calosi, P., Clusella-Trullas, S., Gravel, S., Hargreaves, A. L., Leiva, F.P., Verberk, W.C., Olalla-Tárraga, M.Á., and Morales-Castilla, I. (2019). Thermal tolerance patterns across latitude and elevation. *Philosophical Transactions of the Royal Society B*, *374*(1778), 20190036.

Sweka, J. A., and Wagner, T. (2022). Influence of seasonal extreme flows on brook trout recruitment. *Transactions of the American Fisheries Society*, *151*(2), 231-244.

Thériault, V., Dunlop, E. S., Dieckmann, U., Bernatchez, L., and Dodson, J. J. (2008). The impact of fishing-induced mortality on the evolution of alternative life-history tactics in brook charr. *Evolutionary Applications*, 1(2), 409-423.

Thornton, M.M., Shrestha, R., Wei, Y., Thornton, P. E., Kao, S., and Wilson, B. E. (2020). Daymet: Daily Surface Weather Data on a 1-km Grid for North America; Version 4. ORNL DAAC; Oak Ridge; Tennessee; USA. https://doi.org/10.3334/ORNLDAAC/1840

Tsai, H. Y., Hamilton, A., Guy, D. R., Tinch, A. E., Bishop, S. C., and Houston, R. D. (2015). The genetic architecture of growth and fillet traits in farmed Atlantic salmon (Salmo salar). *BMC Genetics*, *16*(1), 1-11.

Urban, M. C. (2015). Accelerating extinction risk from climate change. *Science*, 348(6234), 571-573.

Urban, M. C., Bocedi, G., Hendry, A. P., Mihoub, J. B., Pe'er, G., Singer, A., Bridle, J.R., Crozier, L.G., De Meester, L., Godsoe, W., and Gonzalez, A. (2016). Improving the forecast for biodiversity under climate change. *Science*, 353(6304), aad8466.

Urban, M. C., Swaegers, J., Stoks, R., Snook, R. R., Otto, S. P., Noble, D. W., ... and Teplitsky, C. (2023). When and how can we predict adaptive responses to climate change? *Evolution Letters*, qrad038.

Valentine, G. P., Lu, X., Childress, E. S., Dolloff, C. A., Hitt, N. P., Kulp, M. A., Letcher, B. H., Pregler, K. C., Rash, J. M., Hooten, M. B., and Kanno, Y. (2024). Spatial asynchrony and cross-scale climate interactions in populations of a coldwater stream fish. *Global Change Biology*, 30, e17029.

Vellend, M., Baeten, L., Myers-Smith, I. H., Elmendorf, S.C., Beauséjour, R., Brown, C. D., De Frenne, P., Verheyen, K. and Wipf, S. (2013). Global meta-analysis reveals no net

change in local-scale plant biodiversity over time. *Proceedings of the National Academy of Sciences*, 110(48), 19456-19459.

Viechtbauer, W. (2010). Conducting meta-analyses in R with the metafor package. *Journal of Statistical Software*, *36*(3), 1-48. https://doi.org/10.18637/jss.v036.i03.

von Biela, V. R., Sergeant, C. J., Carey, M.P., Liller, Z., Russell, C., Quinn-Davidson, S., Rand, P. S., Westley, P. A. and Zimmerman, C. E. (2022). Premature mortality observations among Alaska's Pacific Salmon during record heat and drought in 2019. *Fisheries*, 47(4), 157-168.

Walker, J. D., Letcher, B. H., Rodgers, K. D., Muhlfeld, C. C., and D'Angelo, V. S. (2020). An interactive data visualization framework for exploring geospatial environmental datasets and model predictions. *Water*, *12*(10), 2928.

Wang, I. J. (2009). Fine-scale population structure in a desert amphibian: landscape genetics of the black toad (Bufo exsul). *Molecular Ecology*, *18*(18), 3847-3856.

Wang, T., Kelson, S. J., Greer, G., Thompson, S. E., and Carlson, S. M. (2020). Tributary confluences are dynamic thermal refuges for a juvenile salmonid in a warming river network. *River Research and Applications*, *36*(7), 1076-1086.

Warren, D. R., Ernst, A. G., and Baldigo, B. P. (2009). Influence of spring floods on year-class strength of fall-and spring-spawning salmonids in Catskill mountain streams. *Transactions of the American Fisheries Society*, *138*(1), 200-210.

Waterhouse, M. D., Blair, C., Larsen, K. W., and Russello, M. A. (2017). Genetic variation and fine-scale population structure in American pikas across a human-modified landscape. *Conservation Genetics*, *18*(4), 825-835.

Wells, Z. R., Bernos, T. A., Yates, M. C., and Fraser, D. J. (2019). Genetic rescue insights from population-and family-level hybridization effects in brook trout. *Conservation Genetics*, *20*(4), 851-863.

Wells, Z. R., McDonnell, L. H., Chapman, L. J., and Fraser, D. J. (2016). Limited variability in upper thermal tolerance among pure and hybrid populations of a cold-water fish. *Conservation Physiology*, *4*(1).

Wenger, S. J., Isaak, D. J., Luce, C. H., Neville, H. M., Fausch, K. D., Dunham, J. B., Dauwalter D.C., Young M.K., Elsner M.M., Rieman B.E., and Hamlet, A. F. (2011). Flow regime, temperature, and biotic interactions drive differential declines of trout species under climate change. *Proceedings of the National Academy of Sciences*, 108(34), 14175-14180.

Wickham, H. (2016). *ggplot2: Elegant graphics for data analysis*. Springer-Verlag New York. ISBN 978-3-319-24277-4, https://ggplot2.tidyverse.org.

Willis, C. G., Ruhfel, B., Primack, R. B., Miller-Rushing, A. J., and Davis, C. C. (2008). Phylogenetic patterns of species loss in Thoreau's woods are driven by climate change. *Proceedings of the National Academy of Sciences*, *105*(44), 17029-17033.

Wood, J. L., and Fraser, D. J. (2015). Similar plastic responses to elevated temperature among different-sized brook trout populations. *Ecology*, 96(4), 1010-1019.

Wood, J. L., Belmar-Lucero, S., Hutchings, J. A., and Fraser, D. J. (2014). Relationship of habitat variability to population size in a stream fish. *Ecological Applications*, 24(5), 1085-1100.

Wood, J. L., Tezel, D., Joyal, D., and Fraser, D. J. (2015). Population size is weakly related to quantitative genetic variation and trait differentiation in a stream fish. *Evolution*, 69(9), 2303-2318.

Woodward, G., Perkins, D. M., and Brown, L. E. (2010). Climate change and freshwater ecosystems: impacts across multiple levels of organization. *Philosophical Transactions of the Royal Society B: Biological Sciences*, 365(1549), 2093-2106.

Wright, S. (1943). Isolation by distance. *Genetics*, *28*(2), 114.

Xu, C. L., Letcher, B. H., and Nislow, K. H. (2010a). Size-dependent survival of brook trout Salvelinus fontinalis in summer: effects of water temperature and stream flow. *Journal of Fish Biology*, 76(10), 2342-2369.

Xu, C., Letcher, B. H., and Nislow, K. H. (2010b). Context-specific influence of water temperature on brook trout growth rates in the field. *Freshwater Biology*, 55(11), 2253-2264.

Yates, M. C., Bowles, E., and Fraser, D. J. (2019). Small population size and low genomic diversity have no effect on fitness in experimental translocations of a wild fish. *Proceedings of the Royal Society B: Biological Sciences*, 286(1916), 20191989.

Yoder, J. B., Clancey, E., Des Roches, S., Eastman, J. M., Gentry, L., Godsoe, W., Hagey, T. J., Jochimsen, D., Oswald, B. P., Robertson, J., Sarver, B. A. J. and Harmon, L. J. (2010). Ecological opportunity and the origin of adaptive radiations. *Journal of Evolutionary Biology*, *23*(8), 1581-1596.

Young, M. K., Guenther-Gloss, P. M., and Ficke, A. D. (2005). Predicting cutthroat trout (Oncorhynchus clarkii) abundance in high-elevation streams: revisiting a model of translocation success. *Canadian Journal of Fisheries and Aquatic Sciences*, *62*(10), 2399-2408.

Zabel, R. W., and Achord, S. (2004). Relating size of juveniles to survival within and among populations of Chinook salmon. *Ecology*, *85*(3), 795-806.

Zastavniouk, C., Weir, L. K., and Fraser, D. J. (2017). The evolutionary consequences of habitat fragmentation: Body morphology and coloration differentiation among brook trout populations of varying size. *Ecology and Evolution*, *7*(17), 6850-6862.

Zimmerman, M. S., Kinsel, C., Beamer, E., Connor, E. J., and Pflug, D. E. (2015). Abundance, survival, and life history strategies of juvenile Chinook salmon in the Skagit River, Washington. *Transactions of the American Fisheries Society*, *144*(3), 627-641.

Zorn, T. G., and Nuhfer, A. J. (2007). Regional synchrony of brown trout and brook trout population dynamics among Michigan rivers. *Transactions of the American Fisheries Society*, *136*(3), 706-717.

Zuur, A. F., Tuck, I. D., and Bailey, N. (2003). Dynamic factor analysis to estimate common trends in fisheries time series. *Canadian Journal of Fisheries and Aquatic Sciences*, *60*(5), 542-552.

VIII. Appendices

Appendix 1: *Chapter 1 Supplementary Materials*

A1.1 - Database construction:

In addition to correlations and sample sizes, other data of interest were compiled within and among studies using information provided by authors. Studies were assigned a unique name and number, then we recorded the publication year, study species (common name, genus, species), location (country, region, system name), habitat type (lotic or lentic), migration behavior (anadromous or freshwater resident), and range portion (native or non-native) associated with each correlation. The precise response and predictor used in each correlation were noted, as were overarching variable types that were eventually used to distinguish different data sets (abudance or growth for responses; temperature or precipitation for predictors). In addition, we included more detailed categorizations of the reponse type (abundance, population growth, stock-recruitment, survival, length, weight, or growth rate) and predictor type (average, maximum, minimum, percentile, PCA, or degree-day). Details about study design (spatial or temporal), data transformation (yes or no, based on whether the correlation contained any type of transformed data), and the data extraction method (correlations directly reported by authors, or based on data extracted from figures or tables) were also documented.

Three descriptors of temporal context were initially recorded: age-class (0, 1, 2+, multiple), season (fall, spring, summer, winter, multiple), and life-stage (incubation, emergence, growing season, overwintering, reproduction, migration, multiple). For age-class, age-0 and age-1 observations were required to be from single cohorts, while age-2+ observations could contain multiple cohorts as long as they were all age-2 or older. We adopted a similar protocol as Kovach et al. (2016) to differentiate seasons, using author descriptions when possible but otherwise assigning specific months to spring (March-May), summer (June-August), fall (September-November), and winter (December-February). To add more detail, life-stages were based on author descriptions of reproductive phenology (e.g. most salmonids spawn in fall or spring) and growing season (e.g. shorter at high latitudes). Another temporal variable was later created for life-stage*age, which was the same as life-stage but with observations from the growing season (which had the largest sample sizes) broken up by age-class. For all temporal variables, instances where multiple shorter time-periods within the level of interest were used (e.g. separate correlations based on mean temperatures for June, July, and August), these were specified to be the same level and treated as repeated measures. Conversely, the 'multiple' category was used for observations where a mix of other age-class categories were sampled (e.g. population size), or if the time-period assessed overlapped with multiple seasons or life-stages (e.g. annual average temperature or precipitation).

In cases authors where authors did not provide sufficient information to confidently infer the factors described above (especially range portion and life-stage), we referred to species summaries on FishBase (Froese and Pauly 2010) to guide decision-making. Similar to Kovach et al. (2016), we also flagged instances where a variable used in the correlation was inversely related to the process of interest for responses (e.g. mortality, which is negatively related to abundance) or predictors (e.g. winter severity or drought severity, where high values correspond to low temperature or precipitation, respectively). We identified 21 observations from 9 studies with this issue, and corrected it by simply multiplying these correlations by -1. In addition, for cases where coefficients of determination were provided by authors based on non-linear

regression (e.g. Isaak and Hubert 2004, Lobón-Cerviá and Mortensen 2005), we manually extracted the data and re-calculated the correlation coefficient based on linear regression.

Finally, the database was georeferenced in order to index study locations as continuous variables that could be linked to other spatial data. Coordinates (in decimal degrees) were inputted directly if they were reported by authors, or estimated in Google Maps (WGS 84 Web Mercator coordinate system) based on information provided in the study. For studies conducted over large areas, the location of the centermost sampling site was used. After georeferencing, elevation data (in meters above sea level) were inputted directly if reported by authors, or extracted using the *get_elev_point()* function from the *Elevatr* package in R based on coordinates within Amazon Web Service Terrain Tiles (Hollister et al. 2021). The median elevation was used for large study areas with data provided across sampling sites (e.g. in a table), or otherwise inferred from the centermost sampling site. A comparison of elevations directly reported by authors and those estimated in *Elevatr* (n=544) suggested that the two methods yielded similar results (R^2=0.80) and that bias was minimal.

A1.2 - Critical appraisal and data filtering:

Once the initial database was completed (1,735 correlations from 182 studies), B.K.G. conducted a critical appraisal based on thorough evaluations of each study to ensure the suitability, comparability, and independence of observations to the extent possible. Observations from each study were sequentially screened in six steps, as follows:

1.) We verified that the correlation was ascribed to temporal (i.e. same location sampled over multiple years) or spatial (i.e. a wide area sampled over a short timespan) climate variation based on study design, and that salmonid data were not completely fishery-dependent (e.g. landings from commercial or recreational fisheries). Observations were removed if data were fishery-dependent or if spatial and temporal variation were confounded, but retained if they were only partly fishery-dependent (e.g. recruits per spawner based on catch and escapement, growth or year-class strength derived from fishery samples).

2.) We removed any observation where stocking of the focal population with hatchery fish during the study period was explicitly mentioned. We chose to retain observations from naturalized non-native populations or from situations where stocked fish were differentiated (e.g. through unique fin clips or hatchery marks) and removed from calculations.

3.) We excluded any correlations based on data that were potentially incomparable to measures of salmonid abundance (e.g. percentage of total abundance in a given age-class), salmonid growth (e.g. body condition, size data not standardized by age), or the central tendency of a climate variable (e.g. variation in discharge).

4.) We ensured that correlations and sample sizes were entered correctly based on reporting in full-texts or raw data files, and verified that the response and predictor in the correlation were matched at the appropriate temporal or spatial scale (e.g. salmonid data from September could only be linked to climate variables from previous months or seasons). All correlations based on mismatched data were excluded. Observations based

on raw data from figures were also excluded if data could not be confidently extracted (e.g. many overlapping data points).

5.) We removed any duplicate observations within each study and identified cases where multiple studies reported data for the same population. These studies were subsequently screened for duplicates, identifying cases where the exact same response and predictor variables were used across multiple studies. In these cases, we only retained the observation with the largest sample size or, if sample sizes were equivalent, from the most recent study.

6.) Any observations with a sample size less than five were removed, because it is not possible to estimate the sampling variance when calculating standardized effect sizes for these data (Koricheva et al. 2013).

After critical appraisal and filtering, the final database contained 1,321 correlations from 156 studies.

A1.3 - Publication bias in the Abundance-Precipitation data set:

Significant publication bias was detected in the best-fit model for the Abundance-Precipitation data set (see Results), and a series of follow-up analyses were conducted to identify individual studies that contributed most to this pattern. First, residuals were plotted as a function of sample size, which showed a cluster of negative residuals associated with studies with intermediate sample sizes (visible in points with low standard errors in Figure A1.4a). Subsequently, the A-P data set was filtered to retain observations with residuals between -2 and 0, and sample sizes between 15 and 30, which allowed us to identify eleven studies that exhibited negitively skewed residuals (Hartman et al. 1996, Jensen and Johnsen 1999, Carline 2006, Clews et al. 2010, Copeland and Meyer 2011, Kennedy and Meyer 2015, Myrvold and Kennedy 2015b, Neuswanger et al. 2015, Zimmerman et al. 2015, Grossman et al. 2017, Manhard et al. 2017). These studies provided 96 observations, and nearly half of them (n=42) were from a single study by Copeland and Meyer (2011). The eleven studies were not representative of the A-P data set as a whole (total n=362), and were spatially skewed towards two study areas within the Clearwater River drainage in Idaho (Copeland and Meyer 2011, Kennedy and Meyer 2015, Myrvold and Kennedy 2015b), and Spruce Creek in Pennsylvania (Carline 2006, Grossman et al. 2017). The season moderator that was included in best-fit models was also skewed, with 51% of observations in the eleven studies categorized at the 'multiple' level where precipitation was often averaged over 9-12 months (section A1), whereas this level accounted for 35% of observations in the entire data set. Similarly, there were almost no observations from the fall (n=2, or 2% of observations) or spring (n=1, or 1%) in the eleven studies, but these were much more prominent in the full data set (n=25, or 7% for fall; n=34, or 9% for spring). We do not believe these studies were deliberately biased in any way, but rather were impacted by the over-representation of 'multiple' seasons and a broader lack of seasonal contrast. The reason why residuals from the eleven studies are skewed negative is unclear, but may be related to the low number and uneven spatial distribution of observations, coupled with random among-study heterogeneity.

As a first attempt to reduce bias, we removed Copeland and Meyer (2011) from the data set and re-ran the best-fit model, but this did not alleviate funnel plot asymmetry and the Egger test remained significant ($p<0.05$). We subsequently repeated this procedure after removing all

eleven studies listed above, which lessened asymmetry in the funnel plot and yielded a marginally non-significant Egger test (p=0.064). Collinearity was also significantly reduced when the eleven studies were excluded, with the 'winter' (VIF=2.70) and 'multiple' (VIF=1.87) levels of the season moderator exhibiting much lower VIF values compared to the best-fit model based on the entire data set (VIF=6.43 and 6.12, respectively; Table S2; see section 3.3). Estimated coefficients were similar and showed substantial overlap in 95% confidence intervals for best-fit models with (fall LCI, UCI=-0.25, 0.38; multiple=-0.50, -0.04; spring=-0.89, -0.31; summer=-0.40, 0.05; winter=-0.49, -0.02; temporal=0.10, 0.60) and without the eleven studies (fall LCI, UCI=-0.16, 0.56; multiple=-0.48, 0.04; spring=-0.85, -0.25; summer=-0.44, 0.02; winter=-0.41, 0.11; temporal=0.17, 0.69).

A1.4 - 'Multiple' levels within temporal covariates:

Over-aggregated climate data created several challenges in interpreting effects of temporal covariates on salmonid-climate relationships, especially for the season variable. Specifically, the practice of averaging climate data over 6-12 month periods was common in many studies and inhibited the ability to identify seasons or other time-periods with disproportionate impacts on productivity. Moreover, because the 'multiple' season category contained any estimate that could not be ascribed to a single season (see section A1), it includes some effects from the incubation period (late-fall to early-spring in many fall-spawning salmonids) and growing season (late-spring to early-fall in many low-latitude salmonids). Indeed, we believe that this temporal overlap with other time-periods explains why observations from 'multiple' seasons contributed to collinearity (VIF>6) in the best-fit Abundance-Precipitation model, while it was also partly responsible for publication bias in this dataset (see section A1.3).

In order to test whether the inclusion of 'multiple' levels within temporal covariates significantly impacted results in best-fit models, we removed all such observations and re-ran the same model structure in each dataset. Because different temporal covariates were chosen via model selection for each dataset (Tables 1.2 and 1.3), the specific covariate from which observations were removed differed in each case. Specifically, we removed 'multiple' observations from the season covariate (n=129) in the Abundance-Precipitation dataset, from the age-class covariate (n=240) in the Abundance-Temperature dataset, from the life-stage covariate (n=16) in the Growth-Precipitation dataset, and from the life-stage*age covariate (n=45) in the Growth-Temperature dataset. This substantially reduced sample sizes (n=430 observations removed in total), but model coefficients after removing 'multiple' levels had 95% confidence intervals that overlapped substantially with those from the original best-fit model in all four datasets. Therefore, the inclusion of 'multiple' levels did not appear to significantly alter the results or interpretation of my best-fit models.

Table A1.1: Model results for omnibus test of covariates (Wald-type test statistic with p-values based on a Chi-squared distribution), and fixed effect coefficients for best-fit models from each data set (Abundance-Precipitation (A-P), Abundance-Temperature (A-T), Growth-Precipitation (G-P), Growth-Temperature (G-T)). Covariate abbreviations used for coefficients are from Table 1.1.

Dataset	Omnibus Test	Coefficient	Estimate	SE	df	p-value
A-P	4.36	SE(Fall)	0.0769	0.1645	356	0.6403
	(p=0.001)*	SE(Multiple)	-0.2134	0.1213	356	0.0795
		SE(Spring)	-0.5827	0.1507	356	***<0.001****
		SE(Summer)	-0.2219	0.1177	356	0.0601
		SE(Winter)	-0.2268	0.1212	356	0.0622
		S(Temporal)	0.3316	0.1312	356	***0.0119****
A-T	5.46	Intercept	-1.2878	0.3255	602	***<0.001****
	(p<0.001)*	Latitude	0.0189	0.0061	602	***0.002****
		Elevation	0.0002	0.0001	602	***0.0011****
		AC(1)	0.1383	0.073	602	0.0586
		AC(2+)	-0.1145	0.0712	602	0.1082
		AC(Multiple)	0.0019	0.0677	602	0.9776
		S(Temporal)	0.1961	0.0881	602	***0.0264****
		N(Non-Native)	0.3064	0.0983	602	***0.0019****
G-P	7.08	LS(Multiple)	-0.0795	0.1675	59	0.6368
	(p<0.001)*	LS(Emergence)	0.0532	0.2307	59	0.8186
		LS(Growing Season)	0.6091	0.1106	59	***<0.001****
		LS(Incubation)	-0.9576	0.3196	59	***0.004****
		LS(Overwintering)	0.2410	0.1795	59	0.1844
		LS(Reproduction)	0.4776	0.1758	59	***0.0086****
		A(Anadromous)	-0.3613	0.1559	59	***0.024****
G-T	4.08	Intercept	0.0815	0.4845	270	0.8665
	(p<0.001)*	Latitude	0.0067	0.0072	270	0.3554
		Elevation	0.0004	0.0002	270	***0.0122****
		LSA(Emergence)	0.0282	0.1741	270	0.8713
		LSA(Growing Season_0)	0.0612	0.1352	270	0.6511
		LSA(Growing Season_1)	-0.2080	0.1321	270	0.1164
		LSA(Growing Season_2+)	-0.2222	0.1261	270	0.0793
		LSA(Growing Season_Multi)	0.1335	0.2594	270	0.6071
		LSA(Incubation)	0.4604	0.2102	270	***0.0293****
		LSA(Migration)	-0.1516	0.2886	270	0.5998
		LSA(Overwintering)	-0.5486	0.1436	270	***<0.001****
		LSA(Reproduction)	0.0637	0.394	270	0.8717
		H(Lotic)	-0.3374	0.1564	270	***0.0318****

Table A1.2: Summary of post-hoc tests of model assumptions, collinearity (variance inflation factors calculated across all levels of each covariate and within levels of temporal covariates), publication bias, taxonomic effects, and robustness of model results to methodological factors (see Table 1.1) or the inclusion of outlier studies. Results are shown separately for Abundance-Precipitation (A-P), Abundance-Temperature (A-T), Growth-Precipitation (G-P), and Growth-Temperature (G-T) datasets. Asterisks (*) denote significant results, while non-significant statistical tests are marked with NS. Detailed contrasts for robustness tests are shown in Table A1.3.

Best-Fit Model Test	A-P	A-T	G-P	G-T
Homoscedasticity				
Visual assessment	Yes	Yes	Yes	Yes
Collinearity				
Max VIF (All)	4.31	1.39	2.11	1.43
Min VIF (All)	4.31	1.04	2.11	1.22
Max VIF (Temporal)	6.43	1.33	2.27	2.84
Min VIF (Temporal)	1.91	1.24	1.00	1.08
Publication Bias				
Funnel plot asymmetry	Yes	No	No	No
Egger test (SE)	0.83	-0.03	-0.43	-0.04
p-value	0.01*	0.90	0.55	0.91
Year slope	-0.04	-0.01	0.03	-0.02
p-value	<0.01*	0.17	0.15	0.03*
Taxonomic Effects				
Species contrasts	NS	NS		NS
Difference in 95% CI	NS	NS		NS
Robustness				
Response type	NS	NS	*	*
Predictor type	NS	NS	NS	*
Data transformation	NS	*	NS	NS
Extraction method	NS	*	NS	NS
Outlier Exclusion				
Cook's D threshold	1	0.5	1	1
N influential studies	3	6	3	5
Difference in 95% CI	NS	NS	NS	NS

Table A1.3: Detailed results of robustness tests where four methodological variables were added to the best-fit model for each data set (see Methods; variable descriptions and abbreviations in Table 1.1). Contrast coefficients and their p-values are shown, as well as a description of the variable levels used in each contrast. Results are shown separately for Abundance-Precipitation (A-P), Abundance-Temperature (A-T), Growth-Precipitation (G-P), and Growth-Temperature (G-T) datasets. Significant contrasts and p-values are highlighted in bold italic text with an asterisk (*).

Variable Added	Reference Level	Contrast Level	A-P Contrast	p-value	A-T Contrast	p-value	G-P Contrast	p-value	G-T Contrast	p-value
RT	Abundance	Pop. growth	0.046	0.814	0.181	0.231				
		Stock-recruit	-0.189	0.322	-0.228	0.111				
		Survival	0.117	0.237	-0.211	0.069				
	Growth rate	Length					0.153	0.219	0.064	0.602
		Weight					***-0.686***	***<0.001****	***0.520***	***0.001****
PT	Average	Degree day			-0.005	0.970			-0.011	0.955
		Maximum	-0.035	0.743	0.024	0.741	-0.196	0.360	0.099	0.292
		Minimum	0.021	0.844	0.036	0.733	0.078	0.696	***-0.267***	***0.011****
		PCA	-0.024	0.900	0.253	0.530	-0.068	0.790	-0.653	0.062
		Percentile			-0.121	0.485	-0.294	0.130	0.054	0.878
DT	Raw data	Transformed	0.140	0.311	***0.191***	***0.047****	0.039	0.906	0.558	0.052
DM	Extracted manually	Directly reported	-0.086	0.412	***-0.147***	***0.040****	0.162	0.425	0.017	0.872

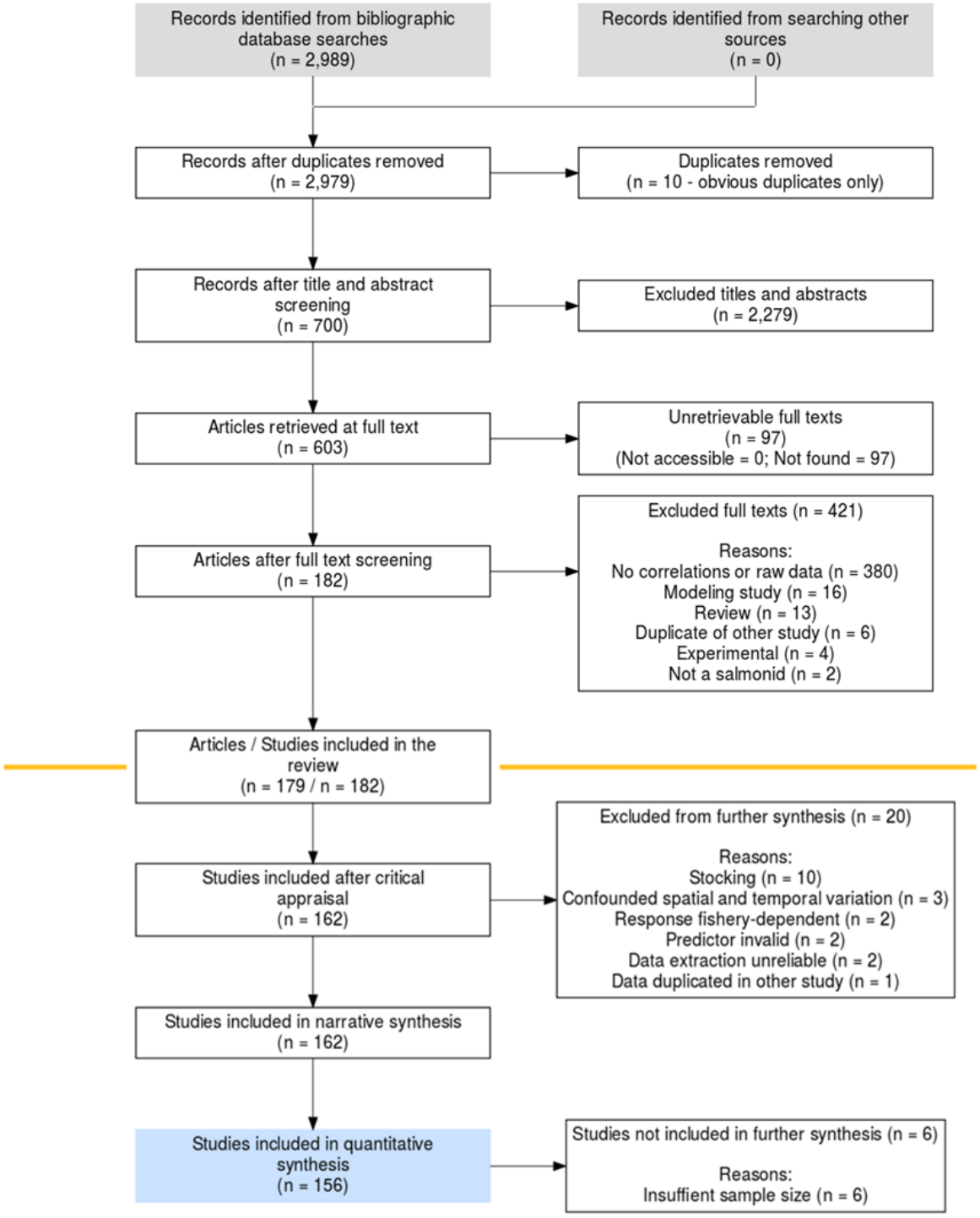

Figure A1.1: Study screening summary, showing each step from the original Web of Science search to the final database after critical appraisal and filtering (see Section A1.3). Flow chart made through the ROSES online tool provided by Haddaway (2020).

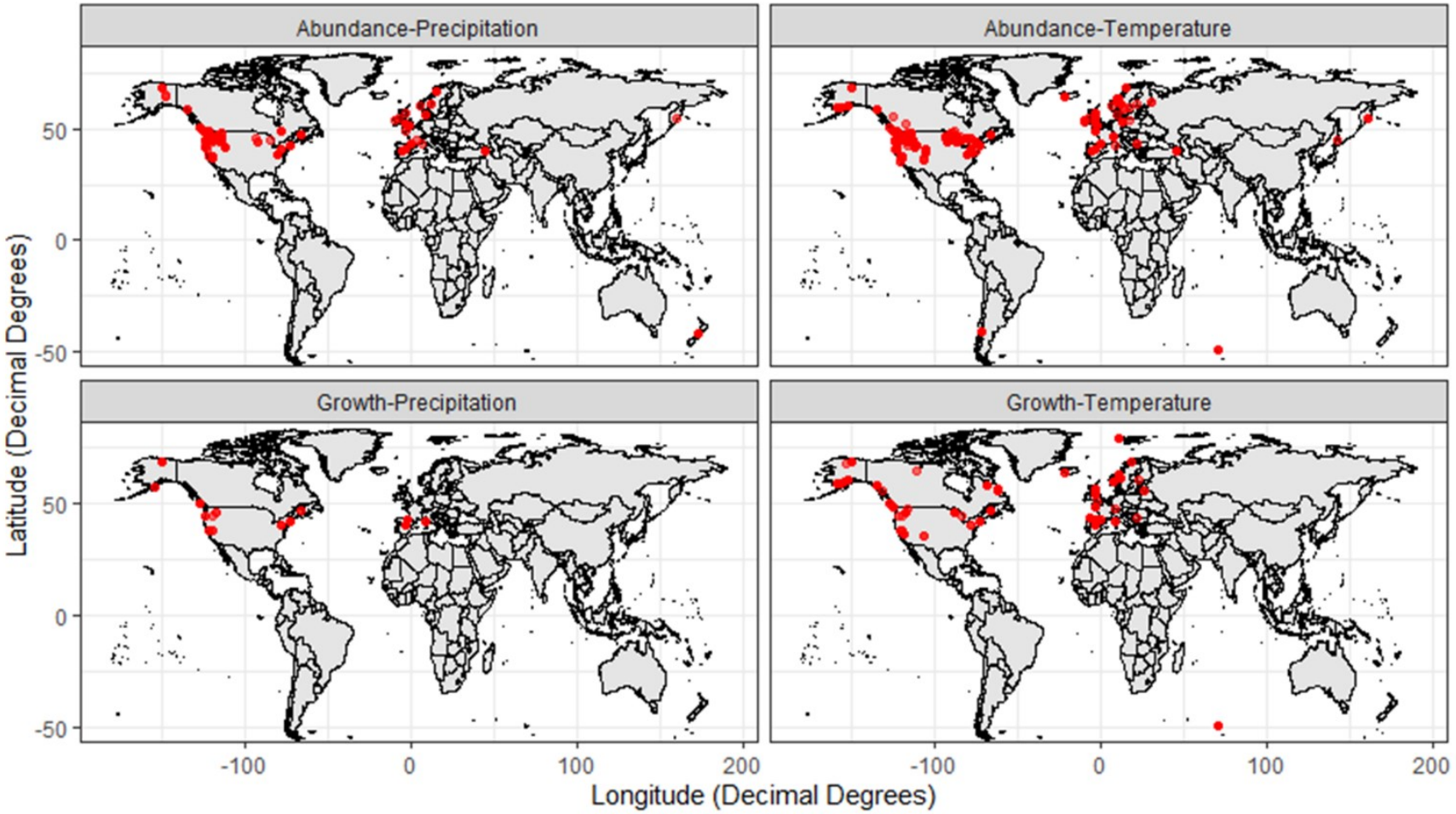

Figure A1.2: Map of georeferenced observations from each dataset. Shape files were taken from the *Maps* package in R (Deckmyn et al. 2021). Map lines delineate study areas and do not necessarily depict accepted national boundaries.

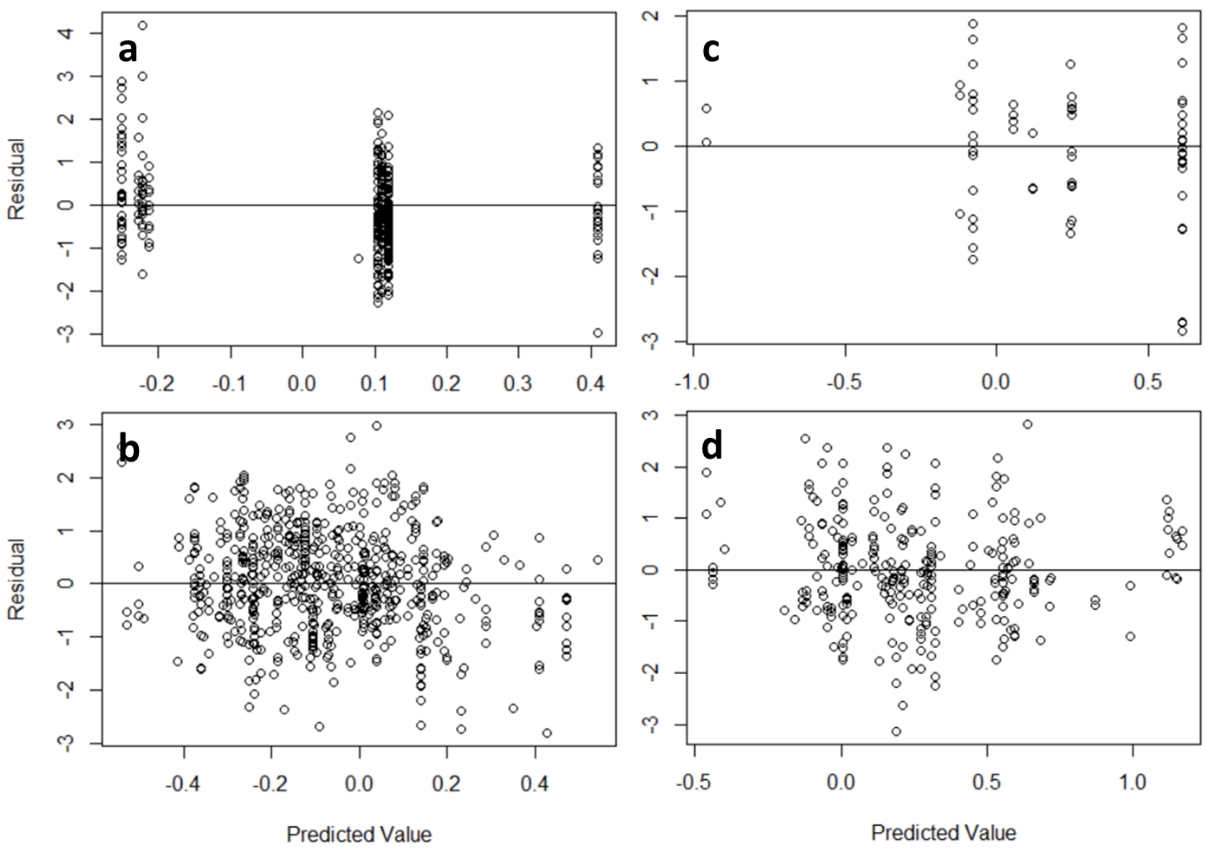

Figure A1.3: Plots of residuals against predicted values from the best-fit models for the Abundance-Precipitation (a), Abundance-Temperature (b), Growth-Precipitation (c), and Growth-Temperature (d) data sets. Details on model structure in each case can be found in Table 1.3.

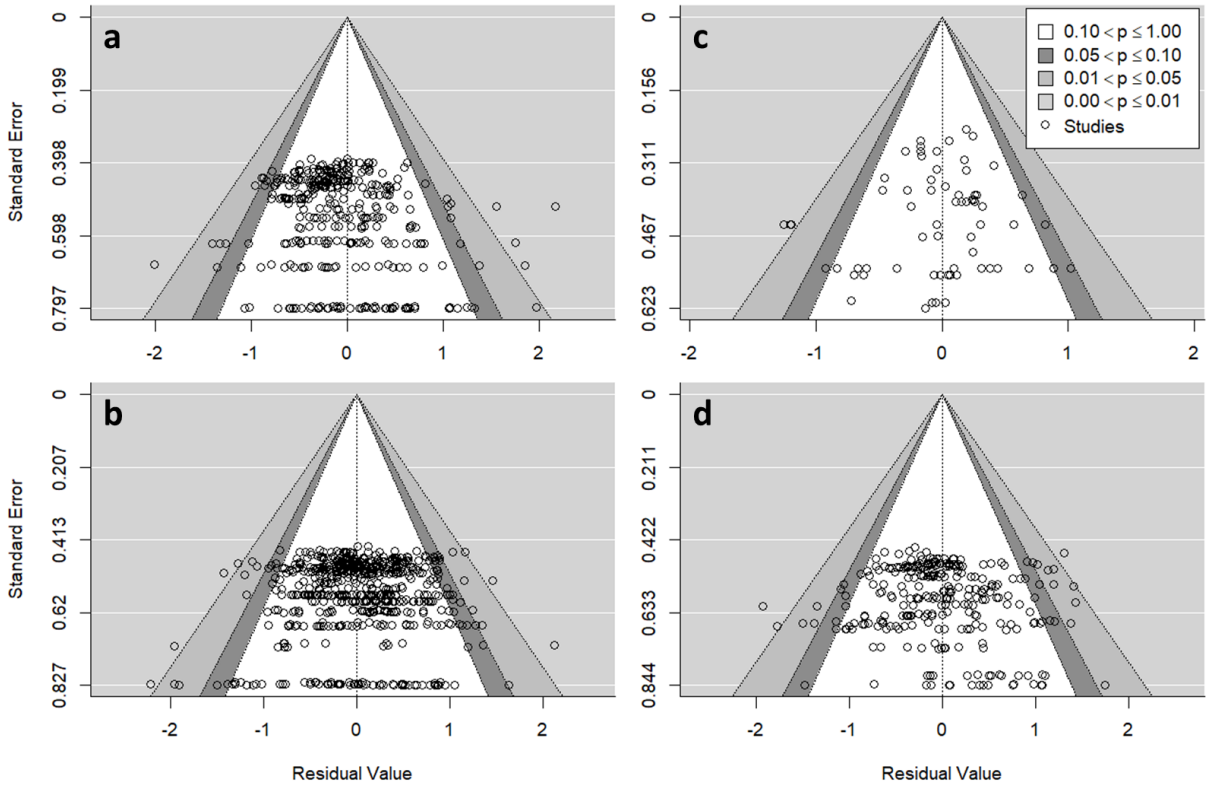

Figure A1.4: Funnel plots showing residual values (x-axis) and standard errors (y-axis) of each observation from the best-fit models for the Abundance-Precipitation (a), Abundance-Temperature (b), Growth-Precipitation (c), and Growth-Temperature (d) data sets. Note the residual asymmetry in panel a, where publication bias is evident in observations with low standard error that are skewed towards negative residual values. Corresponding Egger test results are in Table A1.2.

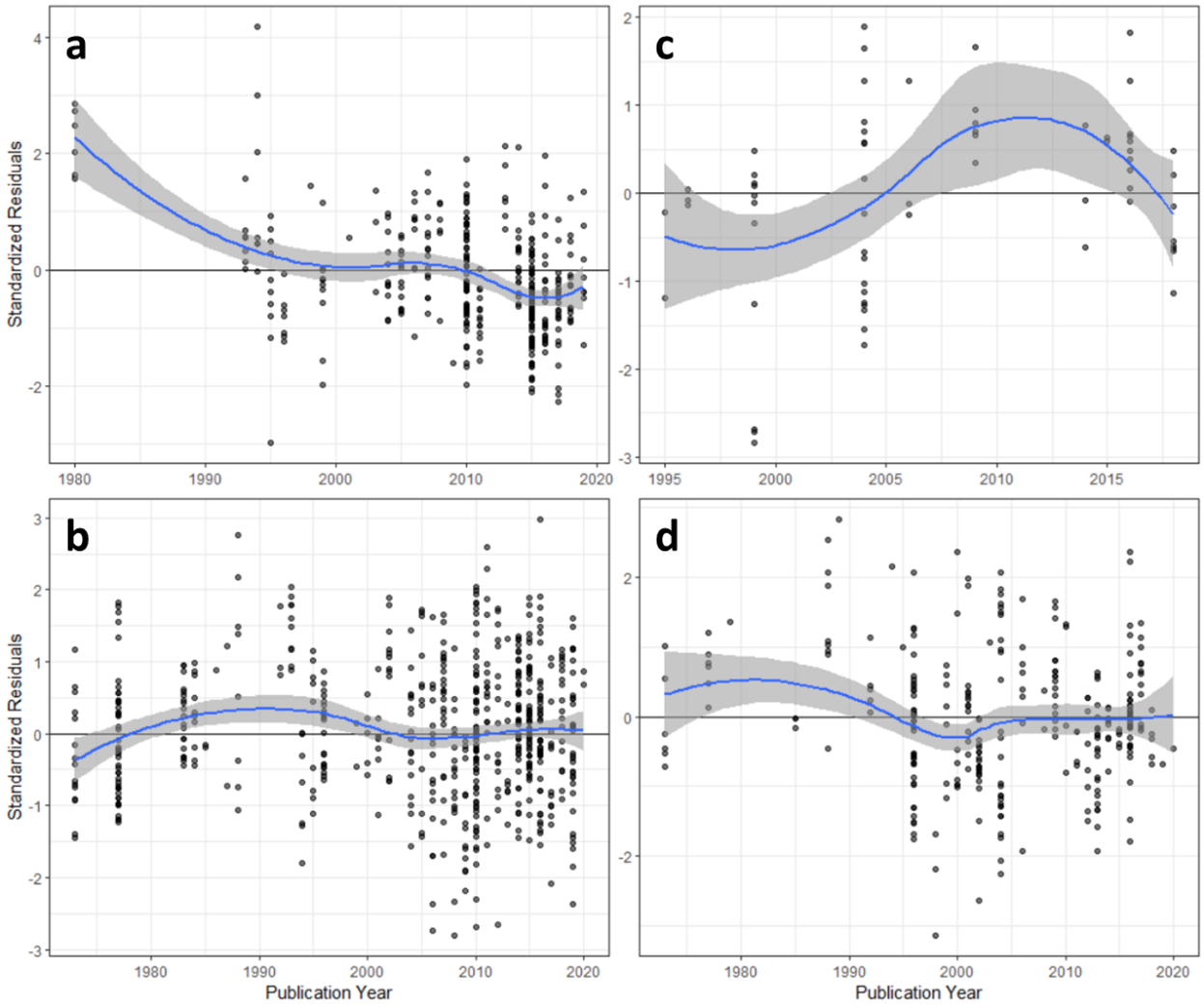

Figure A1.5: Plots of residuals against publication year from the best-fit models for the Abundance-Precipitation (a), Abundance-Temperature (b), Growth-Precipitation (c), and Growth-Temperature (d) data sets. Temporal patterns are visualized with a loess smoother (blue) and its confidence interval (grey shading) in each case. Statistical tests of linear trends with publication year are in Table A1.2.

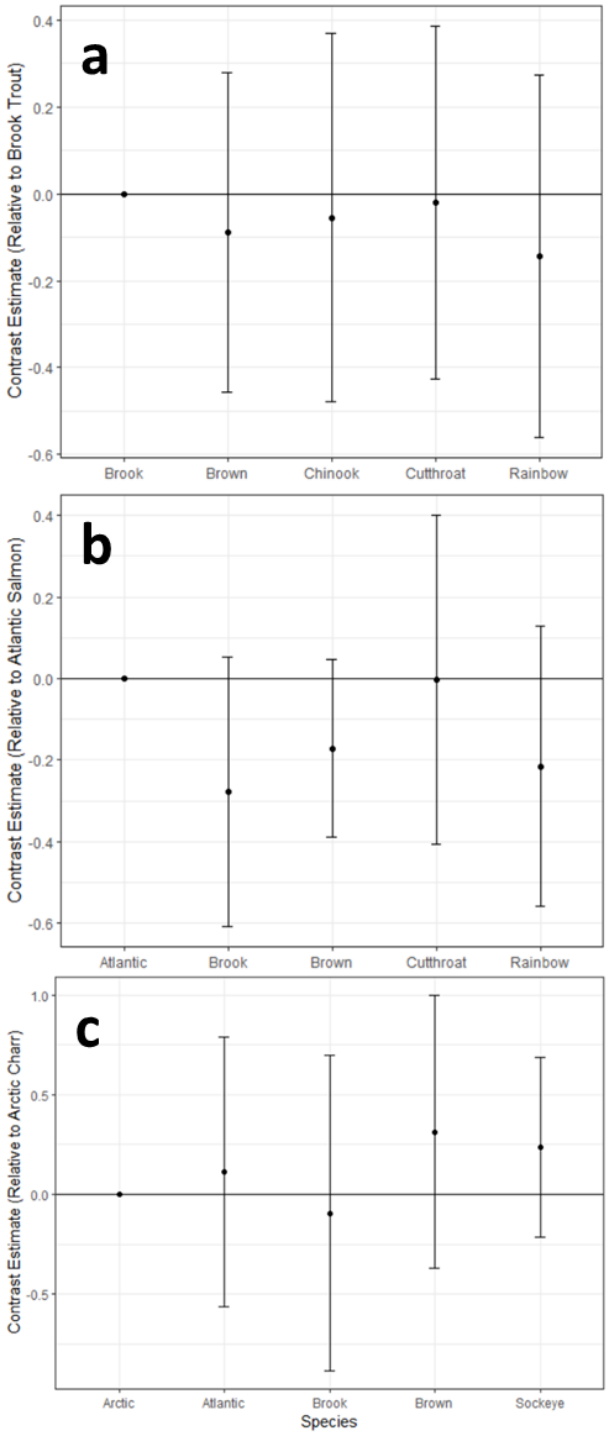

Figure A1.6: Species contrasts and 95% confidence intervals for Abundance-Precipitation (a), Abundance-Temperature (b), and Growth-Temperature (c) datasets subsetted to contain the five species with the greatest sample size in each case. Contrasts were obtained by adding species as an additional covariate to each best-fit model structure (see Methods; Table 1.3). Note that all confidence intervals contain zero, and that the first species listed was used for reference in each set of contrasts.

Appendix 2: *Chapter 2 Supplementary Materials*

A2.1 - Age-specific demographic data:

Histograms of individual fork lengths for each population each year were visually inspected to separate age-1 from age-2+ brook trout. A length cutoff of ~100mm was used in the field for almost all available observations, but these field-based cutoffs were inadequate in many cases, with some populations consistently displaying breaks in their size distributions at smaller or larger lengths. Therefore, we adjusted length cutoffs manually in 5mm increments until age-classes were visually well-separated in histograms. Adjustments were allowed to vary among years but were in the same direction across all years for each population (i.e. cutoffs were only adjusted downwards or upwards, never both). In total, length cutoffs were adjusted for 40 out of 110 observations, with adjustments applied upwards in eight populations (BC, DY, HM, MC, UC, UO, WC, and WN; n=27; range: 105-110mm) and downwards in three populations (LC, LO, and STBC; n=13; range: 80-95mm). The length data with adjusted cutoffs were subsequently filtered to remove all observations <35mm (n=125; <0.5% of total) because these were likely misclassified age-0 fish or data entry errors, and observations from the fall (September or October) were removed unless they were the only data available. This process of yielded 110 years of suitable data from 11 populations (Figure A2.2). While this retrospective adjustment of size cutoffs was not ideal, it was justified because sampling dates varied by 2-4 months among years and Cape Race populations are known to exhibit significant differences in growth, life history, and density-dependence (Hutchings 1993, Fraser et al. 2019, Matte et al. 2020). Moreover, this approach maximized data availability because the data necessary to obtain age-specific mark-recapture estimates were rarely recorded before 2015.

Finally, to calculate age-specific census population size, we multiplied the total census population size (which included all individuals age-1 and older; see Methods) in each population each year by the corresponding proportion of individuals that were classified as age-1 or age-2+ based on filtered and adjusted size distributions. When proportions could not be calculated from length-frequency data (n=12 observations), they were inferred from direct counts of age-1 and age-2+ fish reported in field notebooks during marking (n=10) or recapture events (n=2; Figure A2.3). Similarly, juvenile somatic growth rates were calculated by taking the median fork length of age-1 fish for each population and year, then dividing it by the estimated age in years at the time each age-class was sampled (units of $mm \cdot year^{-1}$). Ages were determined by subtracting the mean population-specific date of reproduction (derived from Wood and Fraser 2015) from the year-specific sampling date and dividing by 365 (Figure A2.4). All growth rates based on sample sizes less than five age-1 individuals (n=5) were removed.

A2.2 - Model robustness:

To ensure that conclusions were robust to connectivity and gaps in time-series, all DFA and GLMM models (described in Sections 2.4 and 2.5) were re-run with a smaller subset of eight populations. WN was excluded because it had a four-year gap (sampling years: 2017-2020) in the middle of its demographic time-series, and MC was removed due to its connectivity with both UC and LC (see Table 2.1). Since LO and UO effectively form a meta-population within the O'Beck drainage (Bernos et al. 2016), data were combined by summing Nc values and calculating the weighted average growth rate across both populations each year. Data from the O'Beck drainage and the seven remaining populations (BC, DY, HM, LC, STBC, UC, WC) formed the subset of demographically independent populations used to re-run models.

Models yielded broadly similar results when data from a subset of eight demographically independent populations were used. Specifically, the re-fitted recruitment DFA had a nearly identical common trend and similar population loadings (r=0.99) to the model based on all data (Figure 2.2a,b), providing further support for a pattern of asynchronous recruitment. The re-fitted growth DFA exhibited different patterns in its common trend (r=-0.01) and loadings (r=-0.09), but loadings were still positive in most populations and displayed more synchrony than recruitment patterns. Similarly, all five re-fitted GLMMs (see Table 2.2) yielded similar fixed effect estimates and the same results when comparing the relative strength of fixed and random effects via variance partitioning. Comparing AICc values of re-fitted models to identify the best-fit DFA covariates and stream temperature metrics also did not change model selection results. Overall, demographic patterns appeared to be largely robust to the influence of connectivity (for MC, LO, and UO) and gaps in time-series (for WN). Moreover, it is notable that removing these populations would have significantly reduced the number of available observations for recruitment (n=93 vs. 122) and juvenile growth (n=78 vs. 105).

A2.3 - Effects of climate extremes:

To assess the influence of climate extremes in Cape Race, we used DayMet data since 1980 (see Section 2.3) to calculate maximum air temperature and precipitation values for the focal time-periods affecting brook trout recruitment (reproduction, incubation, emergence, summer, and winter) and juvenile growth (growing and non-growing season). We then used simple correlations to describe relationships between mean and maximum values, and re-ran all dynamic factor analysis (DFA) models with maximums used as covariates instead of means (n=10 for juvenile growth, n=55 for recruitment; see Section 2.4).

Means and maximums exhibited strong positive correlations during reproduction, emergence, summer, winter, and growing season (r=0.48-0.75). Correlations were weaker during the incubation period and non-growing season (r=0.14-0.52), which were overlapping 5-month periods dominated by winter conditions. Similarly, when maximum values were used as DFA covariates, model selection results were similar to those reported using means (Table A2.1). Specifically, the model with no covariates substantially outperformed all models with a single covariate in analyses of recruitment (ΔAICc>14.3) and juvenile growth (ΔAICc>16.3), which in turn outperformed all models with two covariates (ΔAICc>38.3). This result is likely due to my modest sample sizes, and the fact that adding a covariate to DFA models (regardless of whether it is an average or maximum) requires 11 additional parameters to be estimated. It remains possible that climate extremes are important for Cape Race brook trout demography, but we were unable to detect this effect in the current study, or distinguish it from the effect of average climate conditions within a given period.

A2.4 - Non-linearity in GLMMs:

To assess potential non-linearity in demographic relationships and responses to stream temperature (see Section 2.5), we fit alternative generalized linear mixed models (GLMMs) with a quadratic term added as a fixed effect to each model. However, because the stock-recruitment relationship was fitted as a linearized form of a Ricker stock-recruitment curve, non-linear GLMMs were not explored for this relationship. In all other cases, the quadratic estimate and its standard error were recorded for all models, and the AICc of the non-linear model was compared to the original linear model. During model selection, both linear and non-linear GLMMs were run using maximum likelihood, allowing different fixed effect structures to be compared.

The effect of the quadratic term was generally weak when added to recruit-adult (estimate=-0.02, SE=0.09), density-dependent growth (estimate=0.16, SE=0.09), temperature-recruitment (estimate=0.06, SE=0.11), and temperature-growth relationships (estimate= 3.2e-06, SE=2.1e-05). Additionally, the non-linear model failed to outperform the linear model in all cases, including recruit-adult (ΔAICc= 2.23), density-dependent growth (ΔAICc=-0.45), temperature-recruitment (ΔAICc=1.96), and temperature-growth relationships (ΔAICc=2.29). In cases where linear and non-linear models were within two AICc units of each other (density-dependent growth and temperature-recruitment relationships), the linear model was selected because it is more parsimonious. Thus, the current study found little support for incorporating non-linear relationships into GLMMs, although this could change if more monitoring data are added in future years.

Table A2.1: Model selection results from dynamic factor analysis of recruitment (top) and juvenile growth (bottom) time-series in Cape Race brook trout. All models were run with an identity variance-covariance matrix, and only the top 15 models are shown for recruitment (55 models overall). Note that in both cases, AICc values were lowest in the model with no covariates, which significantly outperformed all models with one covariate (T=air temperature, P=precipitation), which in turn outperformed models with two covariates. The number of parameters estimated (k) increased substantially every time a covariate was added to the model.

DFA Response	Rank	k	Covariates	AICc	ΔAICc
Recruitment	***1***	***11***	***None***	***343.4***	***0.0***
	2	22	T_Emergence	356.0	12.7
	3	22	T_Incubation	359.3	15.9
	4	22	P_Reproduction	364.0	20.7
	5	22	P_Winter	364.7	21.3
	6	22	T_Winter	365.4	22.1
	7	22	P_Incubation	365.5	22.1
	8	22	P_Emergence	366.4	23.0
	9	22	T_Reproduction	366.5	23.1
	10	22	T_Summer	366.5	23.1
	11	22	P_Summer	370.1	26.7
	12	33	T_Incubation + T_Emergence	382.3	38.9
	13	33	T_Emergence + P_Reproduction	384.0	40.6
	14	33	T_Emergence + P_Winter	384.6	41.2
	15	33	T_Emergence + P_Incubation	384.7	41.3
	…	…	…	…	…
Juvenile Growth	***1***	***11***	***None***	***306.4***	***0.0***
	2	22	T_Growing Season	321.0	14.6
	3	22	P_Non-Growing Season	329.8	23.4
	4	22	P_Growing Season	331.1	24.7
	5	22	T_Non-Growing Season	331.4	25.0
	6	33	T_Growing Season + P_Non-Growing Season	354.4	48.0
	7	33	T_Growing Season + P_Growing Season	354.9	48.5
	8	33	T_Growing Season + T_Non-Growing Season	356.5	50.2
	9	33	T_Non-Growing Season + P_Non-Growing Season	363.4	57.0
	10	33	P_Growing Season + P_Non-Growing Season	364.2	57.8

Table A2.2: Model selection results from generalized linear mixed models (GLMMs) relating recruitment and juvenile growth to various measures of stream temperature. Average stream temperature (T) and degree-days since November 1st (DD) were estimated based on empirical air-stream temperature relationships from 2012-2021 (see Chapter 3 for details).

GLMM Relationship	Fixed Effect	AICc	ΔAICc
Temperature-recruitment	T_Reproduction	319.0	2.5
	T_Incubation	320.2	3.7
	T_Emergence	***316.5***	***0.0***
	T_Summer	320.2	3.7
	T_Winter	320.0	3.5
Temperature-growth	T_Growing Season	552.3	12.6
	DD_May1	549.9	10.2
	DD_August31	***539.7***	***0.0***

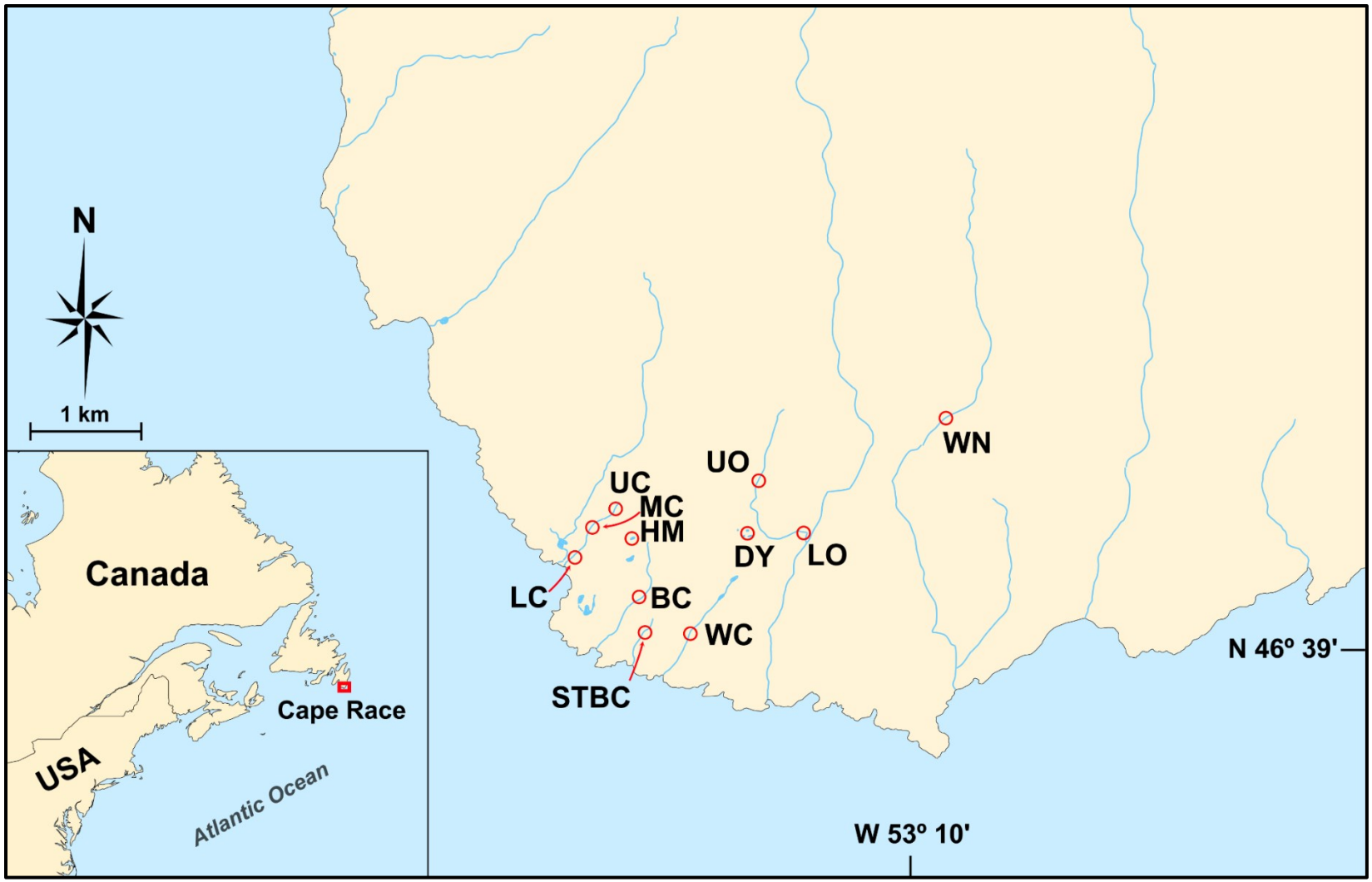

Figure A2.1: Map of the study area, with labels denoting codes for the eleven brook trout populations (red circles) studied in Cape Race, Newfoundland. The full names for each population are provided in Table 2.1.

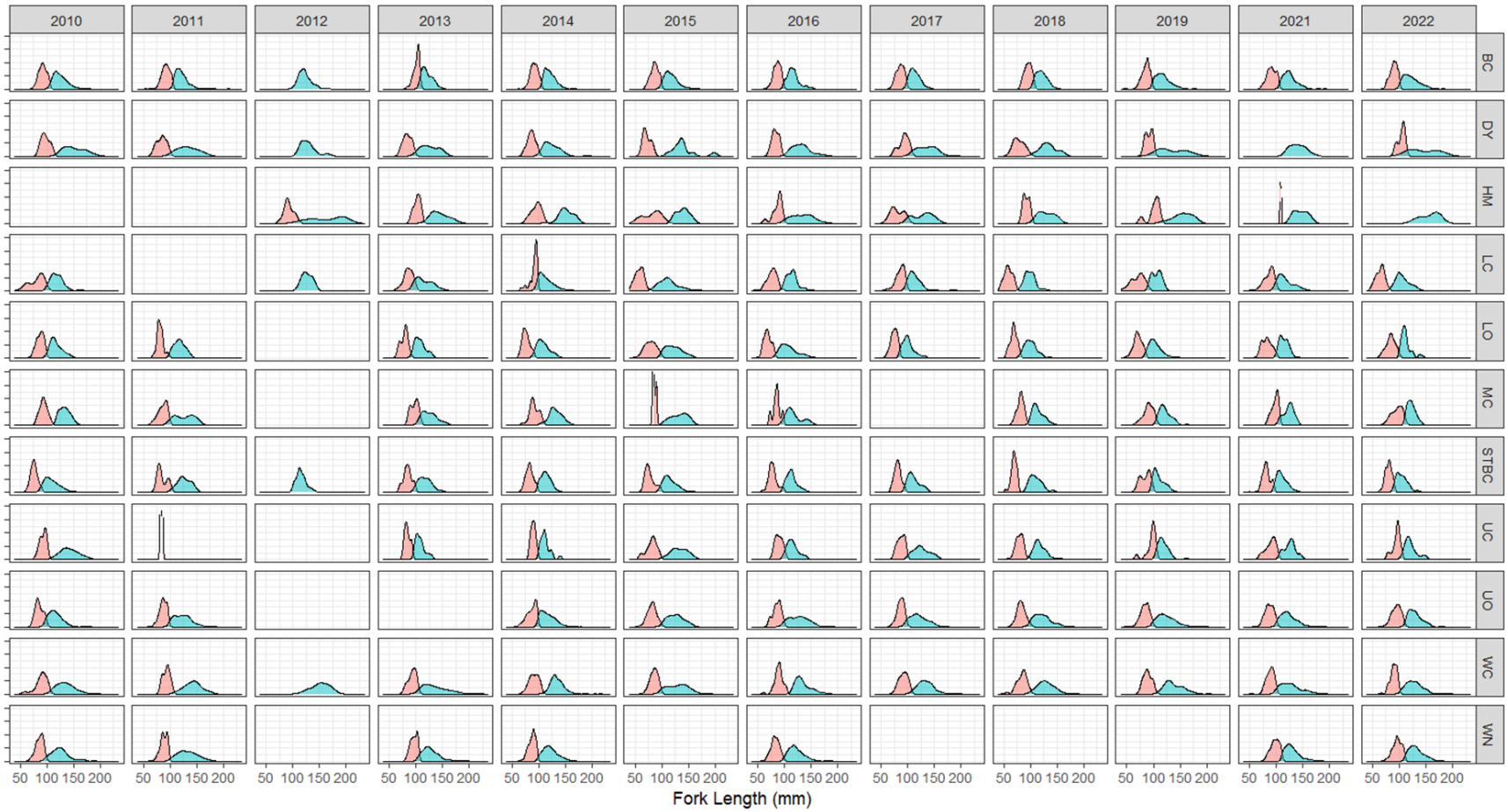

Figure A2.2: Size distributions for eleven Cape Race brook trout populations. Distributions are displayed as smoothed kernel densities for age-1 (pink) and age-2+ individuals (blue) within each population (rows) and year (columns). Empty panels had no data available (see Section A2.1).

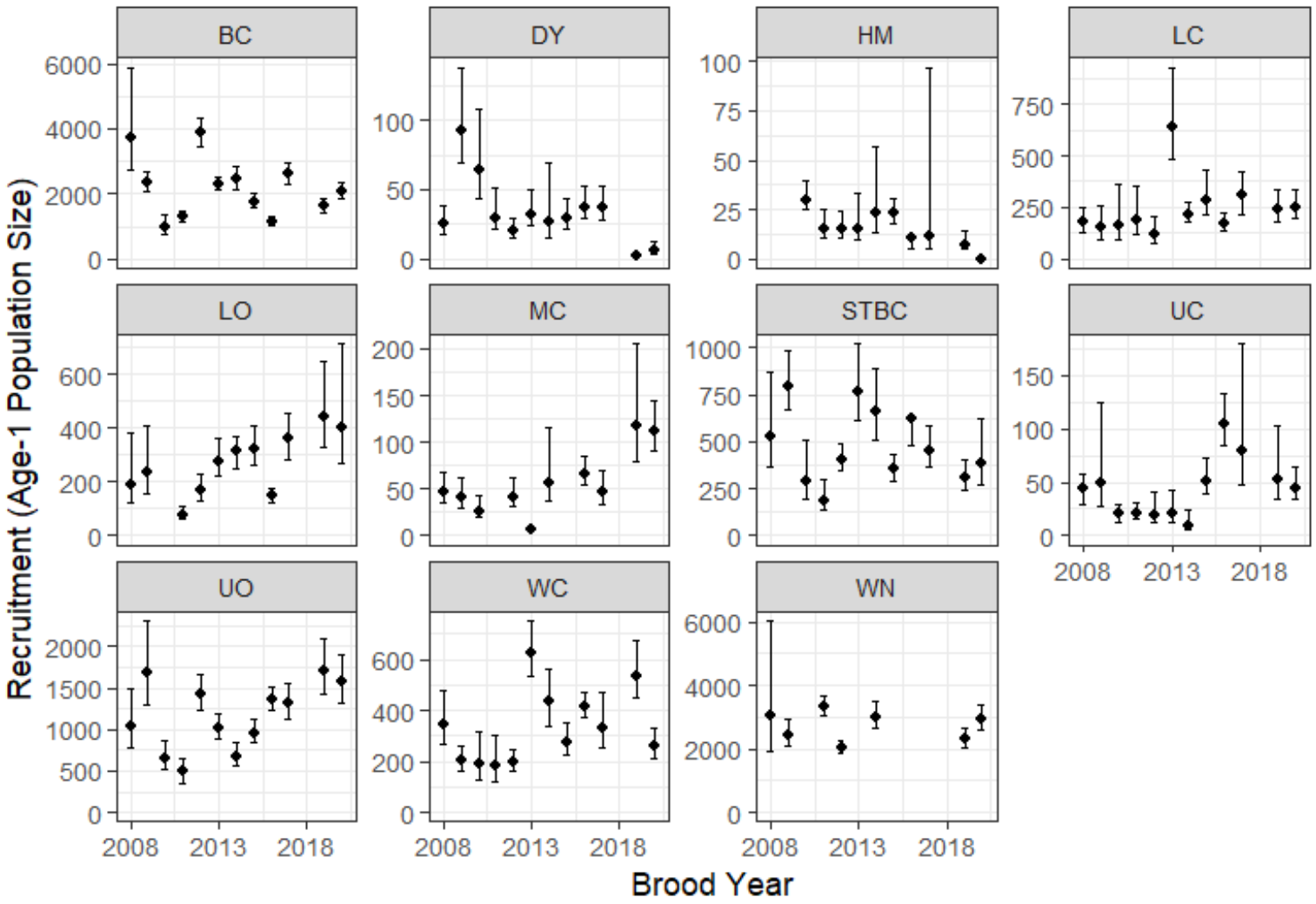

Figure A2.3: Recruitment time-series for eleven Cape Race brook trout populations. Recruitment was estimated as the total census population size multiplied by the proportion of age-1 individuals derived from length distributions or age-specific counts (see Section A2.1 and Figure A2.2). 95% confidence intervals (error bars) were estimated based on recapture proportions observed across all ages.

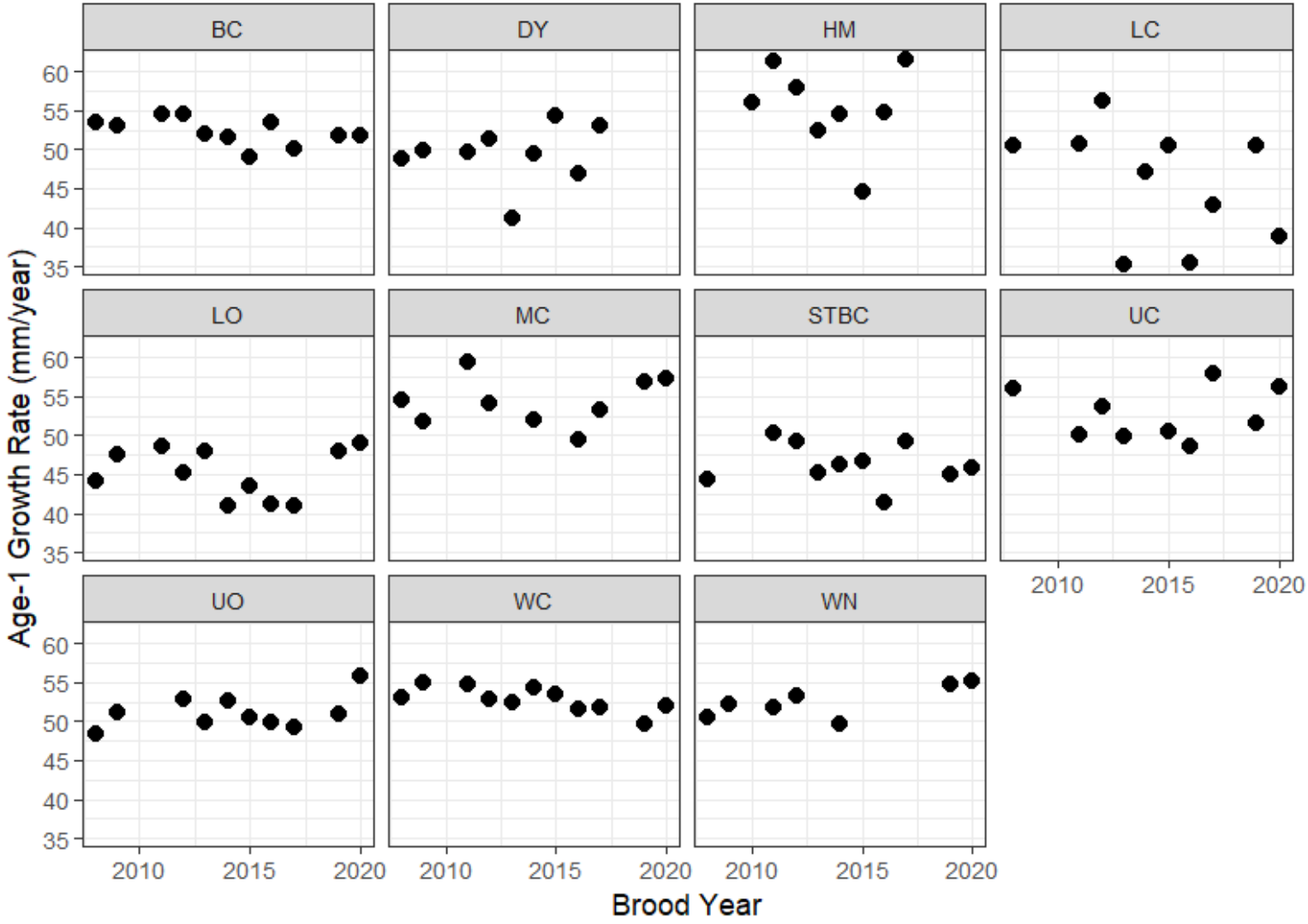

Figure A2.4: Juvenile growth rate time-series for eleven Cape Race brook trout populations. Growth rates were estimated as the median length of age-1 individuals divided by their estimated age at the time of sampling (see Section A2.1).

Appendix 3: *Chapter 3 Supplementary Materials*

Table A3.1: Catchment survey data for ten streams in Cape Race, Newfoundland, Canada. Drainage area is expressed in km^2, gradient is reported as the percent change in elevation divided by stream length, depth is shown in cm, velocity is in $m \cdot s^{-1}$, and relative pond area was calculated as the total perimeter of all ponds divided by stream length. Sinuosity and the width:depth ratio are unitless. Full details on survey methodology are available in Wood et al. (2014).

Stream	Thermal Regime	Drainage Area	Sinuosity	Gradient	pH	Depth	Width:Depth	Velocity	Relative Pond Area
BC	Intermediate	1.4	1.29	24.4	6.32	16.7	15.1	2.01	66
DY	Intermediate	0.1	1.37	2.8	5.83	23.4	5.4	1.50	11
HM	Rainfall	-	-	-	6.27	42.2	34.8	0.00	300
LC	Groundwater	0.1	1.16	51.1	6.28	11.4	10.6	0.99	0
LO	Rainfall	0.2	1.07	10.6	6.57	19.5	18.1	1.77	0
STBC	Groundwater	0.4	1.33	38.2	6.09	21.7	10.4	0.48	0
UC	Intermediate	0.0	1.20	22.1	5.32	24.3	8.8	0.02	16
UO	Rainfall	3.1	1.86	10.6	6.20	20.8	19.2	2.07	82
WC	Intermediate	0.4	1.23	23.8	6.26	17.7	12.9	0.64	20
WN	Intermediate	6.4	1.33	10.3	6.64	23.0	21.5	1.50	0

Table A3.2: Relationships between young-of-the-year brook trout length and degree-days accumulated from November 1st the previous year until the date of capture (see Figure 6). Intercepts, slopes, sample sizes (N), and R^2 values (treating degree-days as a fixed effect) are shown for linear regression models run separately for each stream with no random effects. The same outputs are also shown for a generalized linear mixed model that included stream as a random effect on intercepts and slopes (bottom), where R^2 Fixed and R^2 Random correspond to the variance explained by the fixed and random effects, respectively. Intercept and slope estimates with a p-value <0.05 are marked with an asterisk (*), while those with a p-value <0.001 are marked with two asterisks (**).

Stream	Thermal Regime	Intercept	Slope	N	R^2 Fixed	R^2 Random
BC	Intermediate	11.35**	0.029**	1,660	0.38	-
DY	Intermediate	-2.66	0.039**	194	0.54	-
HM	Rainfall	-6.23	0.035**	29	0.44	-
LC	Groundwater	10.16**	0.017**	294	0.19	-
LO	Rainfall	11.54**	0.019**	119	0.25	-
STBC	Groundwater	-14.31**	0.041**	410	0.36	-
UC	Intermediate	5.90*	0.028**	110	0.60	-
UO	Rainfall	8.92**	0.029**	699	0.33	-
WC	Intermediate	9.09**	0.027**	598	0.29	-
WN	Intermediate	3.71*	0.029**	1,418	0.41	-
GLMM	All	4.54*	0.028**	5,531	0.27	0.35

Table A3.3: Correlations between stream characteristics from habitat surveys (predictors) and parameter estimates for non-linear relationships between daily average air temperature and stream temperature in ten streams in Cape Race, Newfoundland, Canada. Significant correlations without multiple comparison adjustments ($p < 0.05$) are shown in bold italic text. For reference, μ is the minimum stream temperature, α is the maximum stream temperature, γ is the slope at the inflection point, and β is the temperature where the inflection point occurs (see Equation 3.1). Note that all significant correlations became non-significant when applying Bonferroni multiple comparison adjustments ($p > 0.0016$).

Predictor	**μ**	**α**	**γ**	**β**
Drainage Area	-0.48	0.45	***-0.84***	0.48
Sinuosity	-0.28	0.34	-0.30	0.37
Gradient	***0.85***	***-0.87***	0.29	***-0.69***
pH	-0.15	0.19	-0.35	0.37
Depth	-0.12	0.54	0.14	0.48
Width:Depth Ratio	-0.20	***0.63***	-0.07	***0.67***
Velocity	***-0.64***	0.33	-0.48	0.26
Relative Pond Area	-0.01	0.54	0.21	***0.64***

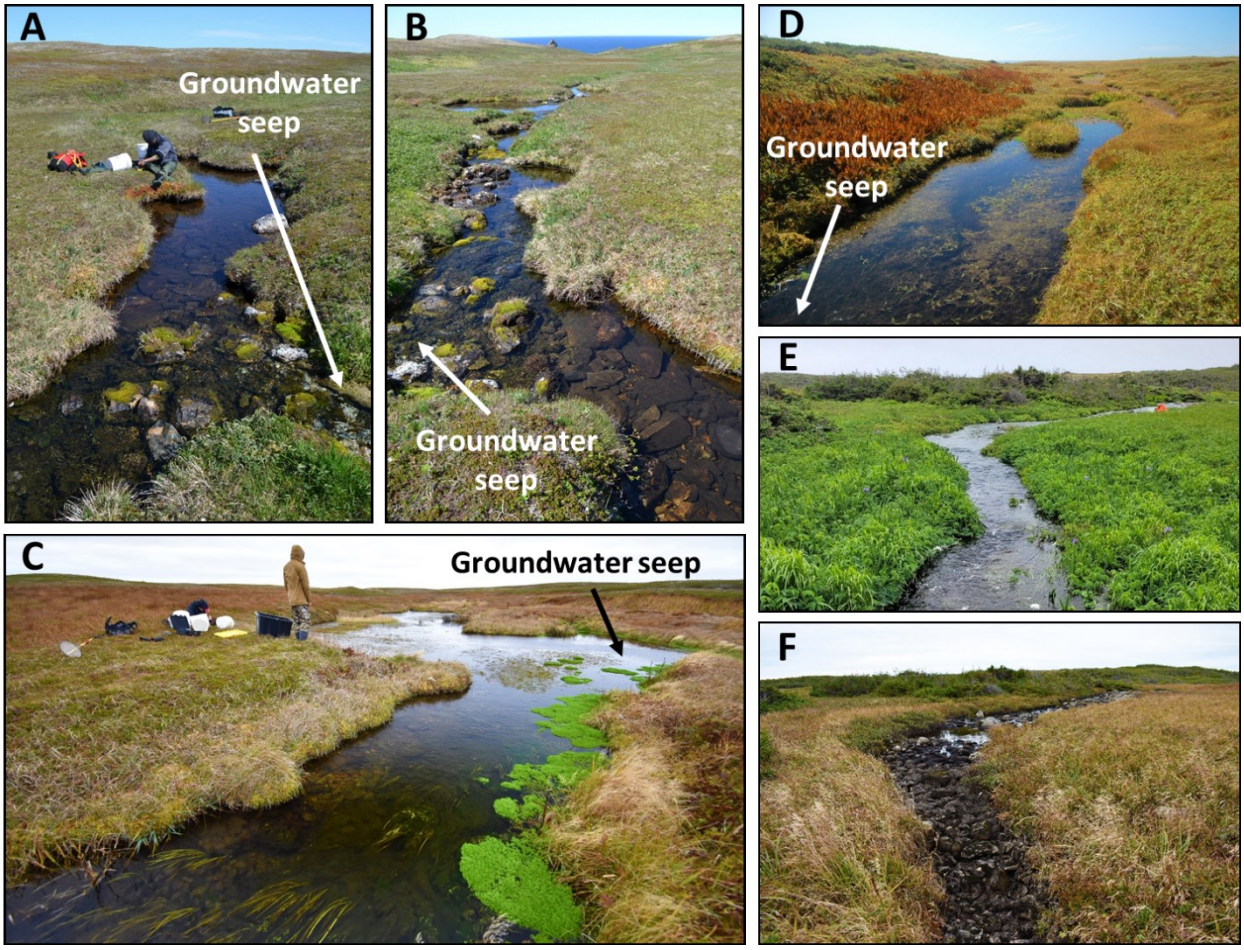

Figure A3.1: Examples of groundwater- and rainfall-dominated streams harboring brook trout in Cape Race, Newfoundland, Canada (photo credits: Dylan Fraser). Panel A (facing upstream) and B (facing downstream, same position): a groundwater seep entering the upper section of Lower Coquita (LC). The seep pours out of the ground 3 m above the confluence with the stream and directly influences the flow, acidity and vegetation downstream. For example, note the tannin-colored water in the bottom right corner of panel B upstream of the groundwater seep that is devoid of aquatic vegetation – here the stream pH is ~5.0-5.3, whereas below the groundwater seep the pH is ~6.3-6.6 and aquatic vegetation is abundant. Panel C: the presence of Miner's Lettuce (*Montia fontana*) (the bright green aquatic plant) below a large groundwater seep that enters a small pond within Bob's Cove River (BC). Panel D: a groundwater-dominated stream characterized by very low current velocity and choked aquatic vegetation (Still There by Chance; STBC). Panels E and F: example of fluctuating streamflow in a rainfall-dominated stream (Upper O'Beck; UO) in the same location in July 2021 (E) and October 2022 (F).

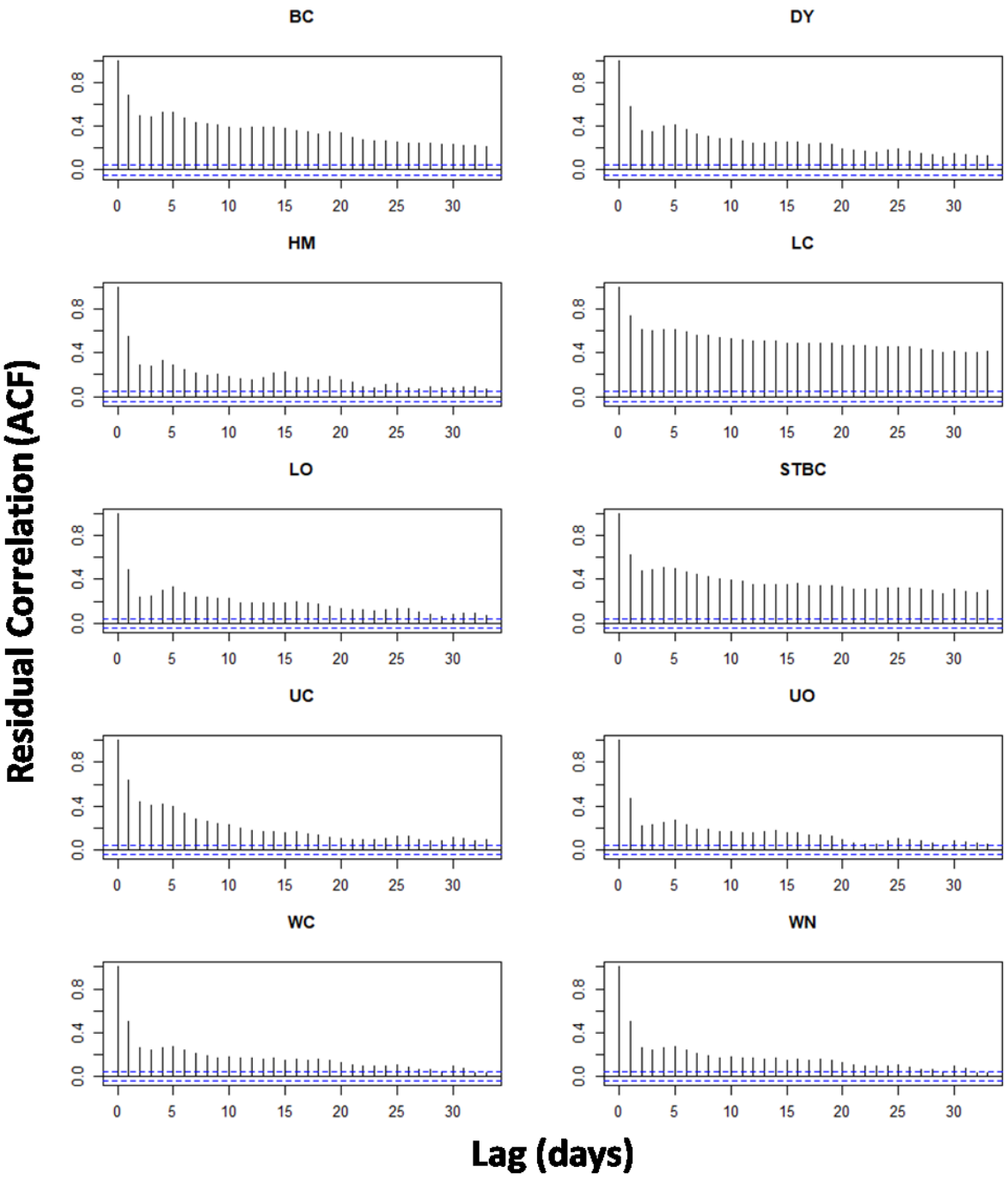

Figure A3.2: Autocorrelation functions based on residual values from air-stream temperature relationships in ten streams in Cape Race, Newfoundland, Canada. Correlations in residuals across various daily time lags (vertical bars) and significance thresholds (blue dashed lines) are shown in each case.

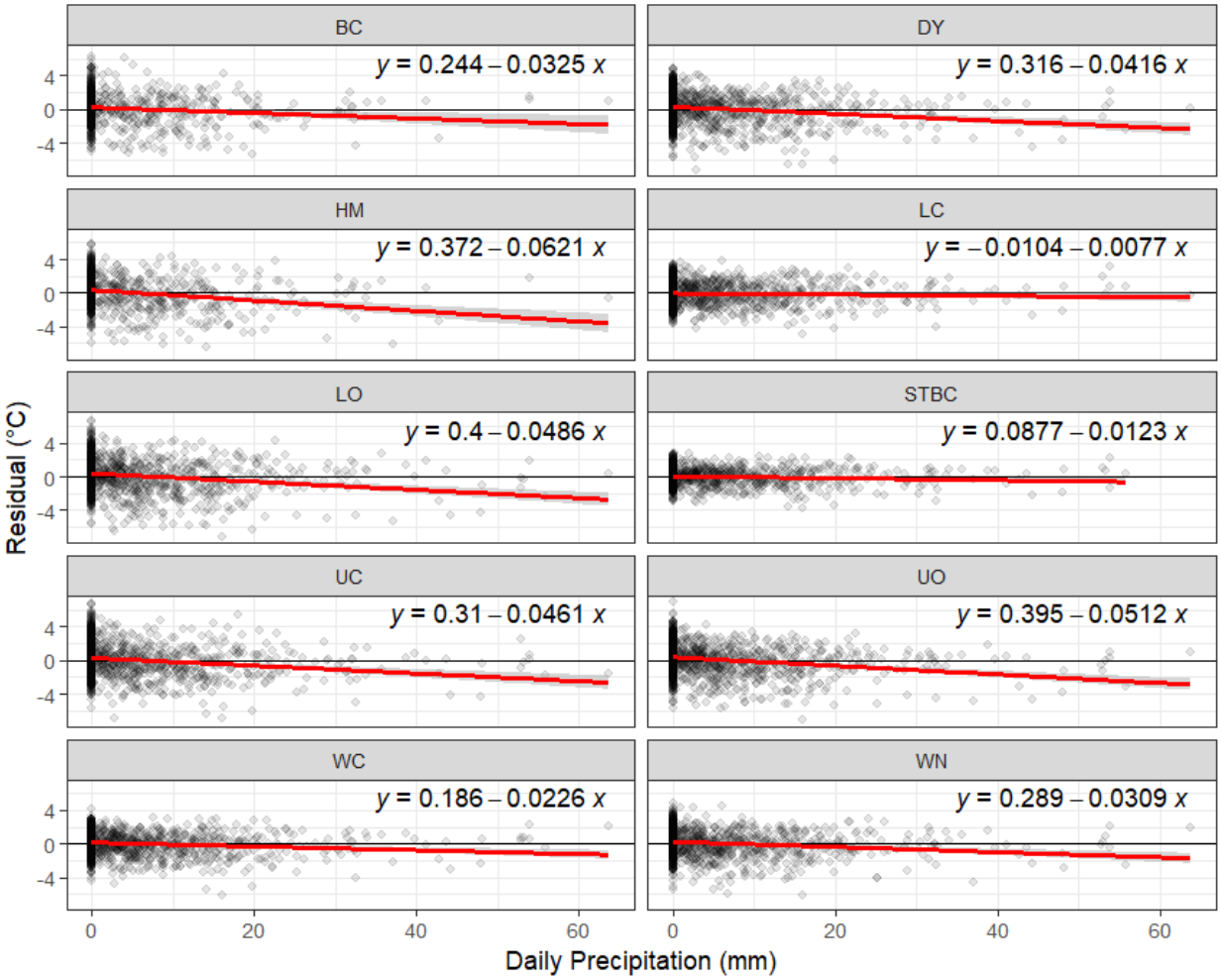

Figure A3.3: Effects of daily precipitation on residual values from air-stream temperature relationships in ten streams in Cape Race, Newfoundland, Canada (panels). A linear trend is shown for each stream (red line), along with its estimated intercept and slope (text in top right corner). Note that all streams exhibit negative slopes.

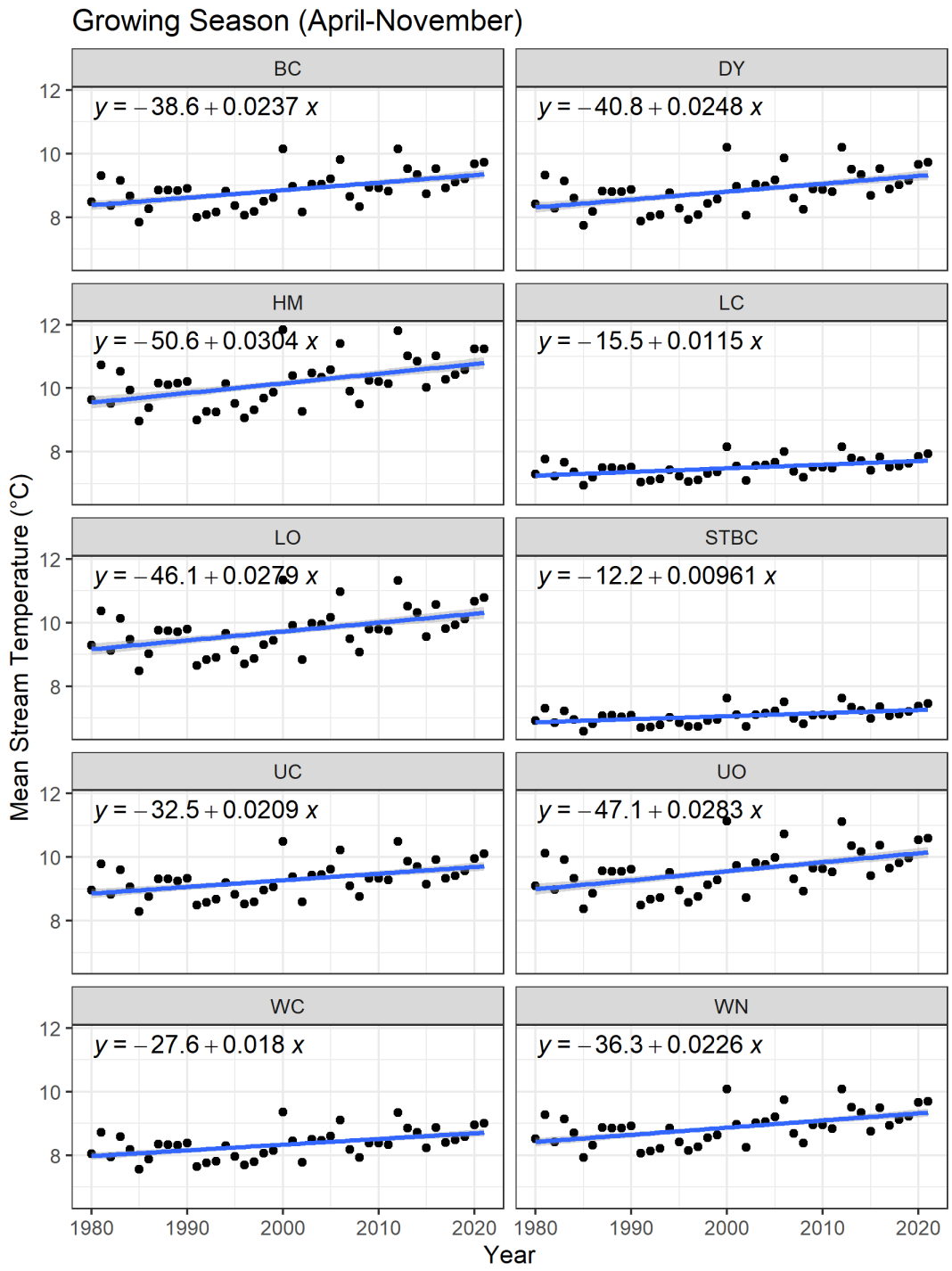

Figure A3.4: Temporal trends in reconstructed mean stream temperature during the growing season (April-November) in ten streams in Cape Race, Newfoundland, Canada. Estimated intercepts and slopes are shown in the top-left of each panel (see also Table 3.2). Note the lower average temperatures and reduced slopes predicted in the two groundwater-dominated streams (LC and STBC).

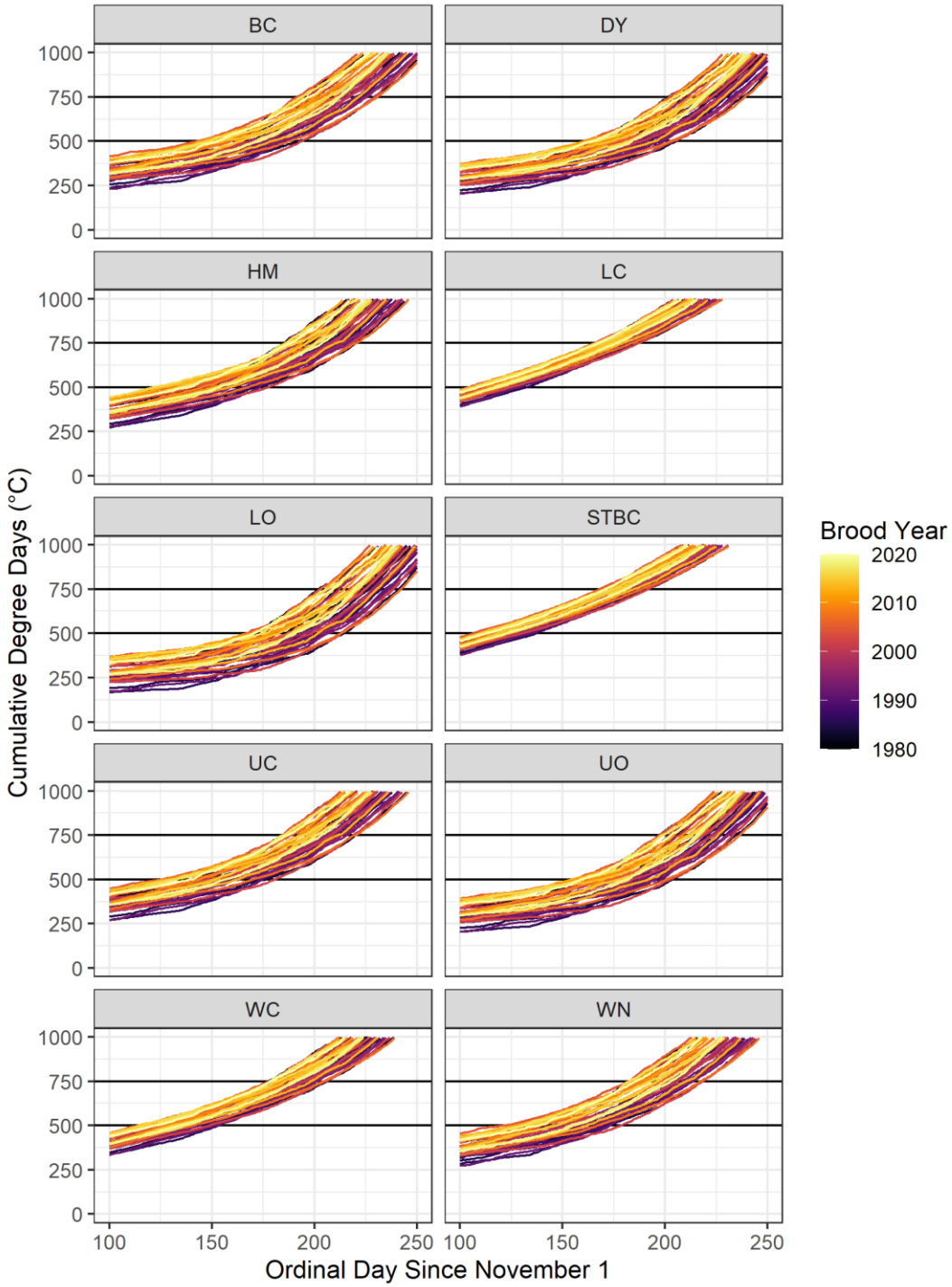

Figure A3.5: Annual variation in reconstructed degree-day accumulation since November 1st in ten streams in Cape Race, Newfoundland, Canada from 1980-2020. Horizontal lines are shown at 500 and 750 degree-days to denote putative thresholds for the timing of hatch and emergence, respectively. The most recent years are plotted in yellow, illustrating phenological shifts (see Table 3.3). Note the earlier phenology and reduced inter-annual variation predicted in the two groundwater-dominated streams (LC and STBC).

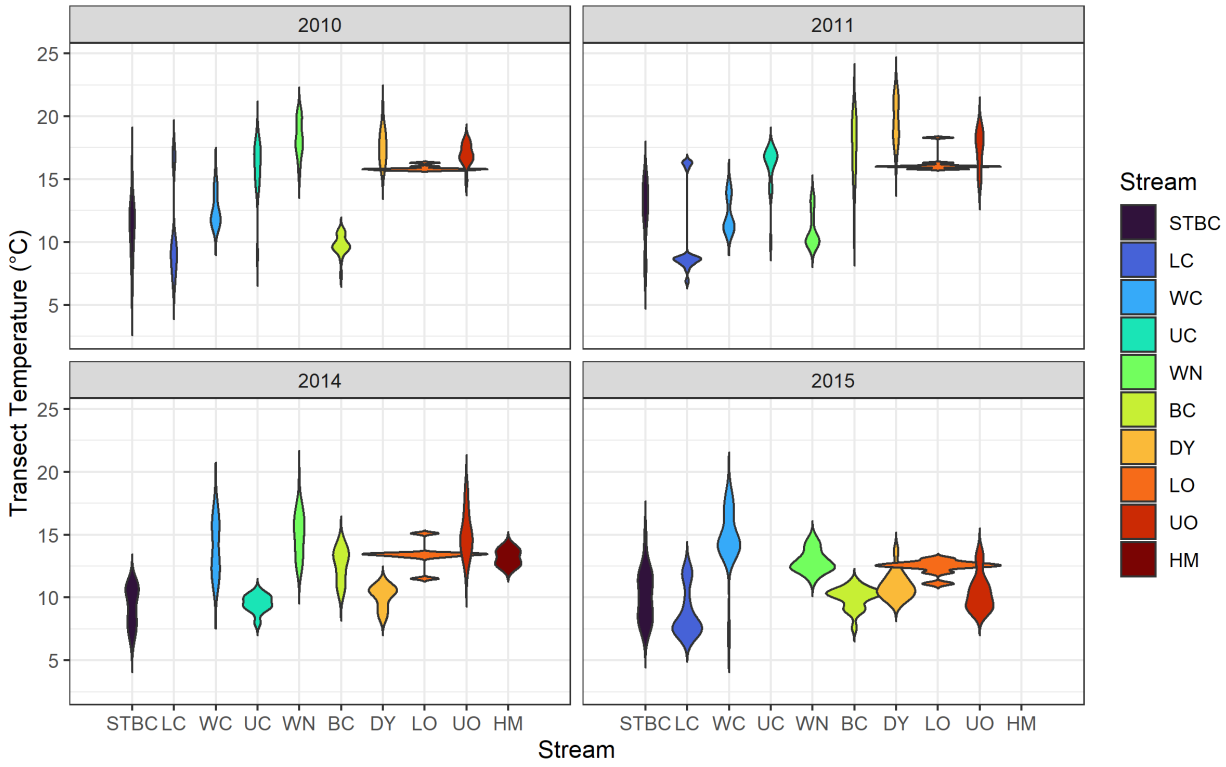

Figure A3.6: Violin plots showing within-stream spatial variation in water temperature recorded during transect surveys in ten streams in Cape Race, Newfoundland, Canada. Transects were performed during four summers between mid-June and early-August (see Wood et al. 2014 for details), but not all streams were sampled each year and were not always sampled in the same order or during the same time of day within years. Note that spatial variation in temperature exceeded 5°C in the majority of cases.